Identification of novel genes controlling sexual development in *Aspergillus* species

Wenyue DU

B.Sc, M.Sc

Thesis submitted to the University of Nottingham (UK)

for the degree of Doctor of Philosophy

March, 2022

Abstract

The overall aim of this PhD project was to gain a better understanding of the genetic controls of sexual development in *Aspergillus* species, a topic of both of fundamental and practical importance. Work covered three areas. First, over 70 genes have already been identified associated with sexual reproduction in *A. nidulans*. In order to maintain *A. nidulans* as a comprehensive model for sexual development in the Ascomycotina, genetic studies were undertaken to determine any role that genes involved in sexual reproduction identified from other ascomycete species, but not yet studied in *A. nidulans*, might have in *A. nidulans i.e.* to investigate whether such genes were universal ascomycete sex genes. To achieve this goal, putative gene homologs were identified in *A. nidulans* by bioinformatic analysis and then gene function characterised by screening for sexual fertility of control versus gene deletion strains. Gene *AN2701.2*, encoding a putative MAPK (mitogen activated protein kinase) scaffold protein, was found to be pivotal for sexual development with gene deletion causing a significant reduction in size of cleistothecia, number of ascospores and ascospore viability. The STRIPAK (striatin-interacting phosphatase and kinases) complex has an essential role in signal transduction. The STRIPAK subunits *AN0164.2* (PP2Ac regulatory unit) and *AN6611.2* (STRIP1/2 unit) were also found to be required for normal sexual development and growth. However, deletion of *AN4632.2* (SLAMP unit) did not show any significant impact on sexual development. The putative transcription factors *AN4813.2, AN1217.2, AN7170.2* and *AN7736.2* were investigated. The *mybA* homolog *AN4813.2* was found to be required for normal sexual development, with gene deletion leading to a significant reduction in numbers of cleistothecia and ascospores, and lowered ascospore viability. *AN4813.2* deletion in addition blocked conidiophore formation, indicating a dual role in sexual and asexual development. Deletion of *AN1217.2* also caused abnormal development of cleistothecia whereas deletion of *AN7170.2* and *AN7736.2* had no impact on cleistothecial formation. Deletion of *AN3147.2*, encoding a glycolipid protein,

reduced the number of cleistothecia and ascospores produced. Deletion of *AN10631.2* had no impact on fruit body formation whilst *AN4891.2*, predicted to encode a histone chaperone, appeared essential for general growth.

Second, the role of high mobility group (HMG) genes in controlling sexual development in *A. fumigatus* was studied. HMG proteins have previously been shown to regulate a wide range of developmental processes in eukaryotic organisms but in the case of fungi, almost all studies have focused only on HMG genes involved in determination of sexual identity. However, recent studies with *A. nidulans* and *Podospora anserina* had revealed the presence of a network of additional HMG genes in the genome, many of which were shown to regulate sexual reproduction in these homothallic/pseudohomothallic species. Studies were therefore undertaken to investigate the possible role of such additional HMG genes in the heterothallic species *A. fumigatus.* Bioinformatic analysis identified seven putative HMG gene homologs in the genome of *A. fumigatus.* Subsequent gene deletion and fertility screening via sexual crossing revealed that five of the HMG homologs were required for normal sexual development. As part of this work, gene deletion of the known sexual development activator gene *nsdC* was conducted as pilot work, and it was found interestingly that loss of fertility was only observed when both mating partners were of the Δ*nsdC* background. This necessitated the construction of highly fertile Δ*kuB* strains of both *MAT1-1* and *MAT1-2* genotype for later characterisation of HMG gene function.

Third, any possible dual role of HMG genes in the regulation of secondary metabolism of *A. fumigatus* was investigated. Levels of the mycotoxins gliotoxin, fumagillin, pseurotin A and helvolic acid were investigated via HPLC in HMG deletant strains of *A. fumigatus*. Both fumagillin and pseurotin A production was reduced in five of the gene deletants, indicating that these HMG genes positively upregulated these secondary metabolites. By contrast, gene deletion had no impact on gliotoxin production.

Overall, studies led to the identification of novel genes involved with sexual reproduction of *A. nidulans*, identified a network of HMG genes regulating

sexual development in *A. fumigtaus*, and provided evidence of the dual role of certain HMG genes in the regulation of both fruit body formation and secondary metabolism.

Ackowledgements

I fully appreciate my supervisors Prof. Paul S. Dyer and Dr. Matthias Brock for helping and supporting throughout my PhD study, and for giving me the opportunity to undertake the project. My thanks go to Matthew Kokolski, Marylin Wagner, Elaine and Robin for assistance and providing the lab materials and equipments. Special thanks go to Dr. Mike Bromley and Zhao, Can at the University of Manchester for helping to start HMG work in *Aspergillus fumigatus*.

Also, thanks go to my colleagues in lab B85 and office B77 for helping me in completing lab works.

Thanks to all my flat-mates in Melton Hall as we have spent many pleasure moments. Special thanks to Jo Mehew from Melton Hall staff team and has encouraged me for so many times.

Sincere thanks to my parents Sun, Ying and Du, Xinsheng for continuously support during my studying and life in the UK. Special thanks go to my dear friend Jiang, Yinyin for cheering me up in difficult times.

Abbreviations

ANOVA	Analysis of variance
BLAST	Basic Local Alignment Search Tool
ble	Phleomycin resistance gene
$CaCl_2 \cdot H_2O$	Calcium chloride monohydrate
$CoCl_2 \cdot 6H_2O$	Cobaltous chloride hexahydrate
$CuSO_4 \cdot 5H_2O$	Copper sulfate pentahydrate
DNA	Deoxyribonucleic acid
EDTA	Ethylene diamine tetraaceticacid
F	*F* factor
$FePO_4 \cdot H_2O$	Iron (III) phosphate monohydrate
$FeSO_4 \cdot 7H_2O$	Ferrous sulfate heptahydrate
H_3BO_3	Boric acid
HCl	Hydrycloride acid
HMG	High-mobility group
hph	Hygromycin B phosphotranferase gene
HPLC-DAD	High Performance Lquid Chromatography-Diode Array Detection
K_2HPO_4	Dipotassium phosphate
KCl	Potassium chloride
KH_2PO_4	Monopotassium phosphate
MAT	Mating-type
MES	Morpholineethanesulfonic acid
$MgSO_4 \cdot 7H_2O$	Magnesium sulphate heptahydrate
$MnCl_2 \cdot 4H_2O$	Manganese (II) chloride tetrahydrate
$MnSO_4 \cdot 4H_2O$	Mangnese sulphate tetrehydrate
$Na_2B_4O_7 \cdot 7H_2O$	Sodium tetreborate heptahydrate
$Na_2MoO_4 \cdot 2H_2O$	Disodium molybdate dihydrate
NaCl	Sodium chloride
$NaNO_3$	Sodium nitrate
NaOH	Sodium hydroxide
ORF	Open reading frame
PCR	Polymerase chain reaction
PEG	Polethylene glycol
pryG	Orotidine 5'-phosphate decarboxylase gene
pyroA	Pyridoxine biosynthesis gene
SDS	Sodium dodecyl sulphate
SEM	Sandard error mean
STRIPAK	Straitin-interacting phosphatase and kinase
Tris	Tris-hydroxymethly-methylamine
$ZnSO_4 \cdot 7H_2O$	Zinc sulphate heptahydrate
Δ	Deletion mutant

Contents

Chapter 1 General Introduction and Literature Review

1.0 The Phylum Ascomycota

Filamentous fungi in the phylum Ascomycota, also called ascomycetes, are traditionally classified by the formation of asci (sac-like meiosporagnuim) during their sexual development cycle (Moore, 2011). Based on the characters of the asci, the phylum can be further divided into three sub-phyla, which are (1) Taphrinomycotina (archi-ascomycetes) which form naked asci; (2) Saccharomycotina (hemi-ascomycetes) which reproduce by budding; and (3) Pezizomycotina (also termed euascomycetes) which produce asci within fruiting-bodies known as ascomata (also termed ascocarps) (Moore, 2011). In addition, phylogenetic research over recent decades has shown that many supposedly 'asexual' fungal taxon are located within the Ascomycota, indicating that they might have cryptic, as yet undiscovered, sexual cycles (Dyer and Kück, 2017).

The majority of described species in the Ascomycota are located within the Pezizomycotina, with the genus *Aspergillus*, the primary subject of studies in the present thesis, being one of the most diverse groups within this sub-phylum (Moore, 2011; Krijgsheld et al., 2013). Representative species include *Aspergillus nidulans*, which is a model organism for cell biology and molecular genetic research; *Aspergillus fumigatus,* which is an opportunistic human pathogen that can cause severe lung disease; *Aspergillus flavus* which can contaminate crops and produces carcinogenic aflatoxins; *Aspergillus oryzae,* which is an important fungus in the Asian food industry; and *Aspergillus terreus*, which generates lovastatin which is used medically to control blood cholesterol levels (Pöggeler et al., 2006; Perez-Sanchez et al., 2017; Challa, 2018; Ibarra et al., 2018). Species within the genus *Aspergillus* reproduce asexually via the

formation of conidiophores and conidia, and certain species can also reproduce sexually via the production of ascomata and ascospores (Krijgsheld et al., 2013; Ojeda-Lopez et al., 2018). In relation to traditional fungal 'dual taxonomy', the epithet *Aspergillus* refers to the anamorphic state genus, while various teleomorphic genera have been described according to the particular characteristics of fruiting body produced during sexual reproduction (Dyer and O'Gormam, 2012; Krijgsheld et al., 2013). For example, the teleomorph of *Aspergillus nidulans* is *Emericella nidulans*, which exhibits the production of Hülle cells and deeply coloured cleistothecia during sexual development, while the teleomorph of *Aspergillus fumigatus* is *Neosartorya fumigata*, which exhibits the production of light-coloured cleistothecia with heat resistant ascopores during sexual development (Dyer and O'Gorman, 2011; Krijgsheld et al., 2013). However, under the recent 'One name, One fungus' convention, a single taxonomic name is now recommended for a given species (Hawksworth et al., 2011). Various environment factors influence whether species of the Ascomycota undergo asexual or sexual development, as will be described below with a particular emphasis on development in *Aspergillus* species, the focus of studies in the present thesis

1.1 Morphological development in the Ascomycota

Members of the Ascomycota may regenerate via asexual development, sexual development and possibly via a parasexual cycle. Each method of reproduction involves the differentiation of particular morphological structures for spore/progeny production as will now be described, with a focus on *Aspergillus* species.

1.1.1 Asexual reproduction: formation of conidiophores and conidia

Asexual reproduction involves the development of conidiophores and conidia in the aspergilli (**Figure 1-1**). After a period of vegetative growth, the aerial hyphal cells differentiate into conidiophore stalks, and some hyphal cells grow vertically to form foot cells (Bennett et al., 1992). In the next stage, conidiophore vesicles form on the aerial stalks in a budding mode of growth, and later these vesicles form primary sterigmata, also called metualae (Bennett et al., 1992). Later, nuclei undergo mitotic division, and the daughter nuclei will move to metula where a septum is formed to separate parental and daughter nuclei (Bennett et al., 1992). Metualae then form secondary sterigmata (also called phialides). As a final stage, nuclei divide mitotically and migrate to form conidia by generating septa (Bennett et al., 1992), with conidial maturation marked by the accumulation of green pigments (Bennett et al., 1992).

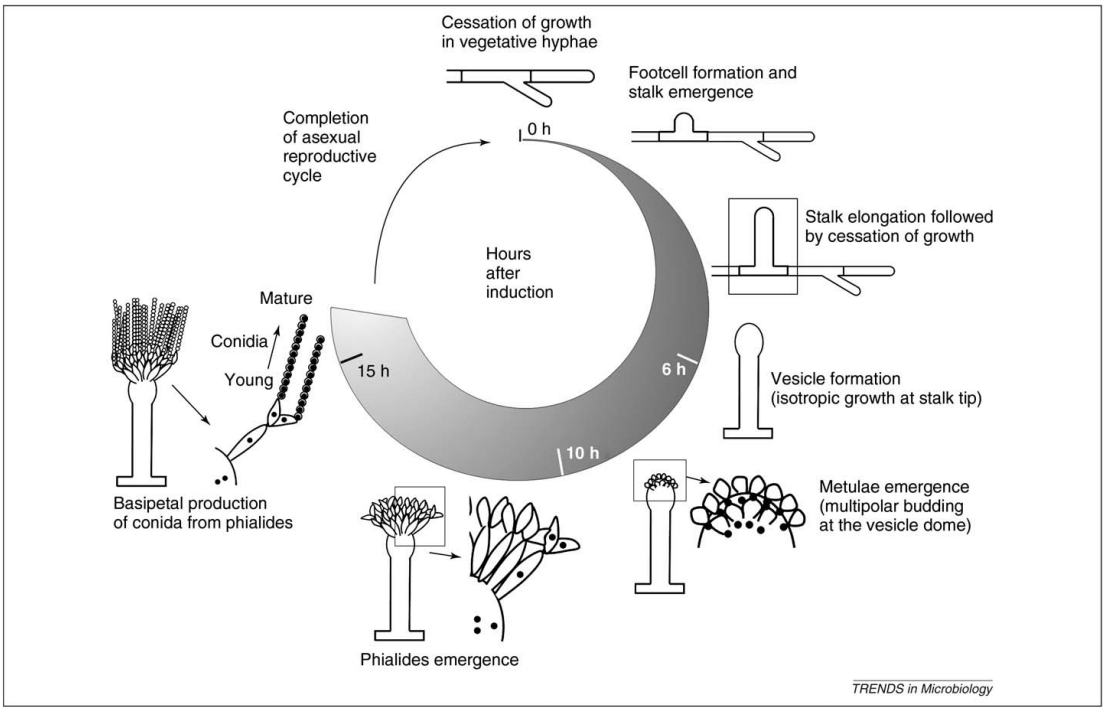

Figure 1-1 Condiophore and conidia formation in *A. nidulans* (Etxebeste et al., 2010). Figure included as an example from *Aspergillus* species. However, note that exact details of condiophores vary within the aspergilli e.g. *A. nidulans*

shows biseriate conidial heads with two rows of phialides, whereas *A. fumigatus* shows uniseriate conidial heads with a single row of phialides.

1.1.2 Sexual reproduction: formation of fruit body and ascospores

The sexual cycle in the Ascomycota involves complex and specific processes of cellular differentiation, many of them particular to a given genus or species. Somatogamy typically occurs under the regulation of mating-type (*MAT*) genes (Pöggeler et al., 2006). In *A. nidulans*, the sexual cycle begins with the formation of a simple and loosely coiled structure with two hyphal branches arising from a mat of aerial hyphal (Sohn and Yoon., 2002). The initial morphogical structure is a coiled lump-like structure in which one hyphae forms the one-celled round head with a tail (likely the ascogonium) and the other hyphae wraps around the core head in spiral loops (Sohn and Yoon., 2002). The coiled lump forms a cleistothecia initial by enlarging the multinuclear core head and further development and tightening of the wrapping hyphae (Sohn and Yoon., 2002). This ascogenous system develops into a young cleistothecia when first Hülle cells (nutrient cells) appear, and peridial hyphae become thickened (Sohn and Yoon., 2002). The inner portion of cleistothecia includes ascogenous cells from which can develop croziers (Sohn and Yoon., 2002). Nuclei in the extending region of the crozier undergo synchronous division, while two compatible nuclei in the bending region of the crozier fuse to form a young ascus in which ascospores are eventually formed (Pöggeler et al., 2006; Moore, 2011).

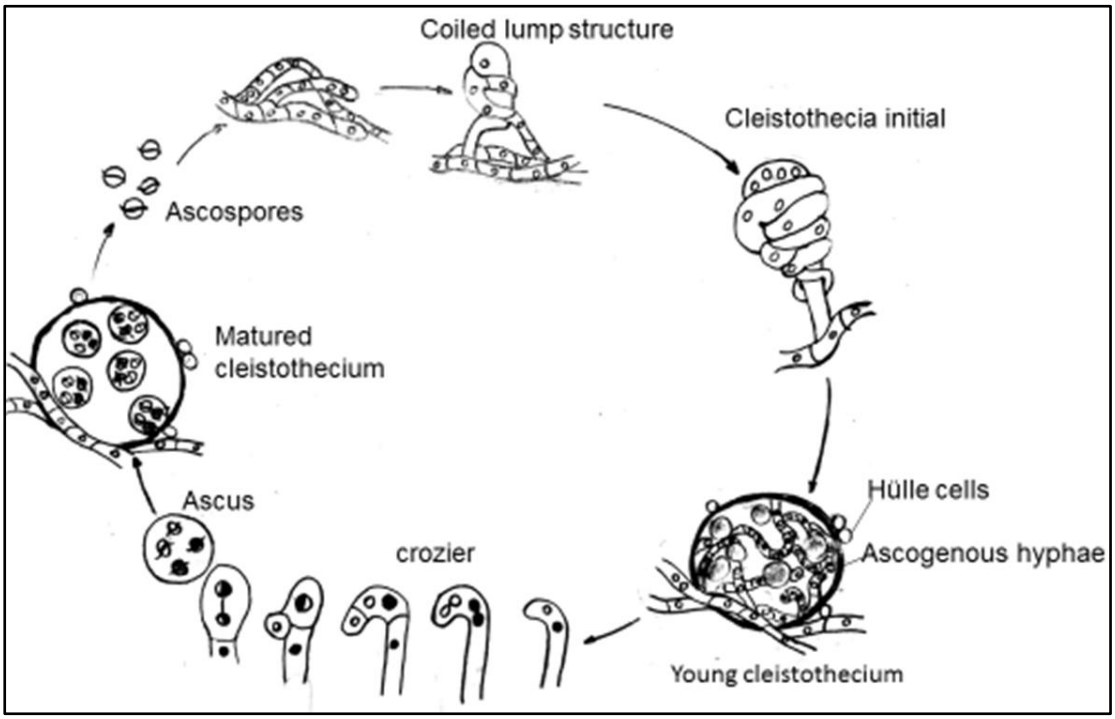

Figure 1-2 Representative example of sexual development in the Ascomycota, showing fruit body formation in *A. nidulans* [according to images from Sohn and Yoon. (2002)]. Two hyphae form a coiled lump structure as the first morphological stage in sexual development, and then develop into a cleistothecia initial. Young cleistothecia can be recognised when Hülle cells appear, and in their interior ascogenous hyphae form crozier tips from which an ascus develops. In the final stage, mature cleistothecium, including asci, are formed. Ascospores are released from the mature cleistothecia and germinate to form a new hyphal colony.

Fruit bodies in the Ascomycota can be classified into four groups based on the morphology of the ascomata (**Figure 1-3**): cleistothecia, which are completely closed spherical structures; perithecia which are more or less closed flask-like with a pore called ostiole; apothecia which are cup- or saucer-like fruit bodies; and pseudothecia which are locules within a surrounding stroma (Pöggeler et al, 2006; Lee et al, 2010).

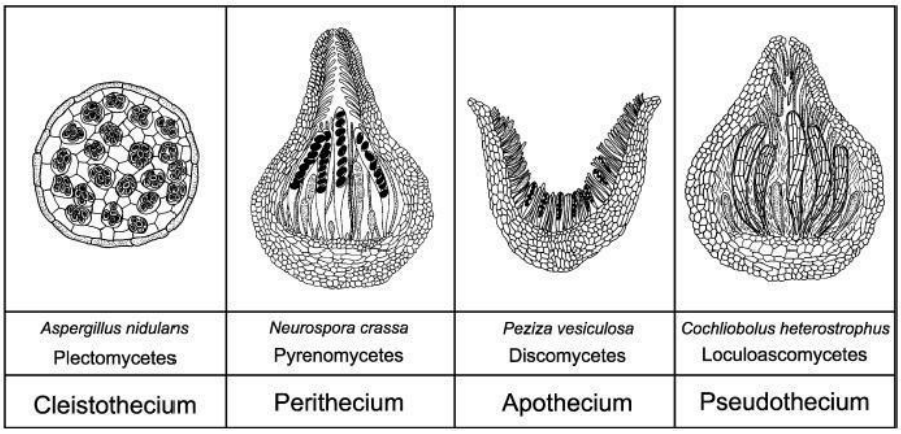

Figure 1-3 The four main types of fruit bodies (ascomata) formed by Ascomycota (Lee et al., 2010).

1.1.3 Homothallism and heterothallism

Ascomycota undergoing sexual reproduction can be classified as homothallic or heterothallic according to the requirement or not for mating partners and the presence of *MAT* loci (Wilson et al., 2015). Some species such as *A*. *fumigatus* and *N. crassa* require compatible mating partners, genetically termed as *MAT1-1* (*MATα*) and *MAT1-2* (*MAT-HMG*), for sexual reproduction to occur and are categorized as heterothallic (Paoletti et al., 2005; Lee et al., 2010). The nuclei of heterothallic species contain either *MAT1-1* or *MAT1-2* loci in their genome (Lee et al., 2010; Dyer et al., 2017). A peptide pheromone produced by one mating type partner initiates the sexual cycle and leads to eventual formation of fruit bodies (Dyer et al., 2017). By contrast, species such as *A. nidulans* are able to complete the sexual cycle without the need for an opposite mating partner, and are instead termed homothallic species, with the genome of these species containing both *MAT1-1* and *MAT1-2* loci (Lee et al., 2010; Dyer et al., 2017). However, most homothallic species are not restricted to self-fertility and retain the ability to outcross under certain conditions (Dyer et al., 2017). Comparing the two different modes of sexual reproduction, a heterothallic breeding system increases the chance of production of genetically varied offspring via gene recombination during the sexual cycle, whereas

homothallism can allow sexual development without the need for a mating partner, which can be advantageous in certain situations (e.g. it can lead to production of environmentally resistant ascospores) despite the fact that clonal offspring are normally produced (Dyer et al., 2017). It is generally thought that homothallism is evolved from heterothallism (Shiu et al. 2000; Dyer et al., 2017; Ojeda-Lopez et al., 2018).

1.1.4 Parasexual cycle and unisexual cycle

Another way in which gene flow can occur in fungal populations is via parasexual reproduction (Lee et al., 2010; Dyer et al., 2017). In this system, hyphae fuse to form a heterokaryon, and then a diploid nucleus can be formed via a rare nuclear fusion event. Mitotic recombination may then occur, accompanied by spontaneous loss of chromosomes (likely via chromosome non-disjunction) leading to restoration of the haploid state (Todd et al., 2007; Lee et al., 2010; Bennett et al., 2016; Dyer et al., 2017).

A further mode is unisexual reproduction, in which species reproduce sexually without a mating partner, and only one mating-type gene is involved, usually the α mating type, in initiating sexual development (Phadke et al., 2013; Bennett et al., 2016; Wilson et al., 2018). For example, *Huntiella moniliformis* is self-fertile but expresses only the *MAT1-2-1* gene, indicating that the species exhibits unisexual reproduction (Wilson et al., 2015). Unisexual reproduction is proposed as a parallel pathway for sexual reproduction which is independent of the need for compatible mating partners (Wilson et al., 2015).

1.2 Model Ascomycota organisms used in research into sexual development

Three main species (*A. nidulans, N. crassa* and *S. macrospora*) have been used in particular as models for sexual development in the Ascomycota, as will now be described.

1.2.1 *Aspergillus nidulans*

Aspergillus nidulans has been used as a model to study sexual morphogenesis in *Aspergillus* species. The species is homothallic (self-fertile) meaning that no other mating partner is required. During the sexual cycle, *A. nidulans* hyphae differentiate into ascogonial coils (female structures) and compatible hyphal partners (male structures) to allow hyphal fusion, which then generates dikaryotic cells and associated development of cleistothecial initials (Sohn and Yoon, 2002; Lee et al., 2010; Bennett et al., 2016). During cleistothecial morphogenesis, nonsporogenous hyphae generate a network of hyphae forming cleistothecial primordia that produce enzymes including diphenol oxidase and laccases, and nurse cells termed 'Hülle' cells which surround the cleistothecium and are thought to provide nutrients and laccases to the developing cleistothecia (Sohn and Yoon., 2002; Lee et al., 2010). Cleistothecia can then mature into smooth, hard, dark-purple spherical shells with a diameter of 125-200 μm (Sohn and Yoon., 2002; Lee et al., 2010; Bennett et al., 2016). The intercellular space of the cleistothecium is filled with thousands of asci which contains 8 haploid ascospores in each ascus, with ascospores generated through nuclei fusion, meiosis and mitosis and eventually forming binucleate cells when mature (Sohn and Yoon., 2002; Lee et al., 2010; Bennett et al., 2016).

1.2.2 *Sordaria macrospora*

Sordaria macrospora has been studied as a model organism for sexual development in filamentous fungal for reasons such as the presence of a short life cycle, it can be easily grown and sex induced under laboratory conditions, it is a homothallic species not requiring a mating partner, and the fact that it solely produces ascospores and not any asexual spore type (Teichert et al., 2020). During 7 days of incubation under optimal laboratory conditions, *S. macrospora* develops ascogonia, protoperithecia and mature perithecia (Pöggeler et al., 2006). The total absence of conidial production is beneficial as it allows research to be focused on fruit body development and minimizes the possible confounding presence of genes involved in the asexual sporulation, which is different from other species such as *A. nidulans* (Pöggeler et al, 2006). Although *S. macrospora* is self-fertile, the strain is able to outcross and allows studies of allele segregation via meiosis (Teichert et al., 2020).

1.2.3 *Neurospora crassa*

N. crassa is a heterothallic species in which fruit bodies (perithecia) are formed within a relatively short developmental time of 14 days (Roche et al., 2014). Under suitable conditions, an *N. crassa* strain of one mating type (A or **a**) forms a female element called protoperithecium, which is the pre-fruiting body, and this structure generates trichogynes to receive a vegetative male cell or conidium from a strain of the opposite mating-type (Metzenberg and Glass, 1990). Once fertilized, the dikaryotic ascogenous hyphae undergoes nuclear fusion, and meiotic events occur, while associated fruiti body (perithecium) development occurs, finally leading to the formation of mature ascospores (Metzenberg and Glass, 1990). The ascospores germinate after a heat shock

and form vegetative mycelium, which may then undergo the asexual or sexual cycles in due course (Metzenberg and Glass, 1990).

Heterokaryon incompatibility needs to be considered as an aspect of the *N. crassa* sexual cycle, as it may have a function in ascospore maturation and germination (Metzenberg and Glass, 1990; Roche. et al., 2014; Wang et al., 2014). Heterokaryon incompatibility (HI) is hypothesized as a self/nonself recognition system, and certain of the corresponding heterokaryon incompatibility (*het*) loci have been shown to have essential functions in perithecial formation during the hyphal and nuclear fusion stages in *N. crassa* (Paoletti and Saupe, 2009; Roche et al., 2014; Wang et al., 2014).

1.3 Genes involved in sexual development

Approximately, 78 genes have been shown to have a function in sexual development of *A. nidulans.* These include genes for environmental sensing which activate early stage of sexual reproduction and activate and upregulate other sexual related genes, genes for signalling the synchronous development of fruit body and meiotic tissues, certain metabolic genes necessary for sexual development and a variety of other genes. These have been reviewed by Dyer and O'Gorman (2012) and summarised as shown in **Figure 1-4**. These genes and associated environmental factors will now be described in further detail below.

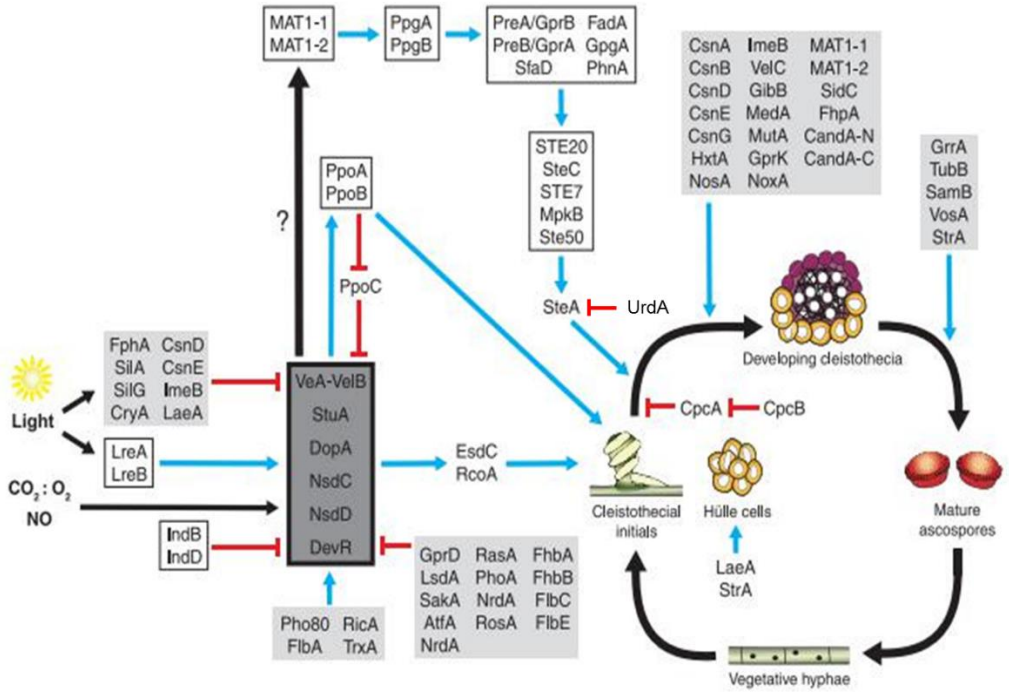

Figure 1-4 Genes regulating sexual development in the aspergilli. Proteins in same box are regarded to act at the same stage of development. Blue arrows indicate activation effects on genes. Red lines indicate repression effects on genes. Black lines indicate connections to different stage of development (Dyer and O'Gorman, 2012). Note that genes ar grouped according to their impact on specific stages of cleistothecial development e.g. genes triggering development of cleistothecial initials versus genes involved with later stages of development such as ascospore formation. Also note that an updated version of this figure will be provided in the final concluding discussion (**Figure 6.1**).

1.3.1 Environmental and endogenous factors involved with sexual development

A variety of external environmental and endogenous factors have been shown to influence sexual development in *Aspergillus* species as will now be described.

1.3.1.1 Light

Sexual morphogenesis of *Aspergillus* species is photo dependent. To induce the sexual cycle of *A. nidulans*, strains must ideally be cultivated in the

dark, with the key regulator being the *veA* 'velvet' gene. VeA is an essential factor in activation of sexual development and inhibition of asexual development in the darkness (Bayram et al., 2008). The VeA protein contains a nuclear localization signal (NLS) sequences at the N-terminus, and at its C-terminus includes a potential PEST domain (so named as the domain contains a high proportion of proline, glutamic acid, serine and threonine residues) which may act as a signal for protein degradation (Calvo et al., 2008; Park et al., 2014; Bayram and Braus., 2021). Deletion of *veA* resulted in a failure in fruit body formation, while overexpression led to production of Hülle cells and cleistothecia in liquid culture, conditions under which only hyphal growth normally occurs (Calvo et al., 2008). Further studies identified that VeA interacts with other proteins such as velvet VelB and KapA to activate fruit body formation (Bayram et al*.,* 2008; Park et al., 2012). VeA and VelB form the so-called 'velvet complex' in the cytoplasm, and in the dark the complex is transported into nuclei via the interaction between VeA and an importin KapA, and sexual development is thus initiated (Bayram et al*.*, 2008). Besides triggering cleistothecial formation, *veA* is also involved in secondary metabolism as discussed later (**Section 1.4**). Another velvet protein is VelC, which contains a putative PEST domain at C-terminus, and which also activates sexual development and may interact with *vosA* for a promotion of VeA-VelB complex formation (Park et al*.,* 2014). It is noted that most laboratory strains of *A. nidulans* contain a truncated NLS domain in VeA, with the arising *veA1* mutant strains [first identified by Käfer (1965)] having higher levels of asexual conidiation in the dark than the wild type and and are consequently less effective in sexual development (Stinnett et al., 2007; Han et al., 2010).

Sexual development of *A. nidulans* can be repressed by red light (680 nm) and blue light (450 nm) (Blumenstein et al, 2005). The red-light sensor is *fphA* (fungal phytochorome), and an *fphA* null strain produced cleistothecia when it

was incubated in red light, while the wild-type formed conidia (Blumenstein et al, 2005; Purschwitz *et al,* 2009). The blue-light sensors are *ireA and ireB* (light response), and these genes act as activators of fruit body formation, given that deletion of either *ireA or ireB* led to a decrease in cleistothecial numbers when the strains were cultivated in dark (Purschwitz *et al,* 2008).

1.3.1.2 Atmosphere

The composition of the gaseous atmosphere can influence fruit body formation in the aspergilli. To induce sexual cycles under laboratory conditions of aspergilli such as *A. nidulans* and *A. fumigatus*, it is recommended to seal plates for accumulation of carbon dioxide (CO_2) as this blocks the electron transport system and leads to a lack of oxygen stress (Han et al., 2003; Ashour 2014; Ashton and Dyer, 2019). In *S. macrospora*, the presence of CO_2 leads to an accumulation of bicarbonate in the cytoplasm, which can influence various essential physiological processes (Elleuche and Pöggeler, 2009). The gene *cas2,* encoding a carbonic anhydrase, is essential for ascospore germination, with the growth defect in *Δcas2* strains being recovered by growth under a higher CO_2 concentration (Elleuche and Pöggeler., 2009).

Nitric oxide (NO) is a signaling compound that triggers nitrosative stress in eukaryotes. To reduce the stress, organisms synthesize flavohemoglobins (FHbs) to convent NO into nontoxic nitrate ions in the presence of oxygen (O_2) (Baidya et al., 2011; Macro et al., 2016). Supplementation of NO in *A. nidulans* promotes cleistothecial formation, consistent with the finding that deletion of *fhbA* resulted in an accumulation of NO and subsequent increased formation of Hülle cells and cleistothecia in *A. nidulans* (Baidya *et al.,* 2011). Besides regulating sexual development, *fhbA* also affects mycotoxin biosynthesis in *A. nidulans,* Δ*fhbA* strains producing less sterigmatocysin (ST) than wild types (Baidya et al*.,* 2011). Other sexual development activators *nsdD* and *steA*

(transcription factors) show increased expressions under elevated NO level that thereby promote fruit body formation (Baidya et al., 2011).

1.3.1.3 Nutrients

Under labotorary conditions, the composition of the growth media may trigger sexual and/or asexual development. For example, the carbon/nitrogen ratio, phosphorus concentration, salt concentration, and presence or absence of manganese and pH all influence levels of cleistothecial formation in the aspergilli (Dyer and O'Gorman, 2011). Amino acid starvation represses cleistothecia development at an early stage, and Hoffmann et al. (2000) identified a c-Jun like transcription factor CpcA and RACK1 like protein CpcB that respond to amino acids in the environment. In the cross-pathway-control (CPC) of amino acid biosynthesis and detection during sexual development, *cpcA* represses fruit body formation under nitrogen limitation, whereas if sufficient amino acids are present, *cpcB* permits cleistothecial formation (Hoffmann et al*.,* 2000). A low phosphorus concentration inhibits sexual development in wild-type strains, while the mutation of gene *phoA*, a cyclin-dependent kinase, allowed fruit body formation under the same conditions, suggesting that *phoA* responds to phosphorus limitation and represses the sexual cycle (Bussink and Osmani, 1998). Another cyclin-like protein encoded gene *An-pho80* positively regulated sexual development when the phosphorus concentration was low (Wu et al., 2004). Salt is another nutrient factor influencing morphological differentiation in *Aspergillus.* For example, the gene *lsdA* senses the concentration of salts and inhibits sexual development when salt concentration is high (Lee et al*.,* 2001).

1.3.1.4 Reactive oxygen species

Reactive oxygen species (ROS) are by-products of the respiratory chain or other enzymatic reactions that taking place in mitochondria, peroxisomes and chloroplasts involving oxygen, and suitable concentrations of ROS act as signaling molecules in cellular communication (Marschall and Tudzynski, 2016). The ROS are formed by NADPH oxidases (Nox) in the endoplasmic reticulum (ER) and mitochondria and affect fungal cell differentiation (Marschall and Tudzynski, 2016). In *A. nidulans*, the gene *noxA* encodes a NADPH oxidase that produces H_2O_2 and other ROS and promotes the maturation of cleistothecia and ascospores, because deletion of *noxA* represses fruit body formation at the stage of cleistothecia initials and blocks ascospores completely (Lara-Ortiz et al., 2003). Similarly, in *S. macrospora* the NOX complex NOX1 regulates oxidative stress response, hyphal fusion, perithecia maturation, and NOX2 controls ascospore germination (Dirschnabel et al., 2014).

1.3.1.5 Oxylipin pheromone

Champe et al. (1987) extracted a family of species-specific hydroxylated linoleic acid derivates from *A. nidulans* that inhibited conidiation and induced cleistothecial formation, with the compounds being termed precocious sexual inducers (psi; Tsitsigiannis et al., 2004). In *A. nidulans*, the gene *ppoA* (psi producing oxygenase) is located in lipid bodies present in Hülle cells and metulae and is involved in psiB production, which then upregulates sexual development (Tsitsigiannis et al., 2004). Two other related *ppo* genes are *ppoB and ppoC*. The deletion of *ppoB* reduces the synthesis of psiBβ molecules and ascospore production, whereas the deletion of *ppoC* increases the production of psiB and subsequently promotes sexual sporulation (Tsitsigiannis et al., 2004). Overall, the triple deletion of *ppo* genes led to an increase in fruit body

formation in *A. nidulans*, which suggests *ppoB* is a suppressor, and the genes *ppoA and ppoC* are antagonistic activators of cleistothecial formation (Tsitsigiannis et al., 2004; Tsitsigiannis et al., 2005).

1.3.2 Regulatory signal transduction cascades, cellular complexes and transcription factors involved in sexual development

A variety of regulatory factors including signal transduction cascades, cellular complexes and various transcription factors have been shown to influence sexual development in *Aspergillus* species as will now be described.

1.3.2.1 Mating Processes: mating-type genes

Mating-type (*MAT*) genes are essential for both heterothallic and homothallic sexual cycles, as they act as master regulators of sexual reproduction (Dyer et al., 2016). *MAT* genes encode proteins that include DNA-binding motifs, which means they can function as transcriptional activators during sexual reproduction (Shui and Glass, 2000; Paoletti et al., 2007). In heterothallic species the *MAT* locus may contain from one to three genes, with the core genes being *MAT1-1-1* (which encodes a protein with an α-domain region containing a DNA binding motif) and *MAT1-2-1* (which encodes a protein with an HMG-domain region containing a DNA binding motif) while in homothallic species the opposite mating-type genes are found either fused together, linked in the same region, or at separate loci in the same genome (Shui and Glass, 2000; Paoletti et al., 2007; Dyer et al., 2016). *MAT* genes normally regulate pheromone signalling in heterothallic species in a mating-type dependent manner, with expression of α- and a-factor-like pheromone precursors and receptors being mating-type dependent (see **Section 1.3.3.2.** below) (Paoletti et al., 2007; Dyer et al., 2016). MAT genes are as well suggested to have a role in nuclear identity during fruit body development, and

be involved in differentiation of Hülle cells (Paoletti et al., 2007). Intriguingly, it has more recently been shown that *MAT* genes might mediate a broader set of cellular processes including asexual sporulation and secondary metabolite production (Dyer and Kück, 2017).

1.3.2.2 Pheromone and G-protein signaling

The G protein signaling is an evolutionarily conserved signal pathway, which comprises three parts: (1) a seven-transmembrane-spanning G-protein-coupled receptor (GPCR), (2) a G protein heterotrimer and (3) an effector. In fungi, the effectors are either cAMP-dependent protein kinases, or mitogen-activated protein kinase (MAPK) cascade (Seo et al., 2004). During fungal sexual reproduction a specific GPCR senses pheromones made by a mating partner and the subsequent G protein signaling regulates sexual development. In the case of *A. nidulans,* an alpha-factor pheromone precursor is produced by the gene *ppgA* and is edited to form a final PpgA peptide mainly under the regulation of *MAT1-1-1* (Dyer et al., 2003; Paoletti et al., 2008; Kilx et al., 2010). Two related pheromone receptor GPCRs in *A. nidulans* are GprA and GprB whose expression is partly controlled by *MAT1-1* and *MAT1-2*, respectively (Paoletti et al., 2007). RNA expression analysis showed that *gprA and gprB* transcripts accumulated after 48 hours of induction of the sexual cycle and were degraded after 96 hours (Seo et al., 2004). Deletions of *gprA* or *gprB* reduced the cleistothecial number and size and the number of ascospores, which also showed reduced viability (Seo et al., 2004). Furthermore, the double mutation blocked cleistothecia formation entirely. Another GPCR, GprD, is a repressor of sexual development and is thought to function upstream of GprA and GprB, as deletion resulted in cleistothecia formation even under unfavorable growth conditions (Han et al., 2004). In *S. macrospora*, the homologous pheromone-percursor/receptor pairs are PPG1/PRE2 and PPG2/PRE1 that have also been

shown to initiate sexual development (Mayrhofer et al., 2006).

In the signaling pathway, the heterotrimeric G-protein exchanges the GDP-bound state to GTP-bound state, which dissociates the heterotrimeric complex into GTP-bound Gα- and Gβγ-subunits, and transmits a signal to the next stage. G-proteins in *A. nidulans* include *fadA*, encoding the Gα-subunit, *sfaD*, encoding the Gβ-subunit, and *gpgA*, encoding the Gγ-subunit (Rosén et al*.,* 1999; Yu et al*.,* 1999; Seo et al., 2005). The FadA-SfaD-GpgA G-protein affects vegetative growth, asexual sporulation, and fruit bodies formation (Rosén et al., 1999; Yu et al., 1999; Seo et al., 2005). In sexual development, the deletion of each gene blocks cleistothecial formation, and a regulator FlbA is involved as the *flbA* mutant strain showed a fluffy-autolytic phenotype which does not support normal sporulation of *A. nidulans* (Yu et al., 1999; Rosén et al., 1999; Han et al., 2008). The regulator FlbA inactives FadA and SfaD, which promotes the expression of EsdC which is activator of sexual development (Han et al., 2008). Another regulator of the Gβγ-subunit is PhnA which is a chaperone, and the deletion abolished fruit body formation (Seo and Yu, 2006). In other Ascomycete specie such as *N. crassa,* G-proteins subunits GNA-1 (Gα), GNB-1 (Gβ) and GNG-1 (Gγ) are also required for female fertility, protoperithecia development and ascospore maturation (Kays et al., 2000; Yang et al., 2002; Kays and Brolovich., 2004; Krystofava and Borkovich., 2005;).

1.3.2.3 Mitogen-Activated Protein Kinase (MAPK) pathway

The Mitogen-activated protein kinase (MAPK) pathway consists of three protein kinases that form a cascade in eukaryotic organisms for signal transduction in cells. In filamentous fungi, there is a dedicated signal pathway which is involved with pheromone response during fungal sexual development. In the case of *A. nidulans* this MAPK module includes the proteins MAP3K (Anste11), MAP2K (Ste7), MAPK (MkpB) and Ste50, which together control

sexual development and secondary metabolism (Bayram et al., 2012). AnSte50 (SteD) is thought to act as an adaptor in the module because deletion abolishes interaction between AnSte11 (SteC) and Ste7 (MkkB), and leads to reduced interaction between Ste7 and MkpB. Ste50 also enhances association of the MAPK module with the plasma membrane (Bayram et al., 2012). Bayram et al. (2012) investigated the localization of the cascade, and their research suggested that the MAPK module AnSte11-Ste50-Ste7-MpkB travels from the outer border of the fungal cell, through the cytoplasm, and to the nuclear envelope to deliver MpkB into the nucleus. Subsequently, MpkB actives a transcription factor SteA to trigger the sexual cycle. MpkB also appears to interact with VeA in the nucleus to influence the production of sterigmatocystin (Bayram et al., 2011). More recently, Frawley et al. (2018) identified a scaffold protein HamE that is a regulator of this MAPK module, with *hamE* mutant strains losing the potential for sexual development. The homologous pheromone signaling module SteC-MkkB-MpkB-SteD-HamE was also assessed in the heterothallic *A. fumigatus*, and was found to regulate asexual development, cell oxidative stress responses, and secondary metabolite production, although any function in fruit bodiy formation remains to be investigated (Frawley et al., 2020).

The MAPK pathway seems to have a ubiquitous role in sexual development of filamentous fungi. For example, in *S. macrospora* the MAPK pathway is encoded by genes *mik1* (MAPKKK), *mek1* (MAPKK) and *mak1* (MAPK) that are essential for perithecia formation, and *pro40* facilitates MAK1 phosphorylation as a scaffold protein (Teichert et al., 2014; Engh et al., 2007). In *N. crassa* the MAPKKK gene *nrc-1* and MAPK gene *mak-2* are responsible for activating hyphal fusion and female fertility (Pandey et al., 2004).

1.3.2.4 Striatin-interacting phosphatase and kinases (STRIPAK) complex

The straitin-interacting phosphatases and kinases (STRIPAK) complex is an evolutionary conserved feature of eukaryotes that mediates a variety of cellular signalling processes. The STRIPAK complex is composed of a number of protein subunits. Detailed investigations identified the serine/threonine phosphatases PP2A and PP2Ac, which act as regulatory and catalytic units, and interact with each other to form a dimer, and this dimeric core offers a platform for striatin to bind with the striatin-interacting phosphatase and kinases (**Figure 1-5**; Goudreault et al., 2008; Kück et al., 2016). Further, the trimeric complex interacts with monopolar spindle-one-binder family protein (MOB3, phocein), which has a role in vesicular trafficking in cells, with the resultant complex being named 'STRIPAK' by Goudreault et al. (2009). The STRIPAK complex in mammalian cells was also found to interact with the cerebral cavernous malformation 3 protein (CCM3) and germinal centre kinase subgroup III (GCKIII kinase), sarcolemmal membrane-associated protein (SLMAP) and/or other associating proteins, and fungal STRIPAK complex interacts with the homologs of GCKIII kinase and SLAMP (Goudreault et al., 2009; Kück et al., 2016; Shi et al., 2016). The STRIPAK complex mediates various signal pathways in mammalian cells. For example, when interacting with GCKIII kinase via the binding with CCM3, the complex regulates the activity of GCKIII that is a key kinase in the Hippo pathway, which regulates cell size and homeostasis, and CCM3 enhances kinase activities of the MAPK pathway to promote cellular processes (Shi et al., 2016). CCM3 and GCKIII, STRIP and MOB proteins have a role in mediating MAPK signalling in the STRIPAK complex, as well (Shi et al., 2016). The striatin unit and complex also participate in nongenomic NR pathway and cytoskeleton remodelling, which responds to steroid and thyroid hormones in the external environment, respectively (Shi et al., 2016).

In fungi, the STRIPAK complex has been shown to control septation, sexual development, hyphal fusion and growth. In the fission yeast *Schizosaccharomyces pombe,* the STRIPAK complex is involved in the septation initiation network (SIN) that regulates cytokinesis, and was named the SIN-inhibitory PP2A complex (SIP; Singh et al., 2011). Regarding filamentous fungi, the STRIPAK complex was first studied in *S. macrospora*. The core subunit PRO45, which is the membrane anchoring unit, was found to bind with other two STRIPAK subunits PRO11 and SmMOB3 which are phosphatase regulatory subunit and kinase activators, respectively (**Figure 1-5**). PRO45 is essential for cell-to-cell fusion and sexual propagation in *S. macrospora* as the pro45 mutant strains failed to fuse hyphae and were sterile (Nordzieke et al., 2015). The homolog of PRO45 in *N. crassa* is HAM-4 which effects morphological development, with deletion of *ham-4* delaying protoperithecium formation and leading to aberrant meiosis and abnormally shaped ascospores (Simonin et al., 2010). At the onset of the present thesis, the only STRIPAK subunit identified from *A. nidulans* was StrA that was found by Wang et al. (2010) to be a homolog of pro11 and which was shown to regulate sexual development in *A. nidulans*. Deletion of *strA* reduced the number and size of cleistothecia and number of ascospores whilst overexpression promoted cleistothecial formation (Wang et al., 2010). StrA localized to the endoplasmic reticulum and nuclear envelope, which suggested a role in the $Ca^{2+/}$calmodulin signaling pathway (Wang et al., 2010).

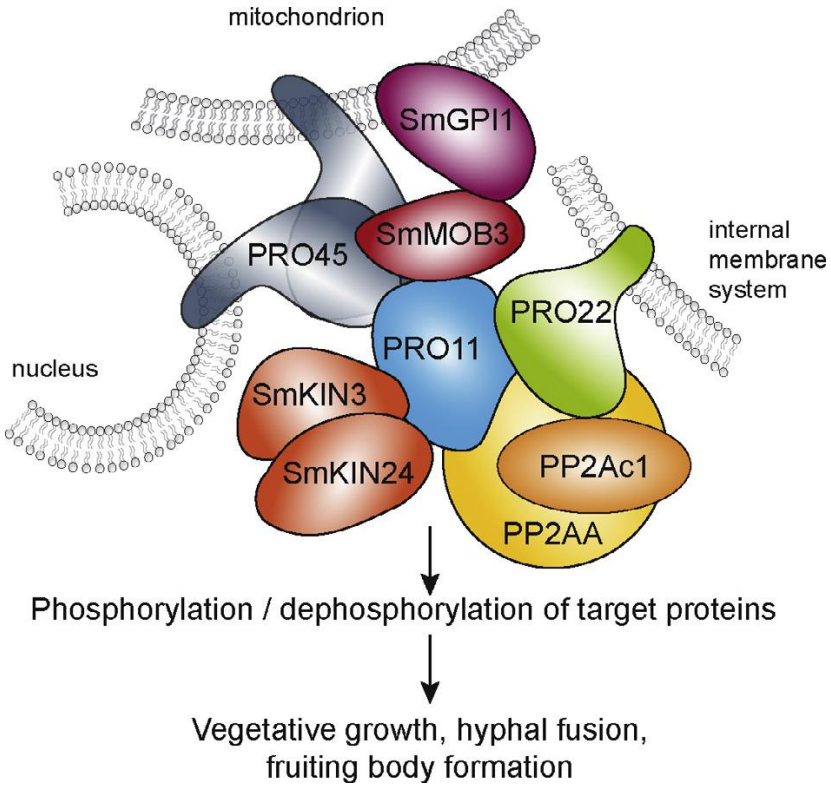

Figure 1-5 Model of the STRIPAK complex in *Sordaria macrospora* (Kück et al., 2016). PRO11 (straitin) acts as platform to interact with the PP2Ac1-PP2AA-PRO22 (STRIP) heterotrimer, PRO45 (SLAMP), SmMOB3 and SmKIN3-SmKIN24 units, and the overall complex is associated with regulatory cellular processes.

1.3.3 Transcription factors

Transcription factors regulate the expression of target genes and are classified by their DNA-binding domains. These include zinc finger domains, homeobox domains, basic helix-loop-helix domains, mating-type domains, and Myb-like domain and so on (Shelest, 2008). A variety of such transcription factors have been identified from *A. nidulans* and have been shown to regulate various stages of sexual development. During early stages of mating, pheromones synthesized under the control of *MAT* genes are detected by cognate GPCRs, which transduce a signal to the pheromone cascade MAPK pathway (Seo et al., 2004; Bayram et al., 2011; Dyer and O'Gorman, 2012). The ultimate effector in this process is *steA,* a transcription factor containing a Zn^{2+} finger domain at the C-terminal and homeodomain at the N-terminal

(Vallim et al., 2000). Vallim et al. (2000) suggested that both domains have the potential to bind DNA, while one of them may function in protein-protein interaction. SteA regulates fruit body development at an early stage, as gene mutation was found to block the formation of cleistothecial initials (Vallim et al., 2000).

Another early effector of G-protein signalling is EsdC (early sexual development), whose expression is repressed by the heterotrimeric FadA-SfaD-GpgA complex (Han et al., 2008). When *veA* expression is induced, and FlbA inactives the FadA-SfaD-GpgA complex, *esdC* is expressed at a high level during the early stages of sexual development (Han et al., 2008). The *nsdC* has a fungal specific C_2H_2 zinc finger motif, featuring with highly conserved DNA-binding domain including six cysteine residues and two zinc atoms to form monomer, homo-or hetero-dimers in DNA interaction in the fungal kingdom (Shelest 2008; Kim et al., 2009).

A further gene relating to G-protein signallling is *nsdD* (never sexual development), which encodes a protein with a zinc-finger domain and is a GATA-type transcription factor required for cleistothecia and Hülle cell differentiation. The expression of *nsdD* is dependent on the G-protein regulator FlbA which is a key element in balancing sexual and asexual development (Han et al., 2001; Han et al., 2008). NsdD accumulates during vegetative and early-stage sexual development, but degrades during conidiation, and its overexpression promote sexual development under conditions normally inhibitory for sex (Han et al., 2001).

In a parallel pathway to *nsdD*, a further zinc-finger protein NosA (number of sexual spores) responds to carbon starvation in *A. nidulans* and promotes sexual development (Vienken and Fischer., 2006). Deletion of *nosA* caused abnormal cleistothecia development in terms of size and number, and also reduced ascospore number. NosA was found to regulate the expression of

CpeA (a catalase-peroxidase) and HxtA (a high-affinity hexose transporter) which are involved with response to nutrient limitation (Vienken and Fischer., 2006). Expression of *nosA* can be repressed by a further zinc-finger protein RosA, which is a repressor for sexual development and is induced under carbon limitation (Vienken et al., 2005; Vienken and Fischer., 2006). Mutation of *rosA* enabled Hülle cell differentiation under submerged growth conditions (Vienken et al., 2005).

Another conserved transcription factor domain in fungi is the bHLH-like structure, with example genes being *stuA* and *devR* (Shelest 2008; Dyer et al., 2011). The gene *stuA* has multiple roles in morphological development of *A. nidulans* including acting as an activator of sexual development (Wu and Miller, 1997). Another bHLH-like transcription factor is *devR*, which induces sexual cycle under conditions of nitrogen limitation (Tüncher et al., 2004).

The COP9 (constitutive photomorphogenesis complex 9) signalosome is comprised of eight subunits, and functions as a metalloprotease to degrade eukaryotic ubiquitin-dependent proteins (Wei and Deng, 2003; Chamovitz, 2009). The subunits are identified by the presence of either a PCI or MPN domain. The former is rich in α-helixes which function to maintain the integrity of the COP9 signalosome (CSN) subunits, while the later is conserved in the CSN5 unit for de-ubiquitination activity (Wei and Deng, 2003; Chamovitz, 2009). In fungi, the CSN complex is critical for sexual development, and in *A. nidulans*, eight subunits have so far been identified (Busch et al., 2003; 2007). The first CSN subunit identified was CsnD that is involved in light signaling, with mutation resulting in defects in fruit body formation (Busch et al., 2003). Later, Busch et al. (2007) identified other CSN subunits including CsnA, CsnB, CsnC, CsnE,CsnF, CsnG and CsnH. Among those subunits, CsnA CsnB, CsnD and CsnG form a stable core as the basis of the complex via PCI domains, and CsnA and CsnD were essential for the assembly of CsnE, with gene mutation

causing a block in fruit body formation (Busch et al., 2007).

1.4 Genes relating to sexual development and secondary metabolism

Genes that regulate sexual development may also be involved in primary and secondary metabolism. For example, sexual development in *A. nidulans* is initiated by the VeA-VelB complex which is imported into the nucleus under darkness. Here it appears that the complex binds with LaeA to promote sterigmatocystin synthesis (Bayram et al., 2008). VosA promotes trehalose biosynthesis which protects ascospores from thermal and oxidative stresses (Kim et al., 2020). In *A. fumigatus,* the over-expression of mating-type genes increased the production of the mycotoxins fumagillin and pseurotin A, and additional upregulation and downregulation of secondary metabolism genes was detected (Yu et al., 2018). In *A. flavus*, the aflatoxin B1 accumulated at significantly higher levels in fertile rather than un-mated strains, and the expression of *MAT1*, *preA* and *preB* were upregulated in highly fertile mated sclerotia (Lius et al., 2022).

1.5 Dynamics of sexual and asexual development

Genes relating to asexual development can be classified into two groups according to their functions in morphological development. Regulatory genes, including *veA*, *fphA, fluG,* have been termed ‘upstream development activators’ (UDAs), which inhibit vegetative growth and initiate conidiophore development, while genes, including *brlA, abaA, wetA,* in the central developmental pathway (CDP) control the development of conidiophore phialide and the production of conidia (Etxebeste et al., 2010). For conidiophore development, in association with FlbE, FlbB is able to form a nuclear complex with FlbD, which activates transcription factors in the CDP such as BrlA, which leads to the subsequent expression of *abaA*, which then activates *wetA* expression to promote conidia

formation (Etxebester et al., 2010). The transcriptional regulator UrdA is an activator of asexual development and a repressor of sexual development because it controls the expression of *brlA, abaA* and *wetA* and inhibits sexual development genes such as *veA, steA* and *nsdD* (Pandit et al., 2018). The gene *stuA* has a dual role in both sexual and asexual development, with deletion causing defective conidiophore formation and reducing the number of cleistothecia initials (Wu and Miller., 1997). Mutation of *vosA* results in reduced conidial spore viability as the spores may lack of cytoplasm and organelles, and the conidia are much less resistant to temperature and oxidative stress (Ni and Yu., 2007).

1.6 Aims of the present study

The overall aim of this PhD project was to gain a better understanding of the genetic controls of sexual development in *Asergillus* species. This is both of fundamental importance, with sexual development being a key biological process, but also of practical importance as it was hoped that insights gained could be used to manipulate the sexual cycles of important fungal species (both beneficial and pathogenic species) for reasons such as strain improvement and for use as a tool for genetic analysis (Dyer and Ashton 2016), as well as elucidating possible reasons for asexuality in economically important fungi (Dyer and Kück, 2017). Linking in with this, the key study aims were as follows.

(1) To further develop our understanding of the genetic control of sexual development in *A. nidulans.*

Over 70 genes have already been identified as being required for normal sexual development in *A. nidulans* (Dyer and O'Gorman, 2012). However, in the past decades a growing number of additional genes have been identified as being essential for sexual development in other ascomycete fungi such as *Sordaria* and *Podospora* species, with multiple roles proposed in cellular

processes including signal transduction, transcriptional control, stress response and heterokaryon incompatibility. However, any potential role in sexual reproduction in the aspergilli has not been shown for the majority of such genes. In order to maintain *A. nidulans* as a comprehensive model for sexual development in the Ascomycotina, genetic studies were therefore undertaken to determine any role that these 'additional' genes might have in the control of sexual development in *A. nidulans* to investigate whether the genes were indeed universal ascomycete sex genes. Target genes included members of the striatin-interacting phosphatases and kinases (STRIPAK) complex, transcription factors, heterokaryon incompatibility determinants, and signal pathway units. As an initial part of this work experimental work was to be undertaken to optimise conditions under which the sexual cycle of *A. nidulans* can be induced *in vitro* to facilitate later screening of the fertility of transformant strains.

(2) To investigate the role of high mobility group (HMG) genes in controlling sexual development in the heterothallic species *A. fumigatus*

High mobility group (HMG) proteins have been shown to regulate a wide range of developmental processes in eukaryotic organisms and comprise a large group of sub-classes of protein families (Idnurm et al., 2008). In the case of fungi, HMG genes are best known for their role as ancestral genes with an essential role in the determination of sexual identity, namely the MATA_HMG and MATα_HMG families (Martin et al., 2010). However, recent genomic and experimental investigations in *A. nidulans* and *P. anserina* have revealed the presence of a series of additional HMG genes in the genome, which have been shown to form a network regulating sexual reproduction in these homothallic and pseudohomothallic species, respectively. It was therefore aimed to determine if a similar network of HMG genes was present in *A. fumigatus*, and to assess whether any difference in gene function was present in this

heterothallic species. This was to involve a combination of bioinformatic analysis followed by gene deletion experimental work, including the construction of highly fertile *ΔkuB MAT1-1* and *MAT1-2* mating strains.

(3) To investigate any dual role of high mobility group (HMG) genes in secondary metabolite biosynthesis of *A. fumigatus*

Genes related to sexual development have previously been shown to affect the production of secondary metabolites in fungi. For example, the VeA-VelB complex induces cleistothecial formation in *A. nidulans*, and at the same time promotes production of the mycotoxin sterigmytocystin (Bayram et al., 2008). However, at the start of the present studies it was unknown whether HMG family genes, including mating-type (*MAT*) genes, had any role in the regulation of secondary metabolism in fungi. Therefore, work was undertaken to evaluate any link between HMG genes and secondary metabolite production in *A. fumigatus*, focusing on mycotoxins such as fumagillin and gliotoxin which are thought to have a role in virulence and are thus of biomedical interest. Studies were to involve screening for suitable media for mycotoxin production and then testing for mycotoxin production via HPLC in both wild type and *ΔHMG* knock-out strains.

Chapter 2 General Materials and Methods

The following chapter describes general materials and methods applicable to experimental work in more than one chapter of the PhD thesis. Where experimental materials and methods are only relevant to a single chapter, then they will be described in that chapter.

2.1 Materials

Various growth media were used for cultivation of fungal stocks as follows. All chemical reagents were supplied by Sigma, UK (at analytical grade if available) unless specified otherwise.

2.1.1 Media

***Aspergillus* Complete Medium (ACM)**

ACM was prepared by dissolving the following components in 900 mL distilled water (DW): 10 g D-glucose powder (Fisher Scientific, UK), 1 g yeast extract powder (Oxoid, UK), 2 g peptone (Bacto, France), 1 g casamino acids (Bacto, USA), 0.075 g adenine, 10 mL *Aspergillus* vitamin solution, and 20 mL *Aspergillus* salt solution according to Paotetti et al. (2005). 20 g agar (Sigma, UK) when necessary, and the pH was adjusted to 6.5 with the final volume made up to 1 L by addition of distilled water. The medium was autoclaved at 117℃ for 30 min.

***Aspergillus* vitamin solution**

Aspergillus vitamin solution stock was prepared by dissolving the following components: 400 mg p-aminobenzoic acid (Duchefa Biochmie, The Netherland), 50mg thiamine HCl (Sigma, UK), 2 mg d-biotin, 100 mg nicotinic acid, 250 mg pyridoxine hydrochloride, 1.4 g choline chloride and 100 mg riboflavin in 1 L distilled water.

***Aspergillus* salt solution**

Aspergillus salt solution stock was prepared by dissolving the following components: 26 g KCl, 26 g $MgSO_4 \cdot 7H_2O$, 76 g KH_2PO_4 in a suitable volume

of distilled water. 10 mL *Aspergillus* trace elements (see below) were then added with, and the solution was made up to a final volume of 1 L with distilled water.

***Aspergillus* trace elements solution**

Aspergillus trace element solution was prepared by dissolving the following components: 40 mg $Na_2B_4O_7 \cdot 7H_2O$, 800 mg $CuSO_4 \cdot 5H_2O$, 800 mg $FePO_4 \cdot H_2O$, 800 mg $MnSO_4 \cdot 4H_2O$, 800 mg $NaMoO_4 \cdot 2H_2O$, and 8 g $ZnSO_4 \bullet 7H_2O$ in 1 L distilled water.

***Aspergillus* Minimal Medium (AMM)**

AMM was prepared by dissolving the following components in 900 mL distilled water: 20 g D-glucose, 6 g $NaNO_3$, 0.52 g KCl, 0.52 $MgSO_4 \bullet 7H_2O$, 1.52 g KH_2PO_4, 2 g peptone, 1 crystal $ZnSO_4 \bullet 7H_2O$, 1 crystal $FeSO_4 \bullet 7H_2O$ (Acros, USA) and 20 g agar when necessary. The pH was adjusted to 6.5, and the final volume was made up to 1 L with distilled water. The medium was autoclaved at 117℃ for 30 min.

Glucose Minimal Medium (GMM)

GMM was prepared by dissolving the following components in 900 mL distilled water : 10 g D-glucose, 6 g $NaNO_3$, 0.52 g KCl, 0.52 $MgSO_4 \bullet 7H_2O$, 1.52 g KH_2PO_4,1 mL Hutner's trace element solution, and 20 g agar when necessary. The pH was adjusted to 6.5, and the final volume was made up to 1 L with distilled water. The medium was autoclaved at 117℃ for 30 min.

Glucose Glutamine 10 (GG10)

GG10 (Geib and Brock., 2017) was prepared by dissolving the following components in 900 mL distilled water: 9 g D-glucose, 1.46 g glutamine (Acros, USA), 50 mL 20X Salt stock (-N), 1 mL Hutner's trace element solution, 218.6 g sorbitol (as an osmotic stabilizer for transformations), and 20 g agar when necessary. The pH was adjusted to 6.5, and the solution was made up to a final volume of 1 L with distilled water. The medium was autoclaved at 117℃ for 30 min.

20X Salt Stock (-N)

20X Salt Stock (-N) was prepared by dissolving the following components: 10.4 g KCl, 10.4 g $MgSO_4 \cdot 7H_2O$, 30.4 g KH_2PO_4 in 1 L of distilled water. The solution was autoclaved at 121 ℃ for 15 mins.

Hutner's Trace Elements solution

Hutner's trace elements (Hunter et al., 1950) solution was prepared by dissolving the following components: 10 g EDTA, 4.4 g $ZnSO_4 \cdot 7H_2O$, 2.2 g $MnCl_2 \cdot 4H_2O$, 1 g $FeSO_4 \cdot 7H_2O$, 1 g $CoCl_2 \cdot 6H_2O$ (Fisher, UK), 0.32 g $CuSO_4 \cdot 5H_2O$, 0.22 g $(NH_4)Mo_7O_{24} \cdot 4H_2O$ in 100 mL distilled water.

Sorbitol Minimal Agar (SMA)

SMA was prepared by dissolving the following components: 10 g D-glucose, 40 mL 25X MN Salt, 1 mL 1000X trace element solution 218.7 g D-sorbitol, 15 g agar in 1 L distilled water.The medium was adjusted to pH 6.5 and autoclaved at 117 °C for 30 mins. 20mL of a 50X $MgSO_4$ stock solution was added aseptically when the medium was used.

50X $MgSO_4$ solution

50X $MgSO_4$ solution was prepared by dissolving the following components: 26 g $MgSO_4 \cdot 7H_2O$ in 1 L, and the solution was autoclaved at 121 °C for 15 mins.

25X MN salts solution

25X MN Salts solution was prepared by dissolving the following components: 150 g $NaNO_3$, 13 g KCl, 38 g KH_2PO_4 in 1 L distilled water, and the solution was autoclaved at 121 °C for 15 mins.

1000X trace elements solution

1000X trace elements solution (Szewczyk et al., 2006) was prepared by dissolving the components: 2.2 g $ZnSO_4 \cdot 7H_2O$, 1.1 g H_3BO_3, 0.5 g $MnCl_2 \cdot 4H_2O$, 0.5 g $FeSO_4 \cdot 7H_2O$, 0.17 g $CoCl_2 \cdot 6H_2O$, 0.16 g $CuSO_4 \cdot 5H_2O$, 0.15 g $Na_2MoO_4 \cdot 2H_2O$, 5.0 g EDTA· Na_2 in 80 mL distilled water. The solution was boiled in order to dissolve the compounds, and then cooled the solution to approximal 60 °C and adjusted to pH 6.5 with NaOH. The solution was cooled to room temperature and made up to 100 mL with distilled water.

MN+URI broth

MN+URI broth was prepared by dissolving the following components: 40 mL 25X MN salts solution, 1 mL 1000X trace elements solution, 12.5 g D-glucose, 1.25 g casamino acids, 1 g uridine (Acros, USA) in 1 L distilled water. The broth was adjusted to pH 6.5 and autoclaved at 117 °C for 30 mins. 20 mL 50X $MgSO_4$ stock solution was added aseptically when the broth was used.

Malt Extract Broth (MEB)

MEB was prepared by dissolving the following components: 20 g malt extract, 1 g peptone, 20 g D-glucose in 1 L distilled water. The medium was autoclaved at 117 ℃ for 30 mins.

Czapek Dox Broth

Czapek Dox Broth was prepared by dissolving the following components: 30 g sucrose (Fisher, UK), 3 g $NaNO_3$, 0.5 g KCl, 0.5 $MgSO_4 \cdot 7H_2O$, 1 g KH_2PO_4, 0.01 $FeSO_4$ (Acros, USA) in 1 L distilled water. The broth was autoclaved at 121 ℃ for 15 mins.

Uridine/Uracil Stock

Uridine/Uracil stock was prepared by dissolving the following components: 5.6 g uridine and 6.1 g uracil in 100 mL distilled water. The solution was autoclaved at 121 °C for 15 mins.

Pyridoxine Stock

Pyridoxine stock was prepared by dissolving 0.1 g pyridoxine HCL in 100 mL distilled water and filter-sterilized by passing through a 0.22 μm syringe membrane filter (Sartotius, Germany).

Oatmeal Agar

Oatmeal agar was prepared by dissolving 40 g oatmeal (Odlums Irish pinhead, Irish) in 1 L tap water (O'Gorman et al., 2009). The mixture was heated to boiling point and then simmered at a lower heat for 45 mins. The liquid was filtered through cheese cloth to remove solid residues and autoclaved at 117 °C for 30 mins.

2.1.2 Solutions and buffers

0.01% Tween 80

0.01% Tween was prepared by dissolving 1 mL of Tween 80 in 1 L of distilled water. The solution was aliquoted into 10 ml glass universals and autoclaved at 121 °C for 15 min.

0.5 M Ethylene di-anmine tetra-acetic acid (EDTA) stock

0.5 M EDTA was prepared by dissolving 181.1 g EDTA in 1 L distilled water and adjusted to pH 8.0. The solution was autoclacved at 121 °C for 15 min.

50X TAE (Tris Acetate EDTA) buffer

The 50X TAE buffer was prepared by dissolving 242 g of Tris and 57.1 mL of glacial acetic acid in 100 mL of 0.5 M EDTA stock solution, the buffer was diluted by 900 mL distilled water.

70 % EtOH

70 mL of ethanol was added to 30 mL of distilled water.

TE buffer

The TE buffer was prepared by dissolving 6.05 g Tris and 0.2 mL 0.5 M EDTA in 100 mL distilled water.

Mycelia wash buffer

Mycelia wash buffer was prepared by dissolving 148 g $MgSO_4 \cdot 7H_2O$ in 1 L distilled water and autoclaved at 121 °C for 15 mins.

NM buffer

NM buffer was prepared by dissolving 58.5 g NaCl and 4 g morpholineethanesulfonic acid (MES) in 1 L distilled water. The solution was adjusted to pH 5.8 and autoclaved at 121 °C for 15 mins.

Protoplast wash buffer

The wash buffer was prepared by dissolving 44.7 g KCl and 6 g Tris in 1 L distilled water. The buffer was adjusted to pH7.0 and autoclaved at 121 °C for 15 mins.

STC buffer

STC buffer was prepared by dissolving 21.87 g sorbitol, 0.12 g Tris, and 0.74 g $CaCl_2 \cdot H_2O$ in 100 mL distilled water. The solution was adjusted pH to 7.5 with HCl and autoclaved at 117 °C for 30 mins.

60 % PEG 3350 solution

60 % PEG 3350 solution was prepared by dissolving 60 g PEG 3350 (Fisher, UK), 0.12 g Tris base, and 0.74 g $CaCl_2 \cdot H_2O$ in 100 mL distilled water. The solution was adjusted to pH 7.5 with HCl and autoclaved at 121 °C for 15 mins. The PEG solution was filtered through a 0.22 μm syringe membrane filter to remove any precipitate directly before use.

Potassium Phosphate Monobasic solution (PPM)

PPM was prepared by dissolving 0.34 g KH_2PO_4 in 100 mL distilled water and autoclaved at 117 °C for 30 mins.

Potassium Phosphate Dibasic solution (PPD)

PPD was prepared by dissolving 0.435 g K_2HPO_4 in 100 mL distilled water before being autoclaved at 117 °C for 30 mins.

Colony PCR Solution

The solution was prepared by dissolving 58 mg NaCL, 121 mg Tris-HCl ,and 292 mg EDTA in 100 mL distilled water. The solution was adjusted to pH7.5.

1 M NaOH

The 1 M NaOH solution was prepared by dissolving 4 g NaOH in 100 mL distilled water.

2.2 Methods

2.2.1 Fungal Strains

Fungal strains were routinely cultured on ACM (**Section 2.1.1**), with slopes supplemented with additional nutrients if required for auxotrophs. These ACM slopes were prepared by pouring around 10-15 mL of agar medium into sterile universal 30 ml tubes set at an angle. The inoculated strains were incubated at 28 °C in the light, or 37 °C for 3-5 days before short-term storage for up to 3 months at 4 °C in a fridge. For longer-term storage, conidia were harvested and suspended in 1.5 mL of a sterile 10 % glycerol solution in sterile cryovials. The cryovials were stored either under liquid nitrogen in a cryovessel or in a minus 80 °C freezer.

Aspergillus nidulans

The parental *A. nidulans* strain used for most studies was strain 2-258 which has the genotype *pyrG89-, pyroA4-, nkuA::argB, veA+,* therefore requiring supplements to a final concentration of 1.12g/L uridine, 1.22g/L uracil and 50 µg/L pyridoxine. This strain was a gift from O Bayram (Dublin, Ireland) and chosen for use as it is a fertile laboratory strain with useful selective markers, as well as having the *veA+* genotype (unusually for laboratory strains). Transformants generated during studies are listed in **Appendix 7**.

Aspergillus fumigatus

The parental *A. fumigatus* strains were wild type 47-51 (*MAT1-1*) and 47-55 (*MAT1-2*) which previous studies had established as being highly fertile (O'Gorman et al., 2009; Swilaiman et al., 2020).

2.2.2 Spore suspensions

Spore suspensions were prepared by agitating conidiating slopes with 0.01% Tween 80 (**Section 2.1.2**) using a sterile 1000 µL tip. The spore concentration was quantified using an improved Neubauer haemocytometer. The spore suspension was diluted to a final desired concentration with 0.01% Tween 80. To calculate the spore concentration in spores/mL, the average number of spores per square of the improved Neubauer haemocytometer was multiplied by either 4 $x10^6$ when the spores were counted in medium squares, or 2.5 x 10^5 when they were counted in small squares. The spore suspension was then diluted to a final desired concentration with 0.01% Tween 80.

2.2.3 DNA extraction

Aspergillus strains were grown in 50 mL ACM broth (**Section 2.1.1**) (with pyridoxine and/or uridine and uracil as necessary) for 24 hour at 28 °C by shaking in sterile 250 mL flasks at 150 rpm. Resulting cultures were filtered through sterile Miracloth and excess liquid squeezed out with gloved hands, and then cultures blotted between paper towels to remove residual liquid. The material was then ground under liquid nitrogen using a pestle and motor. The Wizard@ Genomic DNA Purification Kit was used for genomic DNA extraction according to manufacturer's instruction as follows. Approximately 10-20 mg of ground powder was added into a 2 mL Eppendorf tube and mixed with 450 µL Nuclei Lysis Solution. The mixture was vortexed and incubated at 65 °C for 30 mins. Then, the mixture was cooled down to room temperature and 225 µL of

protein precipitation solution added. The resultant mixture was vortexed, and then centrifuged at 13,000-16,000 **g** for 3 mins. The supernatant of approx. 600 µL was transferred into a clean 1.5 mL Eppendorf tube, and then 600 µL isopropanol was added. The tube was mixed by repeated gentle inversion, and then centrifuged at 13,000-16,000 **g** for 1 min. The supernatant was discarded, and 600 µL of 70% ethanol was added. After inverting, the tube was centrifuged at 13,000-16,000 **g** for 1 min. The supernatant was removed, and the pellet was washed with 70 % ethanol and centrifuged one more time. After removing the supernatant again, the pellet was dried for 15 mins to remove residual ethanol. 100 µL of DNA rehydration solution was next added. Finally, to fully dissolve the DNA pellet, the mixture was incubated at 68 °C for 1 hour, or left at 4 °C fridge overnight. The DNA concentration was measured by a Nanodrop ND-1000 spectrophotometer (Labtech International). For short term storage, DNA samples were kept at 4 °C in a fridge, and for long term storage, DNA samples were kept at -20 °C in a freezer.

2.2.4 Primer design

Primers were designed using the primer 3 design function of MacVector version 14.0.4 for Macintosh.

2.2.5 Agarose gel analysis

1.2% (w/v) agarose gels were routinely used for experimental studies to resolve DNA fragments. Gels were prepared by dissolving agarose in TAE buffer, and ethidium bromide (EB) was added to a final concentration of 0.2 µg/mL for visualizing DNA. The DNA was mixed with a DNA loading dye and loaded into the wells and electrophoresis run at 100-130V to separate products. A Bio-Rad chemidoc XRS+ was used to capture gel images by using Quantity One 4.6.6 software.

2.2.6 Deletion cassettes synthesis

Deletion cassettes for gene knock outs were obtained where possible from the Fungal Genetics Stock Center in the USA (http://www.fgsc.net/). Primers sets used for amplification of gene deletion fragments are listed in **Appendix 8.** Knock-out cassettes, which were not available from the FGSC, were instead made using fusion PCR (Szewczyk et al., 2006). According to the protocol, the target gene was replaced by a selectable maker flanked by upstream and downstream fragments to facilitate homologous integration (**Figure 2-1;** Primers used are listed in **Appendix 8**). The first step was to amplify upstream and downstream fragments (of the target gene) of about 1,200 bp in size. The cycling condition and program were listed in **Appendix 1** and **Appendix 2**. The primer designed for this purpose were termed P1 and P2 for the upstream fragment and P3 and P4 for the downstream fragment. The 5' end of primer P2 was designed to contain a segment that is identical to the antisense of the 3' end of the selectable marker, and the 5' end of P4 was designed to contain a segment that is identical to the antisense of the 5' end of the selectable marker. The next step was to amplify the selectable marker (see **Appendix 3 and 4 for PCR conditions**) The PCR products from these steps were purified using NucleoSpin Gel and PCR Clean-up kit (Macherey-Nagel, Germany) (according to manufacturer's instructions) prior to the third fusion PCR amplification. In the last step, nested primers P5 and P6 were designed inward of the upstream and downstream fragments, respectively (**Appendix 5 to 6**). The optimal annealing temperature of all primers used in the fusion PCR was around 63 ℃. To amplify the up and down stream fragments, and the selectable marker, a standard PCR cycle was applied using the proof-reading high fidelity enzyme Phusion polymerase (NEB, UK). Genomic DNA from *A.nidulans* 2-258 was used as template for amplification of upstream and downstream fragments.

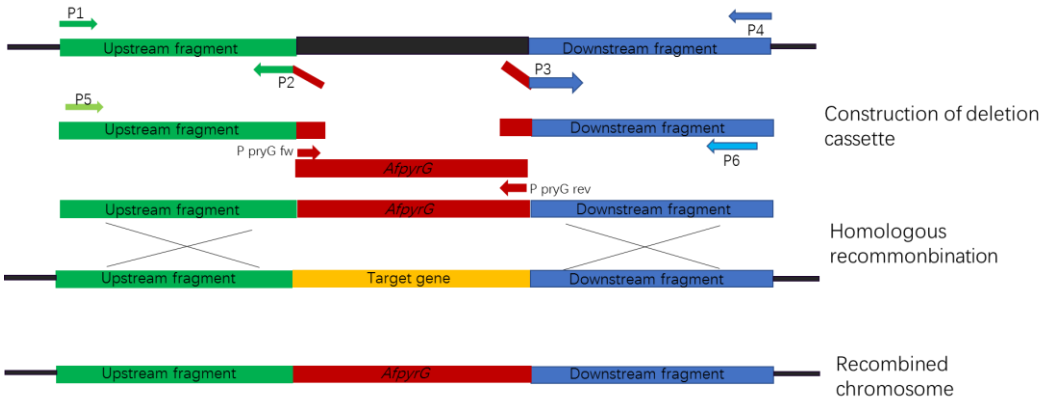

Figure 2-1 Diagramatic illustration of design of gene knock out and replacement process. The putative target gene is replaced by selectable marker *AfpyrG,* Homologous recombination during transformation leads to replacement of the target gene with *AfpyrG.*

2.2.7 Plasmid construction

Due to the large size of the complementation cassettes, it was decided to amplify constructs via a plasmid rather than direct PCR. pUC19 was used as the backbone for plasmid construction for the complementation cassettes (Geib and Brock., 2017) (**Figure 2-2**). The approx. 1 kb of upstream together with the ORF region of the target gene and the approx. 1 kb of downstream were amplified by routine PCR procedures (primers used are listed in **Appendix 10**). The plasmid was then digested via use of an appropriate restriction enzyme to allow insertion of the PCR product. To anneal each fragment in a certain direction, the NEBuilder@ HiFi DNA Assembly Master Mix (New England Biolabs) was used. The amount of each fragment was 0.1 pmol, and the amount was converted into volume by NEBio Calculator (https://nebiocalculator.neb.com/#!/ligation). 10 µL of the HiFi Assembly Master Mix was added into a 200 µL PCR reaction tube, together with appropriate aliquots of the DNA fragments. The final reaction was made up to 20 µL with dH_2O. The mixed sample was incubated at 50 ℃ for 1 hour in the thermocycler.

After incubation, samples were kept on ice for transformation of *E. coli* via electroporation, or stored at -20 °C.

In the plasmid transformation, 2 µL of HiFi Assembly products was diluted into 6 µL of dH_2O, and in the transformation 2 µL of the diluted aliquot was mixed with 50 µL of an electrocompetent *E.coli* suspension. For best results, the tube was kept on ice. Next, 50 µL of the cell-DNA mixture was transferred into a pre-chilled electroporation cuvette, and the electroporator was set at 1,700 V (offering 17 kV/cm field strength0. The sample was electropulsed once and 950 µL of pre-warmed (37 °C) SOC medium was immediately added, and then the sample was transferred into a new 1.5 mL Eppendorf tube and incubated at 37 °C for 1 hour with shaking at 250 r.p.m. Afterward, 100 µL of the transformant mixture was plated on LB agar containing 10 µg/mL ampicillin. After 24-48 hours of incubation at 37 °C, regenerated *E. coli* colonies were selected and screened by restriction enzyme digestion. The correct plasmids were extracted from the colonies by the NucleoSpin Plasmid Purification Kit (Macherey-Nagel, Germany) according to manufacturer's instructions and stored at -20 °C.

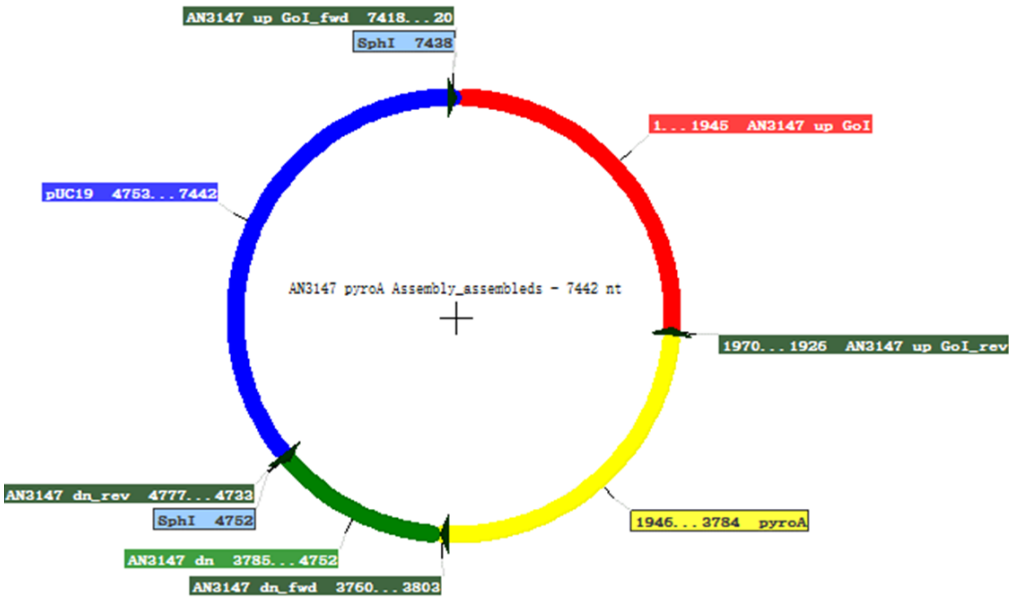

Figure 2-2 The construction of pUC19-AN3147-pyroA plasmid as a representative of plasmid construction. pUC19 backbone shown in blue;

pyroA in yellow [Primers used were pyroA_fwd-C (TGAATTCGAG CTCGGTACCCGGGTGCACCTGATAGGGACATC) and pyroA-rec-C (GTC GACTCTAGAGGATCCCC*GGG*CACTGGACGTTGACATGAC)]; *AN3147.2* upstream and downstream flanking sequences in red and green, respectively (Primers for *AN3147.2* upstream flanking sequence were AN3147 up GoI-fwd (CCTCTAGAGTCGACCTGCAGGC ATG*C*TCCTCATATTCGTGGGTCAAAAC) and AN3147 up GoI-rev (TCTGATGTCCCTATCAGGTGCACCCGACTGCAG ATGTGGCAAAAG); primers for *AN3147.2* downstream flanking sequecne were AN3147 dn-fwd (TTGGTCATGTCAACGTCCAGTGCCCTCCAACTCA ACCAAACAGC) and AN3147 dn-rev (ACCATGATTACGCCAAGCTTGCATG CCCACCCTGATTATGCGAG).

2.2.8 Protoplasting and transformation of *A. nidulans*

Gene deletion and the complementation of target genes were achieved via PEG-mediated protoplast transformation (Szewczyk et al., 2006). The incorporation of identical upstream and downstream regions in the transforming DNA together with use of *nkuA* deletion strains (Ferreira et al., 2006) was designed to promote homologous recombination and allow knock-out of the target genes or recomplementations. In this section, the protoplasting and transformation method applied specifically to *A. nidulans* strains will be described, whilst the particular method of for *A. fumigatus* protoplasting and transformation will be described in **Chapter 4.**

The *A. nidulans* strain 2-258 was incubated at 28 °C on ACM plates (containing uridine/uracil and pyridoxine supplements) for 5 days, and fresh conidial spores were harvested by suspending in 10 mL 0.1% Tween-80 (**Section 2.1.2**). The spore suspension was inoculated in 50 mL MN-URI broth (**Section 2.1.1**) and incubated for 18 hours. The resulting mycelia were harvested by filtering through a layer of sterile Miracloth in a sterile funnel, and then the mycelia were rinsed with the mycelia wash buffer (**Section 2.1.2**). To digest the cell wall, the lysis buffer was prepared on the day of use by the following method: 2.6 g KCl was dissolved into 40 mL PPM (**Section 2.1.2**), and the solution was adjusted to pH 5.8 using PPD (**Section 2.1.2**) and made

up to 50 mL with distilled water. The lysis buffer was sterilized by passing through 0.22 µm syringe membrane filter. For the cell wall digestion step, 1 g of mycelia were transferred into a sterile 50 mL falcon tube by a sterile spoon and was suspended into 10 mL sterile lysis buffer. For 1 g mycelia protoplasting reaction, 9.5 mL lysis buffer was accurately measured, and then 0.5 mL Protoplast F mixture (Megazyme, UK) was added into the lysis buffer and sterilized by passing through 0.22 µm syringe membrane filter. Next, 10 mL sterile Protoplast F solution was added into the mycelia suspension, and then 20 mL of the digestion mixture was transferred into a sterile 125 mL flask and inoculated at 28 °C with shaking at 50 r.p.m. The development of protoplasts was checked at regular intervals by microscope from 1 hour onwards by pipetting 20 µL the mixture onto a microscope slide, looking for evidence of formation of characteristic white spherical structures of 3-5 µm diameter under X40 magnification. Protoplasting was continued for a maximum incubation time of 2 hours to ensure yield of best quality protoplasts. Protoplasts were harvested by slowly pouring the digestion mixture through a double layer of sterile Miracloth in a sterile funnel, and a clean sterile 50 mL falcon tube was used to collect the protoplast suspension. In the next step, a falcon tube with approx. 20 mL of protoplast suspension was filled up to 50 mL with cold NM buffer (**Section 2.1.2**). The tube was centrifuged at 1,408 **g** at 4 °C for 10 mins, thus the protoplasts were pelleted at the bottom. The supernatant was poured off to remove Protoplast F, and then the pellet was resuspended in 1 mL cold STC buffer (**Section 2.1.2**) for counting the number of protoplasts via the haemocytometer method. To remove residual Protoplast F, the falcon tube was filled up to 30 mL with cold NM buffer and centrifuged at 1,408 **g** at 4 °C for 10 mins again. After pouring off the supernatant, the pellet was resuspended with STC buffer and adjusted to the concentration of 5×10^7-1×10^8 protoplasts/ mL.

For transformation, 3-10 µg of an appropriate DNA fragment was mixed with 100 µL of protoplasts suspension in a 15 mL sterile centrifuge tube, and the mixture was incubated for 25 mins at room temperature. In the next step, 200 µL of 60 % PEG3350 solution (**Section 2.1.1**) was added gently drop by drop with a tip cut 1 mL pipette, and then finally 800 µL of 60 % PEG3350 solution was added gently to facilitate the transportation of DNA fragments. The tube contents were mixed gently during the process too. The mixture was then incubated for 20 mins at room temperature. To stop the transformation, the tube was filled to 15 mL with NM buffer and inverted gentle to mix PEG4000 and NM buffer, and the tube was centrifuged at 1,408 **g** at 4 °C for 10 mins to remove PEG3350. Afterward, the supernatant was discarded, and the pellet was resuspended with the 200 µL STC buffer. To regenerate isolates from protoplasts, 150 µL aliquots were then plated onto the selection medium SMA with pyridoxine supplement or control media (**Section 2.1.1**) and incubated at 28 °C for 3-5 days. For the transformation control groups, sterile DNA rehydration buffer (lacking DNA) was added to protoplast suspension, and SMA control plates with uridine/uracil and pyridoxin supplements were used as a positive control group, while the SMA (with pyridoxine supplement) selection plates were marked as the negative control group.

2.2.9 Confirmation of transformant isolates

PCR screening was used to verify the correct knock-out of target genes or recomplementation of genes. The knock-out of the target gene was confirmed by amplification of around 500 bp of the ORF region following a positional PCR screening process illustrated in **Figure 2-3 (**Primer used were listed in **Appendix 9)**. Compared to the positive control (the wild-type strain), a gene deletion transformant should not generate a product from PCR. Colony PCR was applied as a first screen of regenerated *Aspergillus* isolates on selective

media. The mycelia of the candidate gene deletants were picked by sterile toothpicks from the transformation plates, and the mycelia were transferred into 200 µL tubes containing 2 µL of 1 M NaOH and 98 µL of Colony PCR solution (**Section 2.1.2**). The mycelial suspension was boiled at 100 °C for 10 mins (on a thermocycler), and 2 µL of the boiled solution was used in a 20 µL PCR reaction using a Phire polymerase kit according to manufacturer's instructions. In the PCR reaction, the initial denaturation was 98 °C for 30 secs; 30 cycles of 98 °C for 5 secs, 63 °C (using appropriate annealing temperature for respective primers) for 5 secs, 72 °C for 10 secs; 72 °C 1 min for final extension with products than maintained at 4 °C before further analysis by gel electrophoresis.

Transformants giving negative results with the target gene PCR were sub-cultured onto ACM slopes for 5 days, and the spores were collected and incubated at 28 °C or 37 °C for 24 hours and then mycelia were collected for DNA extraction via a Promega Wizard DNA extraction kit (according to manufacturer's instructions). The extracted genomic DNA was used to verify the correct integration of the selectable marker (Primers used were listed in **Appendix 9**). A forward primer was designed to bind to the upstream flank region positioned outside of the deletion cassette, and a reverse primer was designed to bind within the region of the transforming DNA (e.g. the *pyrG* region). Similarly, for the downstream region of the target gene, a forward primer was designed to bind to within the region of the transforming DNA (e.g. the *pyrG* region), and the reverse primer was designed to bind at the downstream flank region positioned outside of the deletion cassette (**Figure 2-3**). PCR was achieved using Phusion Polymerase, the initial denaturation was 98 °C for 2 mins; then 30 cycles of 98 °C for 30 secs, 65 °C (or an appropriate annealing temperature determined by respective primers) for 30 secs, 72 °C for 30 secs; 72 °C 10 min for final extension. The products were then maintained at 4 °C before further analysis by gel electrophoresis. The Isolates giving PCR

amplicons of the predicted size were regarded to be the correct transformant strains (subject to further conformation if necessary by Southern blotting; see later).

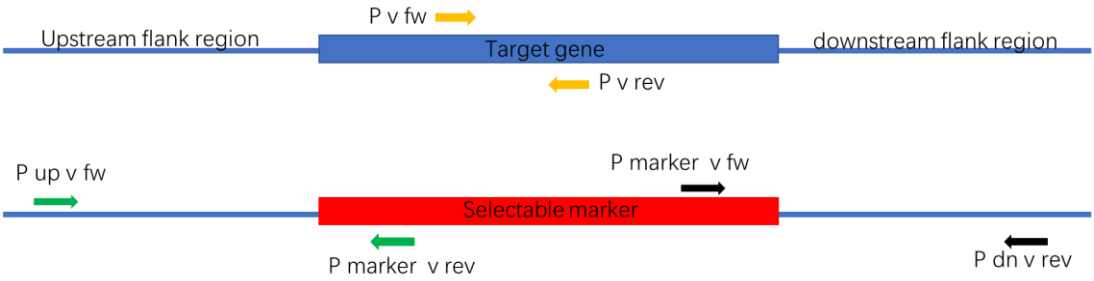

Figure 2-3 Illustration of positional PCR screening process used to verify the replacement of a target gene region. Primer pair P v fw and P v rev was used to confirm the deletion of the target gene (for which a PCR product of approx. 500 bp should be evident in the wild-type control but not in correct transformants). Primer pair P up v fw and P marker v rev (or the pair P marker v fw and P dn v rev) was used to confirm the integration of selectable marker (for which a PCR product of approx.. size 1 kb should be evident in a correct transformant but not in the wild-type control) – note that the flanking primers are positioned outside of the KO cassette.

Chapter 3 Identification of Environmental Conditions and Genes Involved with Fruit Body Development in *A. nidulans*

3.1 Introduction

As previously explained (**Section 1.2.1**), *Aspergillus nidulans* has long been used as a model to study sexual development in Aspergillus species. Under suitable environmental conditions *A. nidulans* hyphae differentiate into ascogonial coils that develop into cleistothecia. When mature, the intercellular space of the cleistothecium is filled with thousands of asci which contain 8 haploid binucleate ascospores in each ascus (Lee et al., 2010; Bennett et al., 2016).

3.1.1 Sexual development in *A. nidulans* – environmental factors

There are many environmental factors, including temperature, pH, and nutrient availability, which can have an effect on sexual and asexual sporulation in fungi (Moore-Landecher, 1996; Dyer et al., 1992). Generally, temperatures from 20 °C to 24 °C are optimal for sexual development of most fungal species, but a minority of fungi can reproduce sexually at temperatures below 10 °C or over 30 °C (Moore-Landecker, 1992). However, the specific conditions for sexual development vary considerably between species, most likely related to the specific ecology of the species involved (Dyer and O'Gorman, 2012). In the case of the model fungus *A. nidulans,* the standard method to induce the sexual cycle involves incubation at 37 °C as first recommended by Pontecorvo (1953). However, trial experiments have suggested that increased numbers of cleistothecia are formed at lower incubation temperatures (Dyer, 2007). In parallel, sexual development in *A. fumigatus* has also been found to be

temperature dependent with ascocarps only being observed at 30 ℃ among various incubation temperatures assayed (O'Gorman et al., 2009). To facilitate further studies of sexual development in *A. nidulans* it would be helpful to know the optimum temperature for such experimental work.

3.1.2 Sexual development in *A. nidulans* – genetic factors

Sexual development in *A. nidulans* has been studied for over half a century and this fungus has been put forward as a model to understand the molecular-genetic control of aspects of the sexual cycle in ascomycete fungi in general. Sexual development is known to be controlled by a network of at least 70 genes encoding various proteins including signal receptors such as pheromone receptors, signal transductors such as MAPK cascades, and effectors such as transcription factors (**Sections 1.3.2 to 1.3.3**; Dyer and O'Gorman., 2012). Many of these genes have been fully characterized and the impact of gene deletion, and in some instances gene overexpression, has been studied in *A. nidulans* and other ascomycete fungi, building on discoveries from *A. nidulans.* However, other ascomycete species, notably *Neurospora crassa* (Dettmann et al., 2013; Iyer et al., 2009; Kim et al., 2012), *Sodaria macrospora* (Teichert et al., 2020), *Podospora anserina* (Saupe et al., 2000; Grogent et al., 2014; Jamet-Vierny et al., 2007), and more recently *Fusarium graminearum* (Kim et al., 2013; Kim et al., 2015; Zhao et al., 2022), have also been used as models to study sexual development in the Ascomcycota. Indeed, certain genes have been identified from these latter species as being critically required for sexual development (e.g. STRIPAK complex, Kück et al., 2016) although their function has not yet been evaluated in *A. nidulans*. Thus, it can be argued that the *A. nidulans* model for sexual development [e.g. as proposed by Dyer and O'Gorman (2012); **Figure 1-4**] might be missing certain key genes.

3.1.2.1 MAPK signalling genes

In the case of the MAPK signaling pathway required for sexual development, this pathway not only requires kinases, but also other associating proteins for correct functioning and to allow association with the correct location in cells. Previous work with *A. nidulans* has established the presence of a AnSte11-Ste50-Ste7-MpkB MAPK cascade, with Ste11, Ste7 and MpkB identified as kinases, while Ste50 acts as an the adaptor (**Section 1.3.2.3**; Bayram et al., 2011). Deletion of Ste50 resulted in no interaction between Ste11 and Ste7 and weakened interaction of Ste7-MpkB, with Ste50 responsible for location of the module at the plasma membrane (Bayram et al., 2011). The homologous cascade in *N. crassa* has been termed the 'MAK-2 cascade', and includes NRC1-MEK2-MAK2 and a Ste50 adaptor (Pandey et al., 2004; Maerz et al., 2008). In addition, a novel protein HAM-5 has been identified in *N. crassa* which is believed to act as a scaffolding protein, with HAM-5 binding with MAK-2 to trigger hyphal fusion via the MAK-2 cascade signaling pathway (Dettmann et al., 2014;Jonker et al., 2014). In *P. anserina*, a similar MAPK1 cascade is required for normal growth and perithecial development, and features a scaffolding protein IDC1 (a homolog of HAM-5) as an essential element for normal fruiting development (Jamet-Vierny et al., 2007).

3.1.2.2 STRIPAK unit genes

Meanwhile, studies using *S. macrospora* have identified the so-called 'STRIPAK' (striatin-interacting phosphatase and kinase) protein complex as having key roles in cellular signal transduction processes in fungi, including those relating to sexual development. The STRIPAK complex is composed of at least seven subunits including a serine/threonine phosphatase catalytic unit PP2Ac, a phosphatase regulatory unit PP2A, and then proteins striatin,

MOB3/phocein, STRIP, SLAMP, and CCM3 (**Section 1.2.3.4**). The complex phosphorylates or de- phosphorylates proteins in the MAPK signal pathway, and thereby regulates various aspects of the morphological development of fungi, for example fruit body development and hyphal cell fusion (Shi et al., 2016; Kück and Stein, 2021). The STRIPAK complex was first studied in fungi in *S. macrospora*. The core subunit PRO45 (SLAMP), which is the membrane anchoring unit, was found to bind with two other STRIPAK subunits PRO11 (Striatin) and SmMOB3, which are a phosphatase regulatory subunit and kinase activator, respectively (Kück et al., 2016). PRO45 was found to be essential for cell-to-cell fusion and sexual propagation in *S. macrospora* with pro45 deletion strains unable to undergo hyphal fusion and were sterile (Nordzieke et al., 2015). A homolog of PRO45 termed 'HAM-4' was detected in *N. crassa* which was also found to effect morphological development such as protoperithecium formation with deletion of ham-4 delaying the protoperithecium formation and leading to aberrant meiosis and abnormally shaped ascospores (Simonin et al., 2010). Finally, the STRIPAK subunit PRO22 was also found to be essential for sexual development in *S. macrospora* with gene mutation resulting in defective protoperithecia maturation apparently due to lack of septa inside the coiled ascogonium (Bloemendal et al., 2010). A homolog of PRO22 'HAM-2' has also been described from *N. crassa* and shown to be required for fruit body formation, with gene deletion preventing hyphal fusion and blocking development at the protoperithecia stage (Xiang et al., 2002). By contrast, the only STRIPAK subunit known in *A. nidulans* at the onset of the present study was StrA, the striatin component identified by Wang et al. (2010). Deletion of *strA* was found to have a striking impact on sexual development, with the formation of abnormally small cleistothecia and defects in ascosporogenesis. In addition, gene deletion caused defects in development of asexual conidia and resulted in decreased mycelium radial growth (Wang et

al., 2010). However, the role of other STRIPAK elements in *A. nidulans* remained to be elucidated.

3.1.2.3 Transcription factor genes

As previously described (**Section 1.3.4**) a series of transcription factors have been identified from *A. nidulans*, which have a vital role in cellular signalling and switching on the expression of target genes. These may be classified by their DNA-binding domains and for example include mating-type domain, zinc finger domain, homeobox domain, basic helix-loop-helix domain, and Myb-like proteins (Shelest, 2008). Although many transcription factors have been characterized in *A. nidulans*, additional transcription factors with possible roles in sexual development have been described from other ascomycetes which have not yet been studied in *A. nidulans*. For example, a bHLH transcription factor *sclR* has been described from *A. oryzae*, which is regarded as an activator of sclerotia formation, and a repressor of conidial sporulation (Jin et al., 2011). In addition, a C2H2 type transcription factor termed *Trire2: 59270* has been reported to influence fruit body formation in *T. reesei* (Linke et al., 2015) but any homolog in *A. nidulans* has yet to be studied).

Homeodomain transcription factors are defined by the presence of a helix-loop-helix-turn-helix structure that consists of about 60 amino acid residues for DNA binding (Bürglin and Affolter, 2016; Holland 2013). Homeobox genes are found throughout the Eukaryota and show high divergence, for example over 200 genes being found in animals and around 100 in plants, but have been much less studied in fungi (Holland, 2013). One fungal example is the homeobox transcription factor *hbx1*, which has been reported to be essential for both asexual and sexual development in *A. flavus* (Cary et al., 2017). However, the role of any homolog in *A. nidulans* has yet to be studied.

The Myb class of transcription factors are defined by the presence of conserved repeating tryptophan residues at the N-terminal region which form a helix-turn-helix structure enabling DNA-binding, and also the presence of repeated has cysteine residues associated with sensing of redox conditions (Pinson et al., 2001). One such Myb transcriptional factor, FlbD has already been described from *A. nidulans.* FlbD contains an Myb domain residue at C46, which act as a redox sensor and plays critical roles in both asexual and sexual development, given that the deletion of *flbD* led to defects in conidiation and fruit body formation in *A. nidulans* (Arratia-Quijada et al., 2012). An additional novel transcription factor MybA (AFUA_3g07070) has been described from *A. fumigatus*, which was reported to regulate conidial formation and maturation via control of the expression of *velB, vosA,* and *wetA*, with the deletion of *mybA* leading to reduction in numbers of conidia and altered conidial survival in water, apparently caused by changes in hydrophobicity of cell wall glycoproteins (Valsecchi et al., 2017). However, this study showed the importance of MybA only in asexual development and any role in sexual reproduction was not investigated. The homeodomain transcription factors contain the helix-loop-helix-turn-helix structure that consists about 60 amino acid residues for DNA binding (Bürglin and Affolter, 2016; Holland 2013).

3.1.2.4 Other possible genes impacting on sexual development

Other sets of genes have also been shown to impact on sexual development in other ascomycete species but have yet to be studied in *A. nidulans*. These include the so-called vegetative incompatibility, heterokaryon incompatibility (HI), genes that mediate self/ non-self recognition of fungal strainsduring vegetative growth. The benefits of vegetative incompatibility may be to prevent the spread of infectious elements, to limit non-adaptive nuclei exploitation and to limit resource plundering during sexual reproduction

(Metzenberg and Glass, 1990; Glass and Kuldau, 1992; Glass et al., 2000; Roche., et al, 2014; Wang et al., 2014). As well as this main role, it has been reported that nonallelic combinations between strains may affect sexual fertility (Glass and Kuldau, 1992; Glass et al., 2000). For example, in *P. anserina,* the *het-C* locus encodes a glycolipid transfer involved in allorecognition (Bastiaans et al., 2014). One of the allelic genes, *het-C2* has been shown to impact on the production of ascospores (Saupe et al., 1994; Bastiaans et al., 2014).

In *S. macrospora*, an ER membrane protein PRO41 has been shown to have a role in fungal sexual differentiation, thought to be, due to modification function of ER function (Nowrousian et al., 2007). Finally, a histone chaperone ASF1 in *S. macrospora* was shown to have a role in sexual development (Gesing et al., 2012; Schumasher et al., 2018).

3.1.3 Aims

The aims of this chapter were two-fold:

(1) To determine the optimum temperature for sexual development of *A. nidulans* to facilitate further experimental studies. This was achieved by inducing the sexual cycle under a range of temperatures between 25 °C to 37 °C, and involved study of representative isolates including wild type, *veA* and *ku* mutant strains.

(2) In order to maintain *A. nidulans* as a model for understanding sexual development in the Ascomycotina it is important that models proposed (**Figure 1-4, Section 1.3**) are as comprehensive as possible in their coverage of genes. However, a series of genes shown to have roles in sexual development in various other ascomycete species have yet to be characterized in *A. nidulans*, as described above. Work therefore aimed to determine if such putative 'universal' pezizomycete sex genes also had a role in sexual development in *A. nidulans.* This was achieved by firstly using bioinformatic analysis to identify

putative homologous genes from *A. nidulans*, and then secondly use of experimental gene manipulation techniques to investigate the function of any candidate genes in cleistothecial and ascospore formation of *A. nidulans*. Target genes comprised the putative MAPK cascade scaffold unit *AN2701.2,* the potential STRIPAK unit genes *AN0164.2*, *AN6611.2* and *AN4632.2*, the putative *mybA* transcription factor *AN4813.2*, the putative homeobox transcription factor *AN1217.2*, the potential transcription factors *AN7170.2* and *AN7736.2,* the potential *het-c2* homolog *AN3147.2*, the putative ER membrane protein *AN10631.2,* the putative histone chaperone *AN4891.2*., and the putative *sclR* and *Trire2:59270* homologs *AN7170.2* and *AN7736.2*, respectively.

3.2 Materials and Methods

3.2.1 Fungal strains and culture conditions

The wild type strains 2-3, 2-137, 2-139, 2-224, 2-227, 2-232, and 2-250; the *veA1* mutant strains 2-149, 2-154, and the *kuA* deletant strain 2-258 were used to investigate the optimal temperature for fruit body development. All strains were obtained from the University of Nottingham BDUN collection (**Table 3-1**). Strain 2-258 was used as the parental strain in subsequent GM work as this was a sexually fertile, *veA* wild-type strain and which contained a *kuA* deletion to allow improved gene targeting in transformation experiments and *pyrG* deletion as a selectable marker (kind gift from O'Bayram, Ireland; note that the *kuA* deletion had no known impact on cleistothecial formation). All strains were cultured on Aspergillus Complete Media (ACM) with 1.12. g/L uridine, 1.22 g/L uracil and 50 µg/L pyridoxine added as supplements as required for auxotrophic strains and to crossing media where relevant. 15 g/L agar was added to make solid media (**Section 2.1.1**).

Table 3-1 Sources of worldwide *Aspergillus nidulans* strains/isolates

Number of strain/isolate	Source Location	Isolation Year	Genetic Markers
2-3	Glasgow (UK)	n/a	Wild-type
2-137	Birmingham (UK)	1960	Wild-type
2-139	Birmingham (UK)	1960	Wild-type
2-149*	Glasgow (UK)	n/a	*pyrG89, pyroA4, nkuA::argB, veA1*
2-154*	Glasgow (UK)	n/a	*yA1, paba A1, nii A4,nkuA::bar, veA1*
2-224**	Gold coast	1982	Wild-type
2-227**	California (USA)	1984	Wild-type
2-232**	Barbados	1987	Wild-type
2-250**	Cardiganshire (UK)	1992	Wild-type
2-258	FGSC	n/a	*pyrG89, pyroA4, nkuA::argB, veA*

*Laboratory strains derived from original Glasgow strain G00.
**Gift from R. Hoekstra.

3.2.2 Optimization of temperature for sexual development in *A. nidulans*

Isolates were grown at 28 °C under lights for 7 days and then conidiospores harvested with 0.01% Tween 80, before being adjusted to a concentration of 1×10^7 spores/mL via counting and calculating spores by a haemocytometer method (**Section 2.2.2**). 10 µL of the resulting spore suspension was pipetted and spread over the surface of ACM in 5 cm Petri dish with a sterile disposable spreader giving a final inoculum of 1×10^5 conidiospores per plate.

The plates were divided into four treatment groups consisting of temperatures of 25 °C, 28 °C, 32 °C and 37 °C, and with 7 replicate plates being set up for each isolate at every temperature. Plates were incubated at the appropriate temperature for an 18 to 24 hours period in the dark and then sealed using two layers of Nescofilm [increased CO_2 levels thought to promote

sexual sporulation; Dyer and O'Gorman (2012)]. Replicates were then placed in single depth [i.e. not stacked; Ashour (2014)]and incubated for 20 days at the respective temperatures in the dark. After incubation, the number of mature cleistothecia (defined as diameter > 100 µm) on the surface of plates was counted in replicate viewing areas of 73.84 mm^2 via microscopy (GX Microscope XTL3101LED at magnification setting 2.5). Numbers of cleistothecia per 73.84 mm^2 were converted into number per 100 mm^2 to allow more direct cross reference of the present study to other study data.

3.2.3 Construction of knock-out cassettes

Where possible, knock-out cassettes for *A. nidulans* gene deletion were obtained from the Fungal Genetics Stock Center (FGSC), USA. The approx. 3.5 kb cassettes provided by FGSC carried a nutrient selectable marker *pryG* (size ca. 1.7 kb) and flanked by approx. 1 kb of target gene specific fragments at the upstream and downstream flanking regions to facilitate homologous integrations. The cassettes were stored at -20 °C. The DNA fragments for transformation were amplified via a Phusion PCR kit (NEB labs, UK). The PCR amplification conditions were: initial denaturation 98 °C 2 min, denaturation 98 °C 30 sec, annealing 63 °C 30 sec, extension 72 °C 2 min, final extension 10 min for 35 cycles. The samples were kept at -20 °C if necessary.

If knock-out cassettes for certain genes were not available from the FGSC then deletion cassettes were constructed following methods described by Szewcyzk et al (2007). The selectable marker *pyrG* was amplified from the FGSC ANID_AN4632.1 plasmid, and the ca.1 kb fragments of the upstream and the downstream were amplified from the parental strain 2-258, respectively suing primers designed for the specific gene based on *A. nidulans* genome sequence data available from the the EnsemblFungi website

(https://fungi.ensembl.org/index.html). The cassette was amplified by fusion PCR (Szewcyzk et al., 2007; **Section 2.2.6**).

3.2.4 Construction of complementation plasmids

To construct complementation cassettes, the nutrient selectable marker *pyroA* was incorporated into cassettes to allow transformant selection. For complementation cassettes, the gene of interest, the *pyroA* marker, and the flanking regions of the target gene were integrated into vector pUC19. The gene of interest was amplified with a ca. 1 kb upstream flanking region by using Phusion PCR kit (NEB labs, UK), as well as the 1 kb downstream flanking region using primers designed for the specific gene based on *A. nidulans* genome sequence data available from the EnsemblFungi website (https://fungi.ensembl.org/index.html). Genomic DNA from *A. fumigatus* Af293 was used as a template, and then the selection marker *pyroA* with a ca.1.7 kb was amplified. The *pyroA* was introduced between the target gene (100 bp downstream from the stop condon), and the downstream flanking region. HiFi DNA assembly master mix was used to link these DNA fragments (**Section 2.2.7**). Plasmid construction was verified by restriction enzyme analysis (*Sma*I and *EcoR*I; **Appendix 28 to 35**). The plasmids were transformed into the competent *E. coli* by electroporation (**Section 2.2.7**). The new plasmids were verified by PCR and restriction enzyme analysis. The *pyroA* fragment for constructing target complementation cassettes was acquired by restriction enzyme *Sma*I digestion and gel purification.

3.2.5 Transformation and gene knock out

Methods for transformation, gene knock out and transformant screening were followed as described in **Sections 2.2.8 and 2.2.9.**

3.2.6 Sexual fertility test

Sexual cultures of *A. nidulans* were set up as described above (**Section 3.2.2**), ensuring that appropriate nutrient supplements (e.g. uridine, uracil and/or pyridoxine) were added to the ACM plates used for production of conidial inoculum and final ACM plates for production of cleistothecia. It is noted that the formation of cleistothecia can be impacted by deletion of *pyrG* and addition of high levels of uracil can be inhibitory to growth (Sun et al., 2013). Therefore, all tests of sexual fertility were routinely performed on ACM supplemented to the same level with uridine and uracil whether or not a supplement was required, with addition of these levels having no recorded impact on sex (Sun et al., 2013). Plates were incubated at 32 °C in the dark and in single depth for 20 days.

After incubation, the number of cleistothecia on the surface of plates was counted in replicate viewing areas as described above (**Section 3.2.2**), and the average sizes of 100 random cleistothecia were measured via microscopy (GX Microscope XTL3101LED at magnification setting 4.0). Furthermore, to evaluate numbers of ascospores produced, an agar plug having a top surface area of 78.54 mm^2 was cut out by a sterile borer, and then the agar plug was transferred into a 1.5mL microfuge tube containing 1mL of 0.01 % Tween 80. In next step, the cleistothecia were removed and crushed by a sterile disposable loop to release ascospores. The tube was vortexed and then a haemocytometer method used to calculate the concentration of ascospore within the suspension. Numbers of ascospores per 78.54 mm^2 were converted into number per 100 mm^2 to facilitate comparison of data to other external studies. The data were analysed by ANOVA via PRISM 9.0.

3.2.7 Ascospore viability

The viability of ascospores produced by control and transformant strains was analysed by growth testing. To obtain relatively pure ascospores, the cleistothecia were cleaned using methods described by Todd et al. (2007). The cleistothecium was viewed under the dissecting microscope, and then picked up by a sterile dissecting needle and rolled along the surface of a 4 % water ager plate to remove hyphae, Hülle cells and conidiophores. The needle was sterilized periodically during cleaning. Around 20 to 30 cleistothecia in total were collected. The cleaned cleistothecia were next transferred into 20 µl sterile 0.01 % Tween 80 solution in a 1.5 mL microfuge tube. The tube was centrifuged at 4°C and 13,000 **g** for 10 mins before cleistothecia in the pellet were ruptured by a sterile disposable loop to release ascospores. 80µL of sterile 0.01 % Tween 80 solution was then added to the tube, which was vortexed to yield a ca. 100 µL ascospore suspension. The concentration of ascospores in the suspension was determined via a haemocytometer method with dilution of the suspension made as necessary to allow accurate counting. Finally, the concentration of the suspension was diluted to $2X10^3$ ascospores/mL for growth testing. A volume of 100 µL of the suspension was added to an ACM plate (with supplements as required) and spread using a sterile spreader (this was estimated to yield a number of around 200 germinating ascospore colonies per plate after incubation). The spread plates were incubated at 28 °C in light for 48 hours. After incubation, colonies on plates were counted and resultant data was analysed one-way ANOVA via the software PRISM9.0.

3.3 Results

3.3.1 Optimum temperature for inducation of the sexual cycle in *A. nidulans.*

The wild type strains (isolates 2-3, 2-137, 2-139, 2-224, 2-227, 2-232, 2-250), the *veA1* mutant strains(isolates 2-149, 2-154), and the *ku* mutant strain 2-258 were utilized to investigate the optimal temperature for sexual reproduction (**Table 3-1**). According to the data analysis, there was a significant difference in production of cleistothecia with temperature, with all *A. nidulans* strains producing highest numbers of mature cleistothecia at 32 °C rather than 25 °C, 28 °C, or 37 °C, except for isolate 2-149 (*veA1*) which produced more cleistothecia at 37 °C [$F(3,240)=16.05$; $p<0.0001$; **Figure 3-1**]. Similarly, there was a difference in ascospore production with temperature, with most isolates developing highest numbers of ascospores at 32 °C, except for isolates 2-149 and 2-154 (both *veA1*) and 2-224 which formed highest numbers at 37 °C [$F(3,240)=3.147$; $p=0.0181$; **Figure 3-1**]. Moreover, there was a significant variation among isolates in fruit body formation [$F(27,240)=2.821$; $p<0.0001$] and ascospore formation [$F(27,240)= 5.268$; $p<0.0001$] under the impact of temperature.

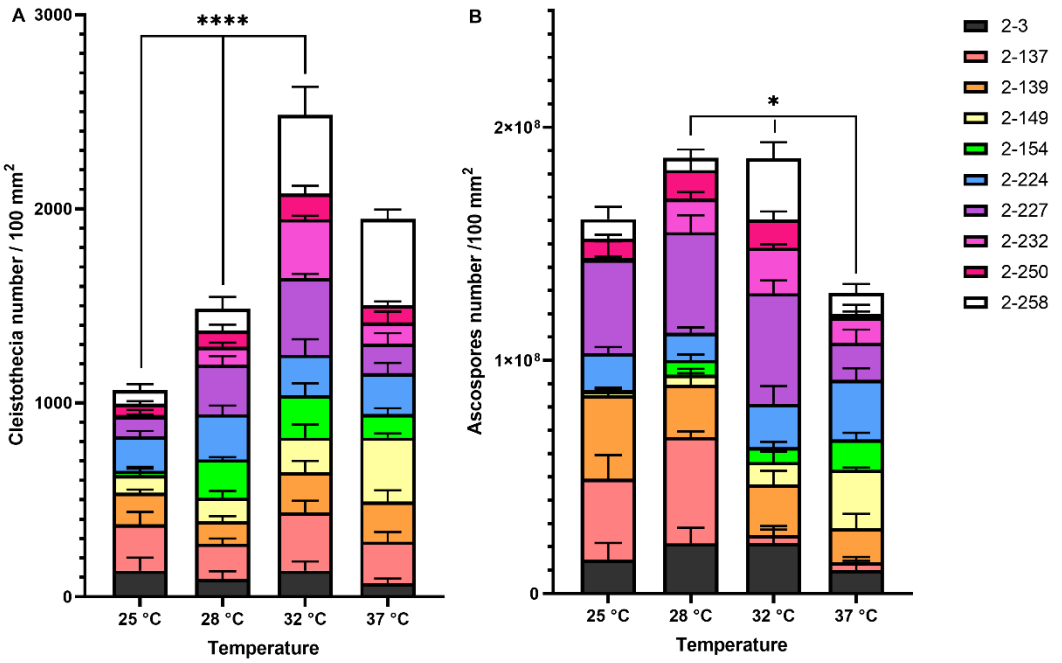

Figure 3-1 Effect of temperature on sexual development in *A. nidulans*. **A** indicates the average number of cleistothecia formed under various temperatures. **B** indicates the average number of ascospores formed under various temperatures. Error bars indicate ± SEM. Each strain contained 7 replicates. Data was analyzed via two-way ANOVA in Prism 9.0.

3.3.2 Construction of gene deletant and complementation strains

Candidate genes with involvement in sexual development were identified *in silico* via BLAST searching with the TBLASTN tool at the Ensembl Fungi website (https://fungi.ensembl.org/Multi/Tools/Blast). A series of gene knock outs were then made in *A. nidulans* strain 2-258, which allowed improved gene targeting for more effient gene transformation (**Section 2.2.8**). Numbers of transformants varied considerably according to the target gene, but it was aimed to select at least two transformants (showing correct integration of knock out cassette) per gene to ensure reproducibility of results. Where an effect was seen on sexual development then gene complementation strains were constructed where appropriate as will now be described.

3.3.2.1 MAPK cascade scaffold unit *AN2701.2*

A putative MAPK scaffolding protein homolog of *P. anserina* IDC1 (XP_011393510.1) was identified via BLAST searches (**Table 3-2**). The identified *A. nidulans* gene *AN2701.2* shared 58.2 % of identity with *idc-1* and gave an E-value of $7.4e^{-165}$. *AN2701.2* shared 62.5 % identity and an E-value of 0.0 with *ham-5* (ABJ96338.2) of *N. crassa* (**Appendix 11**). The coding region of AN2701.2 was 4,898 bp and predicted to encode a polypeptide with 1,570 residues with a WD40 domain at the N-terminal from positions 41 to 312 aa. A *AN2701.2* knock-out cassette was constructed as described in **Section 2.3.4** and the cassette amplified by fusion PCR (**Section 2.2.6; Appendix 23 to 24**; Szewcyzk et al., 2007) and then used for gene knock out. Two transformants (termed ΔAN2701-4 and ΔAN2701-6) showing correct integration of the disruption cassette were then screened for fruit body formation (**Appendix 1; Appendix 25 to 26**).

Table 3-2 Summary of BLAST search results of putative genes related to sexual development in *A. nidulans*

Query seqence		homologous gene in *A.nidulans*			Description	Putative domain
Protein ID	Species	TBLASTN				
		Gene ID	E value	Identity (%)		
XP_011393510.1 (IDC1)	*P.anserina*	AN2701.2	7.40E-165	58.2	Hypothetical protein	WD domain
XP_964080.2 (HAM-4)	*N.crassa*	AN4632.2	5.50E-56	68.3	Hypothetical protein	FHA domain
XP_003352145.1 (PRO22)	*S.macrospora*	AN6611.2	8.40E-164	72.6	Hypothetical protein	STRP domain
XP_962270.2 (PP2Ac)	*N.crassa*	AN0164.2	0	86.6	Hypothetical protein	Serine/threonine-specific phosphatese domain
AFU_3g07070 (MybA)	*A. fumigatus*	AN4813.2	8.50E-69	50.6	Hypothetical protein	Myb-like domain
XP_001825886.1 (SclR)	*A.oryzae*	AN7170.2	8.80E-35	82.4	Hypothetical protein	bHLH domain
XP_006964350.1	*T.reesei*	AN7736.2	9.30E-153	65.7	Hypothetical protein	C2H2 domain
XP_002380469.1 (HBX1)	*A.flavus*	AN1217.2	3.10E-128	87.2	Hypothetical protein	Homeobox domain
AAA20542.1 (HET-C)	*P.anserina*	AN3147.2	5.10E-71	62.9	Hypothetical protein	Glycolipid transfer protein domain
XP_003345657.1 (ASF-1)	*S.macrospora*	AN4891.2	6.90E-68	83.8	Hypothetical protein	Histone chaperone ASF-1 like domain

ΔAN2701-4 and ΔAN2701-6 both showed a dramatic increase in number of cleistothecia formed, but with a significantly reduction in size (ca. 5-fold) as compared to parental and protoplast control strains 2-258O and 2-258P, respectively (**Figure 3-2A-B; Figure 3-3A**). The mutant strains both produced significantly lower numbers of ascospores, which also exhibited a dramatic decrease in viability as compared to the controls **(Figure 3-2C-D**). It was noted that the strains ΔAN2701-4 and ΔAN2701-6 both failed to form cleistothecia on GMM, unlike the parental control, indicating some effect of medium composition on sexual development (**Figure 3-3B**). Due to time limitations, it was not possible to acquire complementation strains in the present study.

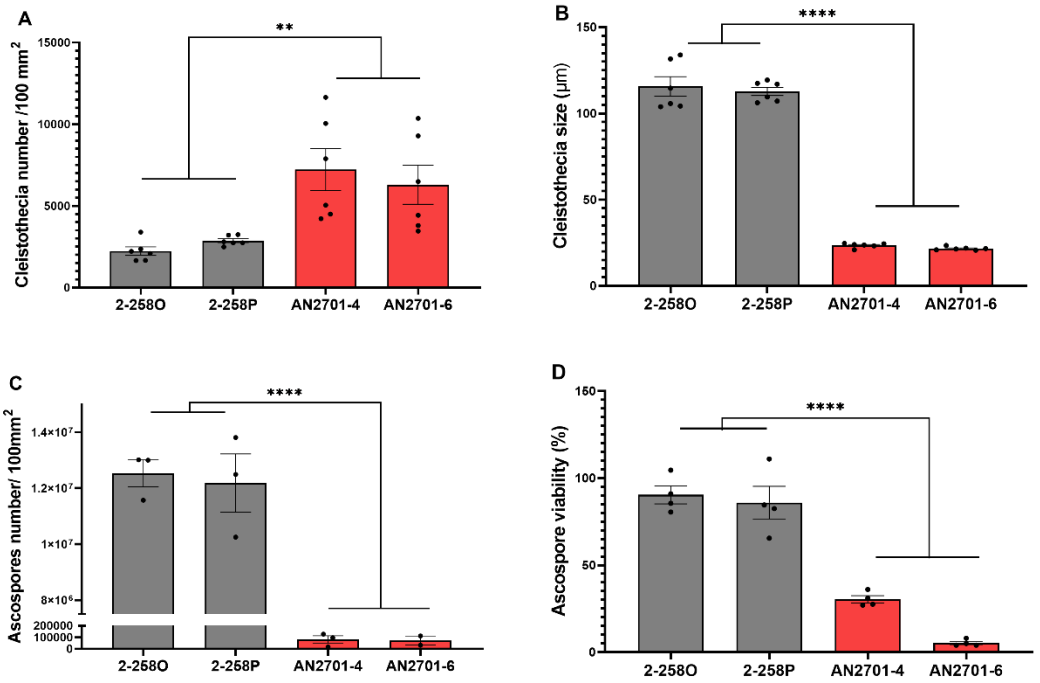

Figure 3-2 Sexual development in Δ*AN2701.2* and control (2-258) strains of *A. nidulans*. A represents number of cleistothecia produced by strains ΔAN2701-4 and ΔAN2701-6 when incubated on ACM at 32 °C in darkness as compared to parental strains 2-258O and 2-258P **B** represents size of cleistothecia (diameter) as measured by microscopy (100 replicates per measurement). **C** represents number of ascospores collected from agar plugs with a defined surface area. **D** represents the viability of ascospores collected from cleistothecia when defined numbers were spread out onto plates. Error bars indicate ± SEM. Dots indicate biological replicates. ** indicates significant difference from the controls at P<0.05; **** indicates significant difference from the controls at P<0.0001.

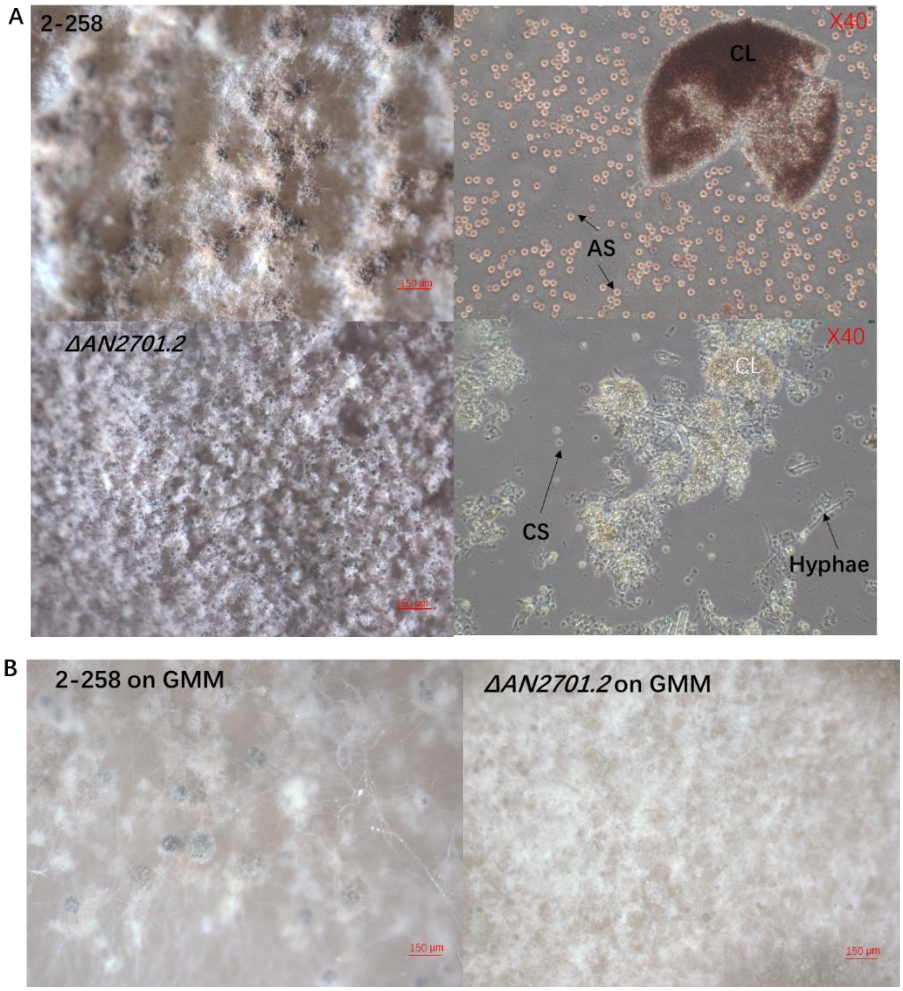

Figure 3-3 Cleistothecia and ascospores formed by control 2-258 and Δ*AN2701.2* strains. A illustrates the fruit bodies formed when strains were inoculated onto ACM. Compared to the control 2-258 strain, the Δ*AN2701.2* strain formed numerous small cleistothecia. **B** represents the sexual development when strains were inoculated onto GMM. Compared to 2-258 control strain, the Δ*AN2701.2* strain failed to form cleistothecia. CL: cleistothecia; AS: ascospores; HC: hülle cells; CS: conidiospores.

3.3.2.2 STRIPAK complex subunits *AN0164.2, AN6611.2* and *AN4632.2*

Three STRIPAK complex subunits were identified. Firstly, a putative phosphatase gene *AN0164.2* was identified based on 86.6% and 85.4% identity to the PP2Ac subunits of *N. crassa* and *S. macrospora*, respectively (**Table 3-2; Appendix 12**). The coding region of the *AN0164.2* gene was 959 bp and the AN0164.2 protein (XP_657768) was predicted to be 299 aa and

contain a serine/threonine-specific phosphatese domain at positions 30-251 aa. Second, a putative tail-anchored membrane protein SLAMP homolog of *N. crassa* HAM-4 (XP_964080.2; Simonin et al., 2010; Shi et al., 2016) was identified. The identified *A. nidulans* gene *AN4623.2* shared 68.3% identify with *ham-4* and returned an E-value of $5.5e^{-56}$, and had 68.3% of identity with *pro45*, the SLAMP unit of *S. macrospora* (**Table 3-2; Appendix 13**). The coding region of gene *AN4632.2* was 2,291 bp and its protein AN4632.2 (XP_662236.1) was predicted to be 746 aa and contain a forkhead-associated (FHA) domain at position 189-247 aa, similar to that identified in *N.crassa* HAM-4. Third, a putative cell morphology and cytoskeleral regulator STRIP unit homolog of *S. macrospora* PRO22 (XP_003352145.1; Bloemendal et al., 2012; Shi et al., 2016) was identified as *AN6611.2*, which shared 72.6% identity to *pro22* with an E-value of $8.4e^{-164}$ (**Appendix 14**). The *AN6611.2* had 72.0% identify with *N. crassa ham-2* (**Table 3-2**). The coding region of gene AN6611.2 gene was 3,370bp, and was predicted to encode a protein of 1,028 aa containing two STRP domains at position 126-451 aa towards the N-terminal and 560-986 aa towards the C-terminal. Attempted gene knock-outs of *AN0164.2* and *AN4632.2* were then made using disruption cassettes from the FGSC, whilst knock out of *AN6611.2* used a newly constructed cassette made by fusion PCR (**Appendix 23 to 24**).

Two transformants (termed ΔAN0164-3 and ΔAN0164-6) showing correct deletion of *AN0164.2* were screened for fruit body formation (**Appendix 7; Appendix 25 to 26**). Cleistothecial formation was reduced significantly in both *ΔAN0164.2* strains as compared to the control strains (**Figures 3-4A and 3-5**). The average number of cleistothecia decreased by over 50% [$F(3,20)=17.36$, $P<0.0001$] and the size was significantly reduced by around 3.7 fold [$F(3,20)=287.2$, $P<0.0001$], with the average size of the *AN0164.2* mutant strains being 34 μm compared to the control strain with an average cleistothecia

diameter of 126 µm (**Figure 3-4B**). Ascospore number was also dramatically reduced in *ΔAN0164.2* strains [F (3,12)=8.997, P<0.0001], indeed it proved impossible to isolate viable ascospores because most of cleistothecia appeared immature (**Figures 3-4C-D**). However, the parental control phenotype was recovered in the AN0164-6C5 complementation strain by reinserting *AN0164.2* back to its original postion in the genome, with the production of mature cleistothecia with viable ascospores (**Figures 3-4A-D and 3-5**

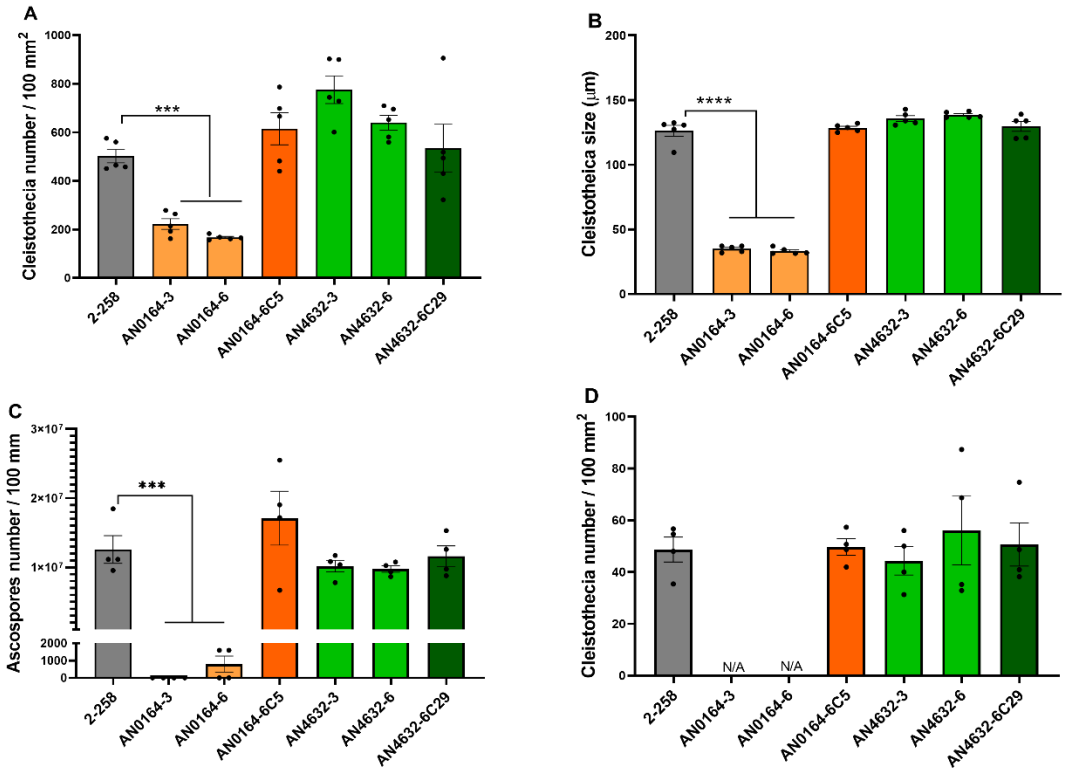

Figure 3-4 Sexual development in Δ*AN0164.2* and Δ*AN4632.2* and control (2-258) and the complementation strain of *A. nidulans*. A represents number of cleistothecia produced by Δ*AN0164.2* and Δ*AN4632.2* strains per unit area as determined by microscopy as compared to parental strain 2-258 and the complement strains AN0164-6C5 and AN4632-6C29, respectively. **B** represents for size (diameter) of cleistothecia as measured by microscopy. **C** represents number of ascospores collected from agar plugs with a defined surface area. **D** represents the viability of ascospores collected from cleistothecia with a defined numbers spread out onto plates. Dots indicate biological replicates in each section. Error bars indicate ± SEM. *** indicates significant difference from the controls at P<0.001; **** indicates significant difference from the controls at P<0.0001.

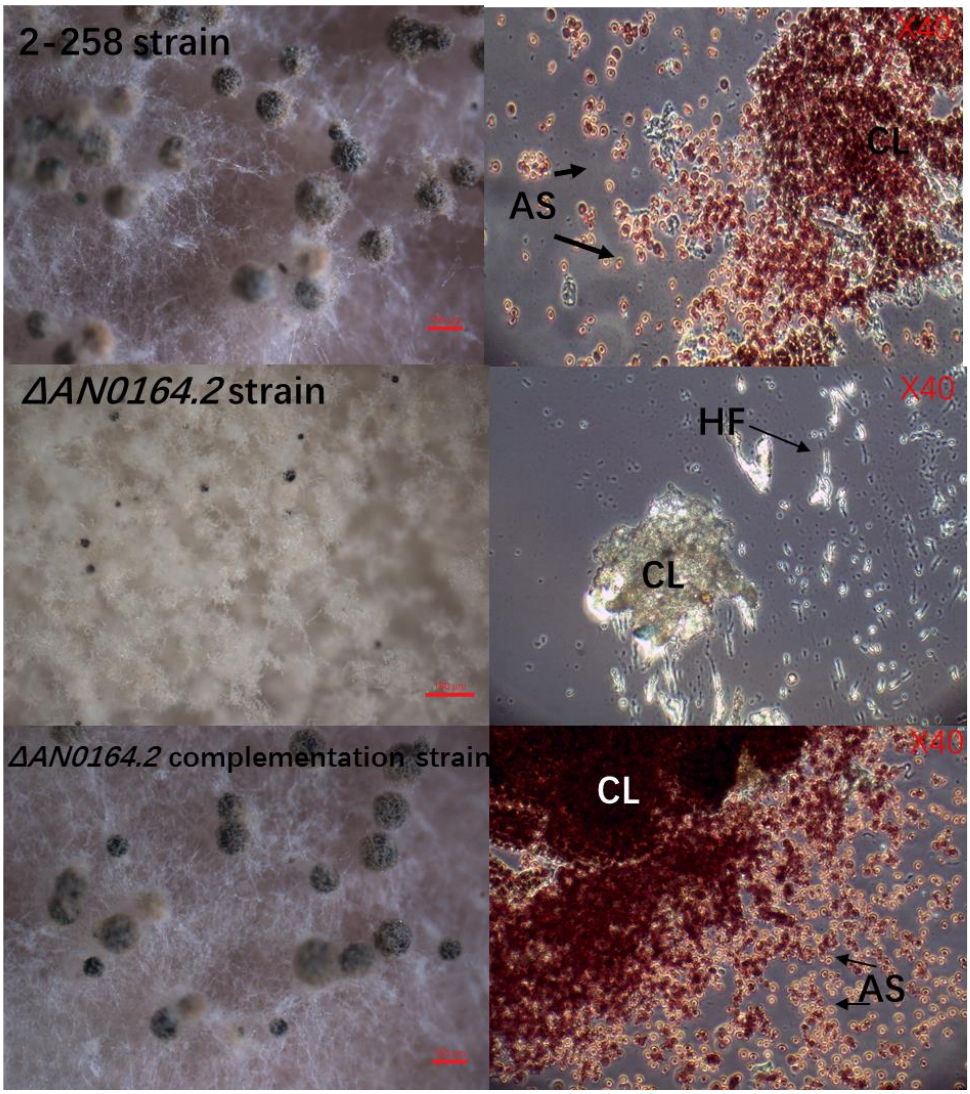

Figure 3-5 Fruit body development of *ΔAN0164.2* and control and complementation strains. Images show a comparison between control strain 2-258, the deletion strain *ΔAN0164.2*, and the complementation strain, *ΔAN0164.2*complementation. CL: cleistothecia; AS: ascospores; HF: hyphae.

Two transformants (termed ΔAN4632-3 and ΔAN4632-6) showing correct deletion of *AN4632.2* were screened for fruit body formation (**Appendix 7; Appendix 25 to 26**). Gene knockout did not appear to greatly affect sexual development (**Figures 3-4A-D and 3-6**). The average number of cleistothecia produced by strain AN4632-3 showed an increase compared to the controls [F (3,20)=17.36, P=0.0015], however the AN4632-6 strain did not show any such difference [F(3,20)=17.36, P=0.2413; **Figure 3-4A**]. In terms of size, strain

AN4632-3 did not show any difference in diameter to the parental strain [F (3.20)=287.2, P=0.0583], but this time strain AN4632-6 produced larger cleistothecia [F(3,20)=287.2, P=0.0073; **Figure 3-4B**]. Ascospore production did not show any differences between the Δ*AN4632.2* deletant and the wild-type strains (**Figure 3-4C-D**). The parental control phenotype was seen in the AN4632-6C29 complementation strain (**Figures 3-4A-D and 3-6**).

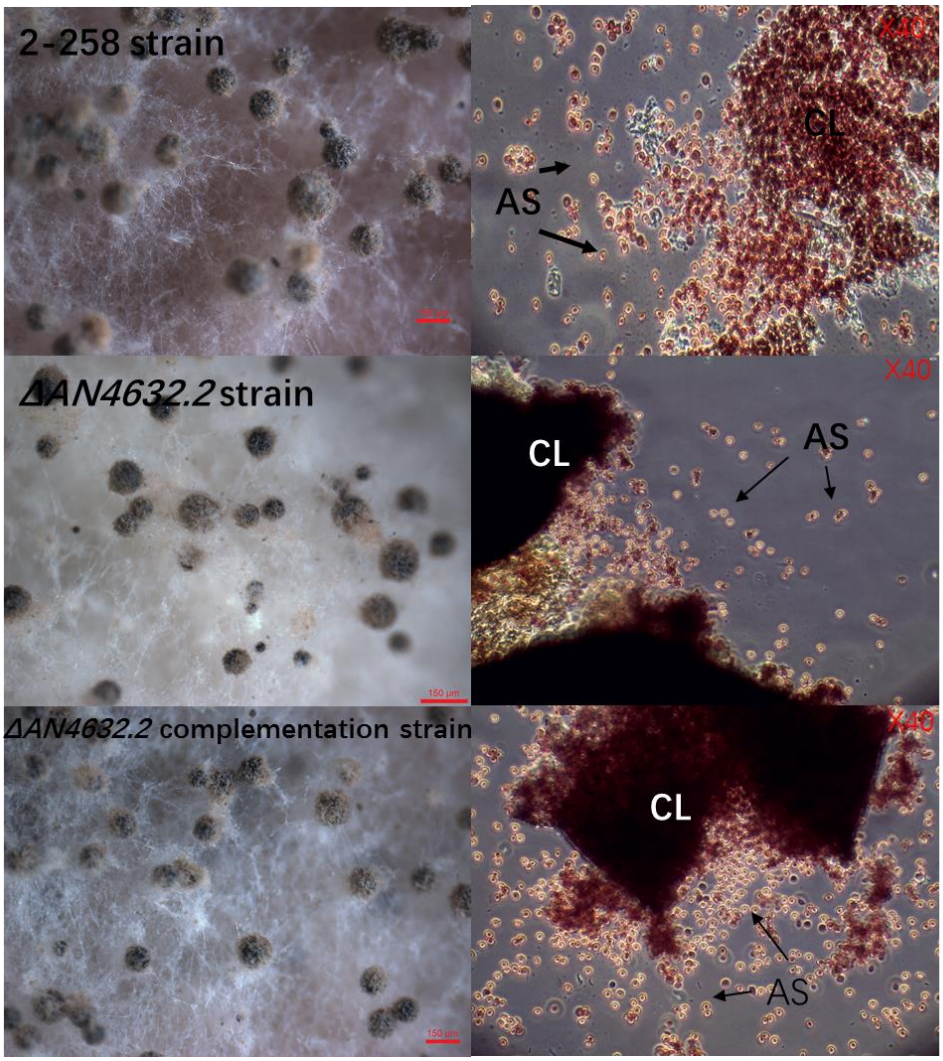

Figure 3-6. Fruit body development of control and *ΔAN4632.2* strain of *A. nidulans*. Images show a comparison between control strain 2-258, the deletion strain *ΔAN4632.2*, and the complementation strain, *ΔAN4632.2*complementation. CL: cleistothecia; CL: cleistothecia; AS: ascospores.

Despite several repeated attempts it was only possible to obtain one deletion strain of *AN6611.2*, and this showed severe defects in vegetative growth (**Figure 3-7; Appendix 25**), precluding further study.

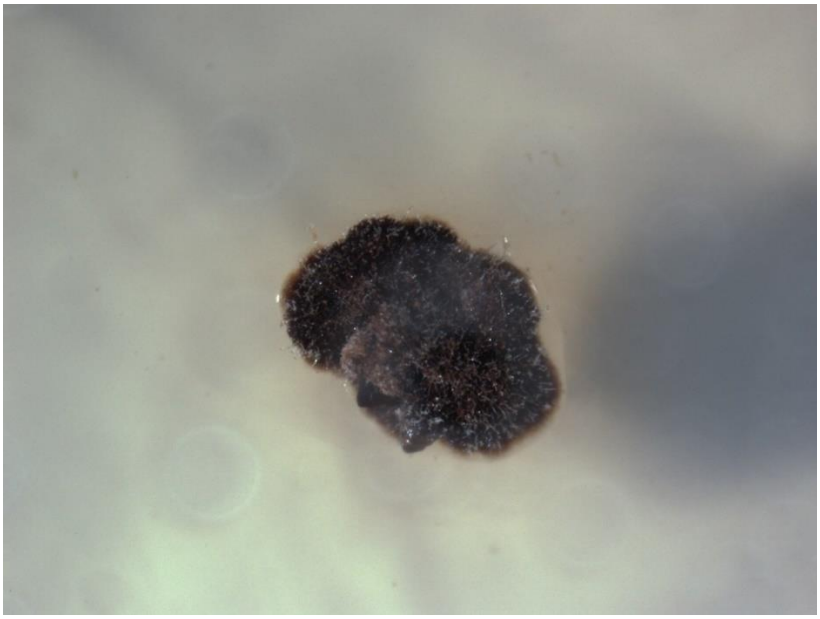

Figure 3-7. Phenotype of the ΔAN6611.2 strain of *A. nidulans* following growth for 14 days at 28 ºC. Black pigmented hyphae slowly aggregated during growth and formed a hard compact structure, instead of normal white radial hyphal growth.

3.3.2.3 *mybA* transcription factor *AN4813.2*

The MybA (XP_754889.2; Valsecchi et al., 2017) protein sequence from *A fumigatus* was used to identify a putative homolog AN4813.2 from *A. nidulans*, which showed an E-value of $8.5e^{-69}$ and identity of 52.3 % to MybA in *A. fumigatus* (**Table 3-2; Appendix 15**). The gene *AN4813.2* is 3,088 bp in length containing four introns and is predicted to encode an 876 amino acid protein (XP_662417.1) with an Myb-like domain located between positions 770 to 827 in the C-terminal portion, similar to the structure of MybA in *A. fumigatus* (Valsecchi et al., 2017). A disruption cassette from the FGSC was used for gene deletion (**Appendix 22**).

Two transformants (termed ΔAN4813-2 and ΔAN4813-14) showing correct deletion of *AN4813.2* were screened for fruit body formation (**Appendix 7; Appendix 25 to 26**). Gene deletion was found to block conidiophore formation and lead to accumulation of an orange pigment in the growth media similar to the mutation of *mybA* in *A. fumigatus* (**Figure 3-8**; Valsecchi et al, 2017). Given the failure to produce conidia, an alternative method had to be devised to inoculate plates for sexual development. This involved culturing both gene deletant and parental strains on ACM (supplemented with uridine/uracil and pyridoxine supplements) for 2 days and then scraping the mycelia off from the surface to make a hyphal suspension, to which sterile glass beads were added. The mixture was vortexed firmly to break long hyphae into short segments. The suspended mycelia was then spread over the surface of a 5 cm Petri dishes containing ACM (with uridine/uracil and pyridoxine supplements as required), and the plates were sealed after 24 hours before being inoculated for 28 days at 32 ℃ in darkness.

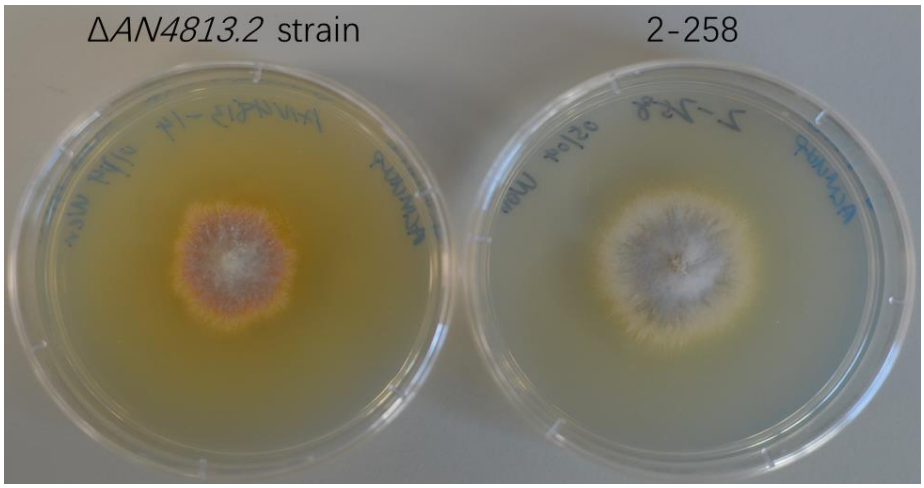

Figure 3-8 Growth phenoptype of Δ*AN4813.2* strain compared to parental 2-258 on ACM. Compared to control strain 2-258, the Δ*AN4813.2* strain failed to form green conidia and produced an orange-brownish pigment.

Compared to the controls, the average number of cleistothecia showed a significant reduction in both ΔAN4813-2 and ΔAN4813-14 [**Figures 3-9 and 3-10**; $F(3,16) = 78.44$; $p<0.0001$]. By contrast, there was no significant difference

in the size (diameter) of cleistothecia when comparing controls and gene deletion mutants [F(3,16)=1.206;p=0.3396], although the data collected suggested that the range of diameter was larger in the Δ*AN4813.2* strains with the larger standard deviation suggesting that there were more unmatured or less developed fruit bodies in the *AN4813.2* deletant strains. Meanwhile, results showed a decline by more than 1,000-fold in production of ascospores in the ΔAN4813-2 and ΔAN4813-14 strains as compared to the control strain [F(3,12)=118.4; p<0.0001]. The proportion of viable spores in the parental strain was 41.3% but the proportion in both Δ*AN4813.2* strains were less than 1% [1.04% in AN4813-2; 0.35% in AN4813-14; F (3,12)=22.93; p<0.0001]. The complementation strain AN4813-2C8 showed restoration of both the number of cleistothecia and also proportion of viable spores (41.3%), and with no significant difference in size to the wild type (**Figures 3-9 and 3-10**).

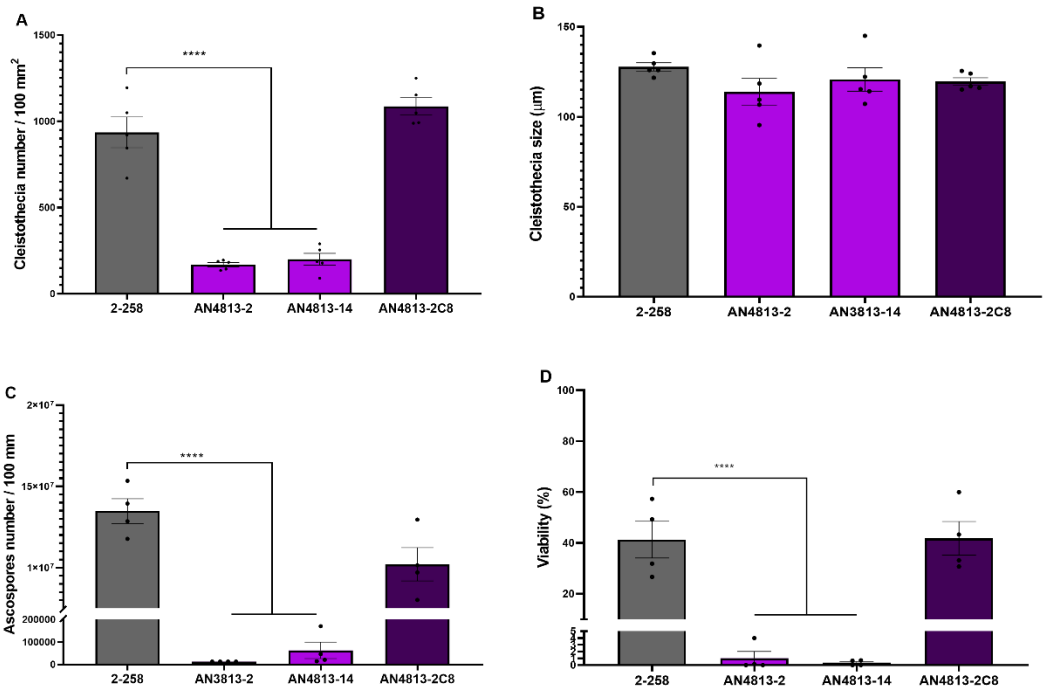

Figure 3-9 Sexual development of Δ*AN4813.2* and control (2-258) and complementation strains of *A. nidulans*. Δ*AN4813.2* strains showed defective cleistothecia and ascospore development when compared to parental strain 2-258 and the complement strain AN4813-2C8. **A** represents the number of cleistothecia produced by the various strains. **B** represents the size (diameter)

of cleistothcia. **C** represents the number of ascospores collected from agar plugs with a defined surface area. **D** represents the viability of ascospores collected from cleistothecia with a defined numbers spread out onto plates. Dots indicate biological replicates in each section. Error bars indicate ± SEM. **** indicates significant difference from the controls at P<0.0001.

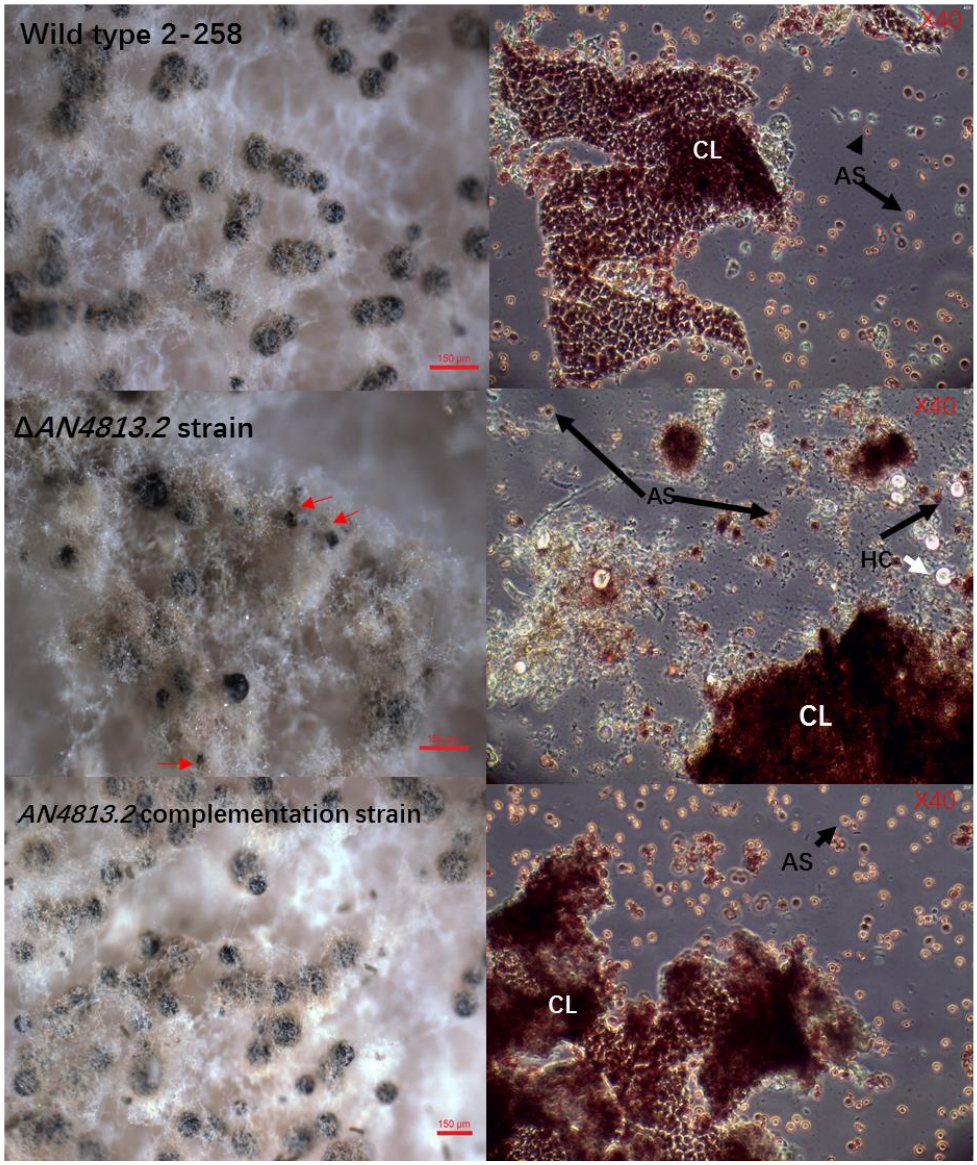

Figure 3-10 Cleistothecial formation by *ΔAN4813.2* and control and complementation strains of *A. nidulans.* The *ΔAN4813.2* strain formed a reduced number of ascospores when compared to the control 2-258 strain and AN4813.2 complementation strain. Cleistothecia of reduced size are indicated by red arrows. CL: cleistothecia; AS: ascospores;HC: hülle cells.

3.3.2.4 Transcription factors *AN1217.2, AN7170.2* and *AN7736.2*

Three different transcription factors with possible involvement in sexual development were investigated. First, sequence of the *A. flavus* homeodomain protein HBX1 (XP_002380469.1) was used to identify a putative homolog AN1217.2 in *A. nidulans*, which showed 87.2 % identity and an E-value of $3.1e^{-128}$ (**Table 3-2; Appendix 16**). The gene *AN1217.2* was 1,873 bp and encoded a putative 566 aa polypeptide whose N-terminal contained a homeobox domain at position 19-99. Second, sequence of the *A. oryae* bHLH protein SclR (XP_001825886.1) was used to identify a putative homolog *AN7170.2* in *A.* nidulans, which shared 82.4 % identity to SclR with an E-value of $8.8e^{-35}$ (**Table 3-2; Appendix 17**). The gene *AN7170.2* was 932 bp and encoded a putative 274 aa polypeptide which formed a bHLH domain. Third, sequence of the *T. reesei* C2H2 protein Trire2: 59600 (XP_006964350.1) was used to identify a putative homolog AN7736.2 in *A. nidulans*, which showed 65.7 % identity and an E-value of $9.3e^{-153}$ (**Table 3-2**). The gene *AN7736.2* was 1,969 bp and encoded a putative 637aa polypeptide with an ankyrin repeating domain (Appendix Figure 8). Knock-out cassettes for ANID_01217.1 and ANID_07736.1 were available from Fungal Genetics Stock Center (FGSC), and fragments were amplified by PCR (**Appendix 23**) whereas the *AN7170.2* knock-out cassette had to be constructed by fusion PCR (**Appendix 23 to 24**).

Two *ΔAN1217.2* transformants were obtained, termed ΔAN1217-6 and ΔAN1217-17, which exhibited correct patterns of knock out integration (**Appendix 25 to 26**). Deletion of *AN1217.2* led to a block of conidiation, similar to the phenotype seen in Δ*hbx1* strains of *A. flavus* (Cary et al., 2017). Therefore, sexual cultures had to be set up using a hyphal-spread technique as described above for *mybA* (**Section 3.2.2.3**). Both *ΔAN1217.2* strains were found to produce significantly lower numbers of cleistothecia than the control strains, whereas the size of cleistothecia, the number of ascospores and the

viability of ascospore were similar to controls [**Figures 3-11A-D and 3-12**; F (3,20)=7, P<0.0001].

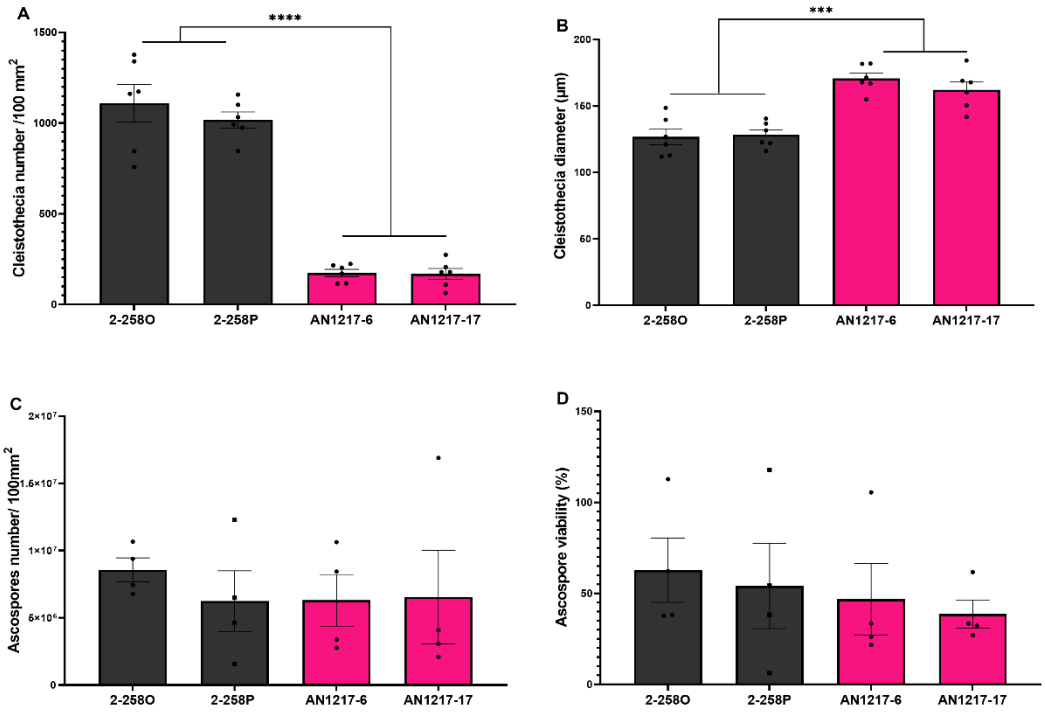

Figure 3-11 Sexual development of Δ*AN1217.2* and control (2-258) strains of *A. nidulans*. Compared to the parental control strains 2-258O and 2-258P, the Δ*AN1217.2* strains formed less cleistothecia although with a larger average size. **A** represents number of cleistothecia produced by the various strains per unit area as determined by microscopy. **B** represents the size (diameter) of cleistothecia size as measured by microscopy. **C** represents the number of ascospores collected from agar plugs with a defined surface area. **D** represents the viability of ascospores collected from cleistothecia when a defined number were spread out onto plates. Dots indicate biological replicates in each section. Error bars indicate ± SEM. *** indicates significant difference from the controls at P<0.001; **** indicates significant difference from the controls at P<0.0001.

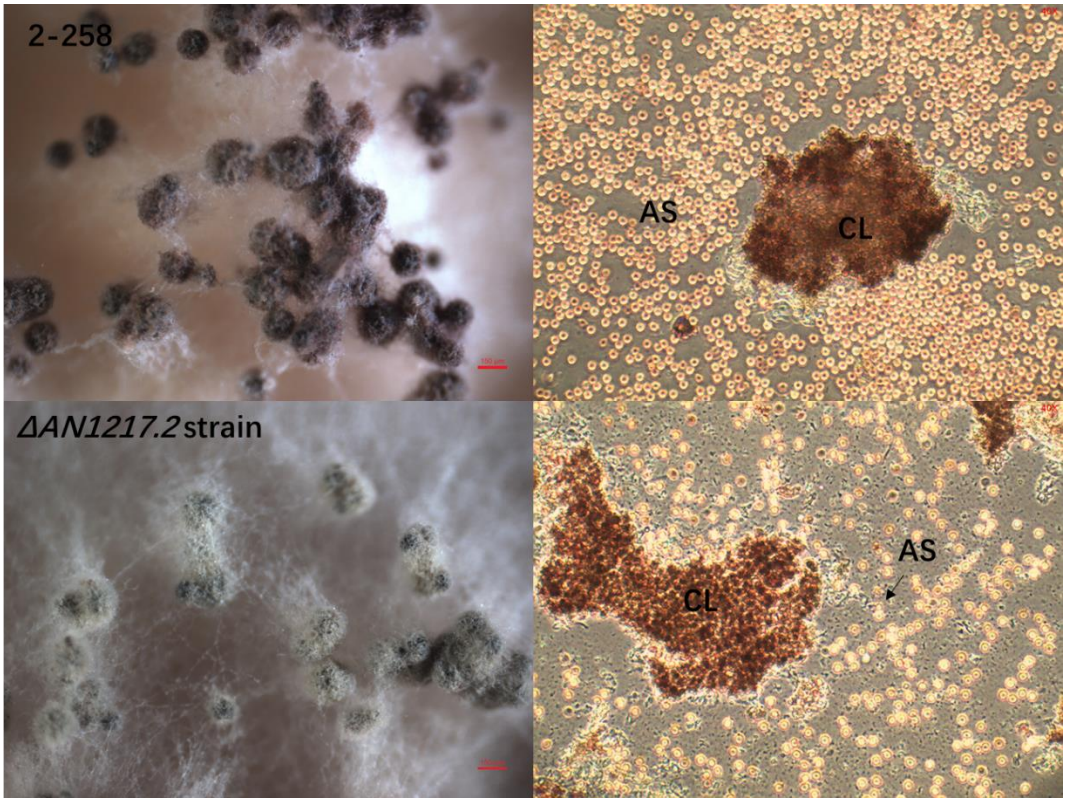

Figure 3-12. Fruit body (cleistothecial) development of *ΔAN1217.2* and control strains of *A. nidulans*. The *ΔAN1217.2* strains were found to produce significantly lower numbers of cleistothecia than control strains, although the size of cleistothecia was similar.CL: cleistothecia; AS: ascospores.

Two *ΔAN7170.2* transformants were obtained, termed ΔAN7170-1 and ΔAN7170-1, which exhibited correct patterns of knock out integration (**Appendix 25 to 26**). Gene deletion did not impact on sexual development in *A. nidulans* in terms of number and size of cleistothecia and numbers of ascospores (**Figures 3-13A-C and 3-14**). However, a significant reduction in ascospore viability was apparent in both of the transformants [F (5,18)=32.00, P<0.005 for AN7170-1; P<0.0001 for AN7170-4; **Figure 3-13D**]. Meanwhile, two *ΔAN7736.2* transformants were obtained, termed ΔAN7736-4 and ΔAN7736-7 which exhibited correct patterns of knock out integration (**Appendix 25 to 26**). Again, gene deletion did not impact on sexual development in terms of number and size of cleistothecia and numbers of ascospores (**Figures 3-13A-C** and **3-14**). However, a reduction in ascospore

viability was apparent in just one of the two transformants (AN7736-7; **Figure 3-13D**).

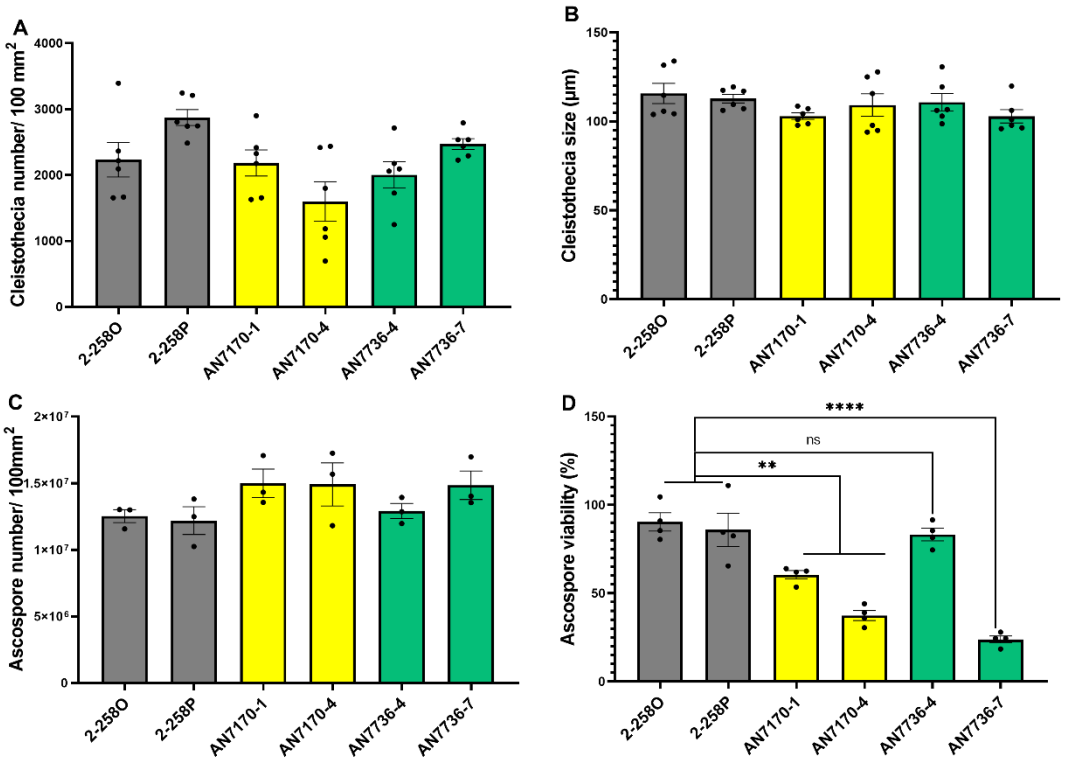

Figure 3-13 Sexual development of ΔAN7170.2 and ΔAN7736.2 and control (2-258) strains of *A. nidulans*. Compared to the parental control strain 2-258O and 2-258P, the gene knock out strains ΔAN7170.2 and ΔAN7736.2 did not show significant differences in cleistothecia development, whilst ΔAN7170.2 strains and strain AN7736-7 showed reduced viability of ascospores. **A** represents number of cleistothecia produced by the various strains per unit area as determined by microscopy. **B** represents the size (diameter) of cleistothecia size as measured by microscopy. **C** represents the number of ascospores collected from agar plugs with a defined surface area. **D** represents the viability of ascospores collected from cleistothecia when a defined number were spread out onto plates. Dots indicate biological replicates in each section. Error bars indicate ± SEM. ** indicates significant difference from the controls at P<0.05; **** indicates significant difference from the controls at P<0.0001.

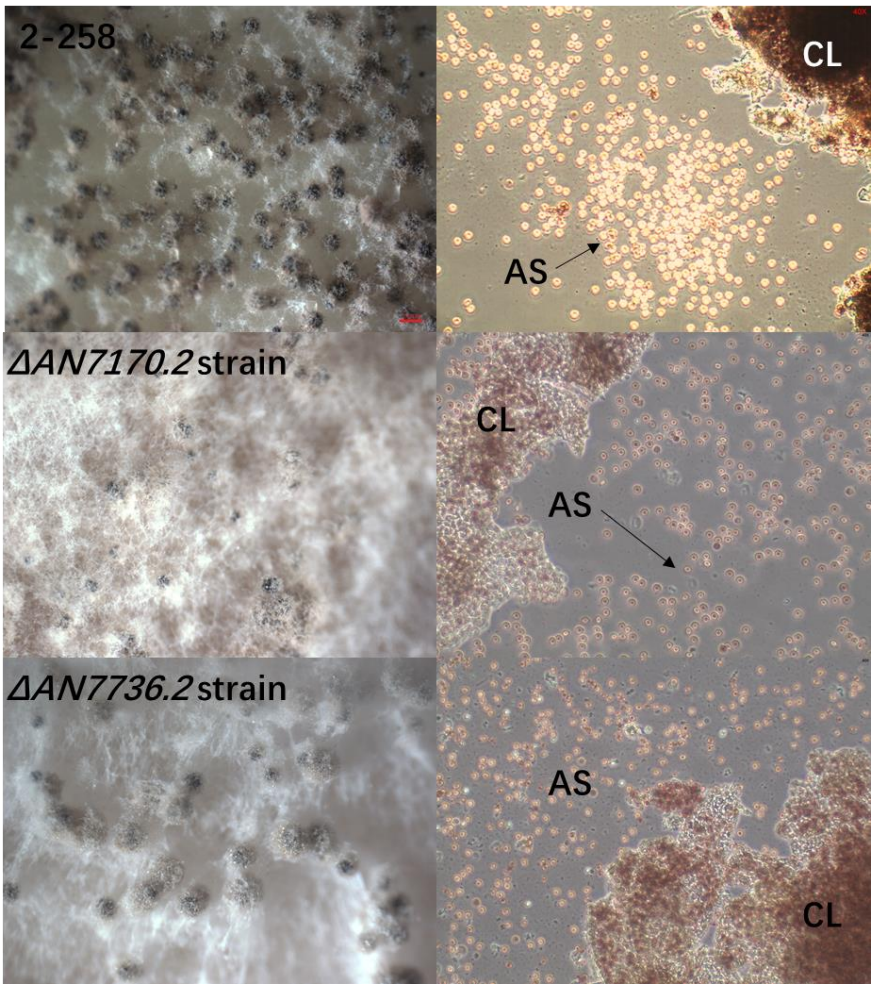

Figure 3-14 Fruit body (cleistothecial) development of *ΔAN7170.2, ΔAN7736.2* and control strains of *A. nidulans* Images show sexual development in the gene knock out *ΔAN7170.2* and *ΔAN7736.2* strains as compared to the 2-258 parental control strain. CL: cleistothecia; AS: ascospores.

3.3.2.5 Other candidate genes – *AN3147.2, AN10631.2* and *AN4891.2*

Three other candidate genes with possible involvement in sexual development were evaluated. Knock-out cassettes ANID_03147.1, ANID_04891.1 and ANID_10631.1 were available for all of these genes from the FGSC and were amplified by PCR (**Appendix 22**).

First, BLAST searching with the HET-C2 sequence from *P. anserina* (AAA20542.1) identified a possible homolog AN3147.2 in *A. nidulans*, which showed 62.9% identity with an E-value of $5.1e^{-71}$ (**Table 3-2; Appendix 19**).

The gene *AN3147.2* is 800 bp in length including four exons and three introns and is predicted to encode a 192 aa poypeptide (XP_660751.1) that belongs to the glycolipid transfer protein superfamily, with an active domain at position 27-191 aa. Two *Δ3147.2* transformants were obtained, termed ΔAN3147-3 and ΔAN3147-10, which exhibited correct patterns of knock out integration (**Appendix Figures 25 to 26**). Gene deletion resulted in a significant reduction in numbers of cleistothecia produced, although there was no change in average size (diameter) of cleistothecia [**Figures 3-15A,B** and **3-16**; $F(3,16)=16.55$, $p<0.0001$]. There was also a significant reduction in the average number of ascospores produced, with over a 50-fold reduction [$F(3,12)=5.566$; $p=0.0125$], although ascospore viability was not impacted (**Figure 3-15C,D**). The complementation strain AN3147-3C15 showed restoration of both the number of cleistothecia and also number of spores (**Figure 3-15A,C**).

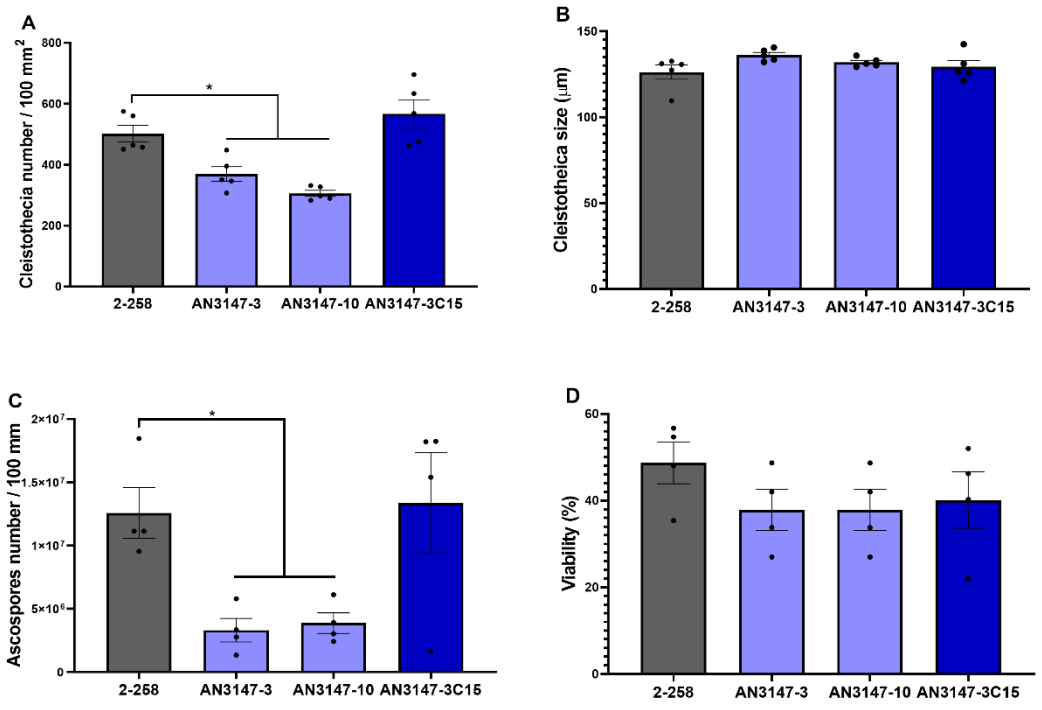

Figure 3-15 Sexual development of ΔAN3147.2 deletion and complementation and control (2-258) strains of *A. nidulans*. ΔAN3147.2 strains showed defects in fruit body formation as compared to parental strain 2-258 and the complement strain AN3147-3C15. **A** represents number of cleistothecia produced by the various strains per unit area as determined by

microscopy. **B** represents the size (diameter) of cleistothecia size as measured by microscopy. **C** represents the number of ascospores collected from agar plugs with a defined surface area. **D** represents the viability of ascospores collected from cleistothecia when a defined number were spread out onto plates. Dots indicate biological replicates in each section. Error bars indicate ± SEM. * represents significant difference from controls at P<0.05.

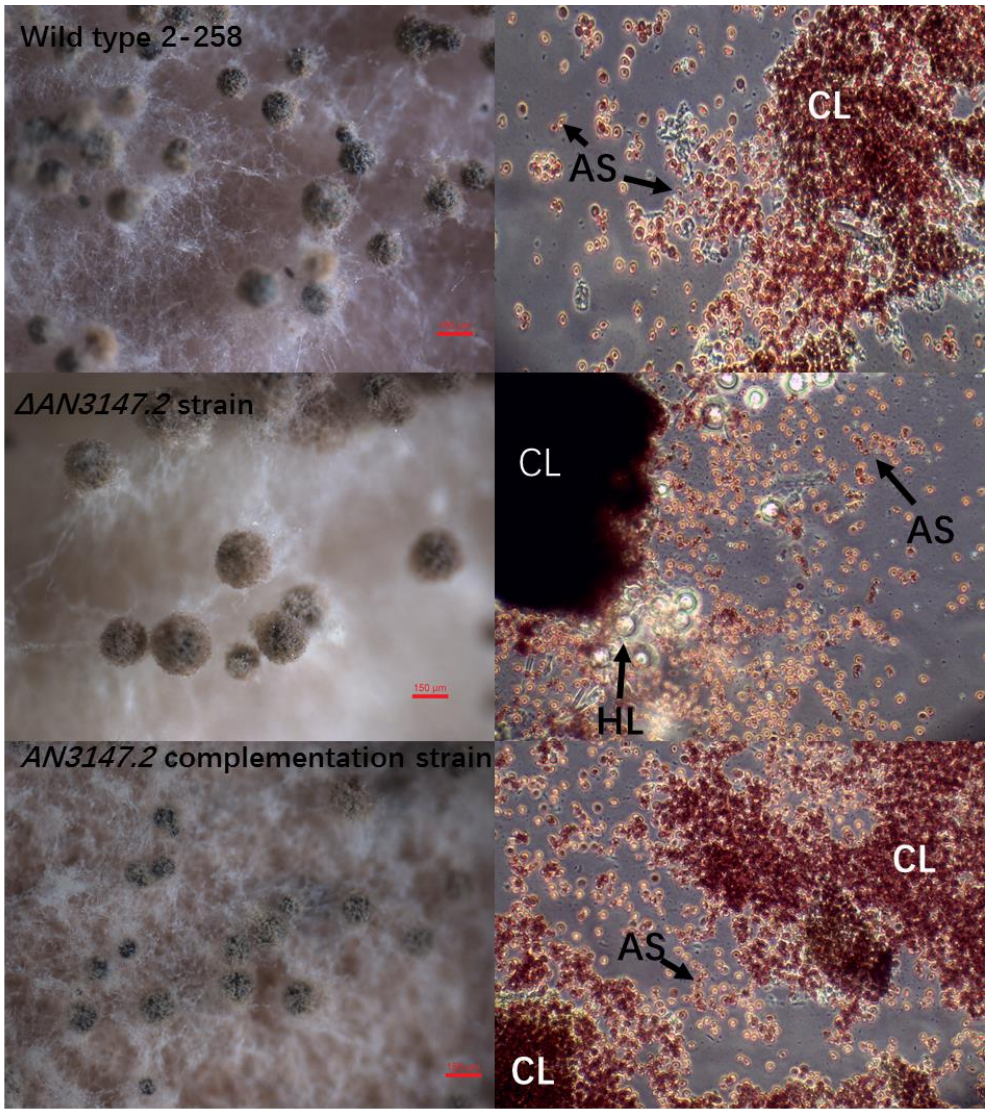

Figure 3-16 Fruit body (cleistothecial) development of *ΔAN3147.2*, complementation and control strains of *A. nidulans.* Images show sexual development in the gene knock out *ΔAN3147.2* strain as compared to the 2-258 parental control strain and *ΔAN3147.2* complementation strain. CL: cleistothecia; AS: ascospores; HL: hülle cells.

Second, BLAST searching with the PRO41 sequence from *S. macrospora* (XP_003347542.1) identified a possible homolog AN10631.2 in *A. nidulans*,

which shared 48 % identity and returned an E-value score of $2.7e^{-20}$ (**Appendix 20**). AN10631.2 showed 50 % identity with HAM-6 (XP_964262.1) from *N. crassa*. This was a relatively low match compared to most other candidate genes (**Table 3.2**) and other possible candidate homologs were identified (results not shown). Due to time limitations work was only persued with AN10631.2 Two *Δ10631.2* transformants were obtained, termed ΔAN10631-5 and ΔAN10631-8 which exhibited correct patterns of knock out integration (**Appendix 25 to 26**). Gene deletion did not result in any significant change in sexual development compared to control strains (**Figures 3-17A-D, 3-18**).

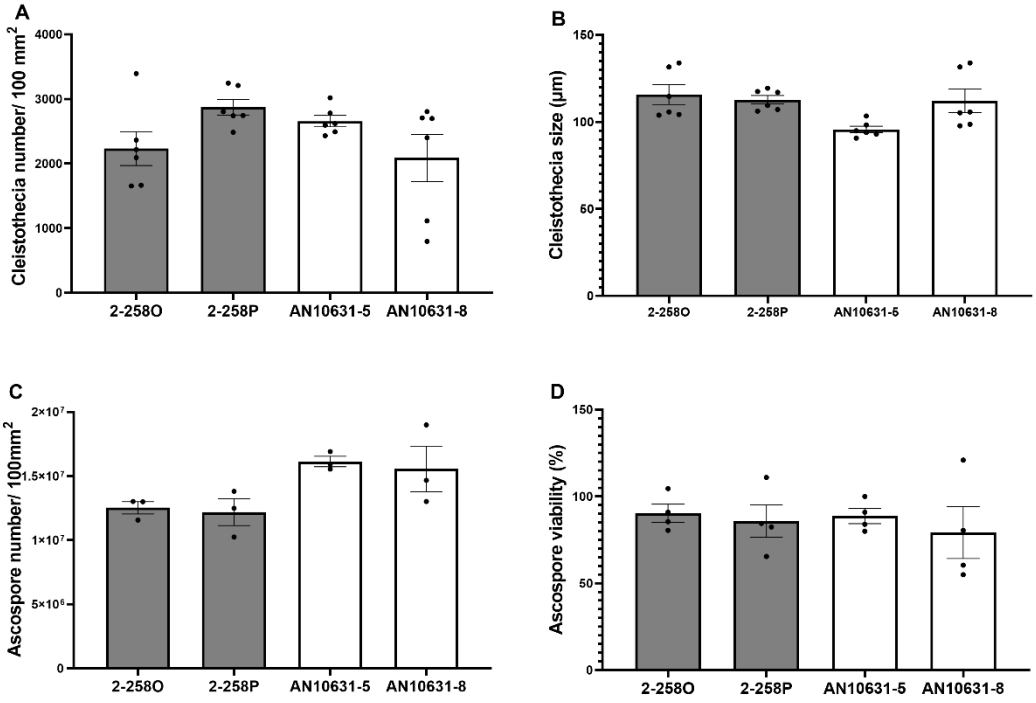

Figure 3-17 Sexual development of ΔAN10631.2 deletion and control (2-258) strains of *A. nidulans*. A represents number of cleistothecia produced by the various strains per unit area as determined by microscopy comperting to parental strains 2-258O and 2-258P. **B** represents the size (diameter) of cleistothecia size as measured by microscopy. **C** represents the number of ascospores collected from agar plugs with a defined surface area. **D** represents the viability of ascospores collected from cleistothecia when a defined number were spread out onto plates. Dots indicate biological replicates in each section. Error bars indicate ± SEM.

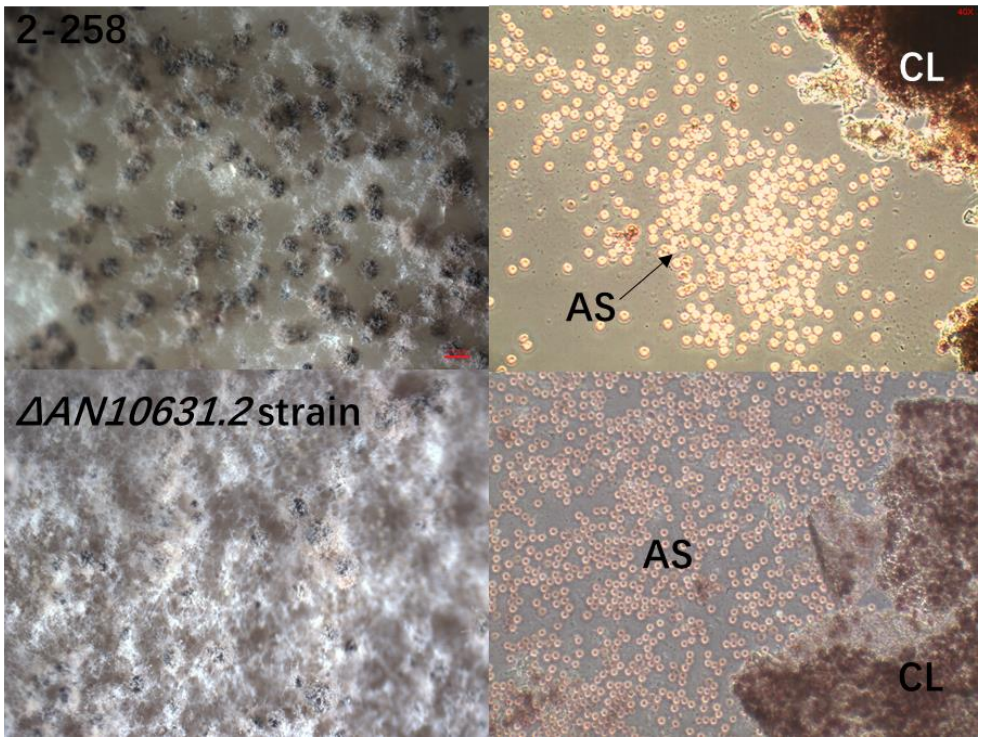

Figure 3-18 Fruit body (cleistothecial) development of *ΔAN10631.2* and control (2-258) strain of *A. nidulans.* Images show sexual development in the gene knock out *ΔAN10631.2* strain as compared to the 2-258 parental control strain. CL: cleistothecia; AS: ascospores.

Third and finally, BLAST searching with the ASF-1 sequence from *S. macrospora* (XP_003345657.1) identified a possible homolog *AN4891.2* in *A. nidulans* that showed 83.8 % identify (**Table 3-2; Appendix 21**). Despite several attempts, it was not possible to obtain any correct *ΔAN4891.2* deletion strains, with the only transformants obtained showing ectopic integration (**Appendix 25**). This suggested that this putative histone chaperone is essential for general growth of the species and work was not pursued.

3.4 Discussion

3.4.1 Optimum temperature for sexual development in *A. nidulans*

Since the pioneering work of Pontecorvo (1951), the sexual cycle of *A. nidulans* has routinely been induced in laboratories worldwide at 37 °C following the procedures first set out by Pontecorvo. However, previous research at the University of Nottingham assessing the effects of various factors on sexual cycle of *A. nidulans* (including sealing plates at different time points, incubating plates in three different stacking arrangements, and incubation at either 32 °C or 37 °C) had suggested that 37 °C might not be the optimum temperature for reliably inducing sexual reproduction in *A. nidulans* (Ashour, 2014).

Following on from the previous study of Ashour (2014), the present work tested the effect of temperature on sexual development in a representative set of wild-type, *veA1*, and *kuB* mutant strains of *A. nidulans*. The wild-type isolates and the Δ*kuB* isolate 2-258 all generally formed maximum numbers of cleistothecia at 32 °C, whereas the *veA1* isolate 2-149 was unusual in forming more cleistothecia at 37 °C. Most isolates showed a reduction in ascospore production at 37 °C, expect for the *veA1* isolates 2-149 and 2-154, and wild-type isolate 2-224, but there was no significant increase in ascospore production for most isolates between 25 °C and 32 °C, despite the increased number of mature cleistothecia observed at 32 °C. The potential reason for this apparent disparity might be that supposed 'immature' cleistothecia under the size of 100 µm in diameter, observed at 25 °C and 28 °C, did actually contain ascospores which would have contributed to the overall level of ascospore formation recorded at these lower temperatures.

Taken as a whole, these results indicate that a temperature of 32 °C is to be recommended for the induction of the sexual cycle in *A. nidulans* when using wild-type strains of *A. nidulans.* This temperature was also adopted for further

experimental work in the present study with the key strain 2-258. However, it is cautioned that most laboratory strains worldwide share a common origin to the *veA1* mutant strains 2-149 and 2-154, so there might not be an advantage to incubation at a lower temperature of 32 °C to induce sex in such strains. Also rates of ascospore germination were not tested at each temperature, and there could conceivably be variation according to incubation temperature.

3.4.2 *A. nidulans* as a model for sexual development in the Ascomycotina

A. nidulans has long been used as a model for understanding sexual development in the Ascomycotina. However, standard models proposed [e.g. those of Pöggeler et al. (2006) and Dyer and O'Gorman (2012)] do not yet include certain genes shown to have roles in sexual development in various other ascomycete species as these have yet to be characterised in *A. nidulans*. Studies were therefore undertaken to determine if such genes influenced sexual development in *A. nidulans* in order to determine if these genes were indeed 'universal' ascomycete sex genes. Overall it was found that the majority of genes investigated did indeed impact on sexual development in *A nidulans.* However, very few of the genes proved to be essential for sexual reproduction, unlike some previously reported genes (Dyer and O'Gorman, 2012), with gene deletion instead mostly resulting in a decrease of production of cleistothecia and ascospore production rather than a total loss. The impact of gene deletion also had some different outcomes to those described for other ascomycete species as will now be discussed (summarised in **Table 3-3**). It should be noted that for all genes under investigation, the approach used was to compare sexual fertility between control and gene deletion strains in terms of number of cleistothecia formed, number of ascospores formed, and the viability of ascsopores. There were no apparent major growth rate differences between most of the control and gene deletion strains. However, this was not formally

investigated and so it is cautioned that slight reductions in growth in gene deletion strains might have partly been responsible for any observed decrease in sexual fertility.

Table 3-3 Phenotype of gene knock out strains in *A. nidulans*

Strain	Sexual fertility			
	No. of cleistothecia	Diameter of cleistothecia	No. of ascospore	Ascospore viability
ΔAN2701.2	Increase	Decrease	Decrease	Decrease
ΔAN6611.2	Defect vegetative growth			
ΔAN4632.2	Normal	Normal	Normal	Normal
ΔAN0164.2	Decrease	Decrease	Decrease	N/A
ΔAN4813.2	Decrease	Normal	Decrease	Decrease
ΔAN7170.2	Normal	Normal	Normal	Decrease
ΔAN7736.2	Normal	Normal	Normal	Normal
ΔAN1217.2	Decrease	Increase	Normal	Normal
ΔAN3147.2	Decrease	Normal	Decrease	Normal
ΔAN10631.2	Normal	Normal	Normal	Normal
ΔAN4891.2	Failed to obtain deletion strain			

3.4.1.2 *AN2701.2* MAPK scaffold protein

The mitogen-activated protein kinase (MAPK) module is a highly conserved signal transduction pathway in eukaryotes. In 2007 an additional member of the module, IDC1 was identified from *P. anserina* which affected protoperithecial formation, with gene deletion resulting in a defect in the transition of ascogonia into protoperithecia (Jamet-Vierny et al., 2007). The homolog HAM-5 was studied in greater depth in *N. crassa*, and evidence provided that it acts as a scaffold protein and is required for hyphal fusion (Dettmann et al., 2014; Jonkers et al., 2014). A homolog *Trire2: 67350* was also shown to effect female fertility in *T. reesei* (Linke et al., 2015). Deletion of the homolog AN2701.2 in the present study was also found to impact on sexual development in *A. nidulans.* Gene deletion resulted in a significant increase in number, but decrease in size, of cleistothecia when the sexual cycle was

induced on Aspergilllus complete media (ACM), together with a drastic reduction in the number and viability of ascospores. This result provides further support for a conserved role of the MAPK module in sexual development in the Ascomycotina. Indeed, during the course of studies, it was discovered that another group had also been studying *A. nidulans* AN2701.2. Frawley et al. (2018) undertook biochemical characterization of the protein and confirmed that AN2701.2 (which they named *hamE*) acts as a scaffold protein that associates kinase phosphorylation and signalling in the AnSte11-Ste50-Ste7-Fus3 module, which is involved in the pheromone signalling and sexual sporulation of *A. nidulans* (Bayram et al. 2012). However, when Frawley et al. (2018) evaluated the impact of *hamE* (AN2701.2) gene deletion, they only screened for sexual development on a glucose minimal medium (which they also used for growth and inducing sexual sporulation). The deletant strain failed to make cleistothecia and it was suggested that *hamE* was essential for sexual development. However, results from the present study showed that sexual development is possible on ACM (albeit at a much reduced level), indicating that nutrient composition can effect outcomes relating to this gene. We also observed a block of sexual development in our ΔAN2701.2 deletion strain when using the same Glucose Minimal Medium as Frawley et al. (2018) (**Figure 3-3**).

3.4.2.2 STRIPAK unit proteins

The STRIPAK complex was first discovered in human and reported to be a mediator of several signal transduction pathway for regulation of cell development (Shi et al., 2016). The homolog in the fission yeast was named the SIN-inhibitory PP2A complex (SIP) for its function in the septation initiation network (Singh et al., 2011). In filamentous fungi, a number of studies involving *Sordaria* and *Neurospora* have revealed that the complex is pivotal for fruit body development (Simonin et al., 2010; Bloemendal, et al., 2012; **Section 1.4.4**).

In the case of *A. nidulans*, Son and Osmani (2009) isolated AN0164.2 as a phosphatase, and their study suggested that AN0164.2 contained an PP2Ac domain similar to that of the human PP2Ac (Goudreault et al., 2008). Deletion of this gene caused defective growth in *A. nidulans* (), but its function in sexual development was not evaluated and the protein was not explored as a possible subunit of the STRIPAK complex (**Figure 1-5; Section 1.3.2.4**) . In the present research, AN0164.2 was identified as a likely PP2Ac component unit in the STRIPAK core. Deletion of AN0164.2 was shown to block fruit body development at an early stage and it proved impossible to isolate viable ascospores because cleistothecia appeared immature. The homolog PP2Ac1 in *S. macrospora* is similarly an essential factor in perithecial formation, hyphal fusion and growth, and has a role in stress resistance (Beier et al., 2016). PP2Ac1 was found to interact with PRO22, the STRIP1/2 unit of the STRIPAK complex (**Figure 1-5; Section 1.3.2.4**). Linked to this, we detected a PRO22 homolog AN6611.2.2 in *A. nidulans*. In the present research, deletion of AN6611.2.2 appeared to have a great impact on development in *A. nidulans*, with severely defective vegetative growth evident (**Figure 3-7**). In *S. macrospora*, PRO22 is associated with the tubular and vesicular vacuolar network, and has a function in ascogonia septation, which is the initial stage of fruit body development (Bloemendal et al., 2010). Therefore, it is possible the AN6611.2 might be involved in the fundamental development of hyphae that is essential for maintaining normal growth.

Another STRIPAK subunit identified in this study was AN4632.2, the putative SLAMP unit (**Figure 1-5; Section 1.3.2.4**). The SLAMP unit in *N. crassa* HAM-4 is regarded as a core unit of its STRIPAK complex (Simonin et al., 2010). However, deletion of AN4632.2 did not appear to impact on sexual development in *A. nidulans.* This was surprising given that the SLAMP unit PRO45 is required for sexual development in *S. macrospora*, and interacts with

other STRIPAK subunits such as the striatin unit PRO11 and MOB3 (Nordzieke et al., 2015). Similarly, in *N. crassa* HAM-4 influences ascospore formation (although formation of perithecia is not affected), and interacts with the homologous units Ppg1 and HAM-2 that are essential for hyphal fusion and fruit body development (Simonin et al., 2010; Dettmann et al., 2013).

The first STRIPAK subunit identified in *A. nidulans* was the striatin unit StrA. This protein regulates sexual development as deletion of the *strA* gene reduced cleistothecia size and ascospore number; while overexpression promoted cleistothecia formation (Wang et al., 2010). StrA localizes to the endoplasmic reticulum and nuclear envelope, which suggests a role in the Ca2+/calmodulin signalling pathway (Wang et al., 2010). Recently, other STRIPAK units were unveiled by tandem affinity purification (TAP), GEP pull-down and LC-MS/MS protein identification methods (Elramli et al., 2019). Following on from these findings, Elrami et al. (2019) proposed that the STRIPAK complex in *A. nidulans* is constructed of MOB3 SipA, SIKE SipB, STRIP1/2 SipC (AN6611.2), SLAMP SipD (AN4632.2), PP2Ac SipE (AN0164.2; PgA), and PP2AA SipF subunits. It was suggested that SipA interacts with StrA in all stages of development including the vegetative growth and the sexual cycle, and as well as with SipB. The gene *sipD* (AN4632.2) was expressed during both developmental stages, but after 48 hours of the sexual cycle the expression reduced dramatically (Elramli et al., 2019). Deletion of SipB, SipC, SipD and SipE decreased hyphal growth rate and conidiation, and blocked fruit body formation (Elramli et al., 2019). The localization of the complex was dependent on StrA, which is thought to act as a platform for the interactions between the subunits. Given StrA as the platform, it was proposed that SipA, SipB-SipD heterodimer and SipC-SipE-SipF heterotrimeric interacts with StrA, respecitively, and finally the fully functional AnSTRIPAK complex is constructed which regulates MpkC for

oxidative stress and MpkB for sexual development via their MAPK pathways (Elramli et al., 2019; Jun et al., 2011).

In conclusion, the STRIPAK complex in filamentous fungi such as *A. nidulans, N. crassa* and *S. macrospora* appears be conserved in both overall structure and function. In *N. crassa*, the complex contains straitin HAM-3, STRIP (HAM-2), SLAMP (HAM-4), MOB-3, PPG1 and PP2AA, with HAM-2 and HAM-3 forming the core components for the assembly of other subunits at the nuclear envelope (Dettmann et al., 2013). In *S. macrospora,* PRO11, PRO22, MOB3, PP2Ac and PP2AA form the central core of the STRIPAK complex (Bloemendal et al., 2012). In *A. nidulans*, StrA forms tetramer via its N-terminal coiled-coil domain and behaves as the scaffold and binds with the other three subcomplex through its C-terminal WD40 repeat domain, including the SipB-SipD (AN4632.2) complex, SipA, and the SipC(AN6611.2)-SipE(AN0164.2)-SipF complex (Elramli et al., 2019; Kück and Stein, 2021). The fungal STRIPAK complex is therefore a key signaling mediator that regulates sexual development, hyphal fusion, stress resistance and secondary metabolism and it is likely that deletion of most sub componets will impact on sexual development (Wang et al, 2010; Bloemendal et al., 2010; Bloemendal et al., 2012; Dettmann et al., 2013; Beier et al., 2016; Elramli et al., 2019; Kuck and Stein, 2021).

3.4.2.3 *MybA* transcription factor protein

The *myb* gene family encodes transcription factors binding to a specific DNA sequence to regulate gene expression and thereby affect cell growth and differentiation (Oh and Reddy, 1999). A putative *myb* transcription factor *AN4813.2* was here identified in *A. nidulans*, with results indicating that it is an activator of conidiation and involved in later stages of fruit body development. Deletion of *AN4813.2* first resulted in defects in asexual conidiation together

with production of an unknown orange pigment, although hyphal growth appeared not to be effected. The phenotype of defective asexual conidiation is similar to that seen following mutation of *mybA* in *A. fumigatus* where MybA was shown to strongly regulate the expression of *wetA* [a gene regulating conidia formation (Ojeda-Lopez et al., 2018)]*, vosA and velB* during conidial development and trehalose metabolism in *A. fumigatus* (Valsecchi et al., 2017). In the present research, conidiation was also blocked following deletion of *mybA*, suggesting that it might also regulate expression of *wetA, vosA* and *velB* genes in *A. nidulans* as well. Second, *mybA* deletion impaired sexual development in *A. nidulans*, significantly reduced numbers of mature cleistothecia with smaller and less mature cleistothecia being evident. However, null *AN4813.2* strains were still able to form cleistothecia and Hülle cells. Gene deletion also greatly affected ascospore production, with ascospore numbers dramatically reduced in the mutant strains and ascospore viability was impaired. This is importantly believed to be the first report of the role of the MybA family on fungal sexual development, as difficulties in inducing sex in *A. fumigatus* Af293 derivatives had not allowed Valsecchi et al., (2017) to evaluate any impact in sex.

It is possible to speculate about the underlying mechanism of MybA acivity. In *A. fumigatus* MybA was found to control expression of two trehalose synthetic genes in the pathway which leads to production of trehalose phospharylase, therefore *mybA* deletion led to reduced trehalose accumulation that caused a loss of conidial viability (Valsecchi et al., 2017). MybA also regulated the expression of *vosA and velB* during conidial development (Valsecchi et al., 2017). In parallel, Ni and Yu (2007) showed that *vosA* influences levels of conidiospore production and trehalose accumulation in conidia. Therefore, *mybA* deletion might lead to down regulation of *vosA* and *velB*, which are genes required for normal sexual development of *A. nidulans*. The gene *vosA* is highly

expressed in sexual spores and during trehalose synthesis (Kim et al., 2020). Mutation of *vosA* resulted in impaired ascospore viability due to a reduced synthesis of trehalose, which is needed to protect ascospores from environmental stressors such as heat and oxidative chemicals (Kim et al., 2020). VosA also interacts with VeA and VelB to form the velvet complex, which activates sexual development in darkness (Bayram et al., 2008; Park et al., 2014). Given these roles of *vosA* and *velB*, it would be of interest in further work to assess the expression level of these genes and the production of trehalose in *ΔAN4813.2* deletion strains. Looking ahead it would also be of interest to study the role of *mybA* in sexual development of *A. fumigatus* considering the close phylogenetic relationship of the species with *A. nidulans*.

It is noted that *AN4813.2* is not the only Myb-domain transcription factor to have been described from *A. nidulans*. FlbD in *A. nidulans* is a Myb transcription factor that regulates *brlA* expression and is therefore required for asexual conidiation. Gene deletion also effected sexual development, a knock-out strain failing to form the normal external tissues of cleistothecia, instead leaving Hülle cells and naked asci and viable ascospores lacking external peridium tissues (Arratia-Quijada et al., 2012). These results suggest a conserved role for Myb-domain transcription factors in morphological development in the aspergilli. Hypothetically, *AN4813.2* might be not in a central position of sexual development as fruit body development was not impaired at an early stage, but it could act upstream of *vosA* and *velB* which impact ascospore maturation.

3.4.2.4 Transcription factors *AN1217.2, AN7170.2* and *AN7736.2*

Three different transcription factors with possible involvement in sexual development of *A. nidulans* were investigated. First, deletion of the putative homeobox transcription factor *AN1217.2* led to a block in asexual conidiation similar to the phenotype seen in *A. flavus* where Δ*hbx1* strains showed reduced

expression of the conidiation related genes *brlA* and *abaA* (Cary et al., 2017; Ojeda-Lopez et al., 2018). In *A. flavus,* sclerotial formation (and therefore sexual development) was also blocked following deletion of *hbx1,* and the expression of *nsdC* and *veA* decreased as well (Cary et al., 2017). It was therefore hypothesized that *AN1217.2* might be a repressor of sexual development in *A. nidulans*. It may be speculated that the difference in results between *A. flavus and A. nidulans* relates to the different nature of their fruit body types. *A. flavus* forms sclerotia containing cleistothecia that are different in structure to the non-enclosed cleistothecia of *A. nidulans* (Horn et al., 2012; Dyer and O'Gorman, 2012). Taking into account that *hbx1* repressed *nsdC* and *veA* expression in *A flavus*, it would be worthwhile examining further the function of *AN1217.2* in *A. nidulans* by overexpression tests. Indeed, work was begun to study the effect of overexpression of *AN1217.*2 but because of time pressures this work was not completed.

Second, the *sclR* homolog of *AN7170.2* was investigated. Deletion of *sclR* caused reduction of sclerotial formation and promotion of conidiation in *A. oryzae* (Jin et al., 2011) and it was considered might therefore impact negatively on sexual development in *A. nidulans.* However, gene deletion did not impact on the number and size of cleistothecia and ascospore numbers. Unexpectedly though a significant reduction in ascospore viability was apparent. Possible reasons for the differences between *A. oryzae and A. nidulans* might again relate to the different nature of their fruit body types; *A. oryzae* forming sclerotia compared to the non-enclosed cleistothecia of *A. nidulans* (Dyer and O'Gorman, 2012) so that *sclR* might be required principally only for sclerotia formation.

Third, deletion of *AN7736.2* did not influence sexual development although in the homolog *Trire2: 59270* from *T. reesei* the was reported to be involved in sexual development (Linke et al., 2015). Because of limited studies on *Trire2:59270* the possible reason for species specificity remains to be revealed.

3.4.2.5 Other candidate genes - *AN3147.2*, *AN10631.2* and *AN4891.2*

Three final candidate genes with roles in sexual development were investigated. First, a *het-c2* homolog gene, *AN3147.2*, was identified in *A. nidulans* and shown to affect certain aspects of the formation of cleistothecia. The first step in sexual development is hyphal fusion, therefore the self/non-self recognition system associated with the process might be predicted to have a role in sexual development (Dyer et al., 1992). A diverse set of genes are involved in heterokaryon incompatibility including *het* and even mating-type genes in certain species (Pàl et al., 2007). It has been speculated that *MAT* genes may function in vegetative incompatibility to promote initiation of the sexual cycle, while the *het* genes are responsible for allorecognition, to avoid the possible spread of harmful chromosome elements (Pàl et al., 2007). Anwar et al. (1993) identified various *het* loci from *A. nidulans* by protoplast fusion of diverse isolates, and their findings suggest that there might be at least eight and a maximum 18 *het* loci. However, any role in sexual development was not investigated. Although the main function of *het* loci is to avoid mixing of dissimilar nuclei, they might nevertheless have a role in sexual development as well (Dyer at al., 1992; Pàl et al., 2007). In the case of *P. anserina,* the gene *het-c2* encodes a glycolipid transfer protein with a role in vegetative incompatibility, perithecia formation and ascospore production (Saupe et al.,1994; Shui et al., 2000). Deletion of *het-c2* resulted in defects in the number and size of ascospores, which was supposed to be caused by the abnormal distribution of nuclei (Saupe et al., 1994). Bastiaans et al. (2017) later confirmed that *het-c* is a highly diverse gene involved in pathogen-defense and allorecognition, with the *het-c2* variant being the most widely distributed in their study collection. In this study, deletion of the homologous gene *AN3147.2* in *A. nidulans* led to a reduction in cleistothecia production. However, in contrast to studies in *P. anserina* the development of ascospores was not affected greatly

and viability of ascospores showed no significant difference to controls. It may be hypothesised that *AN3147.2* might be involved during the initial stage of fruit body development in *A. nidulans*, with *het* gene divergence involved with regulating hyphal fusion to form cleistothecial initials. However, further work is required to investigate this hypothesis, including studies to determine if *AN3147.2* alleles show diversification consistent with *het* gene activity. Elsewhere, in *N. crassa*, the *tol* gene is associated with heterokaryon incompatibility and the mating-type genes *matA-1* and *mata-1.* Shiu and Glass (1999) hypothesised that *tol* is a divergent *het* locus that affects incompatibility, whilst *matA-1* and *mata-1* act solely in sexual development. Another hypothesis is that TOL interacts with the MATA-1/MATa-1 complex or their downstream products to trigger the incompatibility (Shiu and Glass,1999).

Second, a putative *PRO41* homolog *AN10631.2* was identified from *A. nidulans.* Despite the fact that mutation of *PRO41* resulted in an early block in sexual development in *S. macrospora* (Nowrousian et al., 2007) gene deletion of *AN10631.2* failed to have any impact on sexual development in *A. nidulans*. Although a 'negative' result, this was nevertheless potentially important in illustrating that not all proposed ascomycete 'sex' genes might have genus-wide applicability. However, it is cautioned that AN10631.2 showed only 48-50% identity with PRO41 and HAM-6 from *S. macrospora* and *N. crassa,* respectively. Therefore an alternative explanation might be that *AN10631.2* was not a true homolog of *PRO41.* Indeed, further independent BLAST searching revealed that the actual *PRO41* homolog in *A. nidulans* might be *AN5458* (M Bromley pers comm.) and thus further experimental work is required to verify if a *PRO41* homolog has a role in sexual development of *A. nidulans.*

One final target was the homolog of the ASF-1 histone chaperone, which has been shown to be required for sexual development in *S. macrospora*

(Gesing et al., 2012; Schumasher et al., 2018). However, it was not possible to obtain any viable *AN4891.2* knock-out strains, suggesting that this is an essential gene in *A. nidulans.*

3.4.3 Conclusions

It was established that incubation at 32ºC led to increased levels of cleistothecia and ascospore production for most study strains of *A. nidulans* compared to the 'traditional' 37 ºC temperature of Pontecorvo (1953). This temperature was therefore used in subsequent experimental work.

Screening of a series of potential 'sex' genes that might be required for sexual reproduction revealed that the majority of the candidate genes were indeed involved with sexual reproduction in *A. nidulans* as with other members of the Pezizomycotina, so could be considered genus-wide 'sex' genes. Deletion of some genes had a broadly similar impact on sexual development as with other ascomycete species e.g. the *AN2701.2* MAPK scaffold, and the *AN0164.2* and *AN6611.2.2* STRIPAK genes. However, critically some other genes had a different impact in sex e.g. deletion of the *AN3147.2 het-c* gene did not affect ascospore development (unlike *P. anserina*; Saupe et al., 1994); deletion of the *AN7170.2 sclR* gene resulted in lowered ascospore viability (unlike *A. oryzae*; Jin et al., 2011); and sexual development was still possible, albeit at a reduced level, following deletion of the *AN1217.2* homeobox gene (unlike *A. flavus*; Cary et al., 2017). Meanwhile, deletion of certain genes had no apparent impact on sexual development despite these genes being required for sexual development in other pezizomycete species e.g. the *AN4632.2* STRIPAK subunit gene not being needed (unlike *N. crassa* and *S. macrospora;* Simonin et al., 2010; Dettmann et al., 2013; Nordzieke et al., 2015), and the *AN10631.2* putative *PRO41* gene [unlike *S. macrospora* (Nowrousian et al., 2007), although it is uncertain whether AN5458 might instead be a better match

for *PRO41*]. It was also exciting to report for the first time that the *AN4813.2 mybA* transcription factor gene is required for fruit body development in the Pezizomycotina.

Chapter 4 The Potential Role of HMG Genes in Sexual Development of *A. fumigatus*

4.1 Introduction

The fungus *Aspergillus fumigatus* can cause opportunistic infections in humans, most notably invasive aspergillosis of the lung, especially when patients have compromised immune systems (e.g. leukaemia or lymphoma; Coméra et al., 2007; McCormick et al., 2010; Orciuolo et al., 2007). Key factors that contribute towards the ability of *A. fumigatus* to cause infections are properties of the asexual spores, thermo-resistance, and secondary metabolite production (Ben-Ami et a.l, 2009; McCormick et al., 2010). For example, gliotoxin, a key secondary metabolite produced by *A. fumigatus*, is thought to contribute to virulence. Gliotoxin production is regulated by the gliotoxin biosynthesis cluster, which contain 13 genes, with the expression of some genes being co-regulated with asexual development (Scharf et al., 2012; Schoberle et al., 2014). The evolution of antifungal drug resistance is another complicating factor that has affected the treatment of infections by *A. fumigatus*. Most notably there are now worldwide reports of a sub-set of isolates of *A. fumigatus* which exhibit resistance to azoles, the most widely used antifungal drugs for treatment of aspergillosis (Arendrup et al., 2010).

The main source of infection has long been thought to be via inhalation of asexual conidial spores into lung. However, in 2009 it was reported that *A. fumigatus* is also able to reproduce sexually under certain environmental conditions, providing another possible source of inoculum in the form of ascospores (O'Gorman et al., 2009). Thus, it has been speculated that the sexual cycle might lead to the generation of novel forms of antifungal resistance

and promote the spread of antifungal resistance genes worldwide (Zhang et al., 2017; Swilaiman et al., 2020; Krofanty et al., 2021). Various tandem repeats (TR) in the *cyp51* promotor region have been associated with different azole resistant phenotypes, and a novel TR_{46}^{3} mutation was postulated to have arisen via sexual reproduction from an orginal TR_{46}^{2} genotype (Zhang et al., 2017). Isolates of *A. fumigatus* from world-wide locations have been shown to be able to complete mating and form ascospores, albeit even at a relatively low rate, and therefore outcrossing has made genetic exchange possible (Swilaiman et al., 2020; Krofanty et al., 2021) Therefore a better understanding of the regulation of sexual development in *A. fumigatus* is hoped to provide insights that might be of fundamental interest but also have biomedical applications.

4.1.1 Mating-type (MAT) and high mobility group (HMG) genes

Mating-type (*MAT*) genes act as transcriptional activators that are pivotal in regulating the correct expression of target genes during sexual development as already described **Section 1.3.2.1** (Dyer et al., 2012; Lee et al., 2010). Within the aspergilli, heterothallic species such as *A. fumigatus* are composed of isolates of either MAT1-1 mating type, which contain a *MAT* locus encoding an α-domain MAT1-1 protein, or MAT1-2 mating type, which contain a *MAT* locus encoding a high mobility group (HMG) MAT1-2 protein (Paoletti et al., 2005; Dyer and O'Gorman, 2012). By contrast, homothallic species such as *A. nidulans* contains both α-domain and HMG *MAT* genes in the same genome (Paoletti et al., 2007; Dyer and O'Gorman, 2012). The MAT loci of heterothallic species contain highly diverged regions of DNA in the MAT1-1 versus MAT1-2 mating types, and so these *MAT* locus regions have been named 'idiomorphs' to acknowledge the high sequence divergence (Dyer et al., 2016). It was thought that the α-domain MAT1-1 and HMG MAT1-2 proteins had different evolutionary origins given their high sequence divergence. However, Martin et

al. (2010) investigated the similarity of α-helices found in the α1 domain in MAT1-1 and those found in *SOX_HMG*, which is a conserved HMG protein involved in animal sexual determination. The first three α-helices were found to show significant similarity between MAT1-1 and SOX_HMG, while a fourth helix at the C-terminus was distinct, which indicated that MAT1-1 was in fact a member of the HMG protein family and the encoding gene family was therefore named as *MATα_HMG* (Martin et al., 2010).

More widely, HMG proteins (so called as the first members to be identified were found to exhibit high mobility in gel electrophoresis) are transcriptional activators which can induce gene expression by binding to DNA and causing structural alterations (e.g. bending) that allow easier interactions with other proteins i.e transcription factors (Stros et al., 2007). HMG proteins have been shown to have a wide range of roles in developmental processes in eukaryotic organisms, with various protein super families recognised (Idnurm et al., 2008; Stros et al., 2007). For example, HMG genes involved in animal sexual differentiation have been cataloged into the SOX_TCF_HMG super-family containing T/A rich DNA sequence binding regions. HMG *MAT1-2* genes involved in fungal sexual development have been cataloged into the MATA_HMG family, again containing T/A rich sequence for DNA binding, with genes such as the *mat-HMG* or *MAT1-2* (*MAT2*) in *Aspergillius* species and other Pezizomycotina thought to represent an early diverged group of *HMG* genes (Idnurm et al., 2008). A third super family of HMG genes is the HMGB_UBF_HMG which contain non-specific DNA sequence binding regions (O'Sulliivan et al., 2002). It is fascinating to note that transformation of the human sex determination gene *SRY* into a sterile *ΔMAT2* (synonym *ΔMATA*) *A. nidulans* strain was able to restore sexual development, and that the downstream region of the *A. nidulans MAT2* (*MATA*) ORF (+18 to +36) contained an initiator element *Inr* which shares conserved features of *SRY*,

indicating the common evolutionary functions of the HMG gene family (Czaje et al., 2011). The analysis of *MAT-HMG* gene regulation in *A. nidulans* also identified a silencer element termed 'matA-SE' in the upstream region (-512 to -170) of the *MAT* locus; the deletion of mat-SE promoted *MAT2* (*matA*) transcription, whilst duplication reduced *MAT2* (*matA*) expression, although sexual development was not affected in either situation (Czaje et al., 2011). By contrast, the deletion of the *matA* ORF undoubtably affects sexual development in *A. nidulans*, with deletion of the gene leading to loss of ascospore production although some immature cleistothecia were formed (Paoletti et al., 2007).

At the start of the present studies, the main HMG genes studied in the Pezizomycotina were therefore almost entirely the *MATA_HMG* and *MATα-_HMG* family members (Martin et al., 2010). However, studies at the University of Nottingham by Ashour (2014) and Salih (2016) using the conserved HMG box core amino acid sequence in BLAST searches identified that there were at least five further HMG family members in the genome of *A. nidulans,* and gene deletion of four of these genes impacted on sexual development in *A. nidulans* (Ashour, 2014; Salih, 2016). The *A. nidulans* gene AN3667 was found to be essential for fruit body formation as both deletion and overexpression of this gene repressed cleistothecial formation (Ashour, 2014; Salih, 2016). Other HMG genes including AN1962, AN1267, AN2885, AN4734 (*MAT2*) and AN2755 (*MAT1*) were also shown to be required for normal sexual development, with the deletion of these genes resulting in a reduction in the development of cleistothecia (Salih, 2016). In parallel, Benkhali et al. (2013) detected eight HMG family genes in the genome of *Podospora anserina*. These genes could be classified into various HMG super family sub-members (**Figure 4-1**). Benkhali et al. (2013) systematically deleted all eight HMG genes in *P. anserina*, including MATA_HMG gene family members *PaHMG5* and *PaHMG8*, HMGB_UBF_HMG gene family members *PaHMG2*, *PaHMG3*, *PaHMG4* and

PaHMG6, and HMGB gene family members *PaHMG7* and *PaHMG9*. Their research identified different roles for the various HMG genes. Deletion of PaHMG3, PaHMG4, and PaHMG7 impacted on the distribution of fruiting-bodies on agar plates, although not directly on perithecial maturation. By contrast, deletion of PaHMG6, PaHMG8, PaHMG9 (KEF1) impaired female fertility, but not male fertility whereas PaHMG5 (homolog of *A. nidulans* AN36670) was a critical element in sexual development impacting on both female and male fertility (Benkhali et al., 2013). It was also found that PaHMG5 regulated PaHMG6 and PaHMG8 in an HMG module network (**Figure 4-2**) (Benkhali et al., 2013).

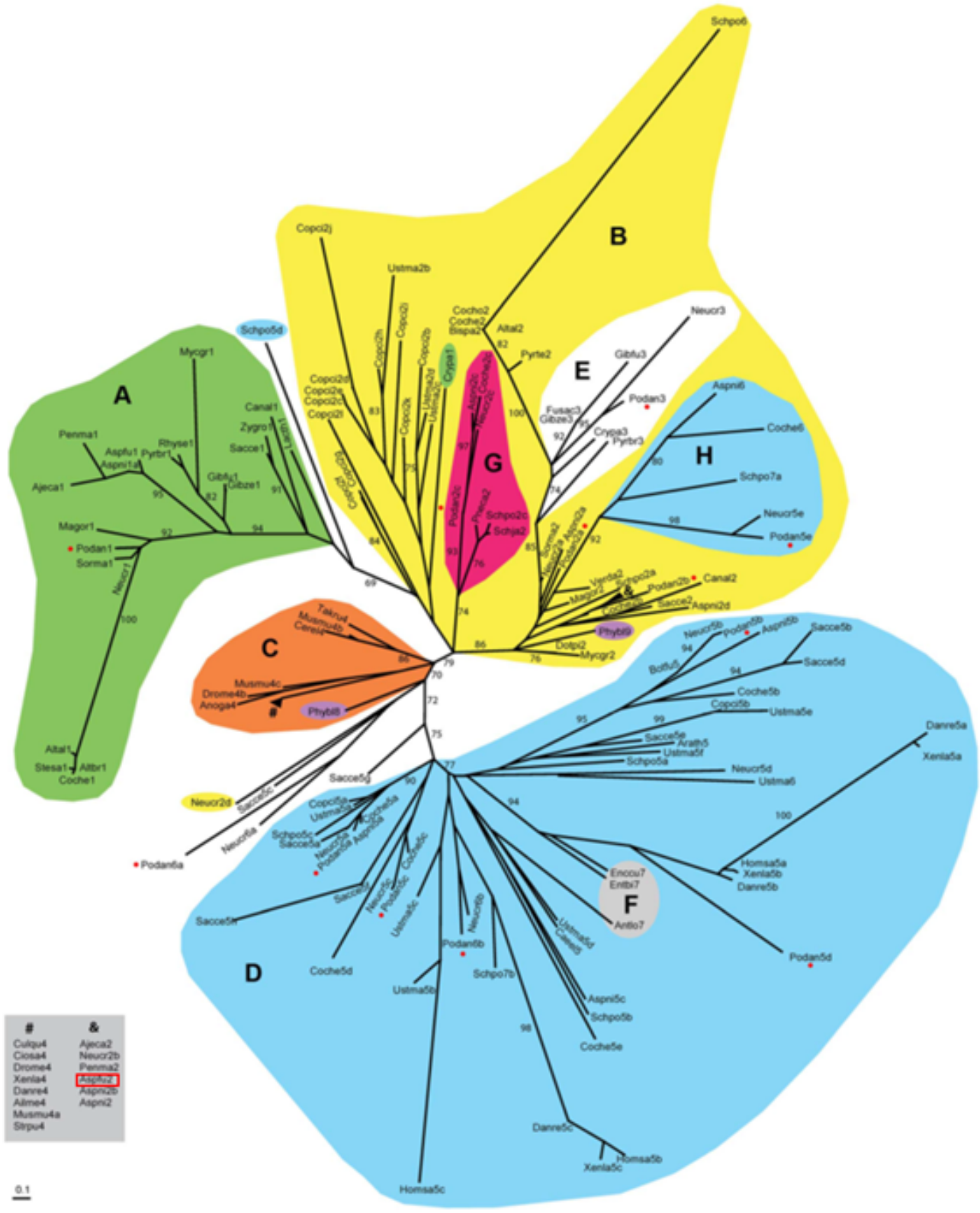

Figure 4-1 Phylogram for the HMG-box superfamily of *P. anserina* (Benkhali et al., 2013). HMG box domains of some plant, animal and fungi were classified into groups according to core amino acid sequenced. The HMG

genes of *A. fumigatus* are highlighted in red rectangle box. MATα_HMG is clade A. SOX-TCF_HMG is clade C, MATA_HMG is clade B, E and G, HMGB-UBF_HMG is clade D, F and H. Aspfu1 belongs to MATα_HMG (clade A); Aspfu2 belongs to MATA_HMG (clade B).

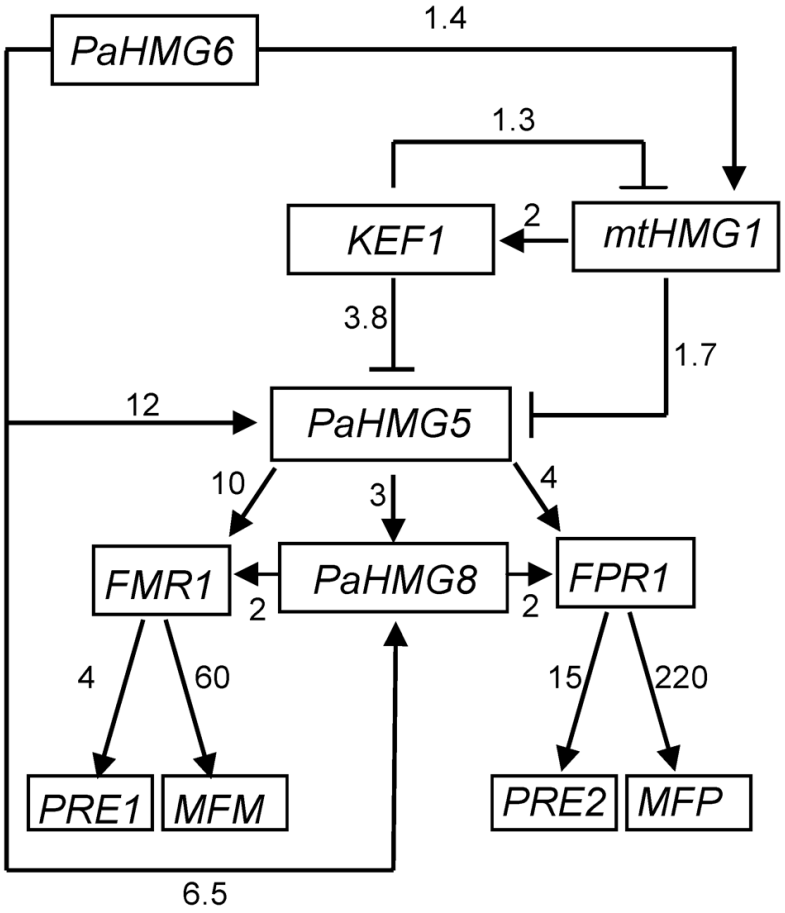

Figure 4-2 Regulatory network of HMG-box genes identifed in *Podospora anserina* (Benkhali et al., 2016). The number next to arrows represents the average FC in gene expression between the wild-type and mutant strains. FC = relative quantity of cDNA for the gene of interest x (geometric mean of relative quantity of cDNA for the normalization genes)$^{-1}$.

Taken as a whole, the studies of Benkahli et al. (2013), Ashour (2014) and Salih (2016) indicate that HMG genes in the genome beyond the classic *MAT-A* (MAT1-2) and *MAT-alpha* (MAT1-1) family genes have potential roles in regulating sexual reproduction in fungi, and might even have further functions given the high number of genes upregulated by the classic *MAT* genes (Dyer & Kuck, 2018).

4.1.2 Aims

The overall aim of work in the present chapter was to determine if HMG gene homologs in *A. fumigatus* have conserved functions in sexual development. This involved bioinformatic analysis to identify HMG gene homologs in *A. fumigatus* followed by gene deletion to determine if this impacted on the ability to form cleistothecia and ascospores. Specifically, HMG gene deletant strains were crossed with isolates of the opposite mating type of both wild-type background and also of the same *Δ*HMG gene deletion background i.e. the related HMG homologs in *A. fumigatus* were knocked out in both MAT1-1 and MAT1-2 background strains, respectively. In addition, as a control the *nsdC* gene in *A. fumigatus* was investigated by gene deletion approaches to determine if this gene is necessary for cleistothecial formation, which would be similar to the known sexual function in *A. nidulans* (Kim et al., 2009).

4.2 Materials and Methods

4.2.1 Strains

Wild-type strains used in experimental work were *A. fumigatus* 47-51 (MAT1-1) and 47-55 (MAT1-2), both highly fertile strains as reported by O'Gorman et al. (2009). In addition two sexually fertile Δ*kuB* strains were used to promote gene targeting in transformations, namely *A. fumigatus* 47-465 (MAT1-1) of Δ*kuB::prtA* background, and 47-466 (MAT1-2) of Δ*kuB::prtA* background. Strain 47-465 originated from progeny of a Δ*kuB* strain 47-51-8 × 47-55 cross, and strain 47-466 originated from progeny of Δ*kuB* strain 47-51-38 × 47-55 cross.

4.2.2 Solutions, buffer and media

KTC (KCl-Tris-$CaCl_2$) buffer

The buffer was prepared by dissolving 4.47 g KCl, 0.12 g Tris and 0.74 g $CaCl_2 \cdot H_2O$ (AnalaR@, UK) in 100 mL distilled water. The solution was adjusted to pH7.5 and autoclaved at 121 °C for 15 mins.

40% PEG 6000 solution

40 % PEG 6000 solution was prepared by dissolving 60 g PEG6000 (Fisher, UK), 0.12 g Tris base, and 0.74 g $CaCl_2 \cdot H_2O$ in 100 mL distilled water. The solution was adjusted to pH 7.5 with HCl and autoclaved at 121 °C for 15 mins. The PEG solution was filtered through a 0.22 µm syringe membrane filter before use to remove any precipitation.

KCl Citric acid buffer

The buffer was prepared by dissolving 4.47 g KCl and 1.05 g citric acid (Fisher, UK) in 100 mL distilled water. The buffer was adjusted to pH 5.8 NaOH and autoclaved at 121 °C for 15 mins.

5 M Potassium Acetate solution

The 5 M potassium acetate (AppliChem, Germany) solution was prepared by dissolving 49 g KAc in 100 mL distilled water.

3 M Sodium Acetate solution

The 3 M sodium acetate solution was prepared by dissolving 24.6 g NaAC in 100 mL distilled water.

DNA extraction buffer

The DNA extraction buffer was prepared by dissolving 12.1 g Tris, 29.2 g NaCl (Fisher, UK) and 100 mL of 0.5 M EDTA in 1 L distilled water. The solution was adjusted to pH 8.0 and autoclaved at 121 °C for 15 mins. After autoclaving, β-Mercaptoethanol was added to a final concentration of 10mM in the sterilized solution.

10% Sodium Dodecyl Sulphate (SDS)

The 10% SDS (Melford, UK) was prepared by dissolving 10 g SDS in 100 mL distilled water.

10X SSC buffer

The 10X SSC buffer was prepared by dissolving 44.12 g Na_3-Citrate (Sigma, UK) and 87.66 g NaCl in 1 L distilled water.

Depurination solution

The depurination solution was prepared by diluting 40 mL 10 M HCl in 1 L distilled water.

Denaturation solution

The denaturation solution was prepared by dissolving 20 g NaOH (Fisher, UK) and 87.66 g NaCl in 1 L distilled water.

Neutralization solution

The neutralization solution was prepared by dissolving 87.66 g NaCl and 60.57 g Tris/HCl in 1 L distilled water. The solution was adjusted to pH 7.5 with HCL.

Washing solution I

The washing solution I was prepared by diluting 200 mL 10X SSC solution and 100 mL 10% SDS in 1 L distilled water.

Washing solution II

The washing solution II was prepared by diluting 100 mL 10X SSC solution and 100 mL 10% SDS in 1 L distilled water.

Solution A

The solution A was prepared by dissolving 11.67g maleic acid (AppliChem, Germany), 8.77 g NaCl, and 3 mL Tween 20 in 1 L distilled water. The solution was adjusted to pH 7.5 with NaOH.

Maleic acid buffer

The maleic acid buffer was prepared by dissolving 11.67 g maleic acid and 8.77 g NaCl. The solution was adjusted to pH 7.5 with NaOH.

Blocking solution

The solution was prepared by 36 mL maleic acid buffer and 4 mL Western blocking reagent (Roche, Germany).

Detection buffer

The detection buffer was prepared by dissolving 12.11 g Tris and 4 g NaCl in 1 L distilled water adjusting to pH 9.5.

4.2.3 Methods

4.2.3.1 Synthesis of deletion cassettes

The deletion cassettes AFUB_004890, AFUB_042900, AFUB_067900 and AFUA_3G01670 and were amplified from the ΔAFUB004890, ΔAFUB42900, ΔAFUB067900, ΔAFUB042890 and (AFUA3G01670) strains (transformant strains utilizing A1163 as parental strain, gift from Bromley group at the University of Manchester; primers used are listed in **Appendix 38 and 55**).

The knock-out cassettes AFUB069370 and AFUB09460 were made using fusion PCR (**Section 2.2.6**) according to the protocol of Szewczyk et al. (2006). The ORF of the target gene was replaced by the selectable maker *hph* that was flanked by upstream and downstream fragments to facilitate homologous integration (primers used are listed in **Appendix 38 and 54**). The genomic DNA from A1163 of *A. fumigatus* was used as the template to amplify the upstream and downstream flanking region. The *hph* was amplified from ΔAFUB004890 strain.

4.2.3.2 Synthesis of plasmids for complementation

The selectable marker *ble* was acquired from plasmid AnPpgA_ble_AttrpCT_pUC19 (gift from M. Brock, University of Nottingham) by restriction enzyme *Not*I digestion. The upstream flanking and gene of interest, and the downstream flanking regions were amplified using strain A1163 as the

template (primers used are listed in **Appendix 40**). The plasmid was constructed by NEBuilder@ HiFi DNA Assembly (**Section 2.2.7**).

4.2.3.3 DNA extraction

The *A. fumigatus* strain was incubated for 24 hours at 37 °C in 50 mL ACM (**Section 2.1.1**) within a 250 mL sterile flask (with 1 mL of 1×10^8 spores/mL spore suspension). Mycelia were harvested by pouring through two layers of sterile Miracloth in a funnel, and the residual broth was squeezed out to dry the sample. The sample was collected in a 15 mL centrifuge tube and freezed in liquid nitrogen. In the next step, the frozen mycelia were ground under liquid nitrogen in a mortar. The resulting powder was collected in a 2 mL Eppendorf tube (filled to 1/3 of the total volume), and then the tube was filled with 500 µL extraction buffer, 60 µL 10 % SDS and 2 µL RNase before incubation at 65 °C for 15 mins. After incubation, 160 µL 5M KAc was added to the sample, which was vortexed to mix, followed by incubation in ice for 5 min, and then centrifugation at 4 °C for 10 mins at 13,000 **g**. The approx. 600 µL supernatant was transferred into a fresh 2 mL Eppendorf tube, and added with 700 µL isopropanol and inverted 30 times for best mixing. The sample was centrifuged at 13,000 **g** for 10 mins, and the supernatant was removed completely (DNA pellet was collected at the bottom). The DNA pellet was resuspended in 400 µL TE Buffer (**Section 2.1.1**) and incubated at 60 °C until the pellet was dissolved completely. Subsequently, 55 µL 3 M NaAc was added to the sample, and the mixture was centrifuged at 16,000 **g** for 5 mins. Afterward, the supernatant was transferred into a new 2 mL Eppendorf tube and mixed with 500 µL isopropanol. The tube was inverted for 30 times, and then centrifuged at 16,000 **g** for 10 mins. The supernatant was discarded, and the DNA pellet was washed with 400 µL 70 % EtOH (**Section 2.1.1**). The sample was centrifuged at 13,000 **g** for 10 mins, and the supernatant was removed. The DNA pellet was dried for 10 mins,

and dissolved in 60 µL of TE buffer (**Section 2.1.1**). DNA samples were used in Southern blotting.

4.2.3.4 Southern blotting

Probes for use in Southern blotting were amplified by replacing partial dTTPs with DIG-UTPs. The PCR reaction solution included 1 µL of 10 mM dATP, dCTP and dGTP separately, 0.7 µL of 10 mM dTTP, 0.5 µL of DIG-UTP; 1 µL of 100 mM forward and reverse primers each; 0.5 µL of Taq polymerase, 5 µL of thermopolymerase buffer, 30 ng of deletion plasmid, and the reaction solution was made up to a volume of 50 µL with dH_2O. The PCR cycles were 95 °C for 30 s as an initial denaturation, followed by 35 cycles of 95 °C for 30 s, 50 °C for 30 s, 72 °C for 60 s, and 72 °C for 5 m as final elongation. The product was gel purified using a NucleoSpin@ Gel and PCR Clean-up kit according to manufacturer's instructions and stored at 4 °C. The genomic DNA of the wild-type and the mutant strains were digested with suitable restriction enzyme overnight. After the digestion, the samples were run on 0.8 % agarose gel for a suitable time. The gel was incubated with depurination solution for 7.5 mins twice followed by rinsing with water between each time, followed by incubation with denaturation solution for 20 mins twice and rinsing with water between each time, and then the gel was incubated in neutralization solution for 15 min twice. The gel was then placed on the wet nylon membrane to transfer the sample via a vacuum blotting system, and the nylon membrane was crosslinked via UV using a Bio-Rad cross linker (Bio-Rad, UK). Afterward, the sample was prehybridized for 1 hour in DIG Easy Hyb solution at 65 °C and 10 µL the DIG probe was added hybridized overnight. Later, the membrane was washed with solution I for 5 mins twice at 65 °C and then solution II for 10 mins twice. The membrane was then washed by solution A for 5 mins at room temperature and followed by rinsing with malic acid buffer. The membrane was incubated in

blocking solution for 30 mins firstly, and then new blocking solution with 0.8 µL of Anti DIG AP Fab-fragment was added and incubated for 30 mins. Afterwards, the membrane was rinsed with solution A for 10 mins twice, malic acid buffer for 5 mins once, detection buffer for 1 min once consecutively. CDP Star reagent was spread onto the membrane, and the membrane was placed in a plastic bag and visualized with a GelDoc system using the chemiluminescence setting. After this the membrane was rinsed with maleic acid buffer and stained with NBT/BCIP buffer. The stain would take several hours or overnight to develop. To stop the staining, the membrane was placed in water with few drops of HCl.

4.2.3.5 PEG mediated protoplast transformation

1 mL of 1×10^8 spores/mL spore suspension from *A. fumigatus* strains were inoculated in 25 mL ACM and incubated at 37 °C for 20 hours in 250 mL flasks with shaking at 150 rpm. After the incubation, the mycelia was filtered through sterile Miracloth and rinsed with sterile distilled water, and then the mycelia was collected and resuspended in distilled water containing 10 mM DTT for 1 hour at 28 °C without shaking. After the incubation, the mycelia were collected by filtering through sterile Miracloth, and rinsed with the KCl solution (**Section 4.2.2**). 1 g of mycelia were weighted and resuspended in 20 mL of the filter-sterilized osmotic solution containing 1.3 g Vino Taste (Geib and Brock, 2017) and 0.1 g Lysing Enzyme (Geib and Brock , 2017). The digesting mixture was poured into a sterile 125 mL flask and inoculated at 28 °C with shaking at 50 rpm. After incubating the mycelia mixture for 1.5 to 2.5 hours, protoplasts were collected by filtering the mixture through a new Miracloth funnel. with the protoplasts suspension collected into a sterile 50 mL Falcon tube. Next, the suspension was centrifuged at 4 °C for 8 mins at 3,220 **g**. The protoplasts pellet was gathered at the bottom. The pellet was resuspended in 1 mL of the KTC

buffer (**Section 2.1.2**), and the concentration was counted and calculated by hemocytometer. The optimal concentration of the protoplasts aimed for was between 5 X1 0^7 to 2 X 10^8 protoplasts/mL. In the transformation, 100 µL of the protoplast solution, 25 µL 40 % PEG-6000 (**Section 2.1.2**) and 1-20 µg (in a volume under 10 µL) DNA fragment were mixed gentlly in a 2 mL sterile tube. The mixture was incubated on ice for 25 mins, and then 500 µL of PEG solution was added dropwise and mixed gently with a cut-off 1 mL tip and incubated for 5 mins. After the incubation, 1 mL KTC buffer was added, and the tube was inverted twice to dilute the PEG solution. For colony regeneration, 600 µL of transformed protoplasts was added to top agar containing 0.1µg/L pyrithiamine, 180 mg/L hygromycin or 0.1 µg/L phleomycin, and the mixture was poured on the bottom agar containing the respective antibiotic as the selection agent. The transformation plates were incubated at 37 °C for 3-5 days. Regenerated colonies were picked and the presence of a correct insert confirmed by diagnostic PCR (**Section 2.2.9**).

4.2.3.5 *A. fumigatus* sexual crossing by point inoculation

Culture medium for inducing the sexual cycle of *A. fumigatus* was prepared according to the methods of Ashton and Dyer (2019). 1 L of tap water was added to 40 g Irish pinhead oatmeal in a 2 L flask, and the oatmeal solution was boiled using a hotplate and stirred consistently with a magnetic flea until the mixture reached boiling temperature, and then the temperature of hotplate was lowered to cook/simmer for 45 min. After cooking, the solution was filtered through two layers of cheese cloth to remove any solid oatmeal and refilled to 1 L using tap water. 10 g of agar was added to a 1 L Schott bottle, and 500 mL of the oatmeal solution was added to the bottle and stirred to disperse/dissolve the agar. The bottle was autoclaved at 117 °C for 30 mins. For preparing sexual crossing plates, 25 mL of the oatmeal agar was poured per 9 cm diameter Petri

dish. To inoculate crosses, 1 mL spore suspension of an appropriate isolate/strain was prepared in 0.01 % Tween-80 from 5-7 days old slope cultures grown on ACM (**Section 2.1.1)** and adjusted to a concentration of 5×10^5 conidia/mL using a haemocytometer method. Two 3 µL aliquots of spore suspension from opposite mating types were point-inoculated approx. 4 cm apart onto the oatmeal agar surface, and the mating types were marked on the underside of plates by blue dots for MAT1-2 and red dots for MAT1-1. The plates were sealed with two layers of Parafilm and incubated at 30 °C in the dark for 3-4 months in single depth. The plates were examined periodically to reseal breaks in Parafilm to prevent the agar drying out. Each group of crosses contained four replicates. After 3-4 months, the fertility level was evaluated by counting numbers of cleistothecia using the dissecting microscope and the result was analysed by Prism 9.0 via one-way ANOVA and nested one-way ANOVA.

4.2.3.6 Harvest of ascospores from cleistothecia

Ascospores were harvested from cleistothecia according to methods described by Ashton and Dyer (2019). A mature cleistothecium was isolated from the crossing plate using a fine-point needle (which had been flame sterilized). The cleistothecium was washed by rolling in 20 µL of sterile water on a 4% water agar plate to remove conidia and hyphae. The cleaned cleistothecium was transferred into a sterile 2 mL microcentrifuge tube containing 100 µL sterile 0.01% Tween 80, and the cleistothecium crushed against the wall of the microcentrifuge tube to liberate ascospores. To acquire a sufficiently high enough concentration of ascospores, five cleistothecia were collected in each tube. The volume was adjusted to 1 mL by adding 900 µL 0.01% Tween 80 and the tube vortexed. To kill any remaining conidia and hyphae, the tube was heated for 1 hour at 70 °C. The heat treated ascospore

suspension was then diluted to a suitable concentration and aliquots spread onto selective medium plates for isolating appropriate colonies.

4.2.3.7 PCR mating-type diagnostic

The mating-type of selected colonies was then determined via diagnostic PCR following the method of Paoletti et al. (2005) for *MAT* determination in *A. fumigatus.* The reaction included 100 ng of genomic DNA, 1 μL of 10 mM dNTPs, 1 U of Phusion , 10 μL of 5X HF Buffer, 1 μL of 10 mM MAT1-1 specific primer AFM1 (5'-CCTTGACGCGATGGGGTGG-3'), 1 μL of 10 mM MAT1-2 specific primer AFM2 (5'-CGCTCCTCATCAGAACAACTCG-3'), and 1 μL of 10 mM the common primer AFM3 (5'-CGGAAATCTGATGTCGCCACG-3'). The cycles were 2 mins at 98 °C, 30 cycle of 20 secs at 98 °C, 30 secs at 65 °C, 30 secs at 72 °C, and a final 5 mins at 72 °C and hold sample at 10 °C.

4.2.3.8 Fertility test of *A. fumigatus*

Conidial spores were collected from slope cultures grown on ACM (**Section 2.1.1**) that had been cultured for 3-5 days at 37 °C. The spore concentration was counted and calculated by the hemocytometer method, and the final concentration was adjusted to $1X10^6$ spores/mL. To induce the sexual cycle, 500 μL aliquots of spore suspensions from MAT1-1 and MAT1-2 strains were mixed and vortexed. 50 μL aliquots of the mixture was then plated and spread over the surface of 9 cm diameter oatmeal agar plates (**Section 2.2.1**), and the inoculated plates were sealed immediately with two layers of Parafilm and incubated at 30 °C in the dark in single depth (using four replicate per cross). After 4 weeks of incubation, plates were inspected carefully by microscopy, using a hoovering method to reveal cleistothecia as described by Ashton and Dyer (2019). Numbers of cleistothecia were counted, and the data was

analyzed by an unpaired t-test or other appropriate statistical test including one-way ANOVA by PRISM 9.0.

4.3 Results

4.3.1 Effect of *nsdC* deletion on cleistothecial formation in *A. fumigatus*

In *A. nidulans*, NsdC is a positive regulator of sexual development and is required for formation of cleistothecia and ascospores (Kim et al., 2009). This gene was therefore used in pilot studies to test the possible impact of gene deletion on sexual reproduction in *A. fumigatus*, specifically to investigate if NsdC has a similar role in this heterothallic species. In parallel work at Nottingham, Δ*nsdC A. fumigatus* strains had already been constructed by transformation and selection in the highly fertile 47-51 (MAT1-1) parental background using pyrithiamine as a selective marker for gene deletion (M Brock, pers. Comm.). Two such Δ*nsdC* deletion strains, 47-51-Δ*nsdC5* and 47-51-Δ*nsdC4* were selected as candidates in fertility tests. The two Δ*nsdC* strains were crossed with two wild-type *MAT1-2* strains, namely the highly fertile 47-55 strain and a supposed medium fertility strain 47-107 (Swilaiman et al., 2020). Compared with the wild-type control crosses, there was no significant reduction in numbers of cleistothecia formed by either of the Δ*nsdC* mutants [**Table 4-1**; $F(3,20)=1.369$, $p=0.2820$] i.e. sexual development was retained despite the Δ*nsdC* mutation in one of the crossing partners. This suggested that in the heterothallic species *A. fumigatus*, that the deletion of *nsdC* in the MAT1-1 parental strains might be being complemented by the presence of a functional *nsdC* in the complementary MAT1-2 wild-type mating partners 47-55 and 47-107. To test this hypothesis, cleistothecia formed in the first round of crossing were collected and ascospores were isolated. The harvested ascospores were then subjected to pyrithiamine selection to identify the presence of offspring

with the Δ*nsdC* genotype and then their mating types were identified by PCR (**Appendix 42**; Paoletti et al., 2005). This allowed the selection of progeny that exhibited either a Δ*nsdC* MAT1-1 or Δ*nsdC* MAT1-2 genotype.

Table 4-1 Cleistothecia formed between *MAT 1-1* Δ*nsdC* and *MAT1-2* wild-type strains. Numbers indicate average number of cleistothecia formed on a 9 cm diameter oatmeal agar crossing plate (mean of four replicates) ± SEM.

		MAT1-1 strains		
		47-51	Δ*nsdC4*	Δ*nsdC5*
MAT1-2 strains	47-55	23.00±14.23	13.75±9.52	6.00±5.15
	47-107	22.25±18.50	24.00±11.94	26.75±2.17

Various crosses were then set up between MAT1-1 and MAT1-2 progeny from the first round of crossing, either control crosses to a wild-type partner or a cross to a similar Δ*nsdC* progeny partner of opposite mating type (**Table 4-2**). These matings involved the crossing of MAT1-1 progeny strains Δ*nsdC*-b and Δ*nsdC*-d that arose from crosses between the Δ*nsdC* 47-51 and 47-55 parents; MAT1-1 progeny strains Δ*nsdC*-y and Δ*nsdC*-z that arose from crosses between the Δ*nsdC* 47-51 and 47-107 parents; MAT1-2 progeny strains Δ*nsdC*-a Δ*nsdC*-c that arose from crosses between the Δ*nsdC* 47-51 and 47-55 parents; and MAT1-2 progeny strains Δ*nsdC*-x and Δ*nsdC*-w that arose from crosses between the Δ*nsdC* 47-51 and 47-107 parents, respectively. An additional highly fertile wild-type MAT1-1 isolate 47-267 was also used in this second round of crossing.

Table 4-2 List of wild type, Δ*nsdC* and ascospore progeny isolates (from Δ*nsdC* and wild-type crosses) that were used in Δ*nsdC* sexual fertility test

Strain	Genetic background	Mating type
47-51	Wild-type	*MAT1-1*
47-267	Wild-type	*MAT1-1*
47-51- Δ*nsdC*4	*ΔnsdC::prtA*	*MAT1-1*
Δ*nsdC* a	progeny of 47-51- Δ*nsdC*5 x 47-55; *ΔnsdC::prtA*	*MAT1-2*
Δ*nsdC* b	progeny of 47-51- Δ*nsdC*5 x 47-55; *ΔnsdC::prtA*	*MAT1-1*
Δ*nsdC* c	progeny of 47-51- Δ*nsdC*5 x 47-55; *ΔnsdC::prtA*	*MAT1-2*
Δ*nsdC* d	progeny of 47-51- Δ*nsdC*5 x 47-55; *ΔnsdC::prtA*	*MAT1-1*
Δ*nsdC* x	progeny of 47-51- Δ*nsdC*5 x 47-107; *ΔnsdC::prtA*	*MAT1-2*
Δ*nsdC* y	progeny of 47-51- Δ*nsdC*5 x 47-107; *ΔnsdC::prtA*	*MAT1-1*
Δ*nsdC* z	progeny of 47-51- Δ*nsdC*5 x 47-107; *ΔnsdC::prtA*	*MAT1-1*
Δ*nsdC* w	progeny of 47-51- Δ*nsdC*5 x 47-107; *ΔnsdC::prtA*	*MAT1-2*

The results of the various crosses are shown in **Table 4-3**. In summary, it was found that in almost all crosses where a MAT1-1 Δ*nsdC* strain was crossed with a MAT1-2 wild-type strain that normal sexual development occurred (with the sole exception of Δ*nsdC*-y x 47-107 which failed to form cleistothecia). Similarly, in almost all crosses where a *MAT1-2* Δ*nsdC* strain was crossed with a MAT1-1 wild-type strain then normal sexual development also occurred (with the one exception of the cross Δ*nsdC*-w x 47-267, which failed to form cleistothecia). By contrast, all 16 crosses between MAT1-1 Δ*nsdC* strains and MAT1-2 Δ*nsdC* strains failed to form cleistothecia i.e. this demonstrated that the deletion of *nsdC* in both mating partners lead to a block in fruit body formation in both mating-type backgrounds [**Table 4-3**, $F(23,72)=10.29$; $p<0.0001$; **Figures 4-3 and 4-4**]. There was still no sign of cleistothecial development even after a prolonged six months incubation for these latter crosses. It is further noted that much variation was observed in numbers of cleistothecia formed on the successful crossing plates as shown in **Table 4-3** and **Figure 4-3**. The data was analysed via nested one-way ANOVA due to the variance between crossing groups, and the subsequent analysis suggested that *nsdC* deletion resulted in a reduction of fertility specifically in the *MAT1-1*

background although cleistothecia were still formed [**Figure 4-3**, F (3,20)=3.43, p=0.0366]. However, it is cautioned that relatively few isolates were examined in this pilot experiment so these results regarding impact on *MAT1-1* fertility remain to be verified with a larger sample number.

Table 4-3 Number of cleistothecia formed in crosses between various wild-type and Δ*nsdC* strains. Data compares cleistothecial formation in wild-type x wild-type crosses (47-51 X 47-55, 47-51 X 47-107, 47-367 X 47-107) versus wild-type x Δ*nsdC* crosses (47-51 X Δ*nsdC* (MAT1-2 background), 47-267 X Δ*nsdC* (MAT1-2 background), 47-55 X Δ*nsdC* (MAT1-1 background) and 47-107 X Δ*nsdC* (MAT1-1 background). Numbers indicate average number of cleistothecia formed on a 9 cm diameter oatmeal agar crossing plate (mean of four replicates)± SEM. Data was analysied via nested one-way ANOVA. **** indicates p<0.0001.

		MAT1-1 strains					
		47-51	47-267	Δ*nsdC*-b	Δ*nsdC*-z	Δ*nsdC*-y	Δ*nsdC*-d
MAT1-2 strains	47-55	7 .00±5.72	29.75±7.97	13.75±9.18	2.75±2.06	7.75±7.63	8.25±10.91
	47-107	14.25±8.73	0.25±0.50	4.00±4.69	0.50±0.58	0****	0.5±1.00
	Δ*nsdC*-a	0.50±1.00	1.50±1.73	0****	0****	0****	0****
	Δ*nsdC*-c	5.50±5.92	2.75±5.50	0****	0****	0****	0****
	Δ*nsdC*-x	35.00±21.83	21.25±8.06	0****	0****	0****	0****
	Δ*nsdC*-w	40.75±18.91	0****	0****	0****	0****	0****

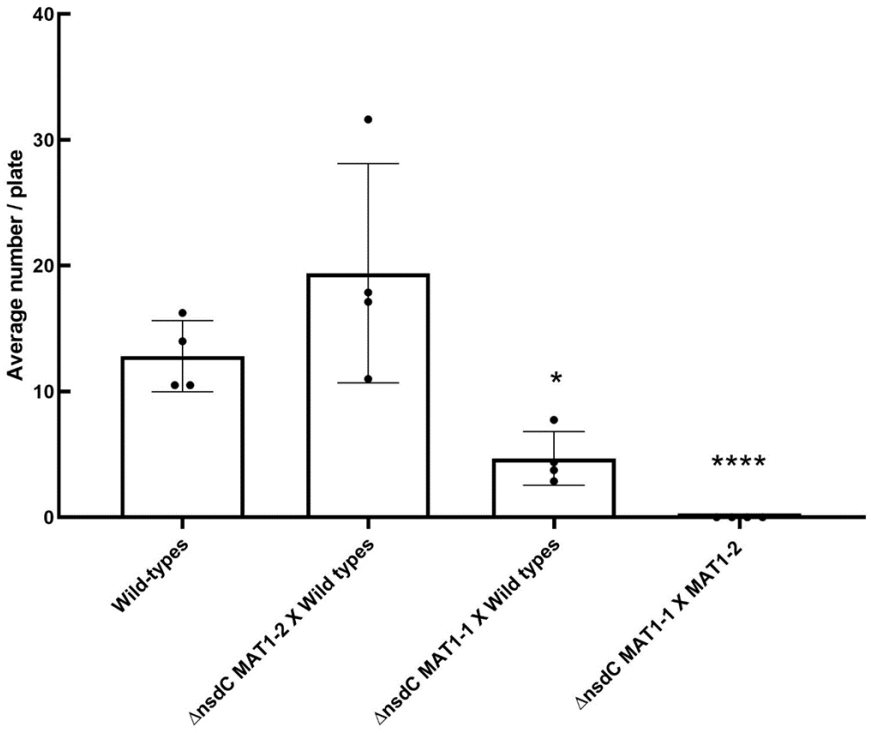

Figure 4-3 Number of cleistothecia formed in various crosses with ΔnsdC and/or wild-type *A. fumigatus* strains. Numbers indicate average number of cleistothecia formed on a 9 cm diameter oatmeal agar crossing plate (mean of four replicates) ± SEM. Data was analysed via nested one-way ANOVA and * indicates $p<0.05$ and **** indicates $p<0.0001$.

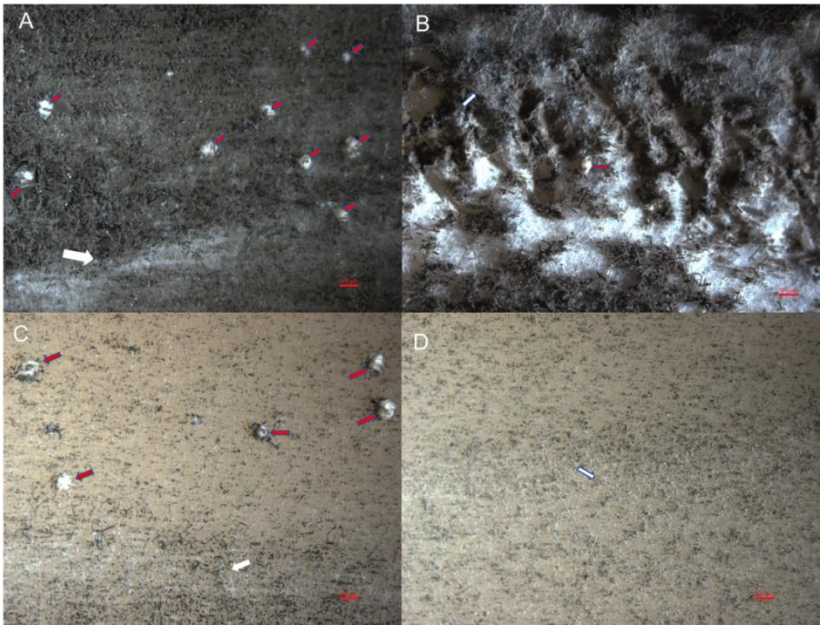

Figure 4-4. **Results of various crosses between ΔnsdC and/or wild-type *A. fumigatus* strains on oatmeal agar following incubation for four months**

in darkness at 30 °C. Red arrow indicates cleistothecia, and white arrow indicates the barrage zone where two mating types of *A. fumigatus* strains met. The magnification factor of the dissecting microscope images is 10X. The scale bar is 500 μm. **A** cleistothecia formed in crosses between strains 47-267 (MAT1-1) and 47-55 (MAT1-2). **B** cleistothecia formed in crosses between 47-267 and ΔnsdC a (MAT1-2). **C** cleistotheica formed in crosses between 47-55 and ΔnsdC b (MAT1-1). **D** lack of cleistotheica in attempted crosses between Δ*nsdC*-a and Δ*nsdC*-b strains.

4.3.2 The construction of highly fertile *A. fumigatus* MAT1-1 and MAT1-2 Δ*kuB* strains

The results of the gene deletion work with *nsdC* described above (**Section 4.3.1**) indicated that in order to assess any impact of gene deletion of putative HMG genes, that it would be necessary to undertake gene deletion in both MAT1-1 and MAT1-2 strains of *A. fumigatus* in case of possible complementation by a wild-type mating partner as seen with the Δ*nsdC* experiments. It was also considered advantageous to conduct such GM work into investigation of genes regulating sexual development using fertile Δ*kuB* strains because the deletion of the *kuB* gene improves the rate of homologous recombination, thereby increasing the success of targeted integration in gene knock-out experiments (Eliana et al., 2006). Although such an *A. fumigatus* Δ*kuB* strain already exists (M Bromley pers. comm.), being a Δ*pyrG* FGSC A1160 derivative, previous work at Nottingham had found that this strain unfortunately is sterile, and the same result was found in trial crosses in which the supplementation of both uridine and uracil into the oatmeal agar medium could not recover fertility.

Therefore, it was necessary to construct Δ*kuB* strains in both MAT1-1 and MAT1-2 *A. fumigatus* backgrounds. The highly fertile strains 47-51 (MAT1-1) and 47-55 (MAT1-2) (O'Gorman et al., 2009) were selected from the Nottingham BDUN collection for this purpose. To start with the *kuB* gene was deleted in the 47-51 (MAT1-1) background, using the selective marker *ptrA* for

pyrithiamine resistance, with transformants selected on medium containing 0.1 g/L pyrithiamine following transformation methods (**Section 4.2.5**). Two MAT1-1 isolates from the parental strain 47-51 were confirmed to be the correct Δ*kuB*::*ptrA* single integrated strains by both diagnostic PCR and Southern blotting. One of these MAT1-1 Δ*kuB*::*ptrA* strains was then crossed with 47-55 (MAT1-2). Progeny were then collected from this cross, and screened for both mating type and the Δ*kuB*::*ptrA* genotype. This allowed identification of the desired Δ*kuB* strains of both MAT1-1 and MAT1-2 genotype, with the strains being coded as 47- 465 (MAT1-1) and 47-466 (MAT1-2) in the BDUN collection (**Appendix 45 to 48**), in which *kuB* had been replaced with *ptrA*.

As a key aim of research was the characterization of genes related to sexual development, the fertility of the Δ*kuB* 47-465 and 47-466 strains were compared to that of the parental strains 47-51 and 47-55. The data indicated that there was no significant difference between the fertility of the parental strains and the Δ*kuB* strains (**Figure 4-5;** p=0.7026; t=0.3930, df=10), all strains showing a similar pattern of variance between replicates in the same cross (**Appendix 41**). Therefore, importantly, these results showed that deletion of *kuB* did not influence the fertility of either MAT1-1 or MAT1-2 strains of *A. fumigatus*.

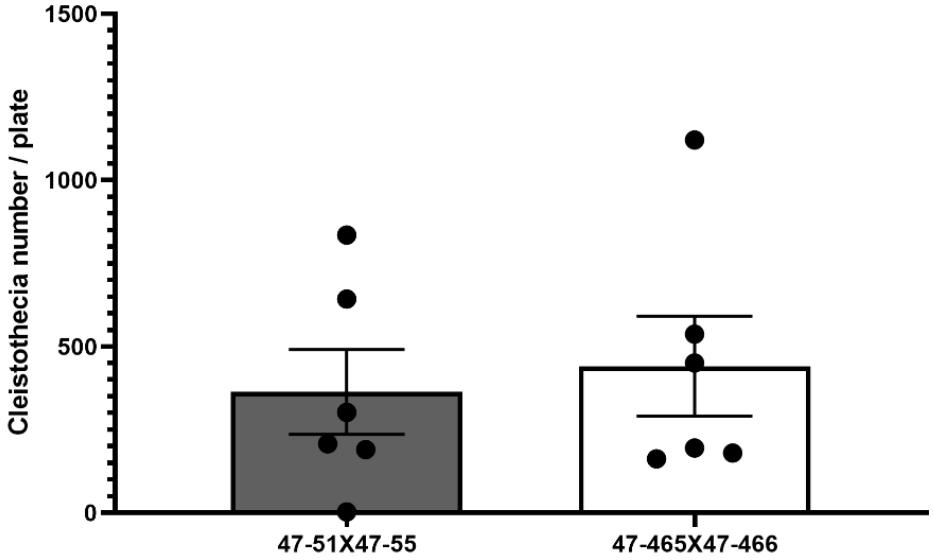

Figure 4-5 Number of cleistothecia formed in crosses between parental wild-type isolates compared to ΔkuB deletion strains. 47-51 (MAT1-1) and 47-55 (MAT1-2) are wild-type high fertility strains and were used as the parental strains to make the *Δku* strains. Strains 47-465 (MAT1-1) and 47-466 (MAT1-2) are from the F1 progeny of *Δku* strain and 47-55, and were also *ku* deletion isolates. Numbers indicate average number of cleistothecia formed on a 9 cm diameter oatmeal agar crossing plate (mean of five replicates) ± the standard error of the mean; dots represent replicates of each group.

4.3.3 Identification of HMG genes in *A. fumigatus*

Protein sequences of the HMG genes previously found in *A. nidulans* (Salih 2016) were used as references to identify seven putative HMG gene homologs in *A. fumigatus* via TBLASTN searches at the EnsemblFungi database (https://fungi.ensembl.org/Multi/Tools/Blast) (**Table 4-4; Appendix 49 to 53**). Gene deletion cassettes were constructed via a fusion PCR method (Szewczyk et al., 2007) with assistance from personnel at the University of Manchester (Manchester Fungal Infection Group, School of Biological Sciences, University of Manchester; Prof. Mike Bromley group) who provided materials and guidance. The *A. fumigatus* strain A1160 was used as the template for synthesising the ca. 1,200 bp upstream and downstream flanking regions. The

selectable marker was the hygromycin B resistance gene *hph* which was used to replace the target HMG gene. The AFUB_009460, AFUB_042900, AFUB_067900, AFUB_069370 and AFUA_3G06170 transformation constructs were synthesized by fusion PCR. The AUFB_004890 and AFUB_037560 constructs were given as gifts by Prof. Bromley (**Appendix 54 to 55**). These HMG genes were then systematically deleted in the *ΔkuB::ptrA* 47-465 (MAT1-1) and 47-466 (MAT1-2) strains (**Section 4.3.2**) and transformants tested for any impact in fertility as described below, together with control and gene complementation strains (made using *ble* as the selectable marker; **Section 4.2.3.2**) where appropriate.

Table 4-4 BLAST search results of putative HMG genes with a possible role in sexual development in *A. fumigatus*

Query sequence in *A. nidulans*	Homologous gene in *A. fumigatus* via TBLASTN			putative HMG domain	Homologous gene in *P. anserina*
Protein ID (Gene ID)	Gene ID	E value	Identity (%)		Gene
XP661271.1 (AN3667)	AFUB_069370	3.00E-81	56.7	HMG box	PaHMG5
XP659566.1 (AN1962)	AFUB_067900	9.40E-120	87	HMG box	PaHMG8
XP660359.1 (AN2755)	AFUB_042900	4.60E-74	68.3	MAT alpha 1	N/A
XP662338.1 (AN4734)	AFUA_3G06170	5.80E-79	55.7	MAT1-2-1; HMG box	N/A
XP754458.1 (AN2885)	AFUB_037560	6.90E-36	94.1	nucleosome binding protein, HMG box	PaHMG6
EAA65860.1 (AN1267)	AFUB_009460	7.20E-05	48.4	HMG box	PaHMG2
CBF89496.1 (AN10103)	AFUB_004890	9.20E-49	79.6	HMG box	PaHMG4

4.3.3.1 *AFUB_069370* is pivotal for fruit body formation in *A. fumigatus*

The amino acid sequence (XP_661271.1) of AN3667 was used to identify a putative HMG homolog in *A. fumigatus*, with this single gene named as AFUB_069370 and AFUA_4G12410 in the genome annotations of A1163 (MAT1-1) and Af293 (MAT1-2), respectively. *AFUB_069370* shared 56.7% amino acid identity with an E-value of $3e^{-81}$ to *AN3667*, AN3667 had previously

shown to be most closely related to PaHMG5 (PODANS1_13940) in *P. anserina*. AFUB_069370 shared 48.9 % identity to *PaHMG5*, and with 40.8 % identity to fmf-1 in *N. crassa* (**Appendix 49**). *AN3667* is 1,561 bp in length and encodes a putative 499 amino acid protein containing the conserved HMG box at residue position from 206 to 276. By comparison, *AFUB_069370* is 1,524 bp, and encodes a putative 507 amino acid protein that includes the HMG box domain at residue position from 195 to 271.

After PEG-mediated protoplast transformation of the *ΔkuB::ptrA* 47-465 (MAT1-1) and 47-466 (MAT1-2) strains, two *AFUB_069370* deletant strains in MAT1-1 background ΔAFUB69370M1a and ΔAFU69370M1b, and two knock-out strains ΔAFUB69370M2a and ΔAFUB69370M2b in MAT1-2 background, were selected and correct integration of the transforming DNA was confirmed by diagnostic PCR (**Table 4-5; Appendix 56 to 57**). Two gene complementation strains, AFUB69370M1C (MAT1-1) and AFUB69370M2C (MAT1-2) were also subsequently made, using transformants ΔAFUB69370M1a and ΔAFUB69370M2a, respectively, as the parental strains (**Table 4-5; Appendix 60 to 62**).

Attempted crosses between strain 47-465 (MAT1-1; *ΔkuB::ptrA*) and the ΔAFUB69370M2a and ΔAFUB69370M2b (MAT1-2) transformant strains failed to form fruit bodies. Similarly, attempted crossing between strain 47-466 (MAT1-2*; ΔkuB::ptrA*) and the ΔAFUB69370M1a and ΔAFUB69370M1b (MAT1-1) transformant strains also failed to form fruit bodies, indicating that strains of the opposite mating-type containing the wild-type form of *AFUB_069370* (synonym *AFUA_4G12410*) could not complement/restore the fertility of the gene deletant strains (**Figures 4-6 and 4-7;** F=4.712, P=0.0006) i.e. deletion of the target HMG gene in MAT1-1 and MAT1-2 background blocked cleistothecial formation indicating that a functional copy of *AFUB_069370* is essential for sexual development in both mating-type partners. However, some aggregated hyphal

structures (that might have been an early developmental phase in formation of cleistothecia?) were evident in these wild-type and gene knock-out strains crosses (**Figures 4-6 and 4-7).** By contrast, attempted crosses between the Δ *AFUB_069370* in MAT1-2 and MAT1-1 strains showed no signs of sexual development even after 8 weeks of incubation. The complementation of the target gene restored the ability of sexual development in both mating-type backgrounds, with no significant difference in numbers between the complementation groups and the wild-type crossing although the complementation strains produced less cleistothecia on average (**Figures 4-6 and 4-7**).

Table 4-5 Wild-type and GM strains used to study functionality of putative HMG family genes in the sexual cycle of *A. fumigatus.*

Strain	Genetic information	Parental strain	Source
47-55	*MAT1-2*, wild type	n/a	Ireland
47-51	*MAT1-1*,wild type	n/a	Ireland
47-51-8	*MAT1-1,nkuB:: ptrA*	47-51	This lab
47-51-38	*MAT1-1, nkuB::ptrA*	47-51	This lab
47-465	*MAT1-1, nkuB:: ptrA*	47-51-8X 47-55	This lab
47-466	*MAT1-2, nkuB::ptrA*	47-51-38X 47-55	This lab
AFUB69370M1a	*MAT1-1,kuB-, AFUB069370::hph*	47-465	This lab
AFUB69370M1b	*MAT1-1,kuB-, AFUB069370::hph*	47-465	This lab
AFUB69370M2a	*MAT1-2, kuB-, AFUA_4G12410::hph*	47-466	This lab
AFUB69370M2b	*MAT1-2, kuB-, AFUA_4G12410::hph*	47-466	This lab
AFUB69370M1C	*MAT1-1, kuB-, hph::AFUB069370, ble+*	AFUB69370M1a	This lab
AFUB69370M2C	*MAT1-2, kuB-, hph::AFUA_4G12410, ble+*	AFUB69370M2a	This lab
AFUB42900a	*MAT1-1,kuB-,AFUB042900::hph*	47-465	This lab
AFUB42900b	*MAT1-1,kuB-,AFUB042900::hph*	47-465	This lab
AFUA3G06170a	*MAT1-2,kuB-,AFUA_3G06170::hph*	47-466	This lab
AFUA3G06170b	*MAT1-2,kuB-,AFUA_3G06170::hph*	47-466	This lab
AFUB67900M1a	*MAT1-1,kuB-,AFUB067900::hph*	47-465	This lab
AFUB67900M1b	*MAT1-1,kuB-,AFUB067900::hph*	47-465	This lab
AFUB67900M1a	*MAT1-2,kuB-,AFUA_4G10820::hph*	47-466	This lab
AFUB67900M2b	*MAT1-2,kuB-,AFUA_4G10820::hph*	47-466	This lab
AFUB37560M1a	*MAT1-1,kuB-,AFUB037560::hph*	47-465	This lab
AFUB37560M1b	*MAT1-1,kuB-,AFUB037560::hph*	47-465	This lab
AFUB37560M2a	*MAT1-2,kuB-,AFUA_3G11610::hph*	47-466	This lab
AFUB37560M2b	*MAT1-2,kuB-,AFUA_3G11610::hph*	47-466	This lab
AFUB04890M1a	*MAT1-1,kuB-,AFUB004890::hph*	47-465	This lab
AFUB04890M1b	*MAT1-1,kuB-,AFUB004890::hph*	47-465	This lab
AFUB04890M2a	*MAT1-2,kuB-,AFUA_1G04550::hph*	47-466	This lab
AFUB04890M2b	*MAT1-2,kuB-,AFUA_1G04550::hph*	47-466	This lab
AFUB09460M1a	*MAT1-1,kuB-,AFUB009460::hph*	47-465	This lab
AFUB09460M1b	*MAT1-1,kuB-,AFUB009460::hph*	47-465	This lab
AFUB09460M2a	*MAT1-2,kuB-,AFUA_1G10040::hph*	47-466	This lab
AFUB09460M2b	*MAT1-2,kuB-,AFUA_1G10040::hph*	47-466	This lab

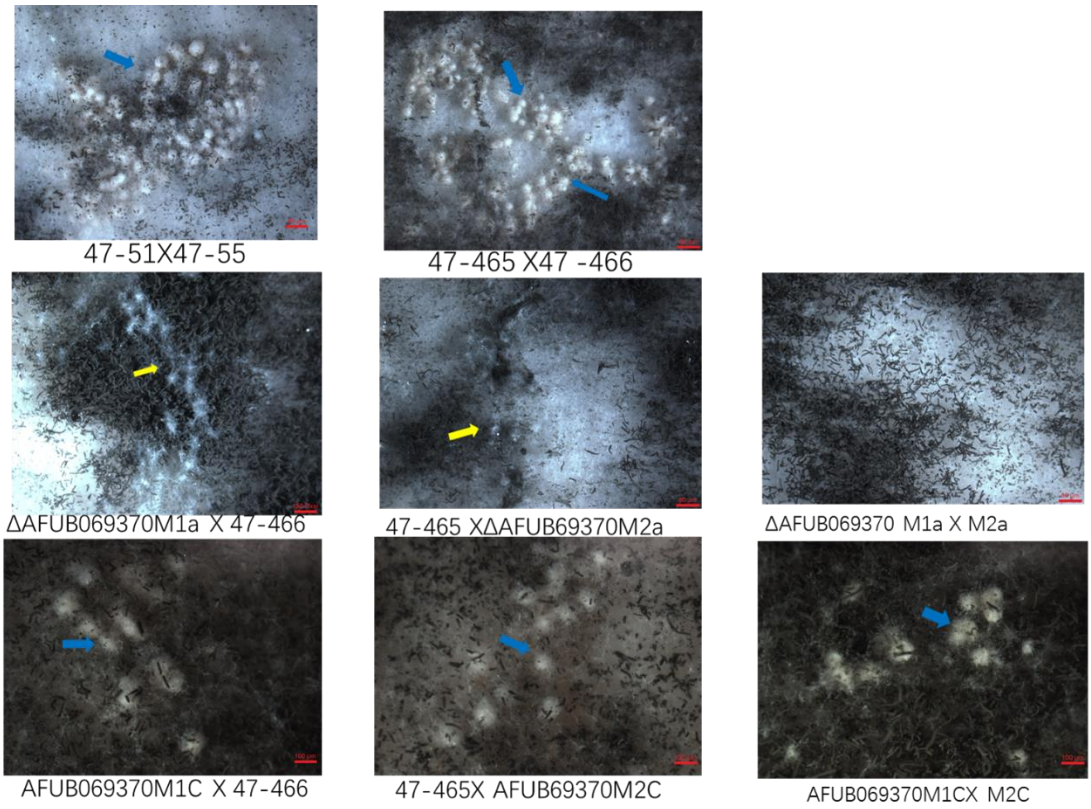

Figure 4-6 Images of crosses to determine impact of gene deletion of AFUB_069370 on sexual development in *A. fumigatus.* Compared to wild-type control strains, crossing of ΔAFUB_069370 with the opposite mating-types showed defects in fruit body development. See description under each figure for specific cross. Blue arrow indicates cleistothecia, yellow arrow indicates aggregated hyphal structure. Red scale bar indicates 80 µm.

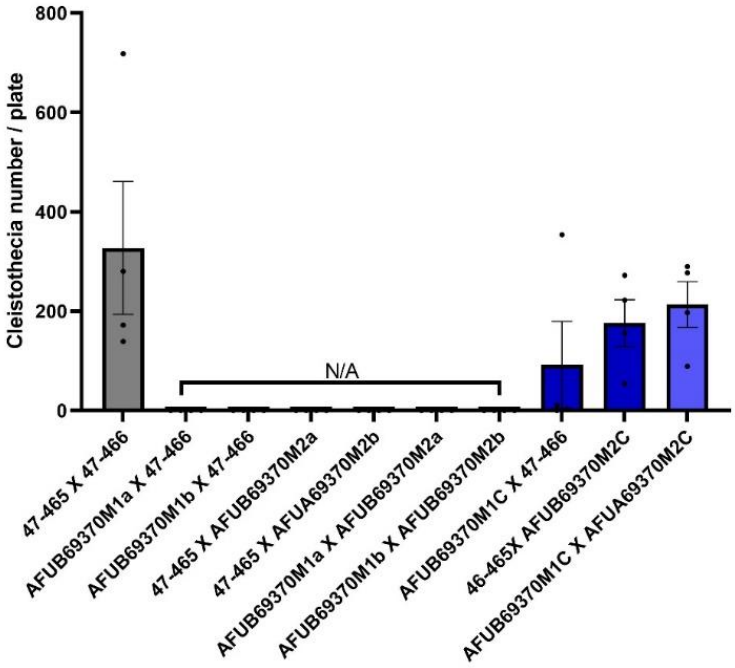

Figure 4-7 Results of crosses to determine impact of gene deletion of AFUB_069370 on sexual development in *A. fumigatus* [F (9, 30)=4.712, p<0.005]***.*** As compared to the wild-type control crossing and AFUB_069370 complement strain crossing, ΔAFUB_069370 exhibited a block in cleistothecia formation. See description on x axis for specific cross. Data shows average number of cleistothecia formed per 9 cm diameter Petri dish (four replicates) ±SEM. The dots represent replicates of each group.

4.3.3.2 *AFUB_067900* is required for fruit body formation in *A. fumigatus*

The *A. fumigatus* gene *AFUB_067900* (synonym *AFUA_4G10820* in Af293 strain) was identified as the homolog of *A. nidulans AN1962*, showing 87% identity with an E-value of $9.4e^{-120}$ to *AN1962*, and shows 71.2 % identify with E-value of $1.3e^{-41}$ to PaHMG8 (PDDNAS_6_4110) in *P.anserina* (**Table 4-4; Appendix 50**). *AN1962* is 2,028 bp in length and encodes a putative 675 amino acid protein containing the conserved HMG box at residue position from 96 to 171. By comparison, *AFUB_067900* is 2,067 bp, and encodes a putative 688 amino acid protein that includes the HMG box domain at residue position from 142 to 210 aa.

Two *AFUB_067900* knock-out strains ΔAFUB67900M1a (MAT1-1) and ΔAFUB67900M1b (MAT1-1), and two deletant strains ΔAFUB67900M2a (MAT1-2) and ΔAFU67900M2b (MAT1-2), and were selected and correct integration of the transforming DNA was confirmed by diagnostic PCR (**Table 4-5; Appendix 49 to 55**). Deletion of *AFUB_067900* (synonym *AFUB_4G10820)* in both the MAT1-1 and MAT1-2 background strains resulted in the absence of fruit body development, although hyphal aggregations were evident on crossing plates with MAT1-2 and MAT1-1 crossing partners, respectively, containing the wild-type *AFUB_067900* gene *i.e*. a functional copy of *AFUB_067900* was required in both mating-type partners for sexual development to occur. There was also no evidence of fruit body development in the double gene deletion ΔAFUB67900M1 x ΔAFUB67900M2 crosses, although hyphal aggregations were again evident (**Figures 4-8 and 4-9; Appendix 56 to 57**).

Unfortunately, there was insufficient time for gene complementation of the ΔAFUB67900M1 and ΔAFUB67900M2 strains.

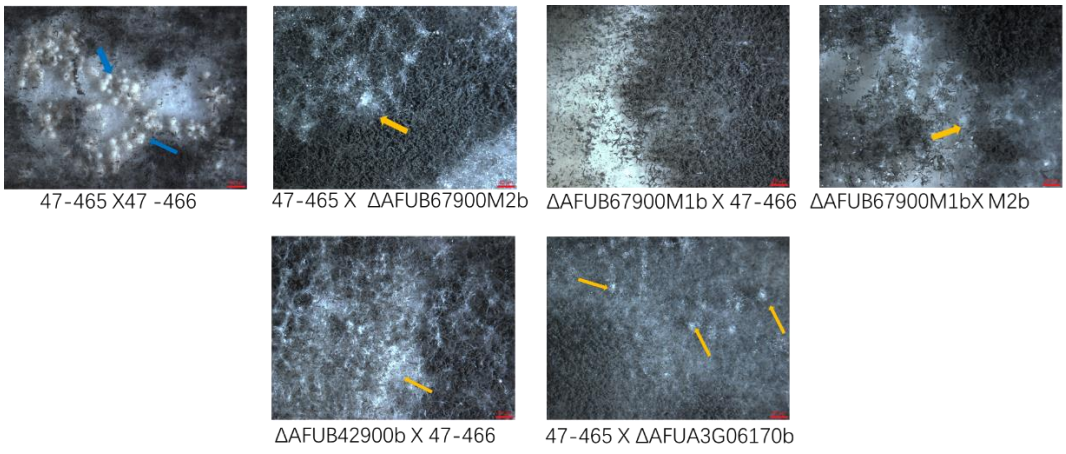

Figure 4-8 Images of crosses to determine impact of gene deletion of *AFUB_067900* on sexual development in *A. fumigatus.* See description under each figure for specific cross. Compared to the wild-type cross 47-465 X 47-466, ΔAFUB_067900 strains formed aggregated hyphal structures instead of mature cleistothecia. Blue arrow indicates cleistothecia, yellow arrow indicates aggregated hyphal structures. Red scale bar indicates 80 µm.

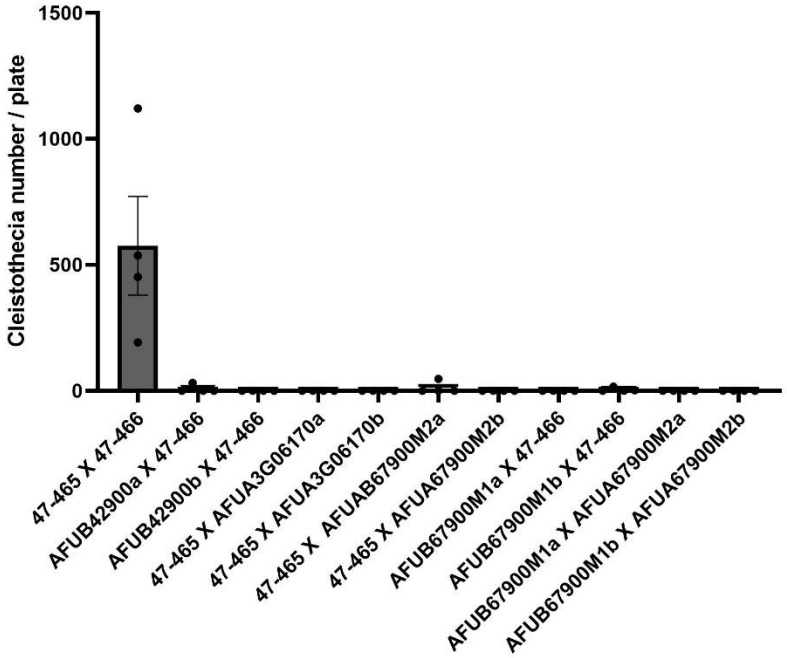

Figure 4-9 Results of crosses to determine impact of gene deletion of *AFUB_067900, AFUB_042900,* and *AFUA_3G06170* on sexual development in *A. fumigatus* [F (10, 33) =3.225, p<0.0001]. Deletion of AFUB_067900, AFUB_042900, and AFUA_3G06170 caused a block in cleistothecia formation as compared to the wild-type control cross. See description on x axis for specific cross. Data shows average number of cleistothecia formed per 9 cm diameter Petri dish (four replicates) ± SEM. The dots represent replicates of each group.

4.3.3.3 Other HMG genes impacting on fruit body formation in *A. fumigatus*

AFUB_042900 was identified as the homolog of *A. nidulans AN2755* showing 68.3 % identity with an E-value of $4.6e^{-74}$, and *AFUB_042900* was 1,107 bp in length and encoded 368 amino acid protein including the mating-tpye protein MATα-1 domain at residue position from 84-139 (**Table 4-4**). *AFUA_3G06170* was identified as putative MAT1-2-1 gene as the homolog of AN4734 sharing 55.7 % identify with an E-value of $5.8e^{-79,}$ and *AFUA_3G06170* (696 bp in length) encoded 322 amino acid protein including the HMG-box domain at residue position from 126 to 194 aa (**Table 4-4**).

Gene deletion of the putative mating type genes *AFUB_042900* and *AFUA_3G06170* demonstrated that both genes are essential for sexual development. Both MAT1-1 gene deletion strains AFUB42900a and AFUB42900b failed to form cleistothecia with a MAT1-2 wild-type partner, and similarly both *MAT1-2* gene deletion strains AFUA3G06170a and AFUA3G06170b failed to form cleistothecia with a MAT1-1 wild-type partner (**Figure 4-8 and 4-9).**

AFUB_037560 (synonym *AFUA_3G11610* in Af293 strain) was identified as a homolog of *A. nidulans* AN2885 sharing 94.1 % identity with E-value of $6.9e^{-36}$, and shared 82.7% identify E-value of $1.3e^{-41}$ to *PaHMG6* (PODAN_1_14230) in *P. anserina* (**Table 4-4; Appendix 51**). *AN2885* was 321 bp in length and encodes a putative 106 amino acid protein, while by comparison *AUFB_037560*, a putative nucleosome binding protein, was 315 bp in length and encoded a putative 104 amino acid protein with an HMB box at residue positions 25 to 93. Deletion of the gene *AFUB_037560* was also found to possibly impact on cleistothecia formation, although the precise effect varied according to the particular transformant used for crossing. The gene deletion strain AFUB37560M1a (MAT1-1 background; **Table 4-5**) produced a greatly reduced number of cleistothecia in crosses with a wild-type partner [$F(6,35)=3.889$; $p=0.0044$] (**Figures 4-10 and 4-11**). However, a second supposedly similar gene deletion strain AFUB37560M1b (also MAT1-1 background; **Table 4-5**) did not show any significant decrease in cleistothecial formation (**Figure 4-11**). When *AFUB_037560* was deleted in the MAT1-2 background, crosses between the two gene deletion strains AFUB37560M2a and AFUB37560M2b with a wild-type partner produced similar numbers of cleistothecia as seen in wild-type crosses (**Figure 4-11**)**.** Finally, when AFUB37560M2a was crossed with AFUB37560M2a then a much reduced number of cleistothecia were produced, although crosses between AFUB37560M1b and AFUB37560M2b did not

shown any such effect (**Figure 4-11; Appendix 56 to 57**). Thus, results with gene *AFUB_037560* were overall inconclusive.

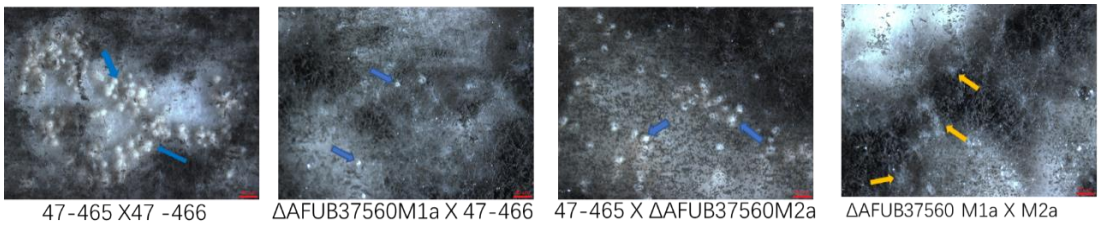

Figure 4-10 Images of crosses to determine impact of gene deletion of *AFUB_037560* on sexual development in *A. fumigatus.* See description under each figure for specific cross. Blue arrow indicates cleistothecia, yellow arrow indicates aggregated hyphal structures. Red scale bar indicates 80 µm.

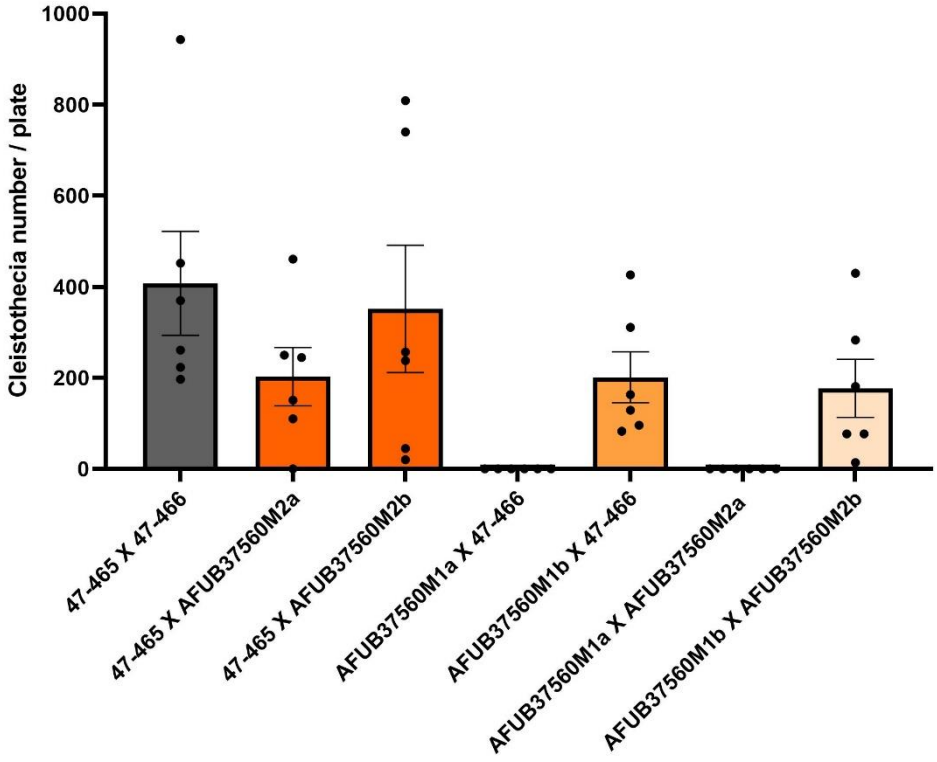

Figure 4-11 Results of crosses to determine impact of gene deletion of *AFUB_037560* on sexual development in *A. fumigatus* [F (6,35)= 3.889, p=0.0044]**.** See description on x axis for specific cross. Data shows average number of cleistothecia formed per 9 cm diameter Petri dish (four replicates) ± SEM. The dots represent replicates of each group.

AFUB_009460 (synonym *AFUA_1G10040* in Af293) was identified as a homolog of *A. nidulans AN1267* with 48.4% identity (E-value: $7.2e^{-05}$) and was 1,200 bp in length and encoded a putative 399 amino acid protein with an HMB box at residue positon from 317 to 383 aa (**Table 4-4; Appendix 53**). *AFUB_009460* shared 32.1 % identify to *PaHMG2* (PODANS_1_7390) with e-value 0.0071. *AFUB_004890* (synonym *AFUA_1G04550* in Af293) was identified as a homolog of *A. nidulans* AN10103 with 79.6% identity and an E-value of $9.2e^{-49}$, and was 930 bp in length encoding a putative 309 amino acid protein with an HMB box at residue position from 108 to 177. *AFUB_004890* shared 51. 3 % idenitity to *PaHMG4* (PODANS_1_11050) with an E-value $1.8e^{-17}$ (**Table 4-4**; **Appendix 52**). Deletion of *AFUB_009460* and *AFUB_004890* (**Table 4-4**), did not show any clear effect on fruit body formation in *A. fumigatus*, whether crosses were made to wild type or gene deletant crossing partners [F (12,39)= 3.022, p=0.0044] (**Figures 4-12 and 4-13; Appendix 56 to 57**).

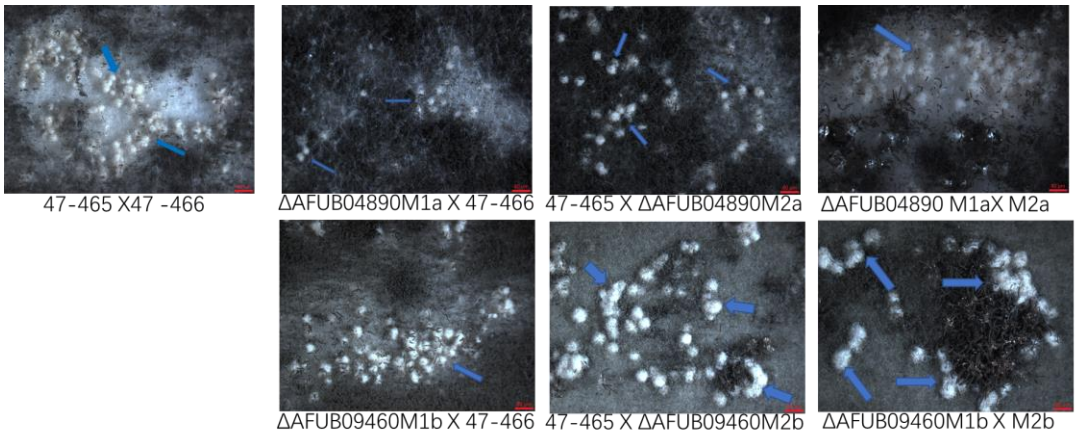

Figure 4-12 Images of crosses to determine impact of gene deletion of *AFUB_004890* and *AFUB_009460* on sexual development in *A. fumigatus*. See description under each figure for specific cross. Blue arrow indicates cleistothecia. Red scale bar indicates 80 µm.

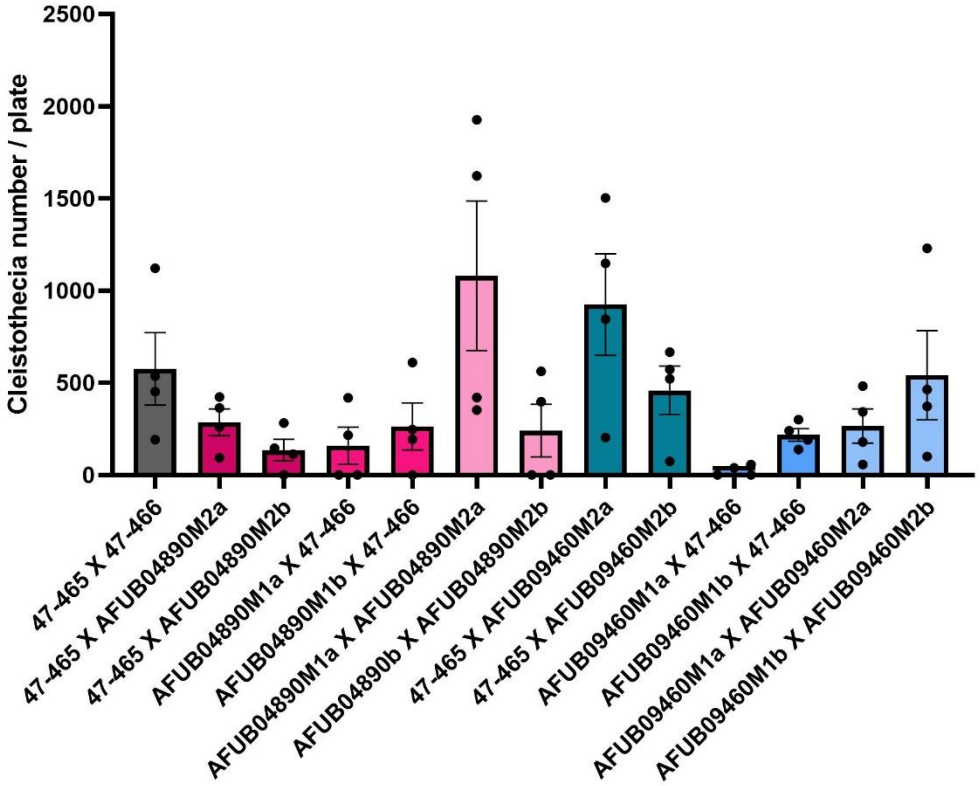

Figure 4-13 Results of crosses to determine impact of gene deletion of *AFUB_004890* and *AFUB_009460* on sexual development in *A. fumigatus.* See description on x axis for specific cross. Data shows average number of cleistothecia formed per 9 cm diameter Petri dish (four replicates) ± SEM. The dots represent replicates of each group. Data was analyzed via ANOVA, showing a significant variation in number of cleistothecia formed in different crosses [F (12, 39) =3.022 and p=0.0044].

4.4 Discussion

The discovery of a sexual reproduction in *A. fumigatus* has opened up the possibility of undertaking methods of classical genetic analysis that rely on the presence of a sexual cycle (O'Gorman et al., 2009). The ability to induce sexual reproduction under controlled laboratory conditions also means that the species can now be used as a model for the aspergilli to study genetic factors controlling sexual reproduction in a heterothallic species, whereas most previous work has been based on research on the homothallic species *A. nidulans* (Todd et al.,

2007; Dyer and O'Gorman, 2012). Work in the present chapter combined genetic manipulation work and sexual crossing to gain various insights into genes effecting sexual reproduction in *A. fumigatus.*

4.4.1. NsdC is an essential element for fruit body development of *A. fumigatus*

The *nsdC* gene is so named for its function in sexual development because gene mutation causes never any sexual development (Kim et al., 2009). The *nsdC* gene has been studied in depth in *A. nidulans*, where it was found to encode a C2H2 type zinc-finger protein (Kim et al., 2009). Two different size mRNA transcripts were detected, with a 2.6 kb mRNA playing an essential role as a promoter of sexual development and repressor of asexual development (Kim et al., 2009). In work described in the present chapter it was found that deletion of *nsdC* in both mating partners blocked the formation of cleistothecia in *A. fumigatus i.e*. exhibiting a similar function as *nsdC* in *A. nidulans*. In other work, Cary et al. (2012) reported that mutation of *nsdC* in *A. flavus* led to a failure in sclerotia production. Taken together, these results indicate that *nsdC* has a conserved role in sexual development for both homothallic (*A. nidulans*) and heterothallic (*A. fumigatus, A. flavus*) *Aspergillus* species. It has recently become apparent that *nsdC* also has more broad roles other than simply the regulation of sexual development, with the gene also having a role in maintaining hyphal growth, as for both *A. nidulans* and *A. fumigatus* the vegetative growth rate was decreased in deletion mutants compared to wild-type strains (Kim et al. 2009; Castro et al., 2021). In addition, other functions of *nsdC* are control of cell wall structure and cell wall and calcium stress response in *A. fumigatus* (Castro et al., 2021), and regulation of secondary metabolite synthesis in *A. flavus* (Cary et al., 2012).

One particularly interesting finding from the present studies into *nsdC* was that it was found to be necessary to knock-out the gene in both MAT1-1 and MAT1-2 mating partners before a significant impact on sexual development was apparent. Thus, when Δ*nsdC* strains (in a MAT1-1 47-51 strain background) were first crossed to wild-type (47-55; MAT1-2) strains, cleistothecia with viable ascospores produced, and it was only when both Δ*nsdC* MAT1-2 and Δ*nsdC* MAT1-1 strains were crossed that sexual development was abolished. This indicated that the function of *nsdC* in the mutant strains could be complemented by the presence of a wild-type allele in the mating partner, which presumably donated a functional protein. This was very useful to know for the subsequent analysis of HMG gene function. This was also a significant finding as most work on genes involved in sexual regulation in the aspergilli have been conducted with the homothallic species *A. nidulans* where the heterothallic mating aspect would be overlooked. As a result of this finding, high fertility Δ*kuB* strains were constructed in both MAT1-1 (47-465) and MAT1-2 (47-466) backgrounds before gene knock out experiments with putative HMG genes was performed.

4.4.2. A network of high mobility group (HMG) genes govern fruit body development of *A. fumigatus*

High mobility group (HMG) proteins, defined by the presence of a core ca. 79 amino acid domain, have been shown to regulate a wide range of developmental processes in eukaryotic organisms (Stros et al., 2007). In the case of the fungal kingdom, HMG genes are best known for their role as ancestral genes with an essential role in the determination of sexual identity (Idnurm et al., 2008; Dyer and O'Gorman 2012). For example, in the aspergilli two complementary members of the HMG family have been identified, namely the MATA_HMG and *MATα_HMG* families (Idnurm et al., 2008; Martin et al.,

2010; Dyer and O'Gorman, 2012). Genes from these families have been shown to be necessary for determination of mating-type identity and are required for sexual reproduction in the aspergilli (Paolettii *et al.*, 2007; Dyer and O'Gorman, 2012). Such *MAT1-1* and *MAT1-2* genes have been identified in numerous *Aspergillus* species (Paoletti et al., 2005; Wada et al., 2012; de Vries et al., 2017). However, other members of the HMG family present in the genome have been less well studied.

In pioneering studies, Salih (2016) identified ten putative HMG genes in the genome of *A. nidulans* by BLASTP searching using sequences from both *A. nidulans* and *P. anserina* HMG core proteins. These genes were then deleted via GM approaches to functionally characterize the putative HMG genes and determine if they had any role in sexual development of the homothallic *A. nidulans*. Besides, the *MAT1* (AN2655) and *MAT2* (AN4734) HMG genes, which had already been characterized (Paoletti et al., 2005; Paoletti et al., 2007; Pyrzak et al., 2008), four additional HMG genes were found to be important for sexual development in *A. nidulans* although other putative HMG genes had no obvious role. Using this data, seven putative HMG genes were identified in *A. fumigatus* in the present study and tested for any possible role in cleistothecial formation. This work identified a network of genes involved in sexual development of *A. fumigatus* as will now be described (**Table 4-6**).

Table 4-6 Phenotypes of HMG gene deletion strains in *A. fumigatus*

	Cleistothecia formation		
Strain	**Gene deletion in MAT1-1 background X WT**	**Gene deletion in MAT1-2 background X WT**	**Gene deletion in MAT1-1 X MAT1-2 background**
AFUB_069370	-	-	-
AFUB_067900	-	-	-
AFUB_042900	-	N/A	N/A
AFUA_3G06170	N/A	-	N/A
AFUB_037560	+	+	+
AFUB_009460	+	+	+
AFUB_004890	+	+	+

+ indicates the present of cleistothecia; - indicates the absence of cleistothecia

4.4.2.1 The *AFUB_069370* gene represents a functionally conserved gene required for sexual development in Ascomycota species

Deletion of *AFUB_069370* in both the MAT1-2 and MAT1-1 background strains resulted in a block in the development of cleistothecia whether the knock-out strains were out-crossed to wild-type or gene deletant strains *i.e.* unlike the previous finding for nsdC, the presence of a functional copy of the gene in one mating partner could not compensate for the deleted gene in the other mating partner. The deletion of the homologous *AN3667* gene in *A. nidulans* was also found to lead to a block in formation of cleistothecia, the three Δ03667.1 transformants strains studied being sterile (Ashour, 2014). Interestingly though, these *A. nidulans* knockout strains instead showed prolific production of Hülle cells, and similarly the△*AFUB_069370 A. fumigatus* strains formed hyphal aggregates when the gene deletion strains were crossed with the wild-type, suggesting that *AFUB_069370* acts at an early point in sexual

morphogenesis. Homologs of *AFUB_069370* in other Ascomycota species have also been shown to be responsible for sexual development as well. In *N. crassa,* the homolog *fmf-1* is required for differentiation of sexual structures, and in *Schizosaccharomyces pombe* the homolog *ste11* is involved with nutrient stress and activation of the sexual cycle.

Meanwhile, in *P. anserina PaHMG5*, which is a homolog of *AFUB_069370*, was reported to be the central regulator that controlled mating (**Figure 4-2**). Deletion of *PaHMG5*, a MATA-HMG family member, blocked the fertility of both male and female strains, which led to no fruit bodies being formed (Benkhali et al., 2013). However, overexpression of the *PaHMG5* did not promote the production of perithecia (the fruit bodies of *P. anserina*) (Benkhali et al., 2013). Similarly, overexpression of *AN3667* in *A. nidulans* did not promote sexual development but caused an abolishment of cleistothecia similar to that seen in the gene deletion stains (Salih, 2016). After 10 days of incubation, the gene overexpression strains only formed a very small colony when comparing to the parental strain (Salih, 2016). It was hypothesized that the overexpression of *AN3667* might have resulted in a decreased vegetative growth rate under these conditions (Salih, 2016). An inhibition of vegetative growth rate was also observed following overexpression of the HMG *MAT1* and *MAT2* genes in *A. nidulans* (Paoletti *et al.,* 2007). It was hoped to overexpress *AFUB_069370* in the present study, but due to time limitations this was not possible.

Regarding the position of PaHMG5 in the regulatory network for sex, Benkhali et al. (2013) provided evidence that *PaHMG5* acts upstream of the mating-type genes *fmr1* and *fpr1*, which indicates a very important role of this HMG genes in sexual development (**Figure 4-2**). *PaHMG5* was found to regulate the expression of other HMG genes including PaHMG6, PaHMG8, KEF1 and mtHMG1, which are all genes relating to sexual development (Benkhali et al., 2013). End-point RNA expression studies in *A. nidulans* also

showed that AN3667 might be a regulator of the *MAT1* and *MAT2* genes in this species (**Figure 4-14;** Salih, 2016). Taken as a whole, the similar function of *AFUB_069370, AN3667* and *PaHMG5* and other homologs indicates a conserved central role of this HMG domain protein in Ascomycota sexual development.

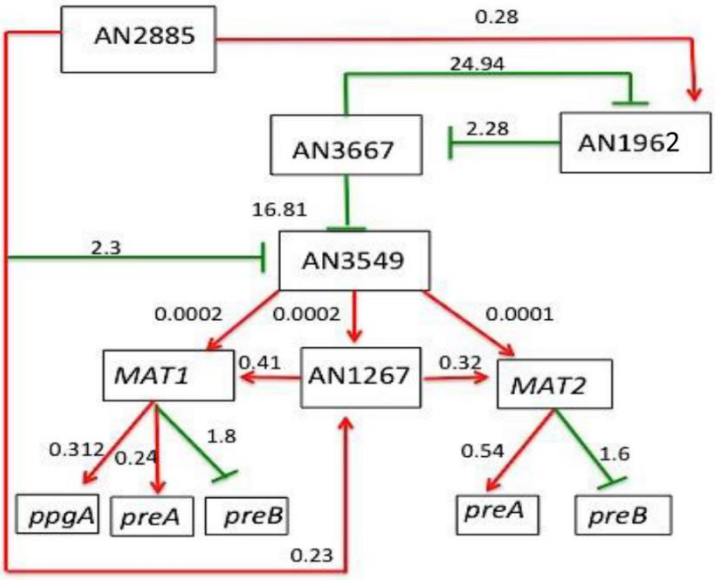

Figure 4-14 Schematic diagram showing the genetic interaction of some HMG genes that regulate mating in *A. nidulans* (Salih, 2016). The red arrows indicate that the genes were induced while the green arrows indicate a suppressive effect of the genes. Numbers represent the fold change in gene transcript level in the mutant strains relative to the parental strain.

4.4.2.2 *AFUB_067900* is a functionally conserved gene required for sexual development in Ascomycota species

Deletion of *AFUB_067900* in *A. fumigatus* led to a loss of cleistothecial formation, and the function of *AFUB_067900* could not be complemented by crossing to a wild-type parent unlike the situation with *nsdC* (**Section 4.3.1**). Deletion of the homolog *AN1962* in *A. nidulans* also caused abnormal development of cleistothecia. However, deletion of this gene did not result in a complete loss of fertility; instead, there was a drastic decrease in the number of cleistothecia formed, which were larger in size compared to the parental

strain (Salih, 2016) i.e. a less severe phenotype than was observed in *A. fumigtaus.* Similar to *AN3667* in *A. nidulans,* the over-expression of *AN1962* caused a reduction in the number of cleistothecia number, but a promotion of cleistothecia diameter (Salih, 2016). Further RNA analysis by Salih (2016) indicated that AN1962 might be a bi-functional regulator of sexual development in an upstream position, thereby controlling the expression of MAT1 and MAT2 downstream (**Figure 4.14**; Salih, 2016). Deletion of another homolog *PaHMG8* caused sterile in female strain in *P.anserina*, and no fruit body was observed in Δ *PaHMG8* crossing plates, and *PaHMG8* regulates mating-type genes expression (Benkhali et al, 2013). Taken as a whole, these results indicate that *AFUB_067900* homologs have a conserved function in fruit body development of filamentous fungi, acting at an upstream position. Due to time limitation, the overexpression of *AFUB_067900 (AFUA_4G10820)* was not attempted in the present study.

4.4.2.3 Deletion of mating-type genes *AFUB_042900* and *AFUA_3G06170* affects fruit body development

It had previously been established that mating-type (*MAT*) genes are essential for fruit body formation and ascosporogenesis in the homothallic species *A. nidulans* (Miller et al., 2005; Paoletii et al., 2007; Salih 2016). Similarly, the deletion of *MAT* genes was also found to completely block cleistothecial formation in *A. fumigatus* in the present study. Deletion of *AFUB_042900* led to defects in cleistothecia formation, whilst the *AFUA_3G06170* deletant strains also failed to form fruit bodies. Mating-type genes have also been shown to be required for sexual reproduction in many other pezizomycete species e.g. *Neurospora crassa* and *P. anserina* (Kim et al., 2012; Grognet et al., 2014). Thus, HMG family mating-type genes are conserved functionally and/or structurally in filamentous fungi. For example,

Pyrzak et al. (2008) replaced the *MAT2* (AN4734) of *A. nidulans* with *MAT1-2* from *A. fumigatus*, and found that the heterologous expression of *MAT1-2* was able to restore fruit body formation in *A. nidulans*. In a similar fashion, the HMG mating-type genes of *N. crass* and *P. anserina* are functionally conserved as shown by the finding that the transformations of *mat-a* and *mat-A1* genes of *N. crassa* into sterile null *mat* strain of *P. anserina* were able to complement the fertilization process, although ascospore failed to form (Arnaise et al., 1993).

4.4.2.4 Other HMG genes may have a species or *MAT*-specific influence on fruit body formation

Although the impact of deletion of *AFUA_037560* of *A. fumigatus* was overall inconclusive, there was nevertheless some indication that gene deletion (strain AFUB37560M1a) specifically in the MAT1-1 background could cause a reduction in number of cleistothecia produced. This phenotype resembles studies with *Pa_HMG6* of *P. anserina* in which gene deletion caused a remarkable reduction in female fertility, with a 50-fold decrease in perithecial formation as compared to the wild-type strain, and with production of a larger modified perithecial neck, whereas a male mutant strain was still fertile (Benkhali et al., 2013). The homolog *AN2885* gene also belongs to the HMG-B family, and the deletion of this gene in *A. nidulans* resulted in reduced fertility compared to the parental strain with a reduction in the number of cleistothecia formed but with those cleistothecia, which were produced having a significantly larger diameter (Salih, 2016). Thus, in contrast to *P. anserina* and *A. nidulans*, there might be genes having a different influence according to the mating type genetic background in heterothallic species such as *A. fumigatus.* However, there was inconsistenty in results concerning deletion of *AFUA_037560* in *A. fumigatus*. For example, strain AFUB37560M1b did not show the phenotype of reduced fertility in the MAT1-1 background seen in AFUB37560M1a. The

reasons why were unclear, but might be caused by factors such as growth rate differences or incorrect deletion of the gene.

In contrast to other HMG genes, the deletion of *AFUB_004890* and *AFUB_009460* had no obvious effect of sexual reproduction in *A. fumigatus*, all deletion strains producing cleistothecia similar to those produced by the parental strain. Similar to *AN10103* in *A. nidualns* and *PaHMG4* in *P. anserina, AFUB_004890* did not affect cleistothecia formation in *A. fumigatus. AN10103* from *A. nidulans* is not involved in sexual development, and the deletion strains were able to form cleistothecia (Salih, 2016). *AN10103* (HmbC) is homologous to *S. cerevisae Hmo1* and *S. pombe Sp-Hmo1*, and belongs to the same clade as *Pa_HMG4* of *P. ansinera* (Benkhali et al. 2013; Karacsony et al., 2014; Salih, 2016). Mutant strains of *Pa_HMG4* are male and female fertile and develop normal perithecia (Benkhali et al., 2013). Mutant strains of *S. cerevisae Hmo1* are characterized by decreased growth rate and other growth defects but show normal sporulation (Lu et al., 1996). Thus, the function of these genes might be specific to each species in terms of development or even in other cellular processes. Similar with *PaHMG2* in *P. anserina* (Benkhali et al., 2013), *AFUB_009460* was found not to have a role in sexual development of *A. fumigatus*. *AFUB_009460* is the homolog *AN1267* which influences number of cleistothecia in *A. nidulans* (Salih, 2016). *AN1267* belongs to the mitochondrial HMGB family, and genes from this family have diverse functions including regulating germination of sexual and asexual spores, mitochondrial DNA replication, protecting cells from reactive oxygen species (ROS), and sterigmatocystin production in *veA1* background strains (Salih, 2016; Karacsony et al., 2014, 2015). Therefore, *AFUB_009460* in *A. fumigatus*. might have functions in the cell other than sexual development.

4.4.3. Closing remarks

By way of conclusion, experimental work in this chapter demonstrated that HMG genes in the genome other than simply the well-known *MAT* genes are also required for sexual development of *A. fumigatus.* Indeed, based on previous work in *A. nidulans* (Salih, 2016) and *P. anserina* (Benkhali et al. 2013) these HMG genes are likely to form a regulatory network, and it would be interesting future work to see if the same 'circuitry' is evident as in *A. nidulans* and *P. anserina.*

It is noted again that for all genes under investigation, the approach used was to compare sexual fertility between control and gene deletion strains in terms of number of cleistothecia formed, number of ascospores formed, and the viability of ascsopores. There were no apparent major growth rate differences between most of the control and gene deletion strains. However, this was not formally investigated and so it is acknowledged that slight reductions in growth in gene deletion strains might have partly been responsible for any observed decrease in sexual fertility.

Finally, it is noted that one side benefit of the present work was the construction of high fertility Δ*kuB* MAT1-1 and Δ*kuB* MAT1-2 strains of *A. fumigatus* that are anticipated to be of use in future mating studies with *A. fumigatus* and to the community in general.

Chapter 5 The effects of HMG genes on secondary metabolism

5.1 Introduction

Fungal secondary metabolites (SMs) have roles in fungi relating to aspects of their biology such as defense against other microbes, response to environmental stressors, virulence and ability to cause disease, and asexual and sexual reproduction (Lim et al., 2012). Hence many fungal SMs show biological activity and as such have impacted on human life in the areas of crop, food and health. Taking *Aspergillus* species as an example, aflatoxins produced by *A. flavus* and sterigmatocystin synthesised by *A. nidulans* are associated with virulence towards plants (Musungu et al., 2016; Tsitsigiannis et al., 2006). *A. fumigatus* produces abundant SMs including gliotoxin, helvolic acid, fumagillin, pseurotin, fumigatin, trypacidin, melanin, fumigaclavin and others, which may enhance pathogenicity of the species (Cramer et al., 2009; Frisvad et al., 2009). Gliotoxin, one key secondary metabolite produced by *A. fumigatus*, targets neutrophils or other phagocytes that promote invasion by inducing apoptosis of these cells, and higher levels of gliotoxin are associated with higher virulence (Orciuolo et al., 2007; Spikes et al., 2008). The presence of bacteria can also increase gliotoxin production by *A. fumigatus* (Comera et al., 2007; Svahan et al., 2014). Pseurotin A represses production of immunoglouline E, but on the other hand, it has an antibacterial function and inhibits loss of bone mass by reducing reactive oxygen species (ROS) levels in bone (Chen et al., 2019; Ishikawa et al., 2009; Mehedi et al., 2010).

Production of these natural compounds normally arises from so-called secondary metabolite gene clusters containing backbone biosynthetic genes, precursor modifying genes, and cluster-specific modifying genes amongst

others such as possible transport protein encoding genes (Lim et al., 2012). Some regulators of SM production have been identified. For example, the LaeA, nuclear methyltransferase, is a regulator of widespread SM production in the Ascomycota. The biosynthesis of sterigmytocystin in *A. nidulans*, penicillin in *Penicillium* spp., gliotoxin in *A. fumigatus*, and aflatoxins in *A. oryzae* are all regulated by LaeA (Bayram et al., 2008; Ben-Amiet al., 2009; Bok and Nancy, 2004; Kale et al, 2008; Kosalkova et al., 2009). Regarding gliotoxin synthesis in *A. fumigatus*, a C_2H_2 type transcription factor *gipA* (gliotoxin inducing protein A) has been shown to induce the expression of gliotoxin cluster genes such as *gliA, gliZ, gliP* and *gliT,* due to the ability of GipA to bind to multiple sites in the gliotoxin cluster (Schoberle et al., 2014).

5.1.1 Fungal secondary metabolites and developmental processes

There is accumulating evidence to suggest that fungal secondary metabolism and developmental processes such as asexual and sexual sporulation may be correlated with each other (**Section 1.4**). Gliotoxin biosynthesis in *A. fumigatus* is regulated by the gliotoxin biosynthetic cluster, which contains 13 genes, and the expression of some genes is correlated with asexual development (Shin et al., 2015). For example, deletion of the conidiation related genes *abaA* and *brlA* reduced expression of the gliotoxin detoxifying gene *gliT* which protects strains from exogenous gliotoxin, and these conidiation related genes down-regulate *gliM* expression which is involved in gliotoxin production (Shin et al., 2015). Elsewhere, the *ppo* genes that produce oxylipins which promote cleistothecial formation in *A. nidulans* have also been shown to influence sterigmatoxystion (ST) and penicillin (PN) synthesis in *A. nidulans,* with the deletion of *ppo* genes repressing ST production but promoting PN synthesis (Tsitsigiannis et al., 2006; Tsitsigiannis and Keller, 2006). SM genes may also have a role in sexual morphogenesis in

fungi as well. PaAflR is an ST specific regulatory gene in *P. anserina*. Over-expression of *PaAlfR* was found to increase ST production but cause sterility in *mat-* strains of *P. anserina* (Shen et al., 2019). The overexpression of another SM related gene *PaStcA*, the core ST polyketide synthetase gene, led to a sterile phenotype and promoted ST synthesis (Shen et al., 2019).

5.1.2 Aims of chapter

A recent study in *A. fumigatus* revealed that biosynthesis of fumagillin, a mycotoxin which reduces macrophage activity, is influenced by mating-type (*MAT*) genes (Yu et al., 2018). Over-expression of *MAT1-1* and *MAT1-2* suppressed fungal growth, but production of fumagillin and expression of the biosynthesis relating genes *laeA, fapR and fmaA* were increased (Yu et al., 2018). However, the extent to which high mobility group (HMG) genes might impact on fungal secondary metabolism in more general is unknown. In previous work in the present study seven putative HMG genes were identified from *A. fumigatus*, and four of these genes were shown to be necessary for fruit body formation. Therefore the aim of work in this chapter was to determine if these HMG genes had any dual role both in secondary metabolites synthesis and sexual development. Production of key mycotoxins including helvolic acid, gliotoxin, pseurotin A and fumagillin was examined in HMG deletion strains of both *MAT1-1* and *MAT1-2* genetic background to assess any potential role of the HMG genes in mycotoxin secondary metabolism.

5.2 Materials and Methods

5.2.1 Materials

5.2.1.1Strains

A. fumigatus strains 47-465, 47-466, AFUB69370M1a, AFUB69370M1b, AFUB69370M1C, AFUB69370M2a, AFUB69370M2b, AFUB69370M2C, AFUB67900M1a, AFUB67900M1b AFUB67900M2a, AFUB67900M2b AFUB42900a, AFUB42900b, AFUA3G06170a, AFUA3G06170b, AFUB37560M1a, AFUB37560M1b, AFUB37560M2a, AFUB37560M2b, AFUB04890M1a, AFUB04890M1b, AFUB04890M2a, AFUB04890M2b, AFUB09460M1a, AFUB09460M1b, AFUB09460M2a, AFUB09460M2b were utilized to investigate the production of mycotoxins (**Table 4-6**).

5.2.1.2 Media

To induce production of pseurotin A, gliotoxin, fumagillin, and helvolic acid，the following media are used.

MEA

MEA was prepared by dissolving the following components: 20 g malt extract, 1 g peptone, 20 g glucose in 1 L distilled water. The broth was adjusted to pH 6.5 and autoclaved at 121 ℃ for 15 mins.

Glucose Minimal Medium (GMM)

GMM was prepared by dissolving the following components: 1 mL trace element solution (**Section 2.1.1**), 6 g $NaNO_3$, 0.52 g KCl, 1.52 g KH_2PO_4, 0.52 g $MgSO_4 \cdot 7H_2O$, 10 g/L glucose in 1 L distilled water. The medium was adjusted to pH 6.5 and autoclaved at 121 ℃ for 15 mins.

Czapek Dox Broth

Czapek Dox Broth was prepared by dissolving the following components: 30 g sucrose, 3 g $NaNO_3$, 1 g K_2HPO_4, 0.5 g $MgSO_4 \cdot 7H_2O$, 0.5 gKCl, 0.01 g $FeSO_4 \cdot 7H_2O$ in 1 L distilled water. The medium was adjusted to pH7.3 and autoclaved at 121 ℃ for 15 mins.

YEG medium

YEG medium was prepared by dissolving the following components: 40 g glucose, 8 g yeast extract in 1 L distilled water. The medium was autoclaved at 121 ℃ for 15 mins.

5.2.2 Methods

5.2.2.1 Induction of mycotoxins

Conidial spore suspensions with a concentration of 1 X 10^7 spores/mL were prepared and 1 mL of the suspension was pre-incubated in MEA for 24 hours at 37 ℃. The mycelia were harvested and transferred into 25 mL GMM in a 250 mL shake flask, and then incubated at 37 ℃ with shaking at 150 rpm (Yu et al., 2018). After 6 days of incubation, 20 mL of liquid culture was extracted with 20 mL of ethyl acetate, and the organic phase was collected. Alternatively, the strains were inoculated in Czapek Dox broth or YEG medium by adding 1 mL of a conidial spore suspension of concentration 1 X 10^7 spores/mL for 7 days.

The incubated solution was filtered through a sterile funnel with one layer of Miracloth to separate the mycelia and broth. The broth (approx. 20 mL) was collected in 250 mL bottle and was adjusted to pH=2 with 6 M HCl to protonate any acidic mycotoxin for better extraction, and then 20 mL fresh ethyl acetate was added to extract the mycotoxin. The ethyl acetate layer was harvested into the 250 mL bulb breaker and evaporated. The residue was re-dissolved in 1 mL

of 10 % DMSO-methanol solution according to methods described by Yu et al. (2018).

5.2.2.2 Preparation of standard solution

Samples including helvolic acid (ApexBio, USA), gliotoxin (Sigma-Aldrich, UK), fumagillin (ApexBio, USA), pseurotin A (Thermo, UK) were dissolved into 10 % DMSO-methanol solvent with concentration of 1 mg/mL respectively and stored as the stock at 4 ℃. The samples were diluted into 400 μg/mL, 200 μg/mL, 100 μg/mL, 50 μg/mL, 25 μg/mL, 12.5 μg/mL, 6.25 μg/mL to prepare a calibration curve.

5.2.2.3 HPLC analysis

Extracts were analyzed by HPLC-DAD (Thermo Ultimate 3000). The mobile phase was a combination of solvent A (H_2O with 0.1% formic acid) and solvent B (100 % acetonitrile): 0% solvent B from 0 to 5 min, 0% to 100% solvent B from 5 min to 30 min, 100% solvent B from 30 to 35 min, 100% to 0% solvent B from 35 to 40 min, and re-equilibration with 0% solvent B from 40 to 45 min. The flow is 0.125 ml/min. Column temperature was 20 ℃. The UV were 254 nm and 335 nm. The HPLC column used was a reverse-phase C 18 column (Accucore C18; length X internal diameter 150X 2.1; particle size 2.6 μm).

5.3 Results

5.3.1 Validation of standard samples qualitatively and quantitatively

Standard samples were analyzed qualitatively and quantitatively (**Figures 5-1 and 5-2**). Pseurotin A showed a retention time of 22.520 min with UV at 254 nm. Gliotoxin showed a retention time of 23.633 min with UV at 254 nm.

Helvolic acid showed a retention time of 30.653 min with UV at 254 nm. Fumagillin showed a retention time of 28.500 min with UV at 335 nm. The calibration curves for the gliotoxin, helvolic acid and pseurotin A standards showed good linearity (R^2 > 0.99) in a concentration range from 400 µg/mL, to 6.25 µg/mL by double dilution, and the calibration curve of fumagillin showed a linearity with R^2 = 0.9698 (**Figure 5-2**).

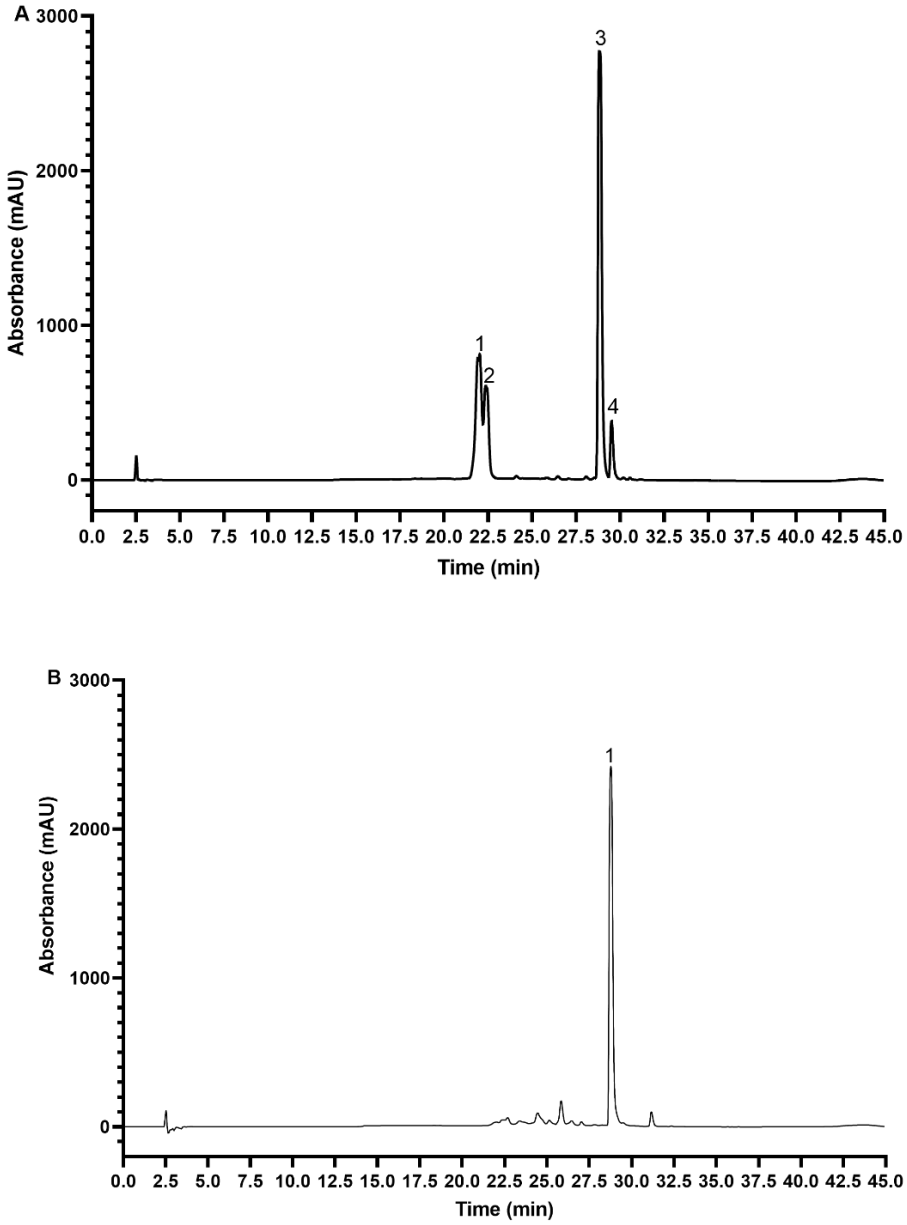

Figure 5-1 Chromatogram of the mycotoxin standards. (**A)** indicates the mycotoxin at 254 nm UV including **1** pseurotin A with retention time 22.520 min, **2** gliotoxin 23.633 min, **3** fumagillin 28.500 min and **4** helvolic acid 30.653 min.

(**B)** indicates **1** fumagillin at 335 nm with retention time 28.500 min. Each standard was detected separately to validate the retention time.

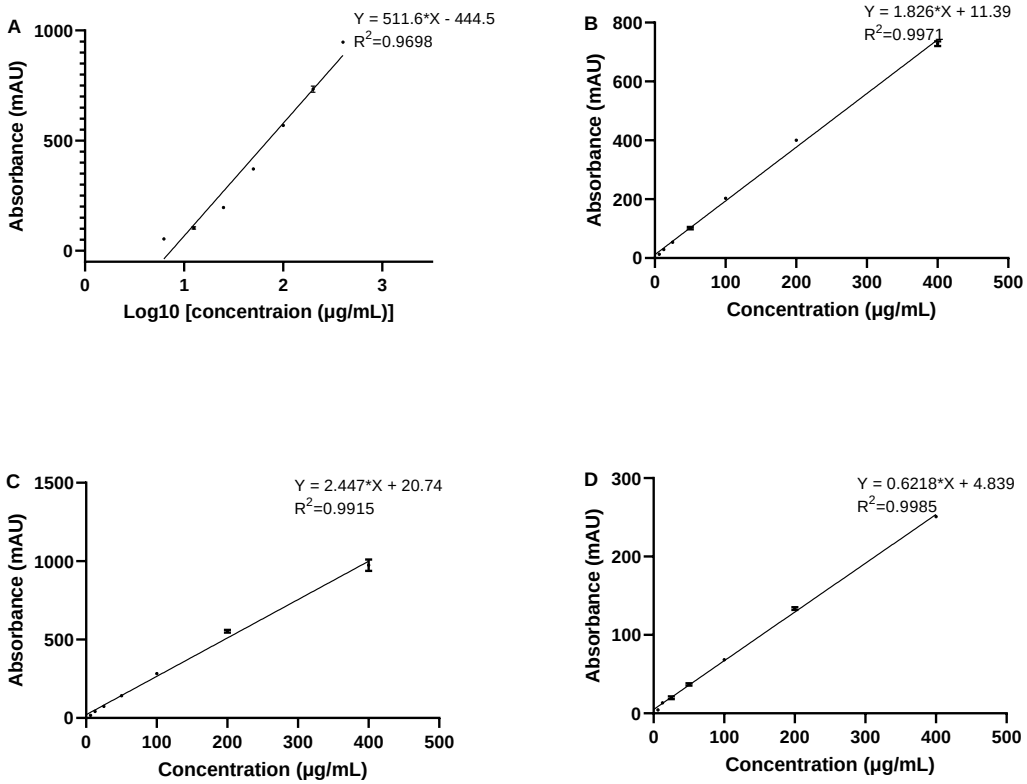

Figure 5-2 Calibration curve of mycotoxin standards. Linear regression equations for each chemical are listed at the upper-right side of each figure. X indicates concentration; Y indicates UV absorbance. **A** represents the linear regression of fumagillin.The concentration value of fumagillin standards were converted into logistic data for better fit of linear regression curve. **B** represents the linear regression of gliotoxin. **C** represents the linear regression of pseurotin A. **D** represents the linear regression of helvolic acid. Each HPLC sample was repeated with three replicates. Error bars indicate ± SEM.

5.3.2 Production of mycotoxin in ΔHMG strains

It was first necessary to identify media that reliably induced secondary metabolite production in the control strains. After 7 days of incubation in test media, secondary metabolites were extracted from the broth and analyzed via HPLC-DAD (**Section 5.2.2.1; 5.2.2.3**). Fumagillin and pseurotin A were detected when strains were incubated in GMM (**Figure 5-4 to 6; Figure 5-8 to**

9), and gliotoxin was detected when strains were incubated in Czapek Dox broth (**Figure 5-10 to11**). However, helvolic acid was not detected via HPLC when strains were incubated in GMM, Czapek Dox broth, MEA or YEG medium despite these media previously being reported to induce helvolic acid (Filtenborg et al., 1990; Yu et al., 2018; Rise et al., 2020).

5.3.2.1 Synthesis of fumagillin in control and ΔHMG strains

The average production of fumagillin differed between MAT1-1 and MAT1-2 backgound strains (**Figure 5-3**). In the MAT1-1 background, fumagillin production did not show a significant difference between gene deletion strains and the wild-type, except for strain Δ AFUB37560M1b. Although the complement strain of Δ*AFUB_0069370* showed a significant increase of fumagillin production [F (13, 28) =16.97, P<0.0001], this was considered a possible artefact caused by the growth difference. By contrast, strains AFUB37560M1b produced significantly higher amounts of fumagillin [F (13,28)=16.97, P<0.0001], whereas Δ AFUB37560M1a did not show differences to the wild-type strain 47-465. Meanwhile, production of fumagillin in the *MAT1-2* background strains did not show significant differences in most Δ*HMG* strains when compared with the wild-type controls, except that Δ *AFUB_009460* strains produced increased amounts of fumgagillin [F (13,28)=16.97, P<0.0001]. Compared to the *AFUB_069370* complementation in MAT1-1 background, AFUB69370M2C recovered fumagillin production [, F(13,28)=16.97, P=0.5705].

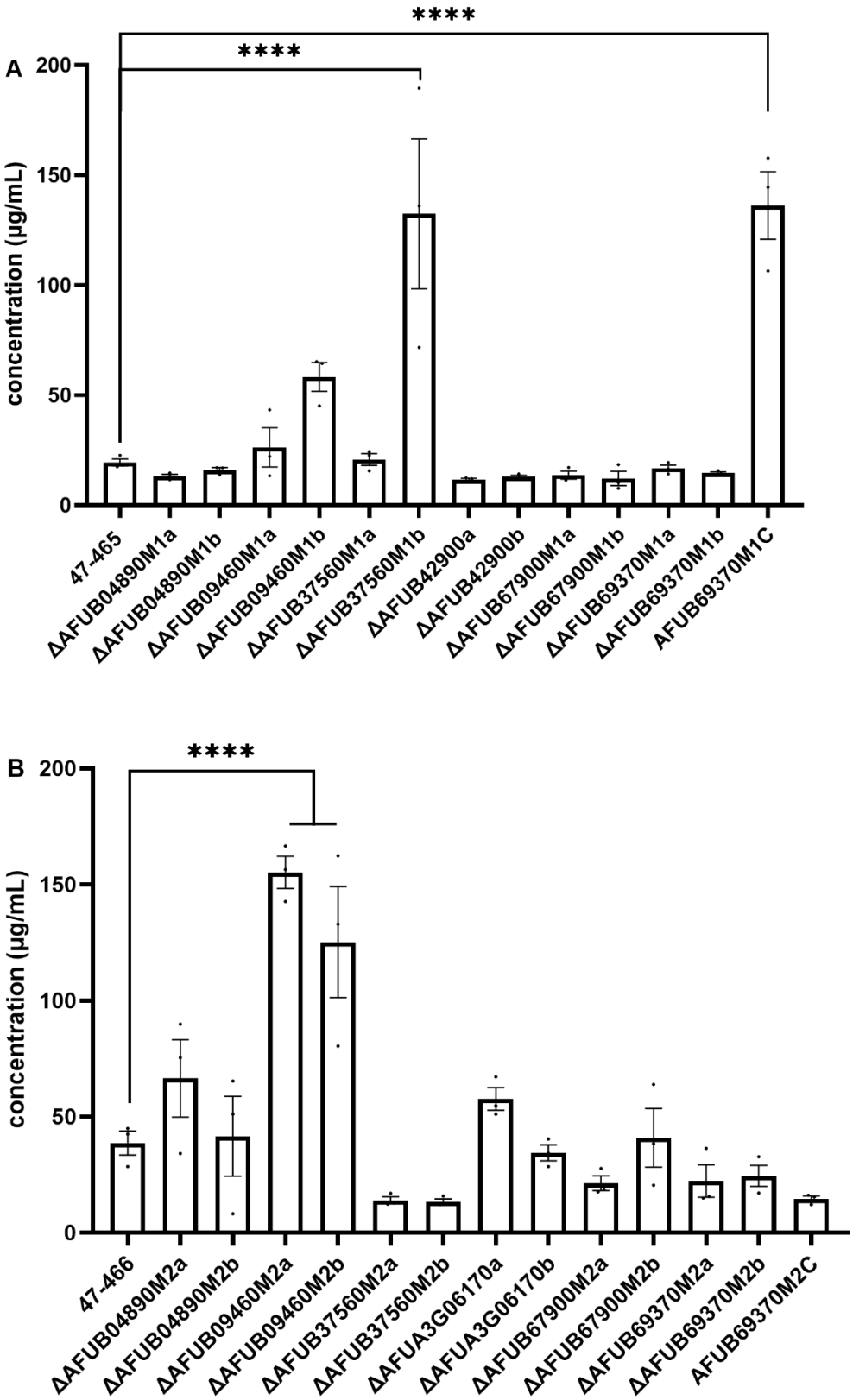

Figure 5-3 Production of fumagillin in control and *Δ*HMG gene strains of *A. fumigatus*. A indicates production of fumagillin from ΔHMG strain in MAT1-

1 background, and **B** indicates production of fumagillin ΔHMG strain in MAT1-2 background. Dots represents the biological replicates, and error bars represent ± SEM. Data was analyzed via one-way ANOVA. **** indicates P<0.0001

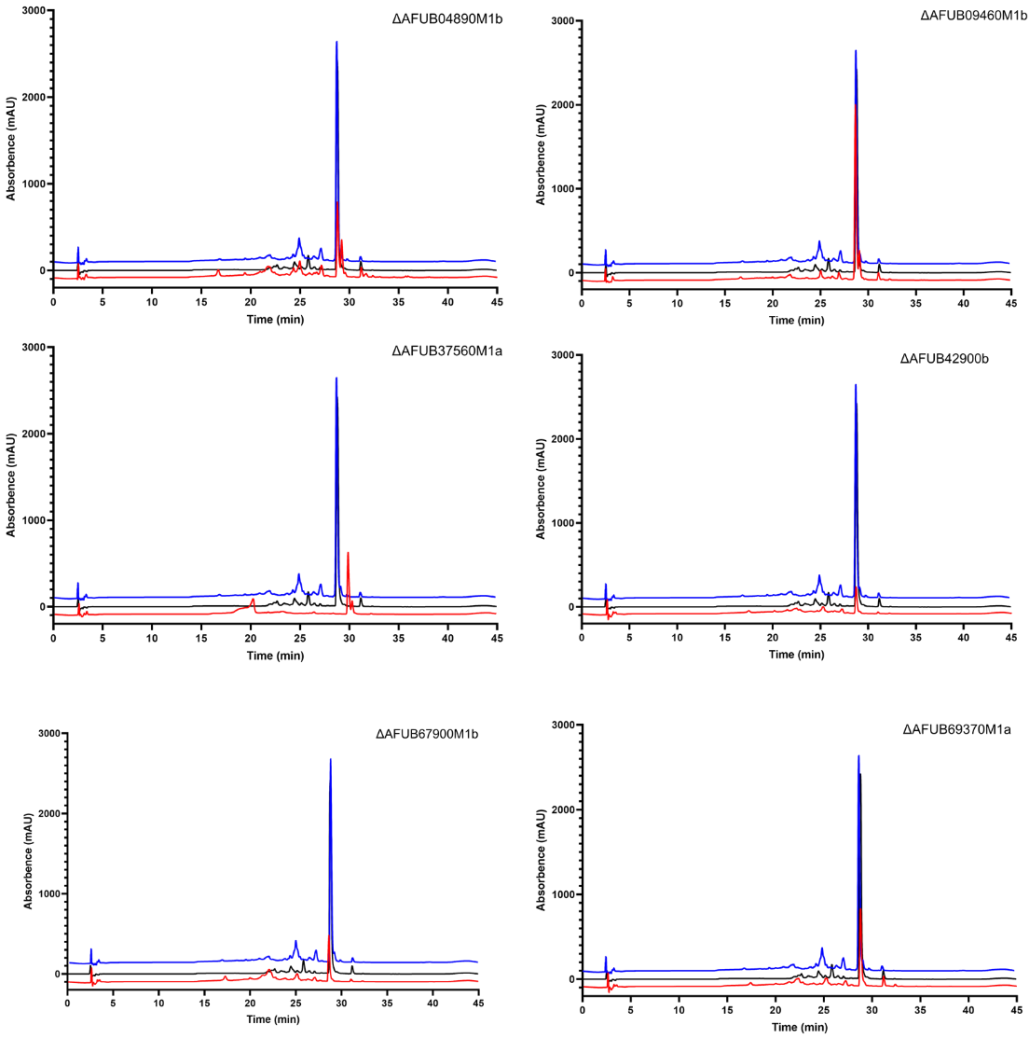

Figure 5-4 Chromatogram of fumagillin production in control and *ΔHMG A. fumigatus* strains of MAT1-1 background. The black line indicates the fumagillin reference. The blue line indicates the parental strain 47-465, and the red line indicates the HMG mutant strain sample, with respective mutant strains indicated by label at top right hand side of graph.

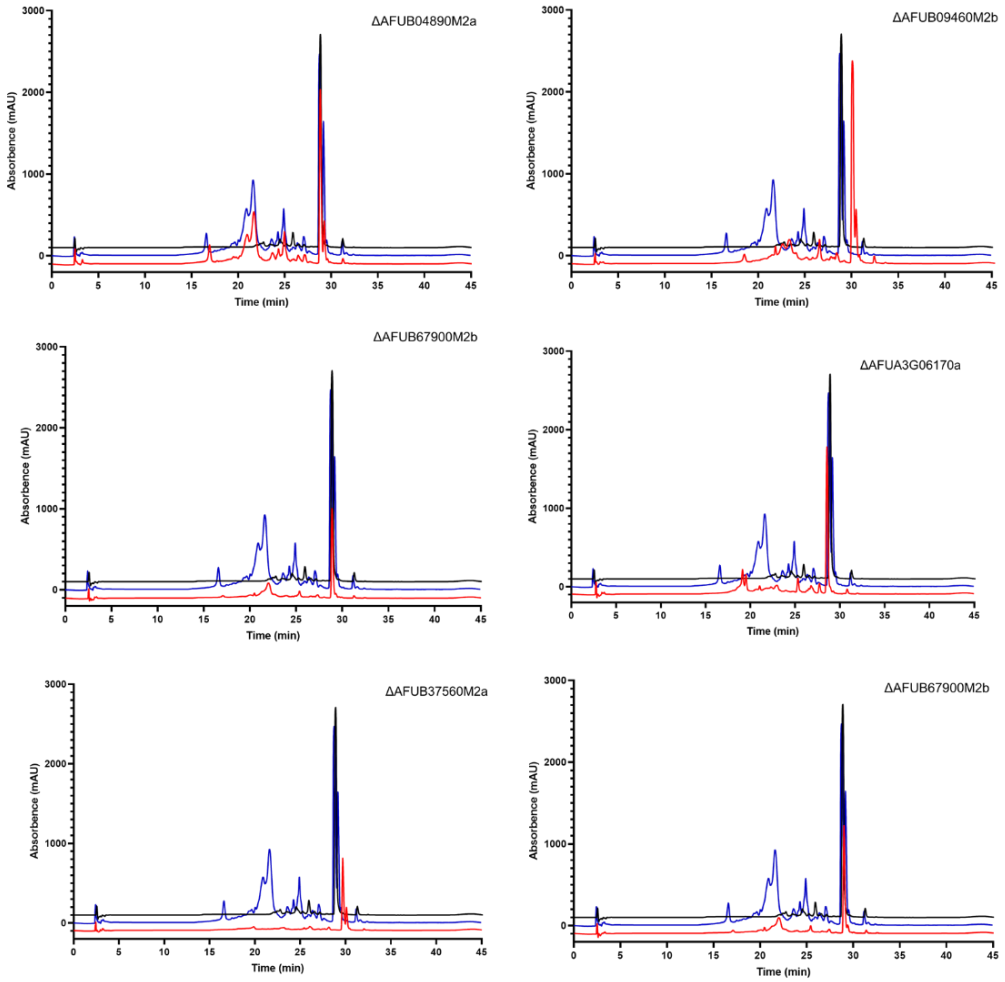

Figure 5-5 Chromatogram of fumagillin production in control andΔHMG strains with MAT1-2 background. The black line indicates fumagillin reference. The blue line indicates the parental strain 47-466, and the red line indicates the HMG mutant strains sample, with respective mutant strains indicated by label at top right hand side of graph.

5.3.2.2 Synthesis of psuerotin A in control and Δ HMG deletion strains

Production of pseurotin A was decreased in many of the ΔHMG strains. This was most prominent in the ΔAFUB69370 strains where deletion of *AFUB_069370* caused a significant reduction in pseurotin A levels in both MAT1-1 and MAT1-2 background strains [**Figure 5-6**; $F(14,30)=9.884$, $P<0.005$ for MAT1 background; $F(14, 30)=13.93$, $P<0.0001$ for MAT1-2 background]. The complementation strains AFUB69370M1C and AFUB69370M2C produced

a relatively higher amount of pseurotin A but did not recover production levels to the wild-type parental levels. Pseurotin A synthesis in ΔAFUB67900 strains was reduced significantly in MAT1-2 background [F (14,30)=9.884, P<0.0001]. In MAT1-1 background, ΔAFUB67900M1a strain decreased in pseurotin A production significantly, while ΔAFUB67900M1b showed on average reduced production [F(14,30)=9.844, p=0.2654]. Similarly, the ΔAFUB42900a strain showed a significant reduction in production with a p-value of 0.0003, but ΔAFUB42900b only showed decrease of synthesis on average with p-value of 0.1065, which does not support the decrease as the significant result. ΔAFUA3G01670b produced significantly less pseurotin A (p<0.0001), but the ΔAFUA3G06170a strain did not support the decrease significantly (P=0.1495) even the average production was lower than the wild type. This may be caused by variations in growth ability of strains. Deletion of *AFUB_037560* caused a reduction in synthesis of pseurotin A in the MAT1-2 background of both strains [F (14, 30) =13.93, p<0.0001] and .In MAT1-1 background, strain ΔAFUB37560M1a showed a significant reduction in pseurotin A synthesis [F(14,30)=9.844, P<0.0005), but ΔAFUB37560M1b did not show any decrease of pseurotin A production (P=0.9994). Deletion of *AFUB_009460* caused a non-significant decrease of pseurotin A production in the ΔAFUB09460M1a, ΔAFUB09460M1b, and Δ AFUB09460M2a strains, but reduction of pseurotin A production in ΔAFUB09460M2b was significant when compared to the wild-type (P<0.0001). Even through the phenotype of *AFUB_009460* mutant strains produced less pseurotin A, the data did not suggest that this HMG gene is important for pseurotin A synthesis. Deletion of *AFUB_004890* did not affect pseurotin A production in either mating-type background.

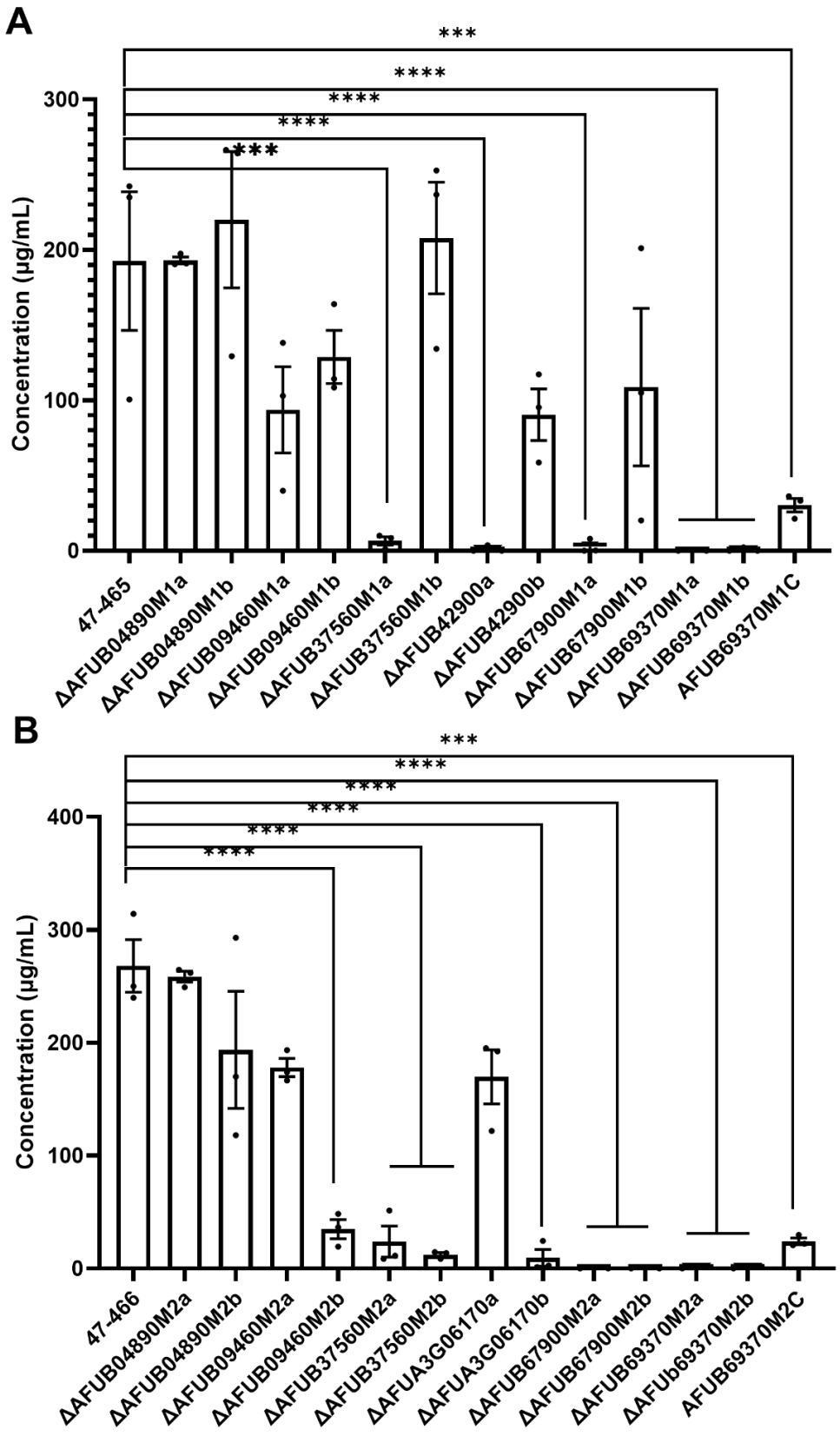

Figure 5-6 Production of pseurotin A in control and *Δ*HMG gene strains of *A. fumigatus* **A** indicates production of pseurotin A from ΔHMG strain in MAT1-

1 background, and **B** indicates production of pseurotin A ΔHMG strain in MAT1-2 background. Dots represents the biological replicates, and error bars represent ±SEM. Data was analyzed via one-way ANOVA. *** indicates $p<0.005$; **** indicates $p<0.0001$.

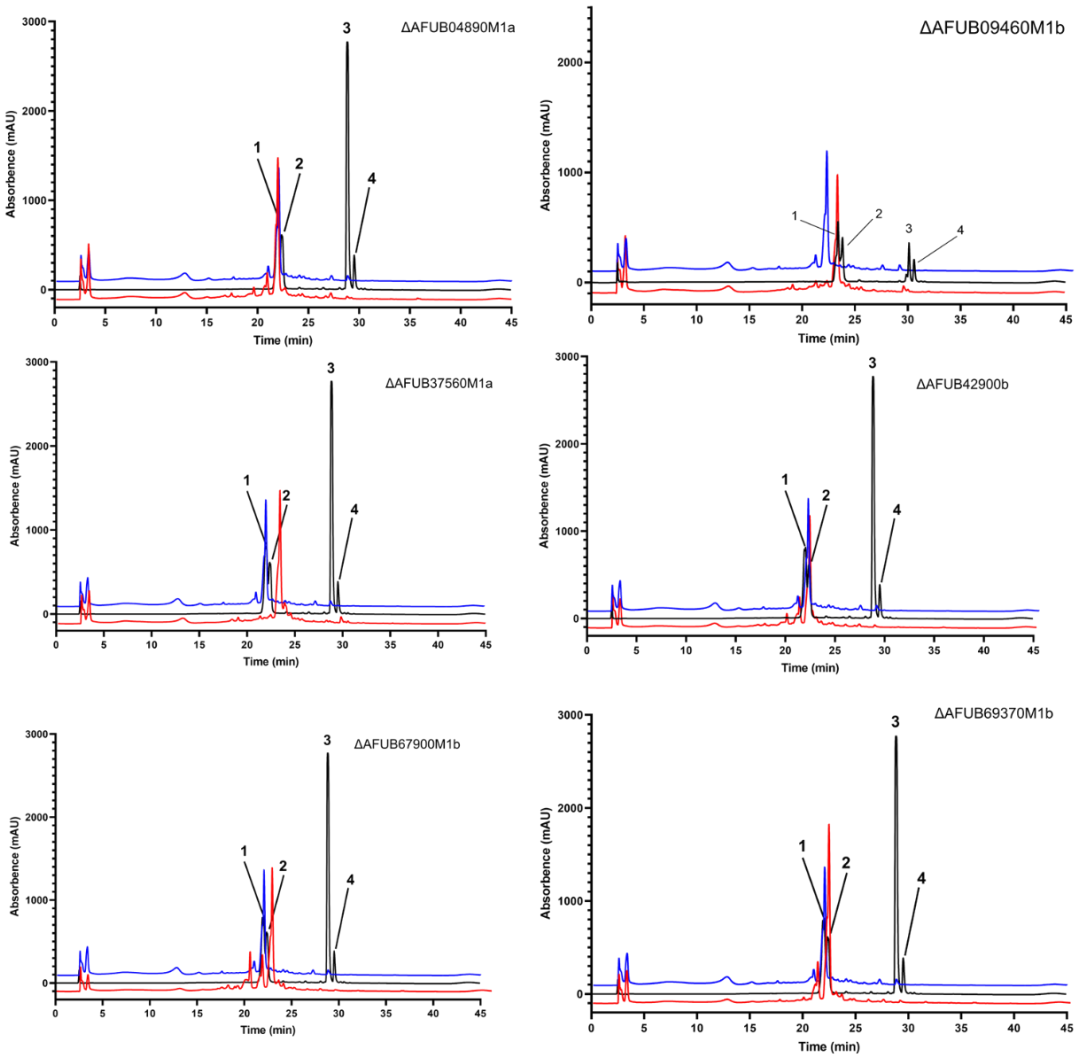

Figure 5-7 Chromatogram of pseurotin A in control andΔHMG strains with MAT1-1 background. The black line indicates mycotoxin reference. The blue line indicates the parental strain 47-465, and the red line indicates the HMG mutant strain sample with respective mutant strains indicated by label at top right hand side of graph. **1** pseurotin A, **2** gliotoxin, **3** fumagillin and **4** helvolic acid.

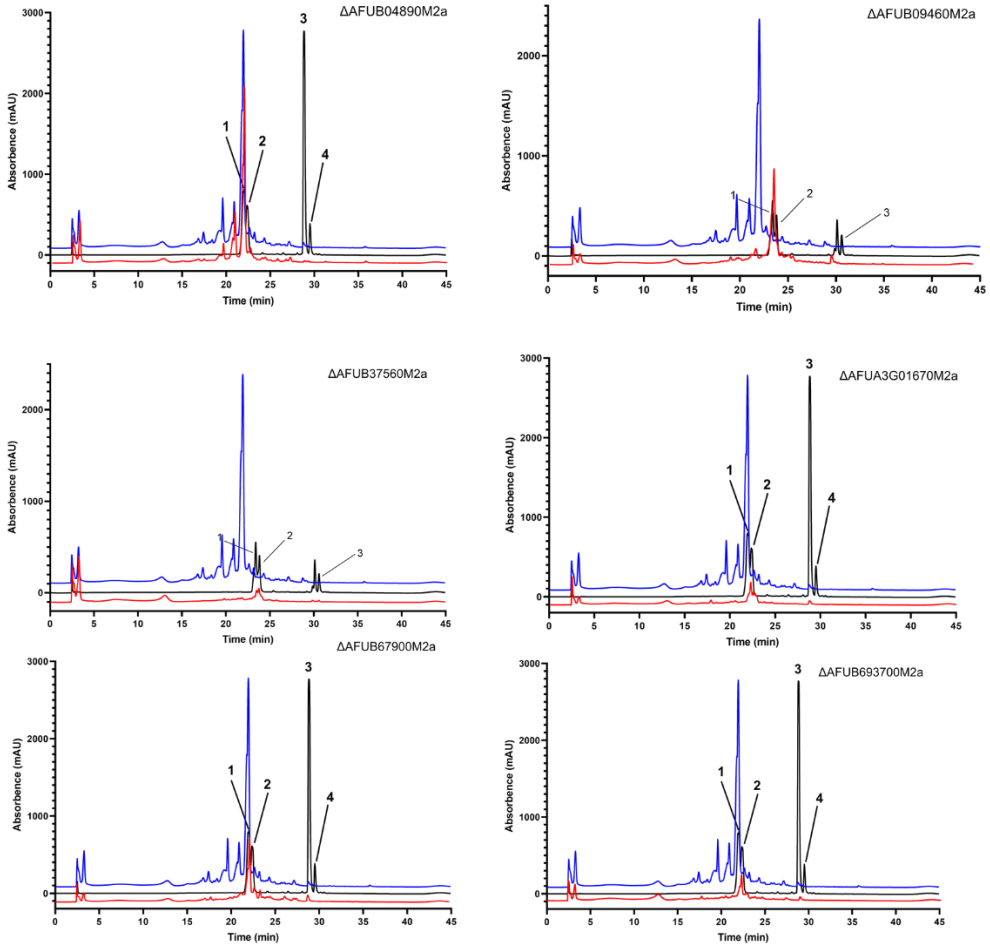

Figure 5-8 Chromatogram of pseurotin A in control and ΔHMG *A. fumigatus* strains of MAT1-2 background. The black line indicates mycotoxin reference. The blue line indicates the parental strain 47-465, and the red line indicates the HMG mutant strain sample with respective mutant strains indicated by label at top right hand side of graph. **1** pseurotin A, **2** gliotoxin, **3** fumagillin and **4** helvolic acid.

5.3.2.3 Production of giotoxin in Δ HMG strains

Gliotoxin synthesis was induced by incubating control and ΔHMG strains in Czapek Dox medium. Production of gliotoxin did not show any significant differences between the Δ*HMG* strains in either of the MAT1-1 or MAT1-2 backgrounds [**Figure 5-9**;F(13,28)=0.9948, P=0.4811 for MAT1-1 background strains; MAT1-2 background strains: F (13, 28)=0.8835, P=0.5782 for MAT1-2

background strains]. Strains AFUB04890M1a, AFUB09460M1a, AFUB09460M2a and AFUB67900M2b produced higher amount of gliotoxin than the wild-types, but the increase did not follow a recognizable pattern or trend.

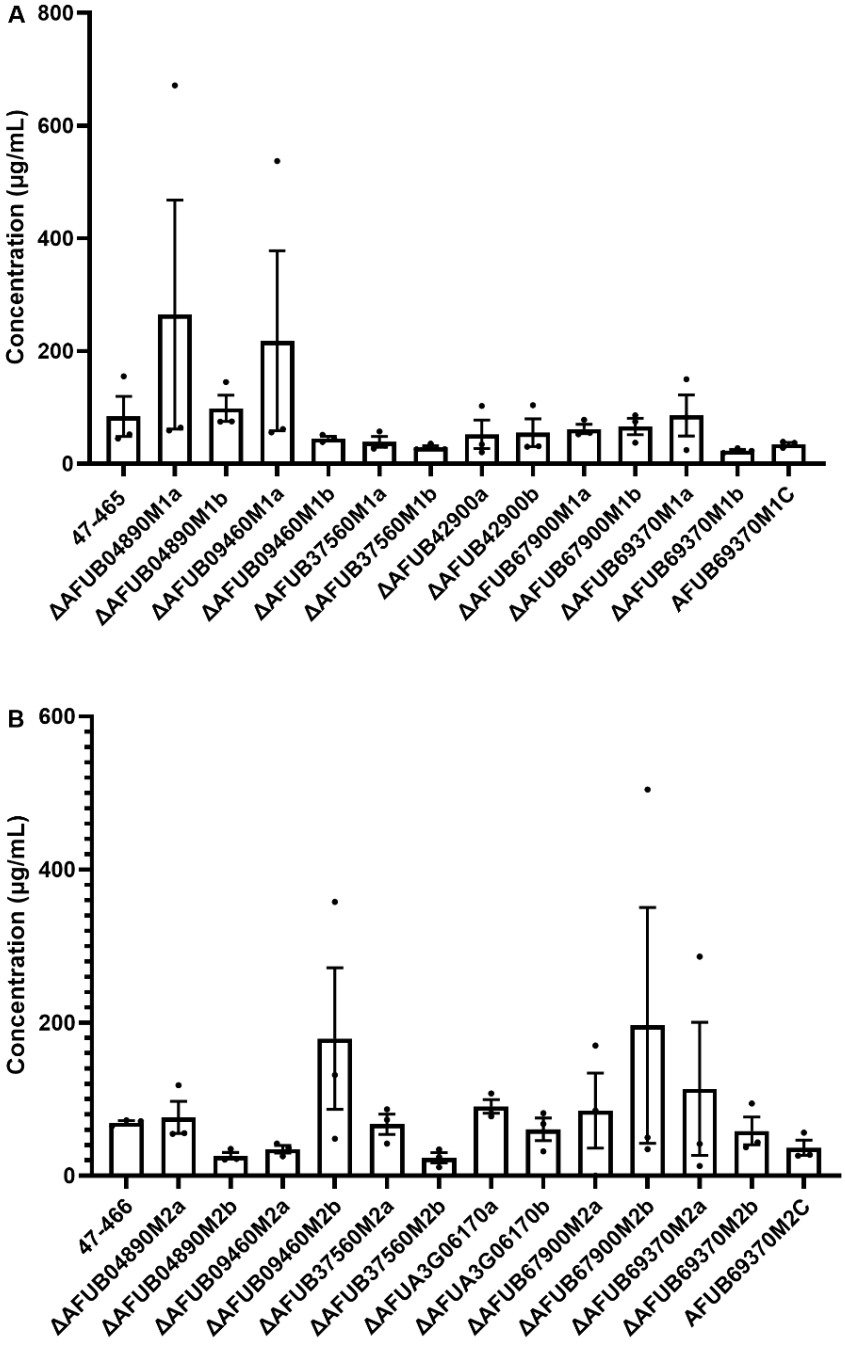

Figure 5-9 Production of gliotoxin in control and *Δ*HMG gene strains of *A. fumigatus*. A indicates production of gliotoxin from ΔHMG strains in MAT1-1 background, and **B** indicates production of gliotoxin from ΔHMG strains in

MAT1-2 background. Dots represents the biological replicates, and error bars represent ± SEM. Data was analyzed via one-way ANOVA, and non-significant difference was shown between gene deletion strains and the parental strains.

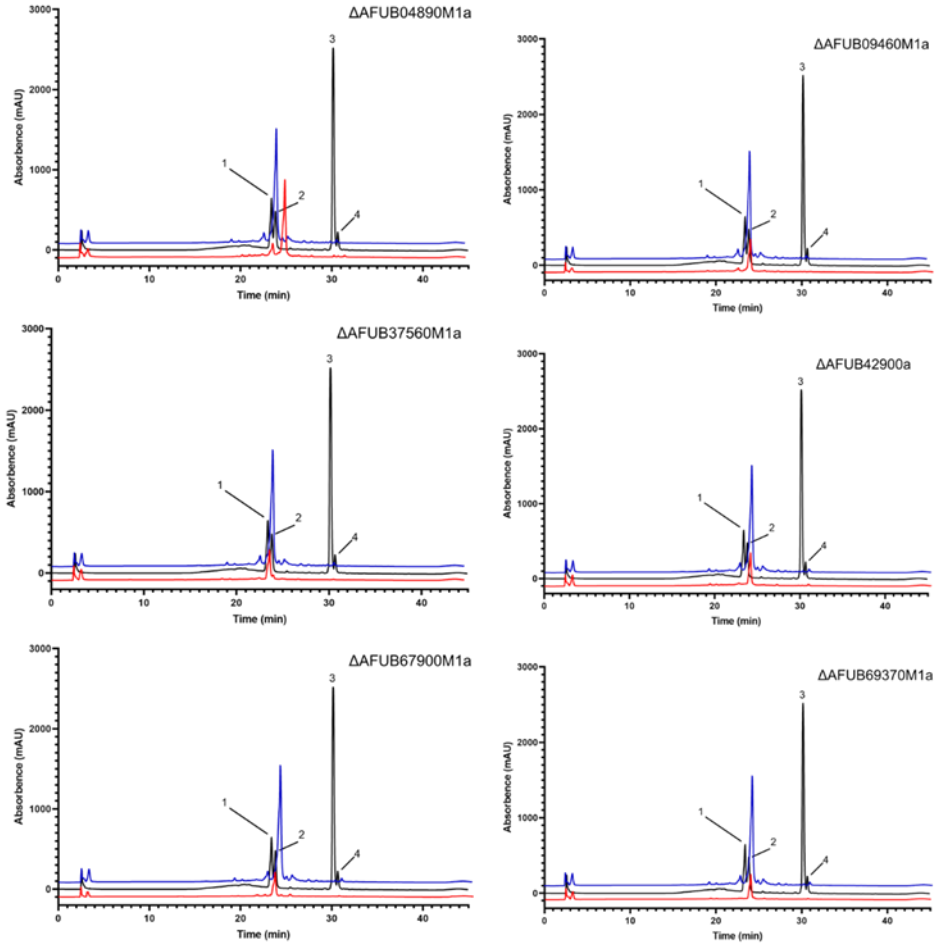

Figure 5-10 Chromatogram of gliotoxin in control andΔHMG *A.fumigatus* strains with MAT1-1 background. The black line indicates mycotoxin reference. The blue line indicates the parental strain 47-465, and the red line indicates the HMG mutant strain sample with respective mutant strains indicated by label at top right hand side of graph. **1** pseurotin A, **2** gliotoxin, **3** fumagillin and **4** helvolic acid.

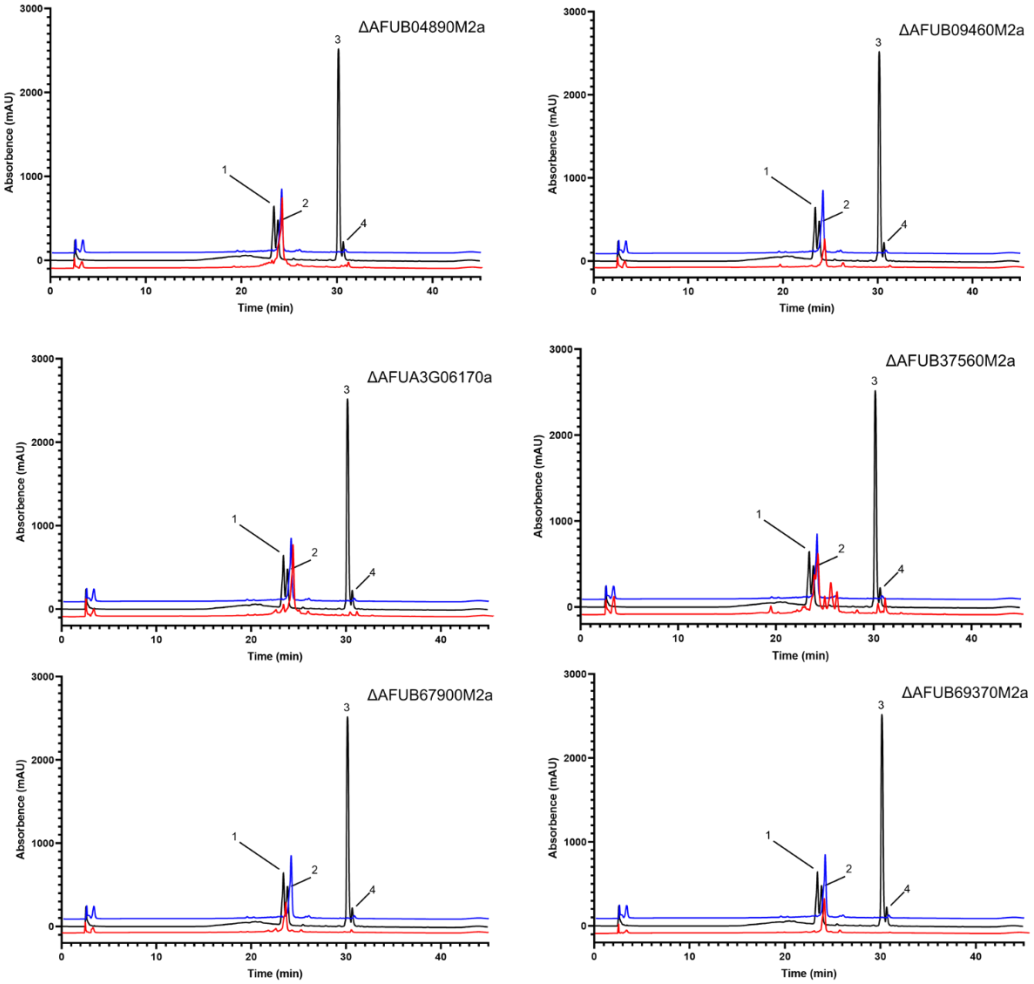

Figure 5-11 Chromatogram of gliotoxin production in control and *ΔHMG A. fumigatus* strains of MAT1-2 background. The black line indicates the fumagillin reference. The blue line indicates the parental strain 47-466, and the red line indicates the HMG mutant strain sample, with respective mutant strains indicated by label at top right hand side of graph. **1** pseurotin A, **2** gliotoxin, **3** fumagillin and **4** helvolic acid.

5.4 Discussion

Genes with roles in fungal sexual development may also be involved in secondary metabolism (Tsitsigiannis and Nancy., 2006; Bayram et al., 2008; Yu et al., 2018; Shen et al., 2019). For example, sexual development in *A. nidulans* is initiated by the VeA-VelB complex being imported into the nucleus in the dark, where the complex binds with LaeA to promote sterigmytocystin synthesis (Bayram et al., 2008). Under conditions suitable for asexual

development, *A. nidulans* is still able to produce the mycotoxin, but production is less than that during sexual development due to the lower level of VeA in the nucleus (Bayram et al., 2008). In the present thesis it was previously shown that a set of HMG transcription factor genes were present in *A. fumigatus* and some (including *AFUB_042900*, *AFUA_3G01670*, *AFUB_067900* and *AFUB_069370*) were shown to be essential for formation of cleistothecia. We therefore speculated that one of more of these HMG genes might have a dual role in regulating development and secondary metabolism. Studies were subsequently undertaken to assess the impact of gene deletion of the HMG genes on secondary metabolite production. Although there were no publications in this area at that point, early on during studies Yu et al. (2018) reported that overexpression of the *MAT1-1* and *MAT1-2* HMG family genes in *A. fumigatus* resulted in an upregulation of fumagillin and pseurotin A production. Fumagillin and pseurotin A are commonly synthesized mycotoxins in *A. fumigatus*, sharing one gene cluster with intermingling of the regulatory genes *fma-PKS, psoF, fma-KR, psoB, psoA* into one super cluster (Frisvad et al., 2009). Thus, our hypothesis appeared correct. Work was therefore continued to investigate the role of the full set of HMG genes on secondary metabolite production in *A. fumigatus* as will now be discussed. The general approach used for all genes under investigation was to compare mycotoxin productin between control and gene deletion strains. There were no apparent major growth rate differences between most of the control and gene deletion strains. However, this was not formally investigated and so it is acknowledged that slight reductions in growth in gene deletion strains might have partly been responsible for any observed differences in mycotoxin production.

It is noted that we also hoped to study the effect of HMG gene deletion on secondary metabolite production in *A nidulans*, but despite concerted efforts it

was not possible to induce sterigmatocystin synthesis in the *A. nidulans* 2-258 strain used elsewhere in the present study.

5.4.1 HMG genes influence synthesis of psuerotin A in both MAT backgrounds

In the previous chapter, the HMG family gene *AFUB_069370* was shown to be required for normal cleistothecia formation. Synthesis of pseurotin A were also found to be influenced by *AFUB_069370* in work conducted in the present chapter. This indicated that Pseurotin A production is positively regulated by *AFUB_069370*, as deletion of the gene caused almost no production of pseurotin A (**Appendix 56 to 57**). Complementation of *AFUB_069370* recovered the production but not back to same level as the wild-types. The homolog *AN3667* in *A. nidulans* is pivotal for sexual reproduction and regulates *MAT1* and *MAT2* mating-type gene expression (Salih, 2016). Given that Yu et al. (2018) found that the *MAT* genes of *A. fumigatus* regulated production of pseurotin A it can be speculated that *AFUB_069370* might regulate pseurotin A production via expression of the *MAT1-1* and *MAT1-2* genes of *A. fumigatus.* However, fumagillin synthesis was not affected by most deletion of most HMG genes, except for AFUB_037560 deletion strain AFUB37560M1b. It is noted that this particular AFUB37560M1b strain also did not show defects in fruit body formation that were seen in deletant strain AFUB37560M1a (**Section 4.3.3.3**), and thus it is possible that the increase in fumagillin production was caused by some artefact such as higher growth rate or incorrect integration of transforming DNA. Similarly, a AFUB_069370 complementation strain produced higher amount of fumagillin, which also may be an artefact of growth rate etc.

Another HMG gene *AFUB_067900* was previously identified as being required for cleistothecia formation, and here again this gene was also shown to be involved with the synthesis of pseurotin A in *A. fumigatus*. Gene deletion

strains showed a decrease in pseurotin A production. The homolog *AN1962* is another HMG protein that was shown to influence the expression of *MAT1* and *MAT2* in *A. nidulans* (Salih, 2016). Therefore, *AFUB_067900* might regulate pseurotin A in a similar way to *AFUB_069370*, which is via expression of *MAT1-1* and *MAT1-2* (Yu et al., 2018).

AFUB_042900 and *AFUA_3G06170* were identified as putative mating-type genes encoding MATα domain and MAT1-2 HMG domain proteins, respectively, which were essential for fruit body formation in *A. fumigatus* (**Section 4.3.3.3**). Deletion of *AFUB_042900* resulted in a lowered pseurotin A production, whilst deletion of *AFUA_3G06170* caused a significant reduction in pseurotin A. This indicated that the *MAT1-1* and *MAT1-2* genes positively upregulate production of pseurotin A, consistent with the findings of Yu et al. (2018). It is noted that over-expression of *MAT1-1* and *MAT1-2* in *A. fumigatus* was found to up-regulate expression of *laeA,* and *fapR*, and *MAT1-2* over-expression up-regulated *psoP* (Yu et al., 2018). For future, work, expression of *laeA* and *fapR* might be investigated inΔAFUB42900 and ΔAFUA3G06170 strains.

5.4.2 HMG gene influences mycotoxin metabolism differently in MAT1-1 and MAT1-2 backgrouds

Deletion *AFUB_037560* caused a reduction in pseurotin A in the MAT1-2 background strains, and a similar reduction in strain AFUB37560M1a which was in the MAT1-1 background strain. However, the deletion of *AFUB_037560* only showed a reduction in cleistothecial formation in the MAT1-1 background strain AFUB37560M1a. In the MAT1-1 background strain AFUB37560M1b did not show any effect on pseurotin A, and there was also no clear change in fruit body formation. Thus, it is possible that *AFUB_037560* has a different influence

on mycotoxin production based on mating-type of the host strain, although this remains speculation due to the limited number of strains used.

Deletion of AFUB_009460 did not influence psuerotin A production in MAT1-1 background, but showed signs of a reduction. In the MAT1-2 background, AFUB09460M2b strain produced significantly decreased pseurotin A. However, AFUB_009460 deletion in the MAT1-2 background caused increased production of fumagillin, while in the MAT1-1 background fumagillin production was not influenced. Unlike other genes, AFUB_009460 was not involved in cleistothecia formation. Overall, the result suggests that HMG genes in different mating-type backgrounds may have a different influence on secondary metabolism in heterothallic species, but this requires further experimental validation to ensure against artefacts such as differences in growth rate which might affect secondary metabolite biosynthesis.

5.4.3 HMG genes were not involved in gliotoxin production

Gliotoxin is an important mycotoxin with a possible role in the virulence of *A. fumigatus* (Spike et al., 2008). Previous studies suggested a link between asexual development and gliotoxin production (Shin et al., 2015). Subsequent work showing links between *laeA* and the conidiation genes *brlA*, *abaA* and *wetA*, which connected primary and secondary metabolism and production of sulfer/methionine metabolites, aromatic amino acid metabolites, products of the gliotoxin synthesis cluster, and DHN-melanin synthesis (Lind et al., 2018). By contrast, synthesis of gliotoxin was not significantly affected by deletion of any of the HMG genes studied in this project, even those related to fruit body formation. The research suggests that gliotoxin synthesis is more likely to be primarily correlated with asexual rather than sexual development (Bayram et al., 2008; Ben-Amiet al., 2009; Bok and Keller., 2004; Kale et al., 2008; Kosalkova et al., 2009).

5.4.4 Conclusion

Production of fumagillin and pseurotin A was affected by deletion of the HMG family genes *AFUB_069370*, *AFUB_067900*, *AFUB_042900,* and *AFUA_3G06170* to different levels, indicating a regulatory role in mycotoxin production for these various genes. The results also hinted that HMG genes in heterothallic species may have a different influence on secondary metabolism according to the mating-type background of the host, although this remains speculation. In future work it will be interesting to investigate the expression of *laeA* in the HMG gene deletion strains given tha LaeA is a key factor in sexual development and control of secondary metabolism.

Chapter 6 General Discussion

Sexual development of *Aspergillus* is regulated by various genes with roles in different processes including sensing of environmental signals, mating, signal transduction and fruit body maturation, and related genes (Dyer and O'Gorman, 2012). Aims of this project were: (1) to identify homologs of 'sex' genes in *A. nidulans* and investigate their function in sexual development; (2) to identify HMG genes in *A. fumigatus* following on from previous studies in *A. nidulans* and investigate their function in cleistothecia formation; (3) to investigate the role of HMG genes in secondary metabolism of *A. fumigatus*.

6.1 Identification of novel 'sex' genes in *A. nidulans*

The study of sexual development in *A. nidulans* was divided into two parts: (1) an investigation of the optimum temperature for fruit body formation, and (2) identification and characteristion of novel 'sex' genes involved in cleistothecia formation. The sexual cycle of *A. nidulans* has been induced at 37 °C world-wide since pioneering work on the species in the last century (Frawley et al., 2018; Pontecorvo, 1951; Todd et al., 2007). However, previous research at the University of Nottingham investigated the laboratory conditions for sex and suggested 32 °C as a better temperature for induction of the sexual cycle in *A. nidulans* (Ashour, 2014). Following on from this previous study (Ashour, 2014), the present work tested the influence of temperature (25 °C, 28 °C, 32 °C, 37 °C) on clestothecia formation in representative strains of *A. nidulans* including wild-type, *veA1* and △*kuB* strains, and it was found that most strains produced more mature cleistothecia (diameter over 100 μm) at 32 °C rather than 37 °C. Therefore, this temperature was adopted for later experimental work involving the sexual cycle in this research.

A. nidulans has been utilised as a model for fungal sexual development research for a long time (Dyer and O'Gorman, 2012; Pöggeler et al, 2006). However, there has been parallel interest in sexual development of other pezizomycete species, with the identification of essential genes for fruit body development in *Neurospora, Sordaria* and *Podospora*, which had not yet been evaluated in *A. nidulans.* In present study, putative genes including *AN2701.2* (MAPK scaffold protein), STRIPAK subunit genes (*AN0163.2, AN4632.2* and *AN6611.2*), transcription factors (*AN4813.2, AN1217.2, AN7170.2* and *AN7736.2*), *AN3147.2* (glycolipid transport protein), *AN10631.2* (transmembrane protein), *AN4891.2* (histone chaperone) have been investigated. *AN2701.2,* also named as *hamE* (Frawlay et al., 2018), was found to be essential for cleistothecia maturation in *A. nidulans*, as deletion caused a significant reduction in size of cleistothecia, number of ascospores and regeneratation rate of ascospores. AN2701.2 was identified as a scafford protein that is associated with pheromone signaling of the AnSte11-Ste50—Ste7-Fus3 module in sexual development of *A. nidulans* (Bayram et al., 2012; Frawley et al., 2018). In this study *AN2701.2* deletants were incubated on ACM, which can be considered a rich nutrient medium, and formed numerous immature cleistothecia (average size of 30 µm; **Figure 3-2B**). However, Frawley et al. (2018) incubated a Δ*AN2701.2* deletion strain on glucose minimal medium (GMM), and cleistothecia formation was blocked (which was also observed in our study for GMM). Therefore, it is possible that nutrient composition can affect the impact of *AN2701.2* on sexual development.

The STRIPAK complex has been reported to be pivotal for sexual development in *Sordaria* and *Neurospora* species as a signaling transduction mediator, especially in the MAPK signaling pathway (Bloemendal, et al., 2012; Kück and Stein., 2021; Simonin et al., 2010; **Section 1.4.4**). In this project, the subunits *AN0164.2* (PP2Ac unit SipE; Elramli et al., 2019), *AN4632.2* (SLAMP

unit SipD; Elramli et al., 2019), and *AN6611.2* (STRIP unit SipC; Elramli et al., 2019) were investigated. Deletion of *AN0164.2* blocked fruit body development in *A. nidulans* at an early stage, which was similar to PP2Ac1 in *S. macrospora* (Beier et al., 2016). Deletion of *AN6611.2* in this research caused a severe defect in vegetative growth, with its homolog PRO22 in *S. macrospora* being associated with the tubular and vesicular vacuolar network (Bloemendal et al., 2010). Therefore, the defective hyphal growth here see in *A.nidulans* might have been caused by a failure to maintain normal cellular functioning. Deletion of *AN4632.2* did not influence cleistothecia formation and ascospore maturation, which was surprising as the homolog HAM-4 in *N. crassa* is required for ascospore formation (Simonin et al., 2010). Other STRIPAK subunits identified in *A. nidulans* include the MOB3 unit SipA, SIKE unit SipB, PP2AA unit SipF, and Striatin unit StrA (Elramli et al., 2019; Wang et al.,2010). StrA acts as a platform to assembly the SipA and SipB-SipD heterodimer and the SipC-SipE-SipF heterotrimeric complex, with the fully functional AnSTRIPAK complex then associating with MpkB signaling to enable sexual development (Elramli et al., 2019; Jun et al., 2011).

Four transcription factors were investigated for their role in fruit body development of *A. nidulans*. Of these, *AN4813.2* was identified to be essential for both sexual and asexual development. In sexual development, deletion of *AN4813.2* led to a reduction in size of cleistothecia, number of ascospores, and ascospore viability, while in asexual development Δ*AN4813.2* strains failed to form conidia. The homolog *mybA* in *A. fumigatus* is involved in asexual development via regulation of *wetA, vosA* and *velB* (Valsecchi et al., 2017). Fruit body formation in *A. nidulans* is related to *vosA* and *velB* (Bayram et al., 2008; Kim et al., 2020; Park et al., 2014), therefore, *AN4813.2* may similarly regulate expression of *vosA* and *velB* during cleistothecia formation, and control expression of *wetA* in conidiation. Deletion of *AN1217.2* caused a failure in

conidiation, which is similar to Δ*hbx1* in *A. flavus* (Cary et al., 2017), but cleistothecia formation was not affected greatly. Δ*AN1217.2* strains formed larger sized cleistothecia with viable ascospores, which suggests that *AN1217.2* might be a repressor of sexual development. *AN7170.2* was identified as homolog of *sclR*, which controls sclerotial formation in *A. oryzae* (Jin et al., 2011), and deletion of *AN7170.2* caused a reduction in rate of regeneration in ascospores, but no impact on number and size of cleistothecia, and number of ascospores. This result suggests that *AN7170.2* might have functions in *A. nidulans* other than fruit body formation. Meanwhile, *AN7736.2* appeared not to have a role in sexual development of *A. nidulans*, as sexual morphogenesis was not impacted in the gene deletion strains, unlike the function of homolog *Trire2 : 59270* in *T .reesei* (Linke et al., 2015).

Other genes investigated with a putative role in sex were *AN3147.2, AN10631.2* and *AN4891.2*. *AN3147.2* was identified as a *het-c2* homolog in *A. nidulans*, and deletion of *AN3147.2* reduced the number of ascospores. *Het-c2* regulates allorecognition which is a key part in heterokayon incompatibility (Pàl et al., 2007). The *het* loci in *A. nidulans* are responsible for avoiding fusion of dissimilar nuclei, which might be important in sexual development, and in *N. crassa tol* (a divergent *het* locus) is associated with mating-type specific heterokaryon incompatibility (Dyer at al., 1992; Pàl et al., 2007; Shiu and Glass, 1999). Hypothetically, *AN3147.2* might regulate hyphal fusion at the initial stage of fruit body development. *AN10631.2* was identified as homolog of PRO41, which is required for an early stage of sexual development at *S. macrospora* (Nowrousian et al., 2007), but here *AN10631.2* was found not to be involved in sexual development. However, further work is required to validate this result as it might be that *AN5458* is the true homolog of *PRO41. AN4891.2* was identified as a putative ASF-1 histone chaperone (Gesing et al., 2012), although it was

not possible to obtain gene deletant strains, suggesting that *AN4891.2* is pivotal for normal cellular functioning and maintenance.

In summary, novel results from this part of the work were: (1) determination of 32 ℃ as the optimum temperature for inducing the sexual cycle in *A. nidulans*; (2) identification of *AN2701.2* (*hamE*), *AN0164.2* (*sipE*), *AN4632.2* (*sipD*), *AN4813.2* and *AN3147.2* as essential genes in sexual development of *A. nidulans.* This allowed an updated model for sexual development to be presented, building on the original model of Dyer and O'Gorman (2012) as shown in **Figure 6-1**.

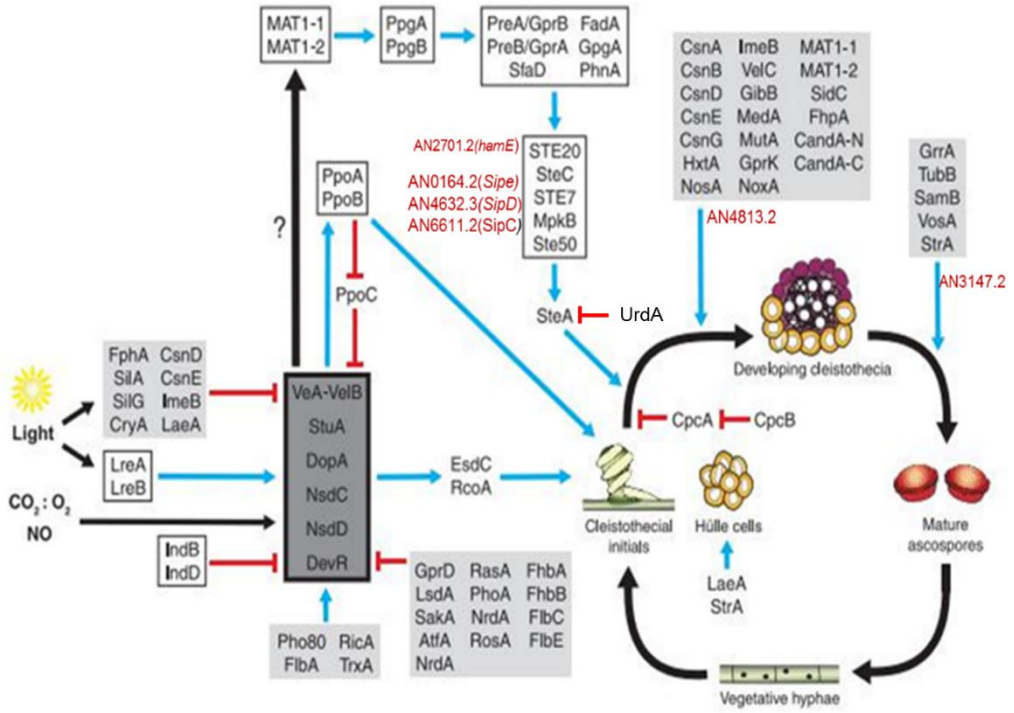

Figure 6-1 Updated model of genetic control of sexual development in *A. nidulans.* The model builds on that proposed by Dyer and O'Gorman (2012) and shows putative placement of the novel proteins involved in fruit body formation characterised in the present study together with other novel proteins identified since the review of Dyer and O'Gorman (2012) e.g. a MAPK scaffolding unit AN2701.2, STRIPAK units AN0164.2, AN4632.2, and AN6611.2 (that are thought to associate with MAPK signal transduction that affect cleistothecia formation) and the transcription factor AN4813.2 related to cleistothecia development, and the glycolipid transfer protein AN3147.2 involved in ascospore maturation.

6.2 Role of HMG genes in fruit body formation of *A. fumigatus*

The transcription factor NsdC has previously been identified to be essential for sexual development of *A. nidulans*, and its homolog in *A. fumigatus* was identified as sharing a highly conserved structure (Kim et al., 2009). Thus, Δ *nsdC* strains in *A. fumigatus* were constructed and tested for their sexual fertility in the project. Deletion of *nsdC* was able to be complemented by a wild-type crossing partner during the sexual cycle, but when double deletion strains were crossed, the crossed failed to form cleistothecia. In other *Aspergillus* species such as *A. flavus nsdC* is a necessary element in sclerotia formation (Cary et al., 2012). Therefore, it may be concluded that *nsdC* has a conserved role in fruit body formation in *Aspergillus* species. In addition, for heterothallic species it is important to complete gene deletion in both crossing partners of opposite mating type, as it is possible that the function of deletant gene might be complemented by the wild-type protein present in the opposite mating type partner during crossing. Consequently, high fertility *kuB* deletant strains 47-465 and 47-466 had to be constructed in the present study.

Previous research had identified a series of HMG group proteins which are important for sexual development in *A. nidulans* (Ashour, 2014; Salih, 2016). In this project, homologous genes were investigated in *A. fumigatus*, and four of these HMG genes were found to be essential for fruit body formation. The HMG gene *AFUB_069370* appears to have a conserved role in sexual development in ascomycota species. Deletion of *AFUB_069370* blocked cleistothecia formation even when the gene deletant strains were crossed with a wild-type partner. In *A. nidulans*, the homolog *AN3667* controls sexual development upstream of mating-type genes, and both deletion and overexpression caused defects in cleistothecia formation (Ashour, 2014; Salih, 2016). Similarly, in *P. anserina*, *PaHMG5* is thought to have a central role in regulating sexual

development (Benkhali et al., 2013). Other homologs including *fmf-1* in *N. crassa* and *ste11* in *S. pombe* are also involved in sexual development (Iyer et al., 2009; Mata and Bahler, 2006; Sugimoto et al., 1991).

Deletion of *AFUB_067900* caused abolishment of cleistothecia formation, and its function could not be complemented by a wild-type crossing partner of the opposite mating type. The *A. nidulans* homolog *AN1962* is also critical for sexual development as deletion and over-expression reduced cleistothecia development, and RNA analysis indicated that *AN1962* acted upstream of the mating-type genes (Salih, 2016). Thus, hypothetically, *AFUB_067900* may act upstream of the *MAT* genes in *A. fumigatus,* but this awaits investigation.

The mating-type genes *AFUB_042900* and *AFUA_3G06170* were found to be required for sexual development in *A. fumigatus*, which is the same as the homologous genes *AN2755 (MAT1)* and *AN4734 (MAT2)* in *A. nidulans* (Paoletti et al., 2007; Salih, 2016). Heterologous transformation of *MAT1-2* from *A. fumigatus* allowed formation of immature cleistothecia in a sterile Δ*MAT2* strain of *A. nidulans* (Pyrazak et al., 2008). Transformation of mating-type genes from *N. crassa* into MAT-deletion sterile *P. anserina* strains promoted the fertilization process (Arnaise et al., 1993).

Results from the present study suggested that HMG gene may influence fertility differently according to the mating-type background in heterothallic species. HMG gene *AFUB_037560* may affect sexual development in the MAT1-1 background *A. fumigatus* more then the MAT1-2 background. Deletion of *AFUB_037560* caused reduction in fruit body formation in MAT1-1 strains, but the deletion did not show difference to the wild-type crossing in MAT1-2 strains. In parallel, in *P. anserina* the HMG gene *Pa_HMG6* is involved in female rather than male fertility (Benkhali et al., 2013).

6.3 Influence of HMG genes on secondary metabolite production

Genes involved in sexual development may have relationships with secondary metabolism, as illustrated by findings involving *laeA* (Lim et al., 2012; Bayram et al., 2008; Ben-Ami et al., 2009; Bok and Keller., 2004; Kale et al., 2008; Kosalková et al., 2009). In *A. fumigatus*, the synthesis of the mycotoxins gliotoxin, fumagillin, pseurotin A and helvolic acid was evaluated in HMG gene deletion strains. *AFUB_069370* affected production of pseurotin A, with gene deletion causing a decrease in the synthesis. Similarly, deletion of *AFUB_067900* reduced the synthesis of pseurotin A. *AFUB_042900* and *AFUA_3G06170* were also shown to be involved in pseurotin A production, respectively. Deletion of *AFUB_037560* caused a reduction of pseurotin A production in MAT1-2 strains, and deletion of *AFUB_009460* increased production of fumagillin in MAT1-2 strains. The results again suggested that HMG genes may have a different impact in isolates of different mating-type background, although this remains speculative until tested with a larger number of isolates.

The research focused on the connections between synthesis of mycotoxin and sexual relating genes in *A. fumigatus*, for the reason that, firstly, control of sexual reproduction or its relating genes might be a novel disease management strategy. For example, regulation of expression in *MAT* genes altered production of fumagillin and pseurotin A (Yu et al., 2018), which might change virulence and further protect immune cells activity (Cramer et al., 2009; Frisvad et al., 2009). In this study, it is possible to control pseurotin A synthesis via down-regulation of *AFUB_069370, AFUB_067900, AFUB_3G06170*, and *AFUB_042900*, which may alleviate stress of lymphocytes and interfere with pathogen production (Ishikawa et al., 2009). Secondly, sexual cycle promotes genetic variations among pathogen populations, and for instance the spread of antifungal resistance gene TR_{46} in natural environment (Zhang et al. 2017).

Thus, thirdly, sexual cycle may facilitate with analysis in genetic basis of pathogenicity factors such mycotoxin synthesis and genetic mutation and its spreading.

6.4 Future work

This study evaluated the optimum temperature for fruit body formation in *A. nidulans*, but ascospore viability was not examined. Thus, as a next step, rate of regeneration in ascospores may be tested. Several novel genes were regarded to be important for sexual development. Of particular interest was *AN4813.2* and it is suggested to act via regulation of the genes *vosA* and *velB*, among others but this was not tested. For future work, to illustrate the putative regulatory function of *AN4813.2* as a transcription factor, it will be worthwhile evaluating expression of *vosA* and *velB* in Δ*AN4813.2* strains. Elsewhere in the present study *AN1217.2* was reckoned to be a repressor of sexual development, thus it will be very interesting to study the effect of overexpression of *AN1217.2* in order to investigate the function in sexual development.

This project completed a study of the effect of HMG gene deletion in *A. fumigatus*, but the effect of gene overexpression on sexual development was not investigated. Overexpression of genes *AFUB_069370* and *AFUB_067900* is worthwhile doing,in order to investigate if they act upstream of the mating-type genes and are bi-functional in sexual development. This might offer exciting possibilities to manipulate fertility levels in low fertility or even sterile fungal strains. Finally, *AFUB_069370* and *AFUB_067900* were found to influence synthesis of fumagillin and pseurotin A. Thus, the effect of these genes on expression of *MAT1-1*, *MAT1-2*, *laeA,* and *fmaB* might be investigated in future studies.

References

Anwar MM, Croft JH, Dales, RB (1993). Analysis of heterokaryon incompatibility between heterokaryon-compatibility (h-c) groups R and GL provides evidence that at least eight *het* loci control somatic incompatibility in *Aspergillus nidulans. Journal of General Microbiology,* **139**: 1599-1603.

Arendrup MC, Mavrídou E, Mortensen KL, Snelders E, Frímodt-Moller N, Khan H, Melchers, WJ, Verweij PE (2010). Development of azole resistance in *Aspergillus fumigatus* during azole therapy associated with change in virulence. *PLoS ONE*: **5**: e10080.

Arnaise S, Zickler D, Glass NL (1993). Heterologous expression of mating-type genes in filamentous fungi. *Genetics*: **90**: 6616-6620.

Arratia-Quijada, J., S nchez, O, Scazzocchio, C., and Aguirre, J. (2012) FlbD, a Myb transcription factor of *Aspergillus nidulans*, is uniquely involved in both asexual and sexual differentiation. *Eukaryotic Cell*, **11**: 1132-1142.

Ashour, A.O. (2014) Control of Sexual Reproduction in Aspergillus Species (Doctoral Thesis). University of Nottingham. Nottinghamshire, pp: 41-90

Ashton GD. and Dyer PS (2019). Culturing and mating of *Aspergillus fumigatus*. *Current Protocols in Microbiology*, ***54***: e87.

Baidya, S., Cary, J.W., Grayburn, W.S., and Calvo, A.M. (2011) Role of nitric oxide and flavohemoglobin homolog genes in *Aspergillus nidulans* sexual development and mycotoxin production. *Applied and Environmental Microbiology*, **77**:5524-5528.

Bastiaans,E., Devets,A.J.M., Aanen, D.K., Van Diepeningen, A.D., Saupe, S. J., and Paoletti, M. (2014). Natural variation of heterokayon incompatibility gene het-C in *Podospore anserina* reveals diversifying selection. *Molecular Biololy and Evolution,* **31**:962–974.

Bayram Ö and Braus GH (2011). Coordination of secondary metabolism and development in fungi: the velvet family of regulatory proteins. *FEMS Microbiology Reviews* **36**: 1-24.

Bayram Ö, Bayram ÖS, Ahmed YL, Maruyama J-i, Valerius O, et al. (2012) The *Aspergillus nidulans* MAPK Module AnSte11-Ste50-Ste7-Fus3 controls development and secondary metabolism. *PLoS Genetics,* **8**: e1002816.

Bayram Ö, Krappmann S, Ni M, Bok JW, Helmstaedt K, Valerius O, Brasu-Stromeyer S, Know NJ, Keller NP, Yu JH, Braus GH (2008). VelB/VeA/LaeA complex cooodinates light signal with fungal development and secondary metabolism. *Science*, **320**: 1504-1506.

Bayram Ö, Sari F, Braus GH, Irniger S (2009). The protein kinase ImeB is required for light-mediated inhibition of sexual development and for mycotoxin production in *Aspergillus nidulans*. *Molecular Microbiology,* **71**: 1278-1295.

Bayram ÖS, Bayram Ö, Valerius O, Park HS, Irniger S, Gerke J, Ni M, Han KH, Yu JH, Braus GH (2010). LaeA control of velvet family regulatory proteins for light-dependent development and fungal cell-type specificity. *PLoS Genetics*, **6**: e1001226.

Beier A, Teichert I, Krisp C, Wolters DA, Kück U (2016). Catalytic subunit 1 of protein phosphatase 2A is a subunit of the STRIPAK complex and governs fungal sexual development. *mBio*, **7**: e00870-16.

Ben-Ami R, Lewis RF, Leventakos K, Kontoyiannis DP (2009). *Aspergillus fumigatus* inhibits angiogenesis through the production of gliotoxin and other secondary metabolites. *Blood*, **114**: 5393-5399.

Benkhali JA, Coppin E, Brun S, Peraza-Reyes L,Martin T, Dixelius C, Lazar N, Tilbeurgh H, Debuchy R (2013). A network of HMG-box transcription factors regulates sexual cycle in the fungus *Podospora anserina. PLoS Genetics*, **9**: e1003642.

Bennett JW, Klich MA (1992) *Aspergillus* Biology and Industrial Applications, Butterworth-Heinemann Press. U.S.A., pp:19-39

Bennett RJ, Turgeon BG (2016). Fungal sex: The Ascomycota. Microbiology Spectrum **4**: Funk-0005-2016.

Bloemendal S, Lard KM, Rech C, Hoff B, Engh I, Read ND, Kück U (2010). A mutant defective in sexual development produces aseptate ascogonia. *Eukaryotic Cell*, **9**: 1856-1866.

Blumenstein A, Vlenken K, Tasler R, Purschwltz J, Veith D, Frankenberg-Dlnkel, N, Fisher R (2005). The *Aspergillus nidulans* phytochrome FphA represses sexual development in red light. *Current Biology*, **15**: 1833-1839.

Böhm J, Hoff B, O'Gorman CM, Wolfers S, Klic V, Binger D, Zadra I, Kürnsteiner H, Pöggeler S, Dyer PS, Kück U (2012). Sexual reproduction and mating-type-mediated strain development in the penicillin-producing fungus *Penicillium chrysogenum*. *Proceedings of the National Academy of Sciences USA* **110**: 1476-1481.

Bok JW, Keller NP (2004). LaeA, a regulator of secondary metabolism in *Aspergillus* spp. *Eukaryotic Cell*, **3**: 527-535.

Bürglin T, Affolter M (2016). Homeodomain proteins: an updata. *Chromosoma*: **125**: 497-521.

Busch S, Eckert SE, Krappmann S, Braus GH (2003). The COP9 signalosome is an essential regulator of development in the filamentous fungus *Aspergillus nidulans. Molecular Microbiology,* **49**: 717-730.

Busch S, Schwler EU, Nahlik K, Bayram O, Helmstaedt K, Draht OW, Krappmann S, Valerlus O, Llpscomb WN, Braus GH (2007). An eight-subunit COP9 signalosome with an intact JAMM motif is required for fungal fruit body formation. *Proceedings of the National Academy of Sciences USA*, **104**: 8089-8094.

Bussink HJ, Osmani SA (1998). A cyclin-dependent kinase family member (PHOA) is required to link developmental fate to environmental conditions in *Aspergillus nidulans*. *The EMBO Journal*, **17**: 3990-4003.

Calvo AM (2008). The VeA regulatory system and its role in morphological and chemical development in fungi. *Fungal Genetics and Biology,* **45**:1953-1061.

Camps SM, Dutilh BE, Arendrup MC, Rijs AJMM, Snelders E, Huynen MA, Verweij PE, Melchers WJG (2012). Discovery of a *hapE* mutation that causes azole resistance in *Aspergillus fumigatus* through whole genome sequencing and sexual crossing. *PLoS ONE*, **7**: e50034.

Cary JW, Harries-Coward PY, Ehrlich KC, Mack BM, Kale SP, Larey C, Calvo AM (2012). NsdC and NsdD affect *Aspergillus flavus* morphogenesis and aflatoxin production. *Eukaryotic Cell*, **11**: 1104-1111.

Cary JW, Harris-Coward P, Scharfenstein L, Mack BM, Chang PK, Wei Q, Lebar M, Carter-Wientjes C, Majundar R, Mitra C, Banerjee S, Chanda A (2017). The *Aspergillus flavus* homeobox gene, *hbx1*, is required for development and aflatoxin production. *Toxins,***9**: 315-333.

Castro PA, Valero C, Chiaratto J, Colabardini AN, Parddeshi L, Silva LP, Almeida F, Rocha MC, Silva RN, Malavazi I, Du W, Dyer PS, Brock M, Loures FV, Wong KH, Goldman GH (2021). Novel biological functions of the NsdC transcription factor in *Aspergillus fumigatus*. *mBio*, **12**: e03102. 20.

Challa S (2018). Pathogenesis and pathology of invasive aspergillosis. *Clinical Pathology*, **12**: 23-32.

Chamovitz DA (2009). Revisiting the COP9 signalosome as a transcriptional regulator. *EMBO reports,* **10**: 352-358. doi:10.1038/embor.2009.33

Champe, S.P., Rao, P., and Chang, A. (1987) An endogenous inducer of sexual development in *Aspergillus nidulans*. *Journal of General Microbiology*, **133**: 1383-1387.

Chen K, Qiu P, Yuan Y, Zheng L, He J, Wang C, Guo Q, Kenny J, Liu Q, Zhao J, Chen J, Tickner J, Fan S, Lin X, Xu J (2019). Pseurotin A inhibits osteolastogenesis and preoventnsoveriectomized-induced bone loss by suppressing reactive oxygen species. *Theranostics,* **9**: 1634-1650.

Coméra C, André K, Laffitte J, Collet X, Galtier P, Maridonneau-Parini I (2007). Gliotoxin from *Aspergillus fumigatus* affects phagocytosis and the organization of the actin cytoskeleton by distinct signaling pathways in human neutrophils. *Microbes and Infection*, **9**:47-54.

Coméra C, André K, Laffitte J, Collet X, Galtier P, Maridonneau-Parini I (2007). Gliotoxin from *Aspergillus fumigatus* affects phagocytosis and the organization of the actin cytoskeleton by distinct signaling pathways in human neutrophils. *Microbes and Infection*, **9**: 47-54.

Cramer RA, Shwab EK, Keller NP (2009). *Aspergilllus fumigatus* and Aspergillosis*. ASM Press. Washington D.C.* Pp: 185-194.

Czaja W, Miller KY, Skinner MK, Miller BL (2014). Structural and functional conservation of fungal MatA and human SRY sex-determining proteins. *Nature Communications*, **5**: 5354.

Czaja, W., Miller, K.Y., and Miller, B.L. (2011) Complex mechanisms regulate developmental expression of the *matA* (HMG) mating type gene in homothallic *Aspergillus nidulans*. *Genetics*, **189**: 795-808.

De Vries R, Riley R, Wiebenga A et al (2017). Comparative genomics reveals high biological diversity and specific adaptations in the industrially and medically important fungal genus Aspergillus. *Genome Biology*,**18**: 28-72.

Dequard-Chablat M and Alland C (2002). Two copies of *mthmg1*, encoding a novel mitochondrial HMG-like protein, delay accumulation of mitochondrial DNA deletions in *Podospora anserina*. *Eukaryotic Cell*, **1**: 503-513.

Dettmann A, Heilig Y, Ludwig S, Schmitt K, Illgen H, Fleiβner A, Valerius O, Seiler S (2013). HAM-2 and HAM-3 are central for the assembly of the *Neurospora* STRIPAK complex at the nuclear envelope and regulate nuclear accumulation of the MAP kinase MAK-1 in a MAK-2-dependent manner. *Molecular Microbiology*, **90**:796-812.

Dettmann A, Heilig Y, Valerius O, Ludwig S Seiler S (2014). Fungal communication required the MAK-2 pathway elements STE-20 and RAS-2, the NRC-1 adapter STE-20 and the MAP kinase scaffold HAM-5. *PLoS Genetics,* **10**: e1004762.

Dirschnabel, D.E., Nowrousian, M., Cano-Dominguez, N., Aguirre, J., Teichert, I., and Kück, U. (2014). New insights into the roles of NADPH oxidases in sexual development and ascospore germination in *Sordaria macrospora*. *Genetics,* **196**: 729-744.

Dyer PS, Inderbitzin P, Debuchy R (2016). Mating-type structure, function, regulation and evolution in the Pezizomycotina. In*: Growth, Differentiation and Sexuality, The Mycota I (3rd edition)* (ed. J Wendland) pp. 351-385. Springer International Publishing, Switzerland.

Dyer PS, Kück U (2017). Sex and the imperfect fungi. *Microbiology Spectrum* **5**:

Dyer PS, Paoletti M Archer DB (2003). Genomics reveals sexual secrets of *Aspergillus. Microbiology Comment,* **149**: 2301-2303.

Dyer PS (2007). Sexual reproduction and significance of MAT in the aspergilli. *Sex in fungi: molecular determination and evolutionary implications. ASM Press, Washington, DC***,** pp: 123-142.

Dyer PS, Ingram DS, Johnstone K (1992). The control of sexual morphogenesis in the Ascomycotina. *Biological Reviews,* **67**: 421-458.

Dyer PS, O'Gorman CM (2012). Sexual development and cryptic sexuality in fungi: insights form *Aspergillus* species. *FEMS Microbiology Reviews*, **36**: 165-192.

Elleuche S, Pöggeler S (2009). β-Carbonic anhydrases play a role in fruiting body development and ascospore germination in the filamentous fungus *Sordaria macrospora*. *PLoS ONE,* **4**: 5177-5193.

Elramli N, Karahoda B, Sarikaya-Bayram O, Frawley D, Ulas M, Oakley CE, Oakley BR, Seiler S, Bayram O (2018). Assembly of a heptameric STRIPAK complex is required for coordination of light-dependent multicellular fungal development with secondary metabolism in *Aspergillus nidulans. Genetics*, **15**: e1008053.

Engh I, Würtz C, Witzel-Schlömp K, Zhang HY, Hoof B, Nowrousian, Rottensteiner H, Kück U (2007). The WW domain protein PRO40 is required for fungal fertility and associates with Woronin bodies. *Eukaryotic Cell,* **6**:831-843.

Etxebeste O, Garzia A, Espeso EA, Ugalde U (2010). *Aspergillus nidulans* asexual development: making the most of cellular modules. *Trends in Microbiology*. **18**: 569-577.

Filtenbrog O, Frisvad JC, Thrane U (1990). The significance of yeast extract composition on metabolite production in *Penicillium . Modern Concepts in Penicillium and Aspergillus Classification* (Samson RA ed). Pp: 433-442.

Ferreira MES, Kress MRVZ, Savoldi M, Goldman MHS, Härtl A, Heinekamp T, Brakhage AA, Goldman GH (2006). The *akuB*^{KU80} mutant deficient for nonhomologous end joining is a powerful tool for analyzing pathogenicity in *Aspergillus fumigatus. Eukaryotic Cell*. **5:** 207-211.

Frawley D, Karahoda B, Bayram OS, Bayram O (2018). The HamE scaffold positively regulates MpkB phosphorylation to promote development and secondary metabolism in *Aspergillus nidulans. Scientific Reports*, **8**: 16588.

Frey S, Reschka EJ, Pöggeler S (2015). Germinal center kinase SmKIN3 and SmKIN24 are associated with the *Sordaria macrospora* striatin-interacting phosphatase and kinase (STRIPAK) complex. *PLoS ONE*, **10**: e0139163.

Frisvad JC, Rank C, Nielsen KF, Larsen TO (2009). Metabolomics of *Aspergillus fumigatus*. *Medical Mycology*, **47**: S53-S71.

Geib E and Brock M (2017). ATNT: an enhanced system for expression of polycistronic secondary metabolite gene clusters in *Aspergillus niger. Fungal Biology and Biotechnology* **4**:10.1186/s40694-017-0042-1

Gesing S, Schindler D, Fränzel B, Wolters DA, Nowrousian, M (2012). The histone chaperone ASF1 is essential for sexual development in the filamentous fungus *Sordaria macrospora. Molecular Microbiology*, **84**: 748-765.

Glass NL and Kuldau CA (1992) Mating type and vegetative incompatibility in filamentous ascomycetes. *Annual Reviews in Phytopathology,* **30**: 201-224.

Glass NL, Jacobson DJ, Shiu PKT (2000). The genetics of hyphal fusion and vegetative incombatibility in filamentous ascomycete fungi. *Annual Reviews in Genetics,* **34**: 165-186.

Goudreault M, D'Ambrosis LM, Kean MJ, Mullin MJ, Larsen BG, Sanchez A, Chaudhry S, Chen GI, Sicheri F, Nesvizhskii AI, Aebersold R, Raught B, Gingras AC (2008). A PP2A phosphatase high dendityinteraction network identifies a novel striatin-interacting phosphatase and kinase complex linked to the cerebral cavernous malformation 3 (CCM3) protein. *Molecular and Cellular Proteomics*, **8**: 157-171.

Grognet P, Bidard F, Kuchly C, Tong LCH, Coppin E, Benkhali JA, Couloux A, Wincker P, Debuchy R, Silar P (2014). Maintaining two mating types: structure of the mating type locus and its role in heterokaryosis in *Podospora anserina. Genetics* **197**: 421-432.

Guruceaga X, Perez-Cuesta U, Cerio AA, Gonzalez O, Alonso RM, Hernando FL, Ramirez-Garcia A, Rementeria A (2020). Fumagillin, a mycotoxin of *Aspergillus fumigatus:*biosynthesis, biological activities, detechtion, and applications. *Toxins*: **12**: 7-33.

Han KH, Han KY, YU JH, Chae KS, Jahng KY, Han DM (2001). The *nsdD* gene encodes a putatibe GATA-type transcription factor necessary for sexual development of *Aspergillus nidulans. Molecular Microbiology*, **41**: 299-309.

Han KH, Kim JH, Moon H, Kim S, Lee SS, Han DM, Jahng KY, Chae KS (2008). The *Aspergillus nidulans esdC* (early sexual development) gene is necessary for sexual development and is controlled by *veA* and a heterotrimeric G protein. *Fungal Genetics and Biology,* **45**: 3310-318.

Han KH, Park JS, Chae KS, Han DM (2010). Simple identification of *veA1* mutation in *Aspergillus nidulans*. *The Journal of Microbiology*, **48**: 885-887.

Han KH, Seo JA, Yu JH (2004). A putative G protein-coupled receptor negatively control sexual development in *Aspergillus nidulans. Molecular Microbiology,* **51**:1333-1345.

Hawksworth DL, Crous PW, Redhead SA, Reynolds DR, Samson RA, et al. (2011). The Amsterdam declaration on fungal nomenclature. *IMA Fungus* **2**: 105-112.

Hoffmann B, Wanke C, LaPaglis SK, Braus GH (2000).c-Jun and RACK1 homologs regulate a control point for sexual development in *Aspergillus nidulans*. *Molecular Microbiology*, **37**: 28-41.

Holland PW (2013). Evolution of homeobox genes. *WIREs Dev Biol*, **2**: 31-45.

Hutner SH, Provasoli L, Schatz A, Haskins CP (1950). Some approaches to the study of the role of metals in the metabolism of microorganisms. *Proceedings of the American Philosophical Society*, **94**: 152-170.

Ibarra BA, Lohmar JM, Stterlee T, McDonald T, Cary JW, Calvo AM (2018). The 14-3-3 protein homolog ArtA regulates development and secondary metabolism in the opportunistic plant pathogen *Aspergillus flavus*. *Applied and Environmental Microbiology*, **84**: e02241-17.

Idnurm A, Walton FJ, Floyd A, Heitman J (2008). Identification of the sex genes in an early diverged fungus. *Nature Letters*: **451**: 193-197.

Ishikawa M, Ninomiya T, Akabane H, Kushida N, Tsujiuchi G, Ohyama M, Gomi S, Shito K and Murata T (2009). Psuerotin A and its analogues as inhibitors of immunoglobulinne E production. *Bioorganic and Medicinal Chemistry Letter*, **19**: 1457-1460

Iyer SV, Ramakrishnan M, Kasbekar DP (2009). *Neurospora crassa fmf-1* encodes the homolog of the *Schizosaccharomyces pombe* Ste11p regulator of sexual development. *Journal of Genetics*, **88**: 33-39.

Jacobsen S, Wittig M, Pöggeler S (2002). Interaction between mating-type proteins from the homothallic fungus *Sordaria macrospora. Current Genetics,* **41**:150-158.

Jamet-Vierny, C., Debuchy, R., Prigent, M., and Silar, P. (2007) IDC1, a Pezizomycotina-specific gene that belongs to the PaMpk1 MAP kinase transduction cascase of the filamentous fungus *Podospora anserina*. *Fungal Genetics and Biology*, **44**: 1219-1230.

Jin FJ, Takahashi T, Matrushima K, Hara S, Shinohara Y, Maruyama J, Kitamoto K, Koyama Y (2011). SclR, a basic helix-loop-helix transcription factor, regulates hyphal morphology and promotes sclerotial formation in *Aspergillus oryzae*. *Eukaryotic Cell*. **10**: 945-955.

Jonkers W, Leeder AC, Ansong C, Wang Y, Yang F, Starr TL, Camp DG, Smith RD, Glass NL (2014). HAM-5 functions as a MAP kinase scaffold during cell fusion in *Neurospora crassa. PLoS Genetics,* **10**: e1004783.

Kale SP, Milde L, Trapp MK, Frisvad JC, Keller NP, Bok JW (2008). Requirement of LaeA for secondary metabolism and sclerotial production in *Aspergillus flavus*. *Fungal Genetics and Biology*, **45**: 1422-1429.

Karácsony Z, Gácser A, Vágvölgyi C,Scazzocchio C, Hamari Z (2014). A dually located multi-HMG-box protein of *Aspergillus nidulans* has a crucial role in conidial and ascospore germination. *Molecular Microbiology*, **94**: 383-402.

Kays AM and Borkovich KA (2004). Severe impairment of growth and differenctiation in a *eurospora crassa* mutant lacking all heterotrimeric Gα proteins. *Genetics*,**166**: 1229-1240.

Kim MJ, Lee MJ, Pham HQ, Gu MJ, Zhu B, Son SH, Haln D, Shin JH, YU JH, Park HS, Han KH (2020).The *velvet* regulator VosA governs survival and secondary metabolism of sexual spores in *Aspergillus nidulans. Genes*, **11**: 102-114.

Kim HK, Jo SM, Kim GY, Kim DW, Kim YK, Yun SH (2015). A large-scale functional analysis of putative target genens of mating type loci provides insight into the reulation of sexual development of the cereal pathogen *Fusarium graminearum. PLoS Genetics,* **11**: e1005486.

Kim HK, Lee S, Jo SM, McCormick SP, Butchko RAE, Proctor RH, Yun SH (2013).Functional roles of FgLaeA in controlling secondary metabolism, sexual development, and virulence in *Fusarium graminearum.PLoS ONE*, **8**:e68441.

Kim H, Wright SJ, Park G, Ouyang S, Krystofova S, Borkovich KA (2012). Roles for receptors, pheromones, G proteins, and mating type genes during sexual reproduction in *Neurospora crassa*. *Genetics,* **190**: 1389-1404.

Kim HR, Chae KS, Han KH, Han DM (2009). The nsdC gene encoding putative C2H2-type transcription factor is a key activator of sexual development in *Aspergillus nidulans*. *Genetics,* **182**: 771-783.

Kishimoto S, Tsunematsu Y, Sato M, Watanabe K (2017). Elucidation of biosynthetic pathways of natural products. *The Chemical Record,* **17**: 1095-1108.

Korfanty G, Stanley K, Lammers K, Fan YY, Xu J (2021). Variations in sexual fitness among natural strains of the opportunistic human fungal pathogen *Aspergillus fumigatus. Infection, Genetics and Evolution,* **87**: 104640.

Kosalková K, Carcía-Estrada C, Ullán RV, Godio RP, Feltrer R, Teijeira F, Mauriz E, Martín (2008). The global regulator LaeA controls penicillin biosynthesis pigmentation and sporulation, but not requefortine C synthesis in *Penicillium chrysogenum*. *Biochimie,* **91**: 214-225.

Krijgsheld P, Bleichrodt R, Veluw GJ, Wang F, Müller WH, Dijksterhuis J, Wösten HAB (2012). Development in *Aspergilllus. Studies in Mycology* **74**: 1-29.

Krystofova S, Borkovich KA (2005). The hetertotrimeric G-protein subunits GNG-1 and GNB-1 form a Gβγ dimer required for normal female fertility , asexual development, and Gα protein levels in *Neurospora crassa*. *Eukaryotic Cell*, **4**:365-378.

Kück U, Stein V (2021). STRIPAK, a key regulator of fungal development, operates as multifunctional signaling hub. *Journal of Fungi,* **7**: 443-453.

Kück U, Beier AM, Teichert I (2016). The composition and function of the striatin-interacting phosphatases and kinases (STRIPAK) complex in fungi. *Fungal Genetics and Biology*, **90**: 31–38.

Lara-Ortíz T, Riveros-Rosas H, Aguirre J (2003). Reactive oxygen species generated by microbial NADPH oxidase NoxA regulate sexual

development in *Aspergillus nidulans*. *Molecular Microbiology*, **50**:1241-1255.

Lee SC, Ni M, Li W, Shertz C, Heitman J (2010). The evolution of sex: a perspective from the fungal kindom. *Mcirobiology and Molecular Biology Reviews*, **74**: 298-340.

Lim FY, Sanchez JF, Wang CCC, Keller NP (2012). Toward awakening cryptic secondary metabolite gene clusters in filamentous fungi. *Methods in Enzymology*, **517**: 303-324.

Lind AL, Lim FY, Soukup AA, Keller NP, Rokas A (2018). An LaeA- and BrlA-dependent cellular network governs tissue-specific secondary metabolism in the human pathogen *Aspergillus fumigatus. mSphere*, **3**: e00050-18.

Linke, R., Thallinger, G.G., Haarmann, T., Eidner, J., Schreiter, M., Lorenz, P., Seiboth, B., and Kubicek, C.P. (2015). Restoration of female fertility in *Trichoderma reesei* QM6a preodives the basis for inbreeding in this industrial cellulose producing fungus. *Biotechnology and Biofuels,* **8**:155-165.

Lius JM, Carbone I, Mack BM, Lebar MD, Cary JW, Gilbert MK, Bhatnagar D, Wientjes C, Payne GA, Moore GG, Ameen YO, Ojianmbo PS (2022). Development of sexual structures influences metabolomic and transcriptomic profiles in *Aspergillus flavus*. *Fungal Biology*, **126**: 187-200.

Lu J, Kobayashi R, Brill SJ (1996). Characterization of a high mobility group 1/2 homolog in yeast. *The Journal of Biological Chemistry*, **271**:33678-33685.

Maerz S, Ziv C, Vogt N, Helmstaedy K, Cohen N, Gorovits R, Yarden O, Seiler S (2008). The nucleat Dbf2-related kinase COT1 and the mitogen-activated protein kinases MAK1 and MAK2 genetically interact to regulate filamentous growth, hyphal fusion and sexual development in *Neurospora crassa. Genetics:* **179**: 1313-1325.

Marcos AT, Ramos MS, MarcosJF, Carmona L, Strauss J, Cánovas D (2016). Notric oxide synthesis by nitrate reductase is regulated during development in *Aspergillus. Molecular Microbiology*, **99**: 15-53.

Marschall R, Tudzynski P (2016). Reactive oxyen species in development and infection processes. *Seminers in Cell & Developmental Biology*, **57**: 138-146

Martin T, Lu SW, Tilbeurgh H, Ripoll DR, Dixelius C, Turgeon BG, Debuchy R (2010). Tracing the origin of the fungal α1 domain places its ancestor in the HMG-box supergamily : implication for fungal mating -type evolution. *PLoS ONE*, **5**: e15199.

Mata J, Bahler J (2006). Global roles of Ste11p, cell type, and pheromone in the control of gene expression during early sexual differentiation in fission yeast. *PNAS,***103**:15517–15522.

Mayrhofer S, Weber JM, Pöggeler S (2006). Pheromones and pheromone receptors are required for proper sexual development in the homothallic ascomycete *Sordaria macrospora. Genetics,* **172**: 1521-1533.

McCormick A, Loeffler J, Ebel F (2010). *Aspergillus fumigatus*: contours of an opportunistic human pathogen. *Cellular Microbiology,* **12**: 1535-1543.

Mehedi MAU, Molla AH, Khondkar P, Sultana S, Islam MA, Rashid MA, Chowdhury R (2010). Pseurotin A: an antibacterial secondary metabolite from *Aspergillus fumigatus. Asian Journal of Chemistry* **22**: 2611-2614.

Metzenberg RL and Glass NL (1990). Mating type and mating strategies in *Neurospora*. *BioEssays*, **12**: 53-59.

Monteiro M, Garcia-Rubio R, Alcazar-Fuoli L, Peláez T, Mellado E (2017). Could the determination of *Aspergillus fumigatus* mating type have prognostic value in invasive aspergillosis? *Mycoses*, **61**: 172-178.

Moore D, Robson GD, Trinci APJ (2011). 21st Century Guidbook to Fungi. Cambrige University Press, New York. Pp: 41-61, 179-197.

Moore-Landecker E (1992). Physiology and biochemistry of ascocarp induction and development. *Mycological Research,* **96,** 705-716.

Moore-Landecker E. 1996. *Fundamentals of the Fungi,* New York: Prentice Hall.

Musungu BM, Bhatnagar D, Brown RL, Payne GA, O'Brain G, Faknoury AM. Geisler M (2016). A network approach of gene co-expression in the *Zea/mays/Aspergillus flavus* pathosystem to map host/pathogen interaction pathways. *Frontiers in Genetics*: **7**:206-219.

Mylona AE, Frensno JM, Palomero F, Loira I, Banuelos MA, Morata A, Dalderon F, Benito S, Suarez-Lepe JA (2016). Use of *Schizosaccharomyces* strains for wine fermentation-effect on the wine composistion and food safety. *International Journal of Food Microbiology*, **232**:63-72.

Ni M and Yu JH (2007). A novel regulator couples sporogenesis and trehalose biogenesis in *Aspergillus nidulans. PloS ONE*, **2**:e970.

Nordzieke S, Zobel T, Fränzel B, Wolters DA, Kück U, Teichert I (2015). A fungal sarcolemmal membrane-associated protein (SLMAP) homolog plays a fundamental role in development and localizes to the nuclear envelope, endoplasmic reticulum, and mitochondria. *Eukaryotic Cell,* **14**: 345-358.

Nowrousian M, Frank S, Koers S, Strauch P, Weitner T, Ringelberg C, Dunlap JC, Loros JJ, Kück U (2007). The novel ER membrane protein PRO41 is essential for sexual development in the filamentous fungus *Sordaria macrospora. Molecular Microbiology***, 64**: 923-937.

O'Gorman CM, Fuller HT, Dyer PS (2009). Discovery of a sexual cycle in the opportunistic fungal pathogen *Aspergillus fumigatus. Nature* **457**: 471-475.

O'Sullivan AC, Sullivan GJ, McStay B (2002). UBF binding in vivo is not restricted to regulatory sequences within the vertebrate ribosomal DNA repeat.*Mol Cell Biol*, **22**: 657–668.

Oh IH. Reddy EP (1999). The *myb* gene family in cell growth, differentiation and apoptosis. *Oncogene,* **18**: 3017-3033.

Ojeda-Lopez M, Chen W, Eagle CE, Gutierrez G, Jia WL, Swilaiman SS, Huang Z, Park HS, Yu JH, Canovas D, Dyer PS (2018). Evolution of asexual and sexual reproduction in the aspergilli. *Studies in Mycology* **91**: 37-59.

Orciuolo E, Stanzani M, Canestraro M, Galimberti S, Garulli G, Lewis R, Petrini M, Komanduri KV (2007). Effects of *Aspergillus fumigatus* gliotoxin and methylprednisolone on human neutrophils: implications for the pathogenesis of invasive aspergillosis. *Journal of Leukoeyta Biology*, **82**: 839-848.

Pál K, Diepeningen AD, Hoekstra RF, Dyer PS, Debets AJM (2007). Sexual and vegetative compatibility genes in the aspergilli. *Studies in Mycology,* **59**: 19-30.

Pandey A, Roca MG, Read ND, Glass NL (2004). Role of a mitogen-activated protein kinase pathway during conidial germination and hyphal fusion in *Neurospora carssa*. *Eukaryotic Cell*, **3**: 348-358.

Pandit SS, Lohmar JM, Ahmed S,Etxebeste O, Espeso EA, Calvo AM (2018). UrdA controls secondary metabolite production and the balance between asexual and sexual development in *Aspergillus nidulans. Genes*, **9**: 570-593.

Paoletti M, Rydholm C, Schwier EU, Anderson MJ, Szakacs G, Lutzoni F, Debeaupuis JP, Latgé JP, Denning DW, Dyer PS (2005). Evidence for sexuality in the opportunistic fungal pathogen *Aspergillus fumigatus. Current Biology* **15**: 1242-1248.

Paoletti, M., Seymour, F.A., Alcocer, M.C., Kaur, N, Calvo, A.M., Archer, D.B., and Dyer, P.S. (2007). Mating type and the genetic basis of self-fertility in the model fungus *Aspergillus nidulans*. *Current Biology*, **17**: 1384-1389.

Park H-S, Nam T-Y, Han K-H, Kim SC, Yu J-H (2014) VelC positively controls sexual development in *Aspergillus nidulans*. *PLoS ONE,* **9**: e89883.

Park H-S, Ni M, Jeong KC, Kim YH, Yu J-H (2012) The role, interaction and regulation of the velvet regulator VelB in *Aspergillus nidulans*. *PLoS ONE,* **7:** e45935. e45935.

Pérez-Sánchez A, Uribe-Carvajal S, Cabrera-Orefiee A, Barrios-González J (2017). Key role of alternative oxidase in lovastatin solid-state fermentation. *Applied Microbial and Cell Physiology*, **101**: 7347-7356.

Phadke SS, Feretzaki M, Heitman J (2013) Unisexual reproduction enhances fungal competitiveness by promoting habitat wxploration via hyphal growth and sporulation. *Eukaryotic Cell,* **12**: 1155-1159.

Pinson B, Brendeford, EM, Gabrlelsen OS, Dalgnan-Fornler B (2001). Highly conserved features of DNA binding between two divergent members of the Myb family of transcription factors. *Nucleic Acids Research,* **29**: 527-535.

Pöggeler S, Nowrousian M, Kück U (2006). Fruiting-body development in Ascomycetes. *The Mycota I. Growth, Differentiation and Sexuality*, pp: 326-355.

Pontecorvo G, Roper J, Chemmons L, Macdonald K, Bufton A (1953). The genetics of *Aspergillus nidulans*. *Advances in Genetics,* **5,** 141-238.

Purschwitz J, Müller S, Kastner C, Schöser M, Haas H, Espeso EA, Atoui A, Calvo AM, Fisher R (2008). Functional and physical interaction of blue- and red- light sensor in *Aspergillus nidulans*. *Current Biology*, **18**: 255-259.

Purschwitz J, Muller S, Fischer R (2009). Mapping the interaction sites of *Aspergillus nidulans* phytochrome FphA with the global regulator VeA and the Whiter Collar protein LreB. *Molecular Genetics and Genomic*, **281**:35-42.

Pyrazak W, Miller KY, Mmiller BL (2008). Mating type protein Mat1-2 from asexual *Aspergillus fumigatus* drives sexual reproduction in fertile *Aspergillus nidulans*. *Eukaryotic Cell,* **7**: 1029-1040.

Ries, LN, Pardeshi L, Dong Z, Tan K, Steenwyk L, Goldman GH (2020). The *Aspergillus fumigatus* transcription factor RglT is important for gliotoxin biosynthesis and self-protection, and virulence. *PLoS Pathogens*, **16**: e1008645.

Roche CM, Loros JJ, McCluskey K, Glass NL (2014). *Neurospora crassa*: looking back and looking forward at a model microbe. *American Journal of Botany*, **101**: 2022-2035.

Rosén S, Yu JH, Adams TH (1999). The *Aspergillus nidulans sfaD* gene encodes a G protein β subunit that is required for normal growth and repression of sporulation. *The EMBO Journal*, **18**: 5592-5600.

Salih NS (2016). Evolution and control of sexual reproduction in *Aspergillus* species (Doctoral Thesis). University of Nottingham. Nottinghamshire, pp: 148-182.

Saupe SJ, Clavé C, Bégueret J (2000). Vegetative incompatibility in filamentous fungi: *Podospora* and *Neurospora* provide some clues. *Current Opinion in Microbiology*, **3**: 608-612.

Saupe SJ, Descamps C, Turcq B, Bégueret J (1994). Inactivation of the *Podospora anserina* vegetative incompatibility locus *het-c*, whose product resembles a glycolipid transfer protein, drastically impairs ascospore production. *Genetics,* **91**: 5927-5931.

Scharf DH, Heinekamp T, Remme N, Hortschansky P, Brakhade AA, Hertweek C (2012). Biosynthesis and function of gliotoxin in *Aspergillus fumigatus*. *Appl. Microbiol.Biotechnol,* **93**:467-472.

Schoberle TJ, Nguyen-Coleman CK, Herold J, Yang A, Weirauch M, Hughes TR, McMurray JS, May GS (2014). A novel C2H2 transcription factor that regulates *gliA* expression interdependently with GliZ in *Aspergillus fumigatus. PLoS Genetics*, **10**: e1004336.

Schumacher DI, Lutkenhaus R, Altegoer F, Teichert I, Kück U, Nowrousian M (2018). The transcription factor PRO44 and the histone chaperone ASF1 regulate distince aspects of multicellular development in the filamentous fungus *Sordaria macrospora*, *Genetics*, **19**: 112-133.

Seo JA, Han KH, Yu JH (2004). The *gprA and gprB* genes encode putative G protein coupled receptors required for self-fertilization in *Aspergillus nidulans. Molecular Microbiology,* **53**: 1611-1623.

Seo JA, Han KH, Yu JH (2005). Mutiple roles of a heterotrimeric G-protein γ-subunit in governing growth and development of *Aspergillus nidulans. Genetics,* **171**: 81-89.

Seo JA, Yu JH (2006). The phosducin-like protein PhnA is required for Gβγ-mediated signaling for vegetative growth, developmental control, and toxin biosynthesis in *Aspergillus nidulans*. *Eukaryotic Cell*, **5**:400-410.

Shelest E (2008). Transcription factors in fungi. *FEMS Microbiology Letters,* **286**: 145-151.

Shen L, Porée FH, Gaslonde T, Lalucque H, Chapeland-Leclerc F, Ruprich-Robert G (2019). Functional characterization of the sterigmatocystin secondary metabolite gene cluster in the filamentous fungus *Podospora anserina*: involvement in oxidative stress response, sexual development, pigmentation and interspecific competitions. *Environmental Microbiology*, **21**: 3011-3026.

Shi Z, Jiao S, Zhou Z (2016). STRIPAK complexes in cell signaling and cancer. *Oncogene*, **35**:4549-4557.

Shin KS, Kim YH, Yu JH (2015). Proteomic analyses reveal the key roles of BrlA and AbaA in biogenesis of gliotoxin in *Aspergilllus fumigatus. Biochemical and Biophysical Research Communications,* **463**: 428-433.

Shiu PKT, Glass NL (1999). Molecular characterization of *tol*, a mediator of mating-type-associated vegetative incompatibility in Neurospora crassa. Genetics, 151: 545-555.

Shiu PKT, Glass NL (2000). Cell and nuclear recognition mechanisms mediated by mating type in filamentous ascomycetes. *Current Opinion in Microbiology*. **3**:183-188.

Simonin AR, Rasmussen CG, Yang M, Glass NL (2010). Genes encoding a striatin-like protein (ham-3) and a forkhead associated protein (ham-4) are required for hyphal fusion in *Neurospora crassa*. *Fungal Genetics and Biology* , **47**: 855–868.

Singh NS, Shao N, McLean JR, Sevugan M, Ren L, Chew TG, Bimbo R, Sharma R, Tang X, Gould KL, Balasubramanian MK (2011). SIN-inhivitoty phosphatase complex promotes cdc11p dephosphorylation and propagates SIN asymmetry in fission yeast. *Current Biology,* **21**: 1968-1978.

Sohn KT, Yoon KS (2002). Ultrastructural study on the cleistothecium development in *Aspergillus nidulans. Mycobiology*, **30**: 117-127.

Son S, Osmani SA (2009). Analysis of all protein phosphatases genes in *Aspergillus nidulans* identifies a new mitotic regulator, Fcp1. *Eukaryotic Cell*, **8**: 573-585.

Spikes S, Xu R, Nguyen CK, Chamilos G, Kontoyiannis DP, Jacobson RH, Ejzykowicz DE, Chiang LY, Filler SG, May GS (2008). Gliotoxin production in *Aspergillus fumigatus* contributes to host-specific differences in virulence. *The Jouranl of Infectious Disease*, **197**: 479-486.

Stinnett SM, Aspeso EA, Cobeno L, Araújo-Bazán L,Calvo AM (2007). *Aspergillus nidulans* VeA subcellular localization is dependent on the importin α carrier and on light. *Molecular Microbiology,* **63**: 242-255.

Stros M, Launhokk D, Crasser KD (2007) The HMG-box: a versatile protein domain occurring in a wide variety of DNA-bind proteins. *Cellular and Molecular Life Sciences*, **64**:2590-2606.

Sugimoto A., Iino Y., Maeda T., Watanabe Y. and Yamamoto M(1991). *Schizosaccharomyces pombe ste11*+ encodes a transcriptionfactor with an HMG motif that is a critical regulator of sexual development. *Genes and Development*, **5**:1990–1999.

Sun XY, Zhu JF, Bao L, Hu CC, Jin C, Harris SD, Liu HW, Li SJ (2013). *pyrG* is required for maintaining stable cellular uracil level and normal sporulation pattern under excess uracil stress in *Aspergillus nidulans. Science China,* **56**: 467-475. doi:10.1007/s11427-013-4480-6.

Svahn KS, Göransson U, Chryssanthou E, Olsen B, Sjölin J, Strömstedt AA (2014). Induction of gliotoxin secretion in *Aspergillus fumigatus* by bacteria-associated molecules. *PLoS ONE*, **9**: e93685.

Swilaiman SS, O'Gorman CM, Du W, Sugui JA, Buono JD, Brock M, Kwon-Chung KJ, Szakacs G,Dyer PS (2020). Global sexual fertitlity in the opportunistic pathogen *Aspergillus fumigatus* and identification of new supermater strains. *Journal of Fungi* **6**: 258.

Szewczyk E, Nayak T, Oakley CE, Edgerton H, Xiong Y, Tacheri-Talesh N, Osmani SA, Oayley BR (2006). Fusion PCR and gene targeting in *Aspergillus nidulans. Nature Protocols* **1**: 3111-3120.

Teicher I, Pöggeler S, Nowrousian M (2020). *Sodaria macrospora*: 25 years as a model organism for studying the molecular mechanisms of fruiting body development. *Applied Microbiology and Biotechnology*, **104**: 3691-3704.

Todd RB, Davis MA, Hynes MJ (2007). Genetic manipulation of *Aspergillus nidulans*: meiotic progeny for genetic analysis and strain construction. *Nature Protocols*, **2**: 811-822.

Tsitsigiannis D and Keller NP (2006). Oxylipins act as determinants of natural product biosynthesis and seed colonization in *Aspergillus nidulans*. *Molecular Microbiology*, ***59***: 882-892.

Tsitsigiannis DI, Kowieski TM, Zarnowski R, Keller NP (2005). Three putative oxylipin biosynthetic genes integrate sexual and asexual development in *Aspergillus nidulans*. *Microbiology,* **151**: 1809-1821.

Tsitsigiannis DI, Zarnowski R, Keller NP (2004). The lipid body protein, PpoA, coordinates sexual and asexual sporulation in *Aspergillus nidulans*. *The Journal of Biological Chemistry*, **270**:11344-11353.

Tüncher A, Reinke H, Martic G, Caruso ML, Brakhage AA (2004). A basic-region helix-loop-helix protein-encoding gene (*devR*) involved in the development of *Aspergillus nidulans. Molecular Microbiology,* **52**: 227-241.

Vallim MA, Miller KY, Miller BL (2000). *Aspergillus* SteA (sterile12-like) is a homeodomain-C_2/H_2-Zn^{+2} finger transcription factor required for sexual reproduction. *Molecular Microbiology,* **36**: 290-301.

Valsecchi I, Sarikaya-Bayram O, Hoi JWS, Laetitia Muszkieta L, Gibbons J, Prevost M, Allet A, Krijnse-Locker J, Ibrahim-Granet O, Mouyna I, Carr P, Bromley M, Aimanianda V, Yu JH, Rokas A, Braus GH, Saveanu C, Bayram O, Latge JP (2017). MybA, a transcription factor involved in conidiation and conidial viability of the human pathogen *Aspergillus fumigatus. Molecular Microbiology,* **105**: 880–900.

Vienken K, Scherer M, Fischer R (2005). The $Zn(II)_2Cys_6$ putative *Aspergillus nidulans* transcription factor repressor of sexual development inhibits sexual development under low-carbon conditions and in submersed culture. *Genetics,* **169**:619-630.

Vienken K, Fischer R (2006). The Zn(II)2Cys6 putative transcription of factor NosA controls fruiting body formation in *Aspergillus nidulans*. *Molecular Microbiology*, **61**: 544-554.

Wada R, Maruyama J, Yamaguchi H, Yamamoto N, Wagu Y, Paoletti M, Archer DB, Dyer PS, Kitamoto K. Presence and functionality of mating type genes in the supposedly asexual filamentous fungus *Aspergillus oryzae. Applied and Environmental Microbiology,* 2819-2829.

Wang Z, Lopez-Giraldez F, Lehr N, Farré M, Common R, Trail F, Townsend JP (2014). Global gene expression and focused knockout analysis reveals genes associated with fungal fruiting body development in *Neurospora crassa. Eukaryotic Cell*, **13**: 154-169.

Wang CL, Shim WB, Shaw BD (2010). *Aspergillus nidulans* striatin (StrA) mediates sexual development and localizes to the endoplasimic reticulum. *Fungal Genetics and Biology*, **47**: 789-799.

Wei N, Deng XW (2003). The COP9 signalosome. *Annual Reviews of Cellular and Developmental Biology,* **19**: 261-86.

Wilson AM, Wilken PM, Nest MA, Wingfield MJ, Wingfield BD (2019). It's all in the genes: the regulatory pathways of sexual reproduction in filamentous ascomycetes. *Genes*, **10**: 330-351.

Wilson AM, Godlonton T, van der Nest MA, Wilken PM, Wingfield MJ, Wingfield BD (2015). Unisesual reproduction in *Huntiella moniliformis. Fungal Genetics and Biology,* **80**:1-9.

Wu D, Dou X, Hashmi SB, Osmani SA (2004). The Pho80-like cyclin of *Aspergillus nidulans* regulates development independently of its role in phosphate acquisition. *The Journal of Biological Chemistry*, **270**: 37693-37704.

Wu J, Miller B (1997). *Aspergillus* asexual reproduction and sexual reproduction are differentially affected by transcriptional and translational mechanisms regulating *stunted* gene expression. *Molecular and Cellular Biology,* **17**: 6191-6201.

Xiang Q, Rasmussen C, Glass NL (2002). The *ham-2* locus, encoding a putative transmembrane protein, is required for hyphal fusion in *Neurospora crassa. Genetics*, **160**: 169-180.

Yang Q, Poole SI, Borkovich KA (2002). A G-protein β subunit required for sexual and vegetative development and maintenance of normal Gα protein levels in *Neurospora crassa*. *Eukaryotic Cell*, **1**: 378-390.

Yu JH, Rosén S, Adams TH (1999). Extragenic suppressors of loss-of-function mutation in the *Aspergillus* FlbA regulator of G-protein signaling domain protein.*Genetics*, **151**:97-105.

Yu Y, Blachowicz A, Will C, Szewczyk E, Gllenn S, Gensberger-Reigl S, Nowrousian M, Wang CCC, Krappmann S (2018). Mating-type factor-specific regulation of the fumagillin/ pseurotin secondary metabolite supercluster in *Aspergillus fumigatus. Molecular Microbiology*, **110**:1045-1065.

Zhang J, Snelder E, Zwaan BJ, Schoustra SE, Meis JF, Dijk K, Hagen F, Beek MT, Kampinga GA, Zoll J, Melchers WJG, Verweij PE, Debets AJM (2017). A novel enrironmenal azole resistance mutation in *Aspergillus fumigatus* and a possible role of sexual reproduction in its emergence. *mBio*: **8**:e00791-17.

Zhao Y, Sun H, Li J, Ju C, Huang J (2022). The transcription factor FgAtrR regulates asexual and sexual development, virulence, and DON production and contributes to intrinsic resistance to azole fungicides in *Fusarium graminearum*. *Biology,* **11**: 326.

Publications to date arising from thesis work

de Castro PA, Valero C, Chiaratto J, Colabardini AC, Pardeshi L, Silva LP, Almeida F, Rocha MC, Silva RN, Malavazi I, **Du W**, Dyer PS, Brock M, Loures FV, Wong KH, Goldman GH (2021). Novel biological functions for the *Aspergillus fumigatus* NsdC transcription factor homolog involved in sexual development. *mBio,* **12**: e03102-20.

Swilaiman SS, O'Gorman CM, **Du W**, Sugui JA, Del Buono J, Brock M, Kwon-Chung KJ, Szakacs G, Dyer PS (2020). Global sexual fertility in the opportunistic pathogen *Aspergillus fumigatus* and identification of new supermater strains. *Journal of Fungi,* **6**: 258.

Appendices

Appendix 1 PCR reaction mix of upstream and downstream fragment amplification

Reagent	Amount per reaction
gDNA (100 ng/μL)	1 μL
Primer P1 for upstream	2.5 μL
or P3 for downstream fragment (1 nM)	
Primer P2 for upstream	2.5 μL
or P4 for downstream fragment (1 nM)	
Phusion High Fidelity polymerase (2 U/μL)	1 μL
dNTPs (10mM)	1 μL
HF buffer (5X)	10 μL
H_2O	Add to 50 μL

Appendix 2 The cycing program of upstream and downstream fragment

Cycle number	Denaturation	Ramp rate	Annealing	Ramp rate	Extension	Ramp rate
1	98 °C, 2 min					
2-34	98 °C,	Ramp to 63 °C at	63 °C,	Ramp to 72 °C at	72 °C,	Ramp to 98 °C at
	30 sec	maximum rate	30 sec	maximum rate	35 sec	maximum rate
35	98 °C,	Ramp to 63 °C at	63 °C,	Ramp to 72 °C at	72 °C,	Hold at 4 °C
	30 sec	maximum rate	30 sec	maximum rate	10 sec	

Appendix 3 PCR reaction mix of selectable marker amplification

Reagent	Amount per reaction
FGSC ANID_AN4632.1 plasmid	2 μL
Primer pryG F/ pryG R (1 nM each)	5 μL
Phusion High Fidelity polymerase (2 U/μL)	1 μL
dNTPs (10mM)	1 μL
HF buffer (5X)	10 μL
H_2O	Add to 50 μL

Appendix 4 The cycling program of selectable marker amplification

Cycle number	Denaturation	Ramp rate	Annealing	Ramp rate	Extension	Ramp rate
1	98 °C, 2 min					
2-34	98 °C,	Ramp to 63 °C at	63 °C,	Ramp to 72 °C at	72 °C,	Ramp to 98 °C at
	30 sec	maximum rate	30 sec	maximum rate	35 sec	maximum rate
35	98 °C,	Ramp to 63 °C at	63 °C,	Ramp to 72 °C at	72 °C,	Hold at 4 °C
	30 sec	maximum rate	30 sec	maximum rate	10 sec	

Appendix 5 PCR reaction mix of deletion cassette amplification

Reagent	Amount per reaction
Purified upstream/downstream fragment (85 ng/μL)	2 μL
Purified pryG fragment (50 ng/μL)	1 μL
Primer P5 (1 nM)	2.5 μL
Primer P6 (1 nM)	2.5 μL
Phusion High Fidelity polymerase (2 U/μL)	1 μL
dNTPs (10mM)	1 μL
HF buffer (5X)	10 μL
H_2O	Add to 50 μL

Appendix 6 The cycling program of fusion PCR

Cycle number	Denaturation	Ramp rate*	Annealing	Ramp rate*	Extension	Ramp rate
1	98 °C, 2 min					
2-11	98 °C, 20 sec	To 70 °C at maximum rate, 1 s. ramp to the annealing temperature at 0.1 °C/sec	63 °C, 30 sec	Ramp to 72 °C at 0.2 °C/sec	72 °C, 2 min	Ramp to 98 °C at maximum rate.
12-16	98 °C, 20 sec	To 70 °C at maximum rate, 1 s. ramp to the annealing temperature at 0.1 °C/sec	63 °C, 30 sec	Ramp to 72 °C at 0.2 °C/sec	72 °C, 2 min Extension for first cycle 2 min, and last cycle 2 min 20 sec**	Ramp to 98 °C at maximum rate.
	98 °C, 20 sec	To 70 °C at maximum rate, 1 s. ramp to the annealing temperature at 0.1 °C/sec	63 °C, 30 sec	Ramp to 72 °C at 0.2 °C/sec	72 °C, 2 min Extension for first cycle 2 min 20 sec, and last cycle 6 min 20 sec**	Ramp to 98 °C at maximum rate.
17-26	98 °C, 20 sec	To 70 °C at maximum rate, 1 s. ramp to the annealing temperature at 0.1 °C/sec	63 °C, 30 sec	Ramp to 72 °C at 0.2 °C/sec		Ramp to 98 °C at maximum rate.

* The aim of this touch-down PCR was to try and improve specificity of primer annealing.

** The increase of extension time was due to potential loss of potency/activity of polymerase enzyme as the PCR progressed.

Appendix 7 Strains utilised in the study of sexual development in *A. nidulans*

Strain/Isolate	Genotype	Parental strain	Source
AN2701-4	*AN2701.2::pyrG*	2-258	This lab
AN2701-6	*AN2701.2::pyrG*	2-258	This lab
AN0164-3	*AN0164.2::pyrG*	2-258	This lab
AN0164-6	*AN0164.2::pyrG*	2-258	This lab
AN0164-6C5	*pyrG::AN0164.2-pyroA*	AN0164-6	This lab
AN4632-3	*AN4632.2::pyrG*	2-258	This lab
AN4632-6	*AN4632.2::pyrG*	2-258	This lab
AN4632-6C29	*pyrG::AN4632.2-pyroA*	AN4632-6	This lab
AN4813-2	*AN4813.2::pyrG*	2-258	This lab
AN4813-14	*AN4813.2::pyrG*	2-258	This lab
AN4813-2C8	*pyrG::AN4813.2-pyroA*	AN4813-2	This lab
AN1217-6	*AN1217.2::pyrG*	2-258	This lab
AN1217-17	*AN1217.2::pyrG*	2-258	This lab
AN7170-1	*AN7170.2::pyrG*	2-258	This lab
AN7170-4	*AN7170.2::pyrG*	2-258	This lab
AN7736-4	*AN7736.2::pyrG*	2-258	This lab
AN7736-7	*AN7736.2::pyrG*	2-258	This lab
AN3147-3	*AN3147.2::pyrG*	2-258	This lab
AN3147-10	*AN3147.2::pyrG*	2-258	This lab
AN3147-3C15	*pyrG::AN3147.2-pyroA*	AN3147-3	This lab
AN10631-5	*AN10631.2::pyrG*	2-258	This lab
AN10631-8	*AN10631.2::pyrG*	2-258	This lab
2-258	*pyrG89*$^{-}$*,pyroA4,nkuA::argB, veA*$^{+}$	n/a	O'Bayram

Appendix 8 List of primers used in construction of gene knock-out cassettes

Primer name	Oligo-nucluetides (5' to 3 ')
AN1217 5'F	GTAACGCCAGGGTTTTCCCAGTCACGACGCAGTGGACACTGCTACTGAG
AN1217 3'R	GCGGATAACAATTTCACACAGGAAACAGCGGAAGAATCAGTCTAGGACG
AN3147 5'F	GTAACGCCAGGGTTTTCCCAGTCACGACGGGTACTTGACAGGTCTTCCT
AN3147 3'R	GCGGATAACAATTTCACACAGGAAACAGCCAGGAGTATGTGGGAGAAGT
AN4632 5'F	GTAACGCCAGGGTTTTCCCAGTCACGACGCACTAGAGCGGATACTGACA
AN4632 3'R	GCGGATAACAATTTCACACAGGAAACAGCATACTGTGTACGAGAGGCTG
AN4813 5'F	GTAACGCCAGGGTTTTCCCAGTCACGACGGTCGGTATGTATCTCCGTTC
AN4813 3'R	GCGGATAACAATTTCACACAGGAAACAGCCTGGATCTATGACGACTGTG
AN4891 5'F	GTAACGCCAGGGTTTTCCCAGTCACGACGACTGAAGTGGGAGTGTCTGT
AN4891 3'R	GCGGATAACAATTTCACACAGGAAACAGCCTACGTACTTATTCCCCAGC
AN7736 5'F	GTAACGCCAGGGTTTTCCCAGTCACGACGCCGTAGTCGGACTTAGAACT
AN7736 3'R	GCGGATAACAATTTCACACAGGAAACAGCCTGCTGTCCGGTACTCTTAT
AN10631 5'F	GTAACGCCAGGGTTTTCCCAGTCACGACGGTAGCCTGTTGTATGCAGTC
AN10631 3'R	GCGGATAACAATTTCACACAGGAAACAGCGCTGGTAGGGTTAGAAGTTG
AN2701 P1	AGCTGGTGGACTTGGAACC
AN2701 P2	ATCCACTTAACGTTACTGAAATCCAGGAGGTAGGCCAATAACG
AN2701 P3	CTCCTTCAATATCATCTTCTGTCGACTGCCTTTTGCTACTCACG
AN2701 P4	AAGCGGCTCAATCTCGTAGC
AN2701 P5	AAGAAGAACACTGCCAGTCC
AN2701 P6	CGCACCCTGAATGGTTAGTC
AN6611 P1	TACGTTATTGGTGCCACTCG
AN6611 P2	ATCCACTTAACGTTACTGAAATCCAGGTAAAGTGCCTCGAACG
AN6611 P3	CTCCTTCAATATCATCTTCTGTCTTTCTTTCCCGCTAAACAAGC
AN6611 P4	GAATCATTGCCAAGCCAGTC
AN6611 P5	AGTCACGGCTTTTCTGAGGA
AN6611 P6	GTACTCAACCTCCCCGACAC
AN7170 P1	GAGGCAACTGGGCTAACTAGG
AN7170 P2	ATCCACTTAACGTTACTGAAATCGCGAGAGCCAGAGAGTTAGG
AN7170 P3	CTCCTTCAATATCATCTTCTGTCGTCTGGCGTTTGAGGTTTTC
AN7170 P4	GTATGTTTGGAGGGGTCAGG
AN7170 P5	TTCCGTCCAGAAAAGACGAG
AN7170 P6	GCGATTATCGACGCTAAGATG

Appendix 9 List of primers used in verification of transformant strains

Primer name	Oligo-nucluetides (5' to 3 ')
AN2701 vFw	TCAGAGCATGTTTCCTGTCG
AN2701 vRv	GCAACGGTACACACTTCACG
AN3147 vFw	GGAGCGGAACAGTGCTAATC
AN3147 vRv	ATGTTGCTTGAGGGTTTTGC
AN4632 vFw	AGCCCGTCAAATACTGATGC
AN4632 vRv	AGGTACGGTTTTTGCATTCG
AN4813 vFw	CAACAAAGCGCTGTTAGACG
AN4813 vRv	TCATATTCCGAGCTCGATCC
AN6611 vFw	ACGGATCGTGACGAATTAGG
AN6611 vRv	GGGACTTGCGACTTGAAGAG
AN7170 vFw	CTTTCTCGCCCAACAACTTC
AN7170 vRv	GTAGCCGCTCATTCATTTCC
AN7736 vFw	ATCAGCCCATAACCGTTGAG
AN7736 vRv	GAGAGCAGGATGCGTAAACC
AN10631 vFw	TGCTCCACCATGATACAACC
AN10631 vRv	CTTGCGACTCATTCCTGATG
AN7336 vFw	ATCAGCCCATAACCGTTGAG
AN7336 vRv	GAGAGCAGGATGCGTAAACC
AN0164 vFw	TGGTTCGTTCCAGCATACCT
AN0164 vRv	GCTCCAAACCGTACTCAACC
AN1217 vFw	ACCCGCAGTGAATCTAATCG
AN1217 vRv	TCACAGTGCCGTAGTTCTGG
AN4891 vFw	TCGAGATCACGTTTGAGTGC
AN4891 vRv	CTGGTCACTCTGGGCTTTTC
pryG v5Rv for up	GAAGTAGCCGAGCAATGAGG
pryG v3Fw for dn	ACGAGTGTTGTGGAGGAAGG
AN3147 PvU	GTGCATGTCTTGCAGATTGG
AN3147 PvD	CCGTCAAGTCCTCGTAGTGG
AN4632 PvU	GGTGACAGTTCCTGCAATCC
AN4632 PvD	CGGCTAGAGTTCTGGCAGTC
AN4813 PvU	GGAGAAAGAGCACGAGCAAC
AN4813 PvD	CACCTCCTGCTTTTCCATTC
AN7736 PvU	CGTGTGAGACCTTGTGCATC
AN7736 PvD	TCGCGGTGGTATTTCTCAAG
AN10631 PvU	TGGTCTCGTAGGTATCGTTCAG
AN10631 PvD	TTGAACGTTCGTCAAACCAC
AN0164 PvU	GAACATAGCTGCCTCAAGCC
AN0164 PvD	CGTCAATCGAAGCATTTCCT
AN1217 PvU	AGCACCACTCAGATGGATCC
AN1217 PvD	GTTGTGCGTACATTCCAAGC

Appendix 10 Primers used in construction of gene complementation plasmids

Primer name	Oligo-nucluetides (5' to 3 ')
pyroA_fwd-C	TGAATTCGAGCTCGGTACCCGGGTGCACCTGATAGGGACATC
pyroA-rev-C	GTCGACTCTAGAGGATCCCCGGGCACTGGACGTTGACATGAC
AN3147 up GoI-fwd	CCTCTAGAGTCGACCTGCAGGCATGCTCCTCATATTCGTGGGTCAAAAC
AN3147 up GoI-rev	TCTGATGTCCCTATCAGGTGCACCCGACTGCAGATGTGGCAAAAG
AN3147 dn-fwd	TTGGTCATGTCAACGTCCAGTGCCCTCCAACTCAACCAAACAGC
AN3147 dn-rev	ACCATGATTACGCCAAGCTTGCATGCCCACCCTGATTATGCGAG
AN0164 up GoI-fwd	CCTCTAGAGTCGACCTGCAGGCATGCCTGAGGCAGGAGATGAGG
AN0164 up GoI-rev	TCTGATGTCCCTATCAGGTGCACCCGTTTGGAAGACGTGTTTGG
AN0164 dn-fwd	TTGGTCATGTCAACGTCCAGTGCCCGCCAAACACGTCTTCCAAAC
AN0164 dn-rev	ACCATGATTACGCCAAGCTTGCATGCTCTCACAAACCCACACCAAG
AN4632 up GoI fwd	GCCAGTGAATTCGAGCTCGGTACCCGGGGGGAGCTCACTTTTGTCG
AN4632 up GoI rev	TCTGATGTCCCTATCAGGTGCACCCTACACAAAGGCTGGGCAC
AN4632 dn-fwd	TTGGTCATGTCAACGTCCAGTGCCCCATGGCTCTGTTATCTGCTC
AN4632 dn-rev	TGCAGGTCGACTCTAGAGGATCCCCGGGTTGCTTTCACTTCCCGATTC
AN4813 up GoI-fwd	GCCAGTGAATTCGAGCTCGGTACCCGGGGGTGGAATGATCTCCTTGTTG
AN4813 up GoI-rev	TCTGATGTCCCTATCAGGTGCACCCCTACTCTACTCGCCTGCC
AN4813 dn-fwd	TTGGTCATGTCAACGTCCAGTGCCCTTGGTTCTTCCGCTATTCTTTC
AN4813 dn-rev	TGCAGGTCGACTCTAGAGGATCCCCGGGCCTGAGTCTGCCTACAGC
AN3147 PvD	CCGTCAAGTCCTCGTAGTGG
AN4813 PvD	CACCTCCTGCTTTTCCATTC
AN4632 PvD	CGGCTAGAGTTCTGGCAGTC
AN0164 PvD	CGTCAATCGAAGCATTTCCT
pyroA 5‘F	AGATTGAGCTGCGTGCCTAC
pyroA 3’R	GTGTCCGATACGAGCTTTGG

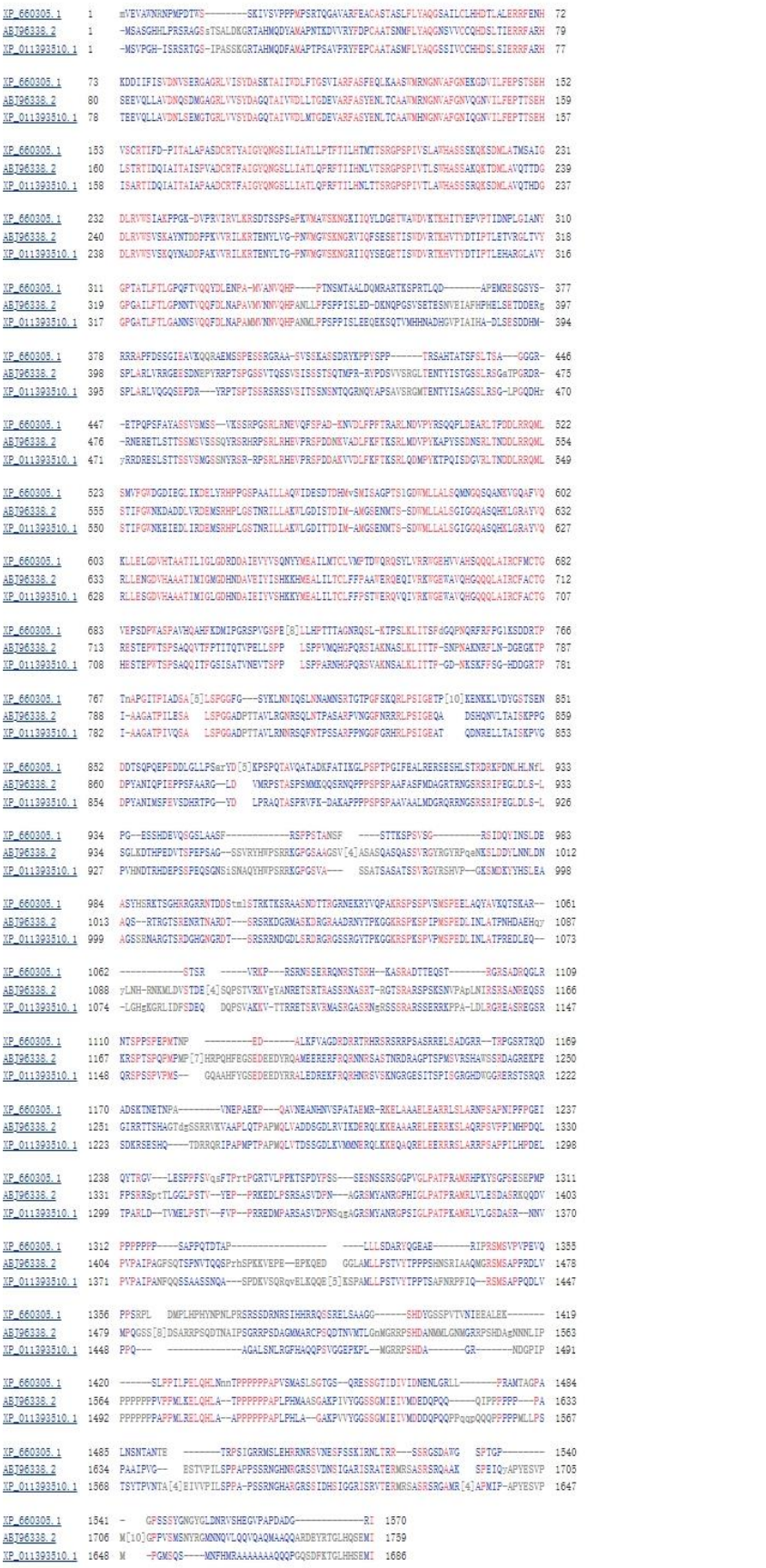

Appendix 11. Alignment of amino acid sequences between *AN2701.2* (XP660305.1), *idc-1(*XP_011393510.1*)* and *ham-5 (*ABJ96338.2*).* Highly

conserved residues are marked in red, while lower conserved residues are marked in blue. The alignment was analyzed via the Constraint-based Multiple Alignment Tool (COBAL; https://www.ncbi.nlm.nih.gov/tools/cobalt/cobalt.cgi?CMD=Web).

Appendix 12. Alignment of amino acid sequences between *AN0164.2* (XP657768.1), PP2Ac unit of *P.anserina* (XP_003437272.1), *S.macropsora* (XP_003346505.1) and *N.crassa* (XP_962270.2). Highly conserved residues are marked in red, while the lower conserved residues are marked in blue.

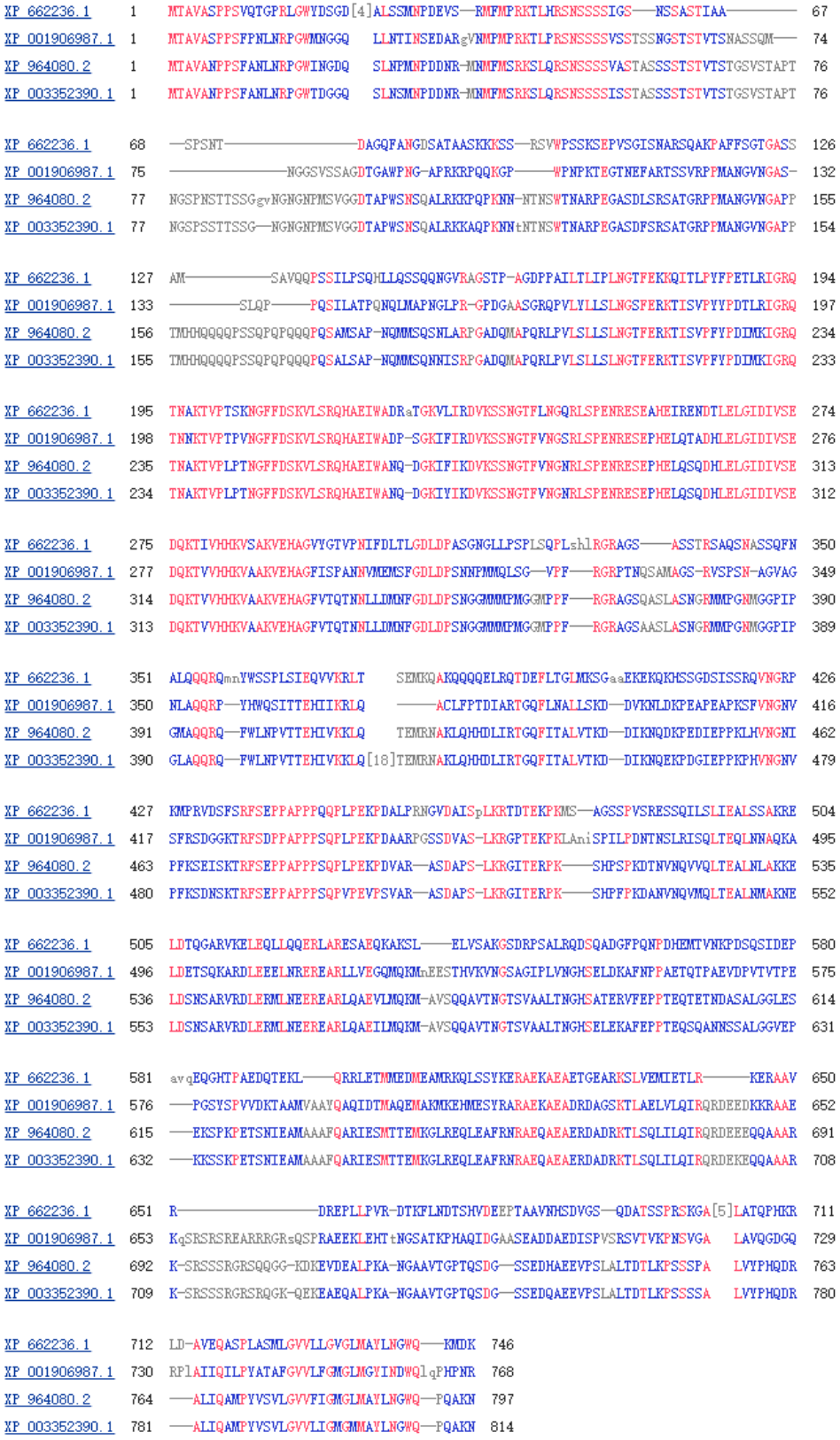

Appendix 13. Alignment of amino acid sequences between *AN4632.2* (XP_662236.1), *P.anserian* (XP_001906987.1), *N.crassa* (XP_964080.2) and

***S.macrospora* (XP_003352390.1).** Highly conserved residues are marked in red, while lower conserved residues are marked in blue.

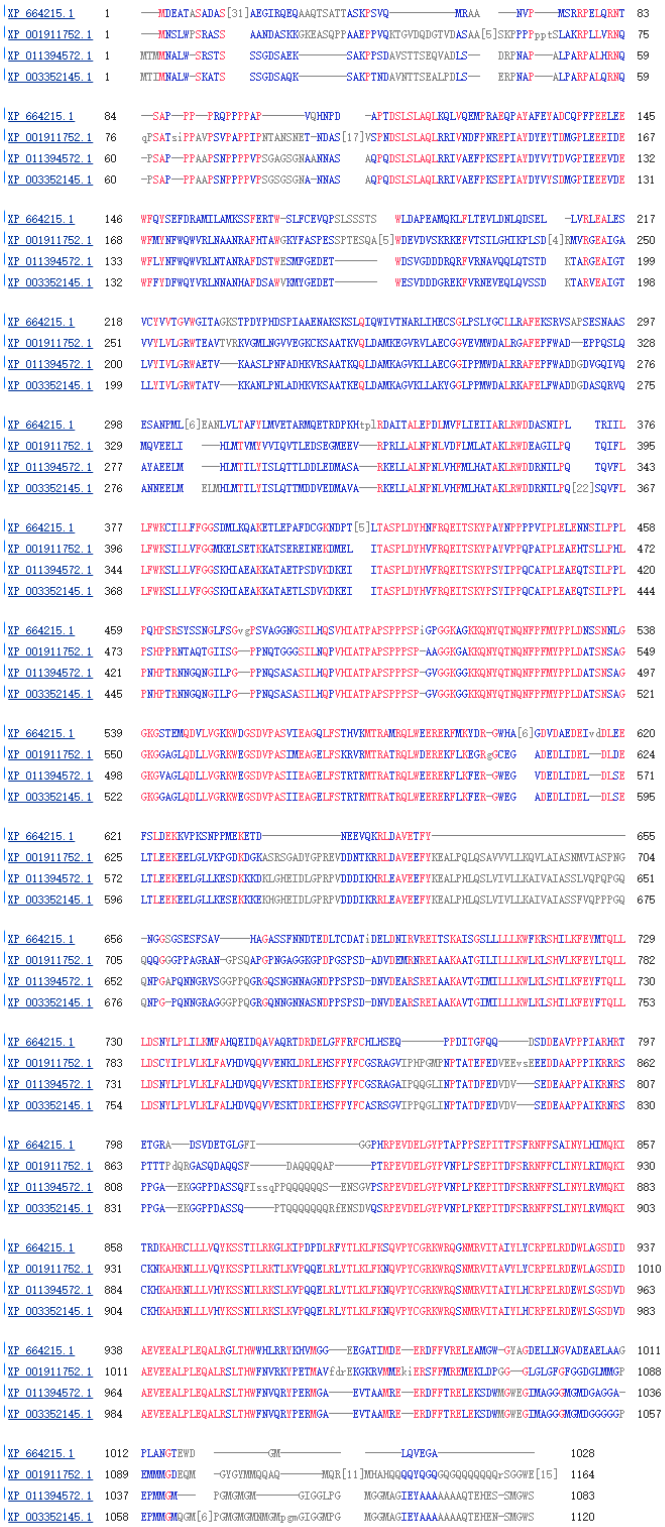

Appendix 14. Alignment of animo acid sequences between *AN6611.2* (XP_662236.1), *P.anserina* (XP_001911752.1), *N.crassa ham2* (XP_011394572.1) and *S.macropsora pro22* (XP_003352145.1). Highly

conserved residues are marked in red, while lower conserved residues are marked in blue.

Appendix 15. Alignment of amino acid sequences between *A. fumigatus mybA* (XP_754899.2) and *AN4813.2 (*XP_662417.1 *).* Highly conserved residues are marked in red, while lower conserved residues are marked in blue.

Appendix 16. Alignment of amino acid sequences between *AN1271.2* (XP_658821.1) and *A.flavus hxb1 (*XP_002380469.1 *).* Highly conserved residues are marked in red, while lower conserved residues are marked in blue.

Appendix 17 Alignment of amino acid sequences between *AN7170.2* (XP_664774.1) and *A.oryzea sclR (*XP_001825886.1*)* Highly conserved residues are marked in red, while lower conserved residues are marked in blue.

Appendix 18. Alignment of amino acid sequences between *AN7736.2* (EAA61251.1) and *Trire2:59600 (*XP_006964350.1*).* Highly conserved residues are marked in red, while lower conserved residues are marked in blue.

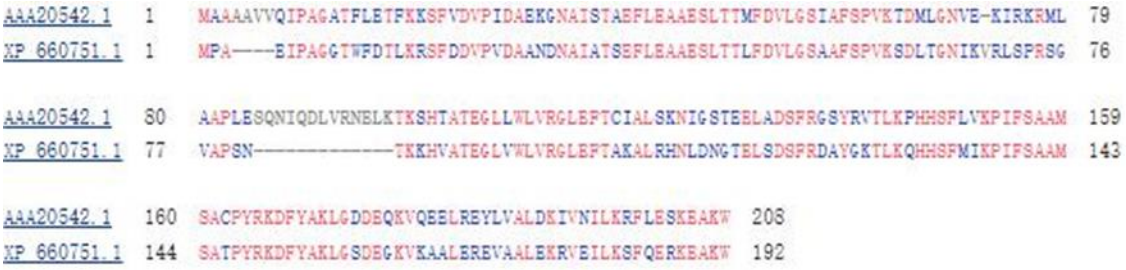

Appendix 19 The alignment of amino acid sequences between *AN3147.2 (*XP_660751.1*)* and *het-c2* (AAA20542.1). Highly conserved residues are marked in red, while lower conserved residues are marked in blue.

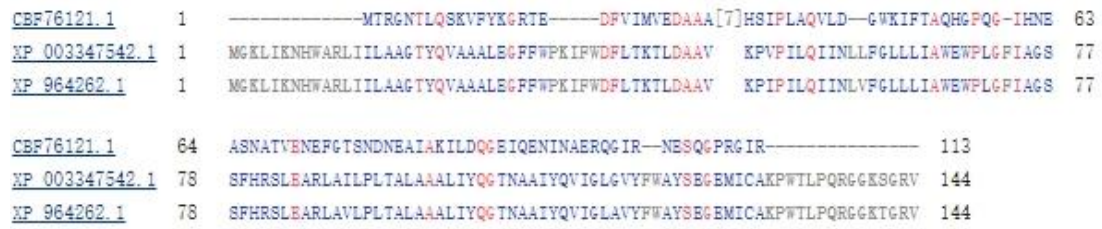

Appendix 20. The alignment of amino acid sequences between *AN10631.2 (*CBF76121.1*), S.macrospora pro41 (XP_0033475742.1)* and *N.crassa* (XP_964262.1) Highly conserved residues are marked in red, while the lower conserved residues are marked in blue.

Appendix 21. Alignment of amino acid sequences between *AN4891.2 (*XP_662495.1*), S.macrospora asf-1 (XP_003345657.1)* and *N.crassa* (XP_958588.1) Highly conserved residues are marked in red, while lower conserved residues are marked in blue.

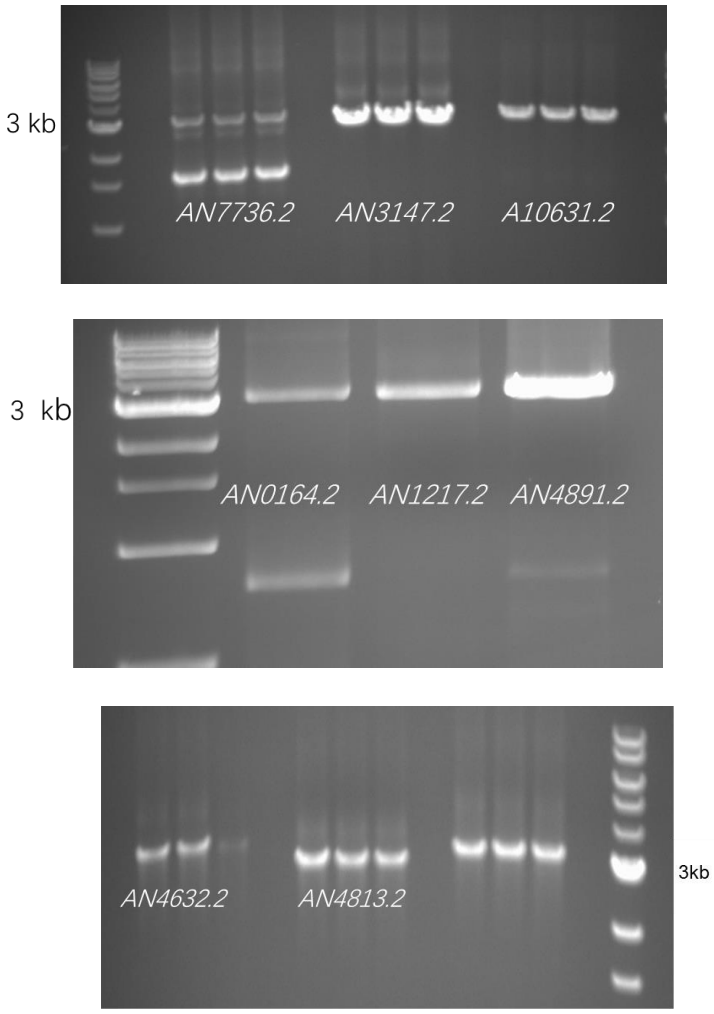

Appendix 22 The amplification of the deletion cassettes of *AN7736.2, AN3147.2, AN10631.2, AN0164.2, AN1217.2, AN4891.2 and AN4813.2* (approx. size 3.5 kb for each fragment).

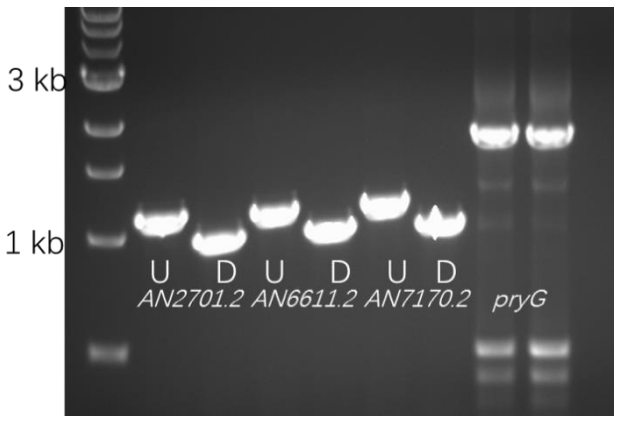

Appendix 23 PCR amplification of the upstream and downstream fragments of *AN2701.2, AN6611.2* and *AN7170.2* (approx. size 1kb of each fragment) and the selectable *pryG* marker (approx.size 1.8 kb).

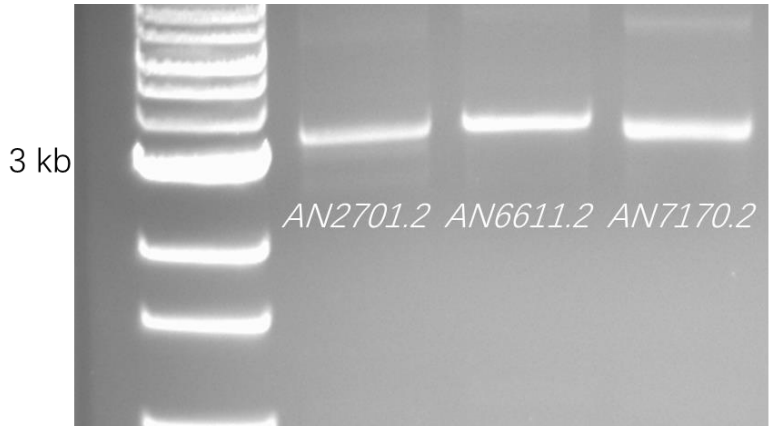

Appendix 24 PCR amplification of the deletion cassettes of *AN2701.2, AN6611.2 and AN7170.2* (approx. size 3.5 kb of each fragment).

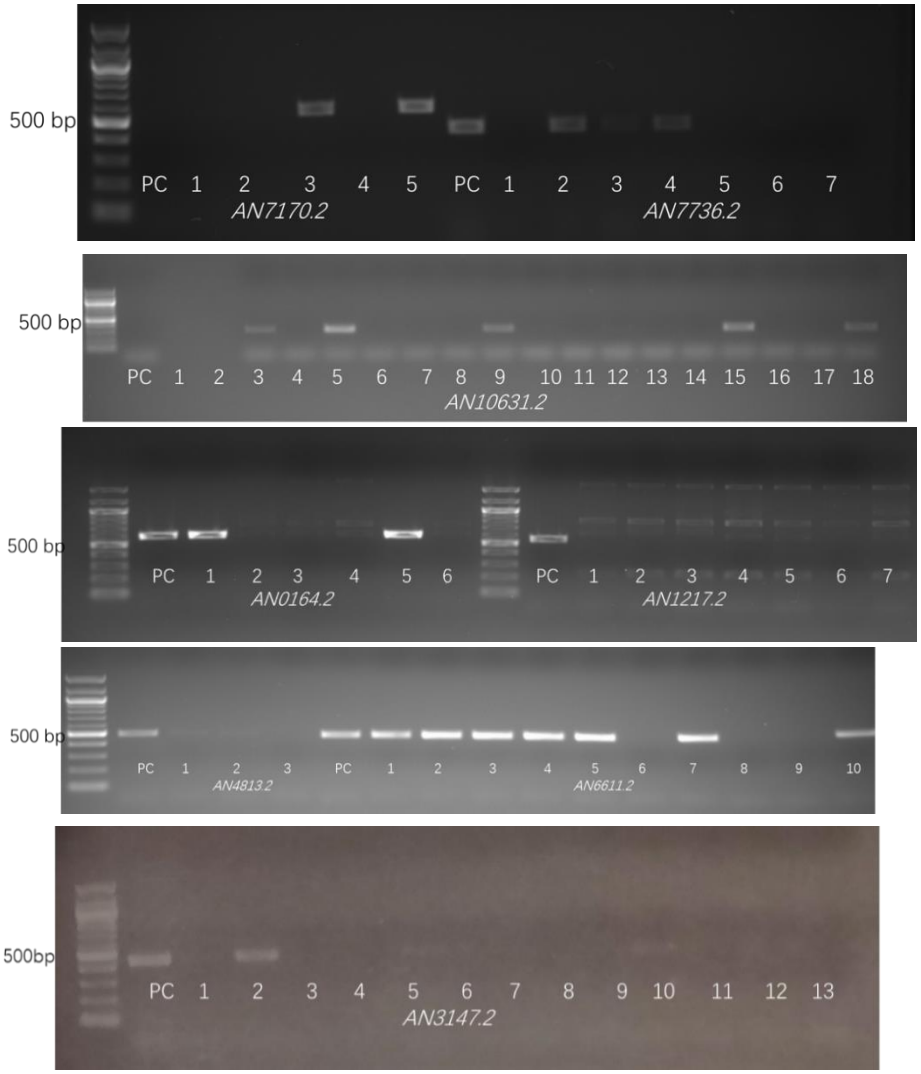

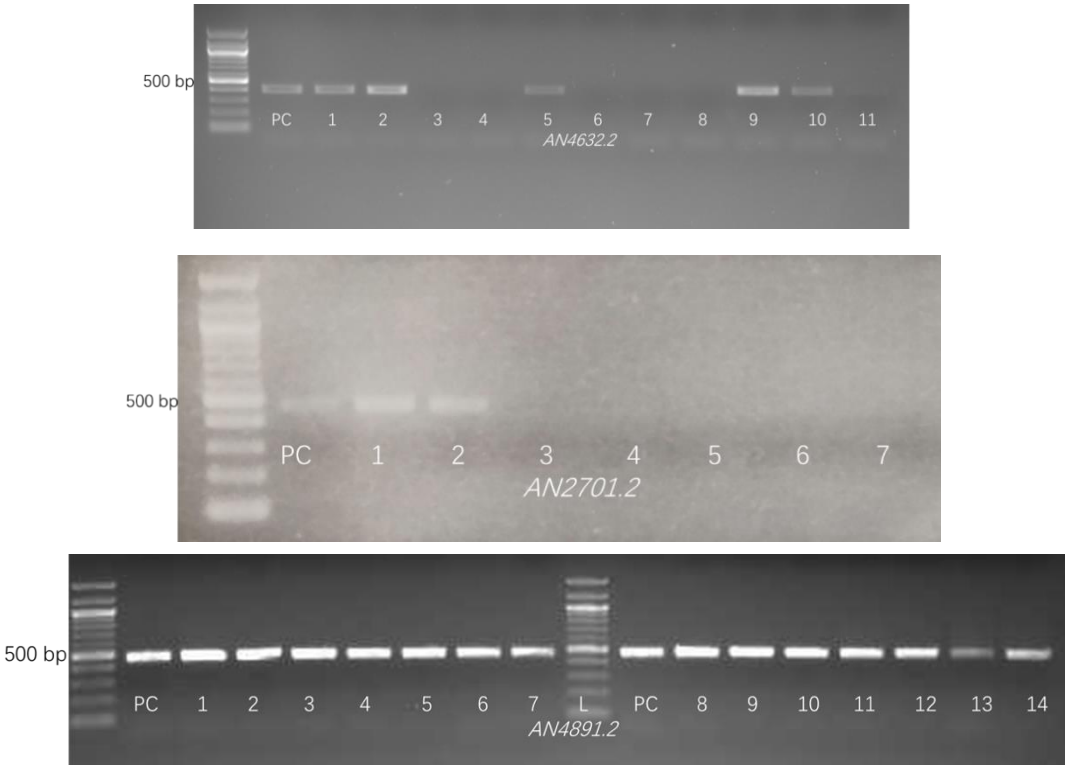

Appendix 25 Verification of knock-out of genes of interest. See annotation on individual gels for the gene being screened. PC indicates positive (parental) control (with an average fragment size of approx. 500 bp).The absence of a band in the numbered transformants indicates replacement of the target genes where as presence of a gene product suggests ectopic transformation.

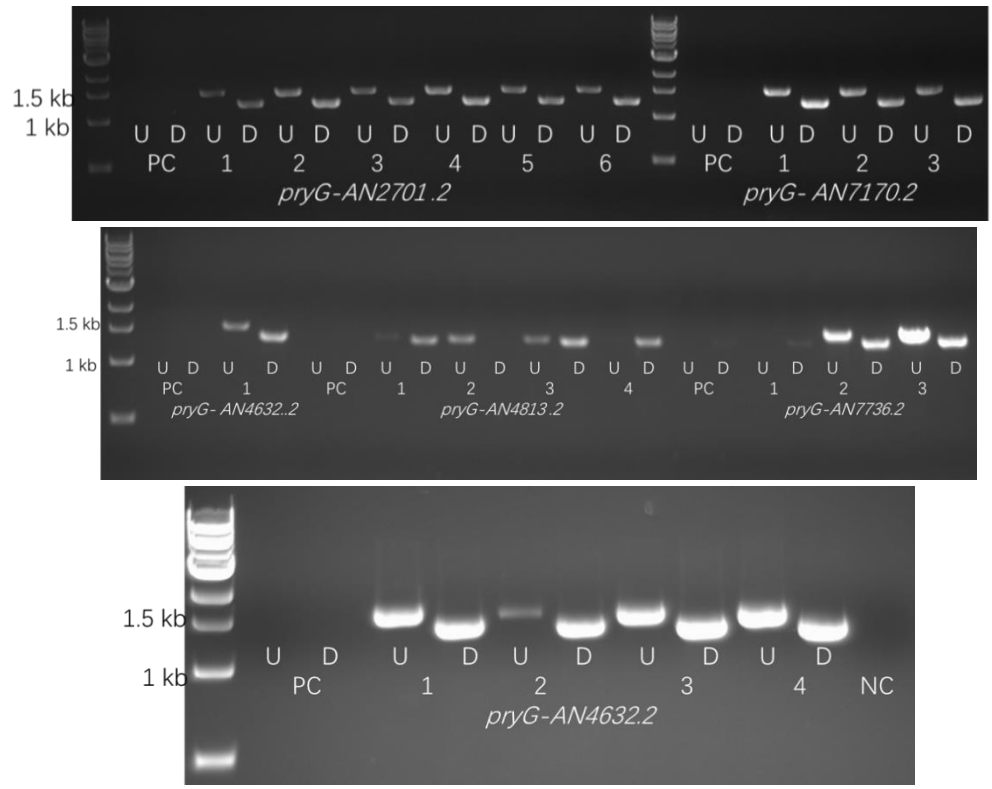

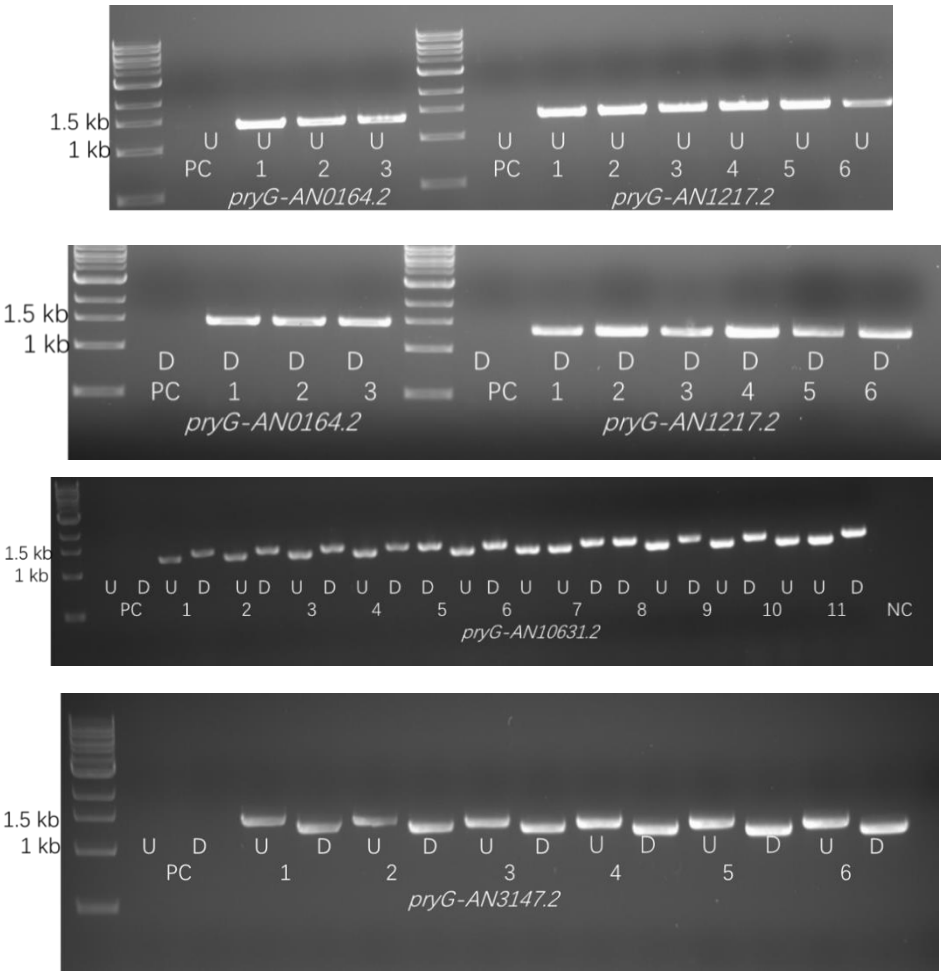

Appendix 26 Verification of integration of *pyrG* at the correct target locus according to positional PCR diagnostics. The letter U indicates a fragment produced with primers sets designed from the upstream flanking region of the target gene and the internal *pyrG,* and the letter D indicates a fragment produced with primets sets designed from the internal *pryG* and the downstream flanking region of the target gene. Diagnostic fragments were all designed to be approx. 1-1.5 kb in size.

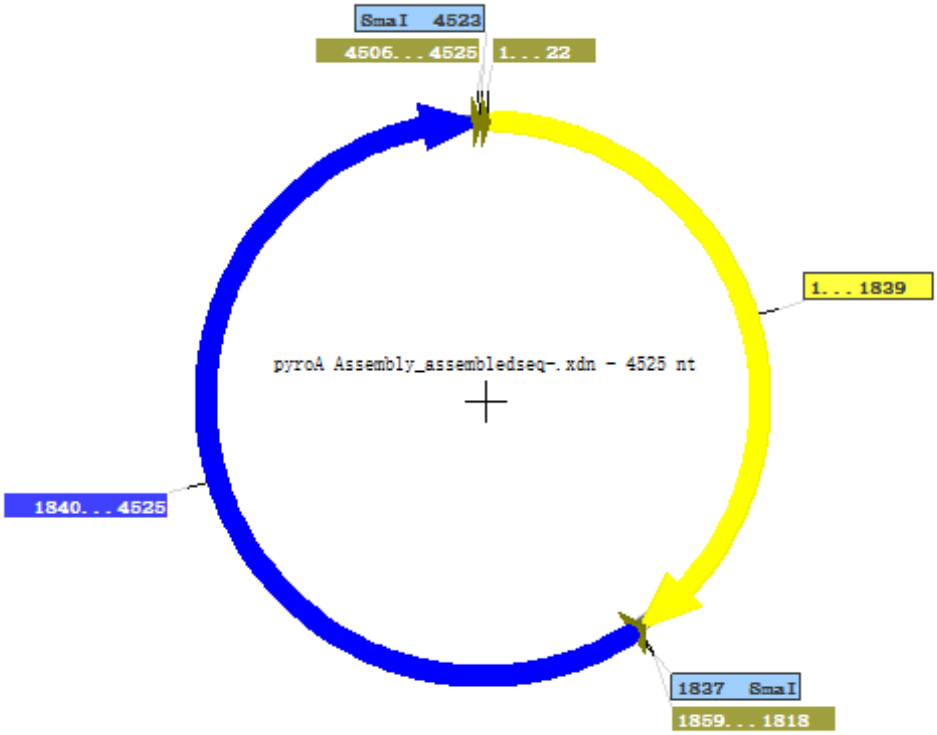
SmaI 4523
4506...4525
1...22
1...1839
pyroA Assembly_assembledseq-.xdn - 4525 nt
1840...4525
1837 SmaI
1859...1818

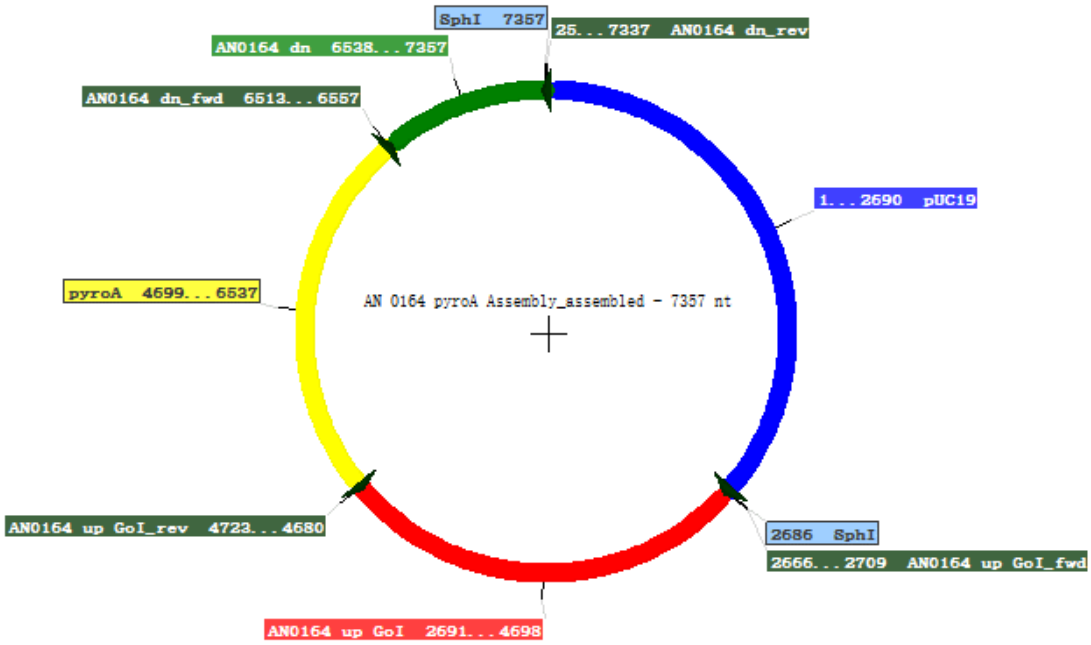
SphI 7357
25...7337 AN0164 dn_rev
AN0164 dn 6538...7357
AN0164 dn_fwd 6513...6557
1...2690 pUC19
pyroA 4699...6537
AN 0164 pyroA Assembly_assembled - 7357 nt
AN0164 up GoI_rev 4723...4680
2686 SphI
2666...2709 AN0164 up GoI_fwd
AN0164 up GoI 2691...4698

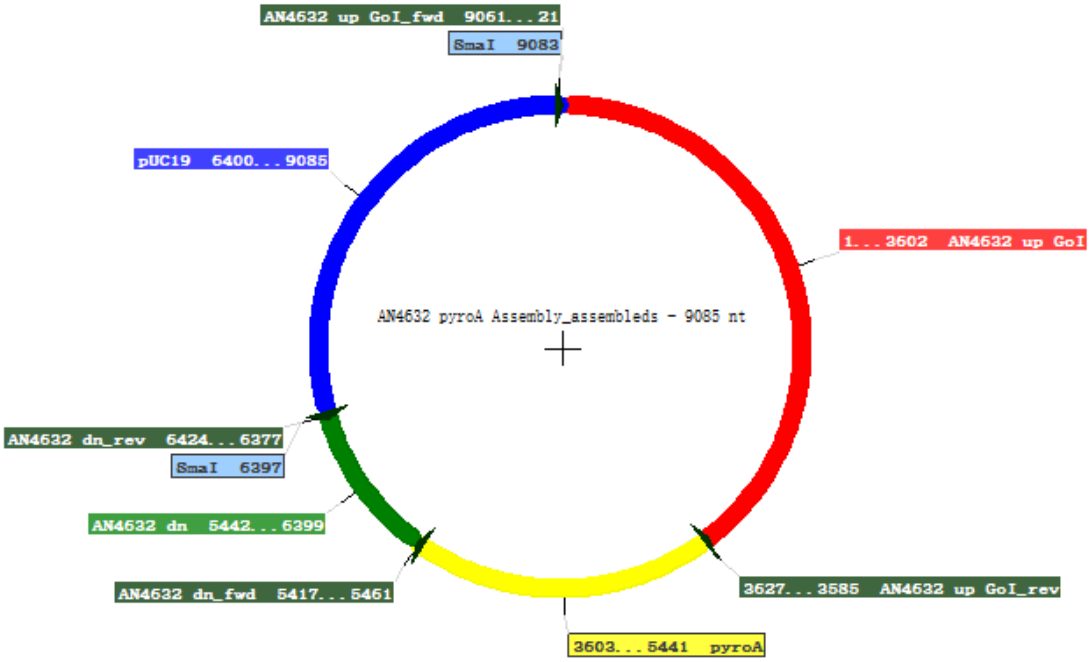
AN4632 up GoI_fwd 9061...21
SmaI 9083
pUC19 6400...9085
1...3602 AN4632 up GoI
AN4632 pyroA Assembly_assembleds - 9085 nt
AN4632 dn_rev 6424...6377
SmaI 6397
AN4632 dn 5442...6399
AN4632 dn_fwd 5417...5461
3627...3585 AN4632 up GoI_rev
3603...5441 pyroA

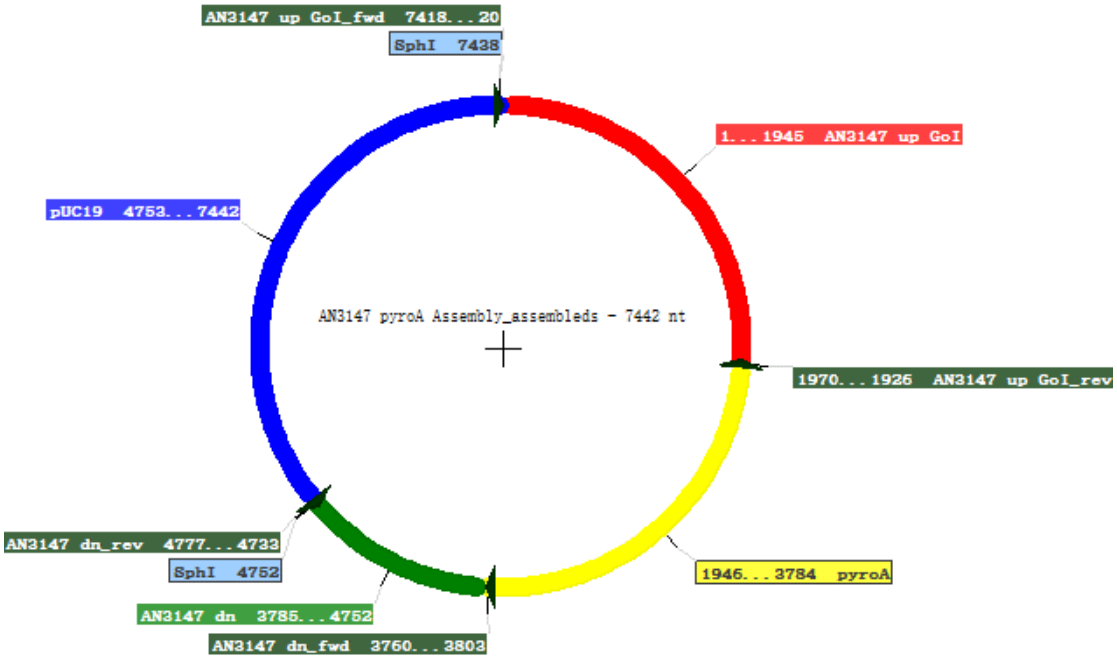
AN3147 up GoI_fwd 7418...20
SphI 7438
1...1945 AN3147 up GoI
pUC19 4753...7442
AN3147 pyroA Assembly_assembleds - 7442 nt
1970...1926 AN3147 up GoI_rev
AN3147 dn_rev 4777...4733
SphI 4752
1946...3784 pyroA
AN3147 dn 3785...4752
AN3147 dn_fwd 3760...3803

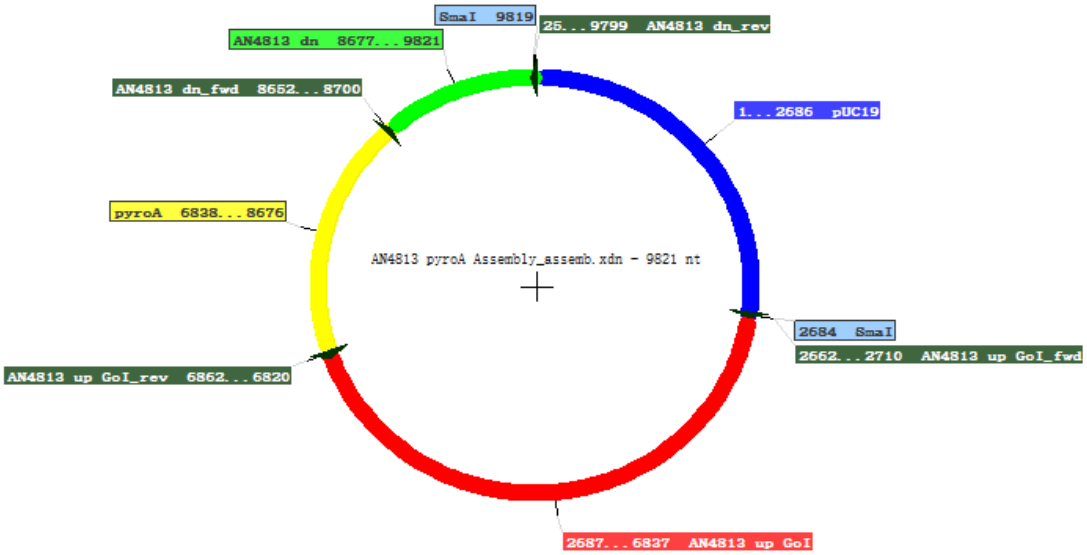

Appenix 27 Construction of the complementation plasmid of the gene of interest *in silica*. The blue line indicates the fragment of the vector pUC19. The red line indicates the upsteam flanking region and the ORF region of the target gene. The yellow line indicates the selectable marker *pyroA*. The green line indicates the downstream flanking region of the target gene.

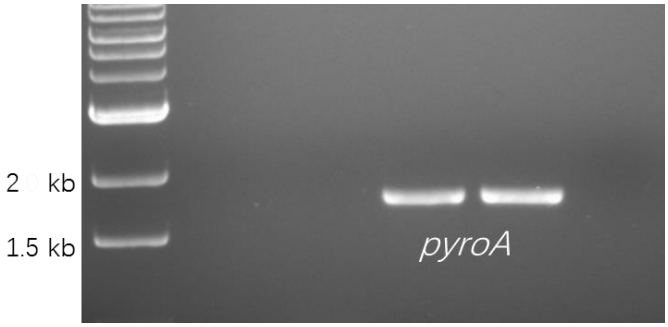

Appendix 28 Amplification of selectable marker *pyroA*. The approx. size was 1.8 kb.

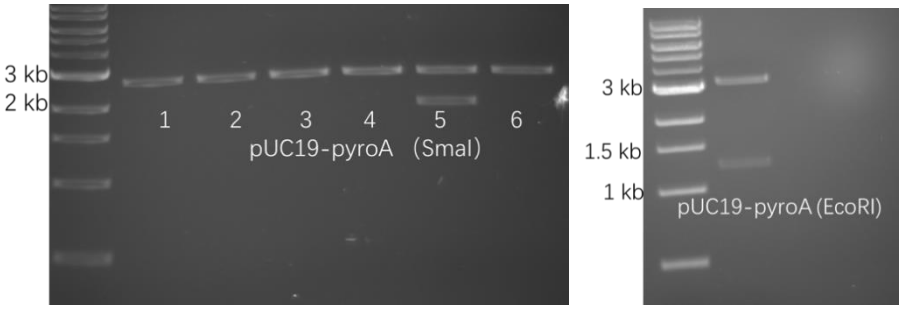

Appendix 29 Selection of the complementation plasmids. The pUC19-pyroA plasmids were digested with *Sma*I and *EcoR*I, and the complementation cassettes were approx. 4.5 kb.

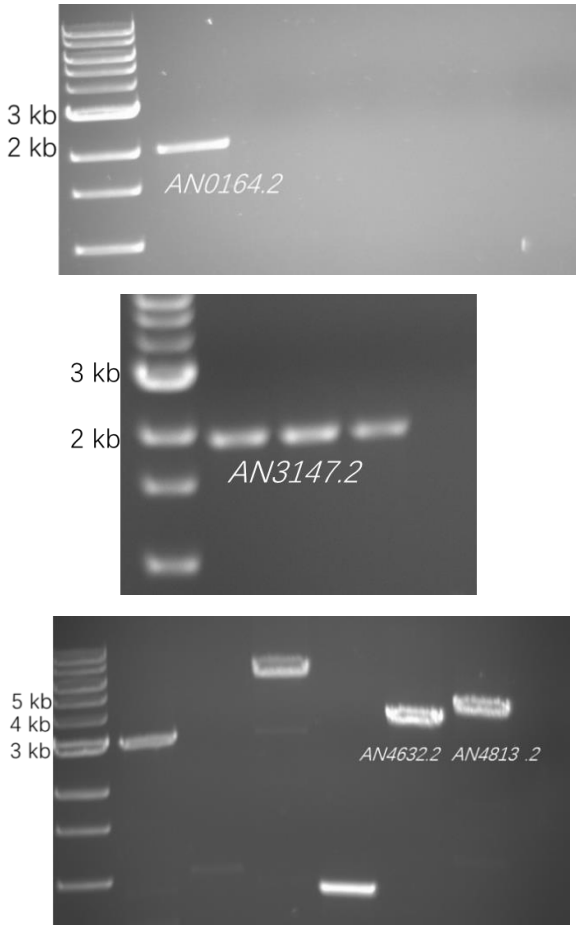

Appendix 30 Amplification of the fragments of the upstream flanking region and the ORF region of the target genes. The approx. sizes of *AN0164.2* and *AN3147.2* was 2.0 kb, resprectively. The approx. size of *AN4632.2* was 3.6 kb. The approx. size of *AN4813.2* was 4.2 kb.

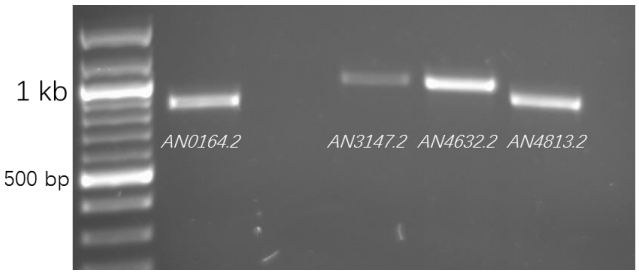

Appendix 31 Amplification of the fragments of the down region of the target genes. The approx. size of each fragment was 1.0 kb.

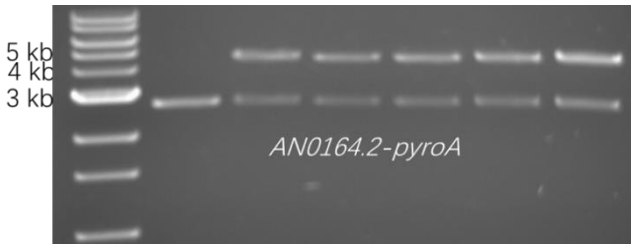

Appendix 32 The selection of the complementation plasmids. The pUC19-AN0164-pyroA plasmids were digested with *Sma*I, and the complementation cassettes were approx. 4.6 kb.

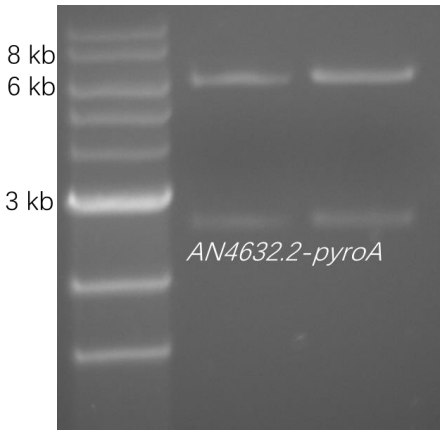

Appendix 33 Selection of the complementation plasmids. The pUC19-AN4632-pyroA plasmids were digested with *Sph*I, and the complementation cassettes were approx. 6.4 kb.

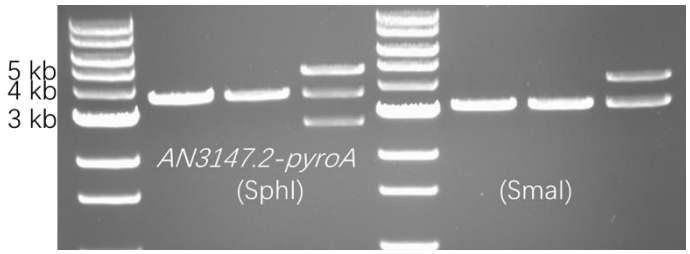

Appendix 34 Selection of the complementation plasmids. The pUC19-AN3147-pyroA plasmids were digested with *Sph*I and *Sma*I, and the complementation cassettes were approx. 4.7 kb when digested with *Sph*I.

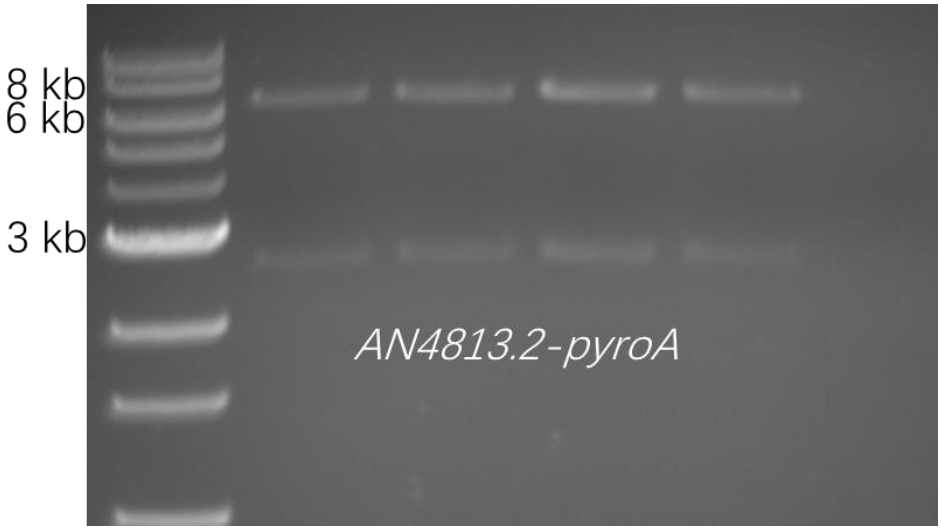

Appendix 35 Selection of the complementation plasmids. The pUC19-AN4813-pyroA plasmids were digested with *Sma*I, and the complementation cassettes were approx. 7.1 kb.

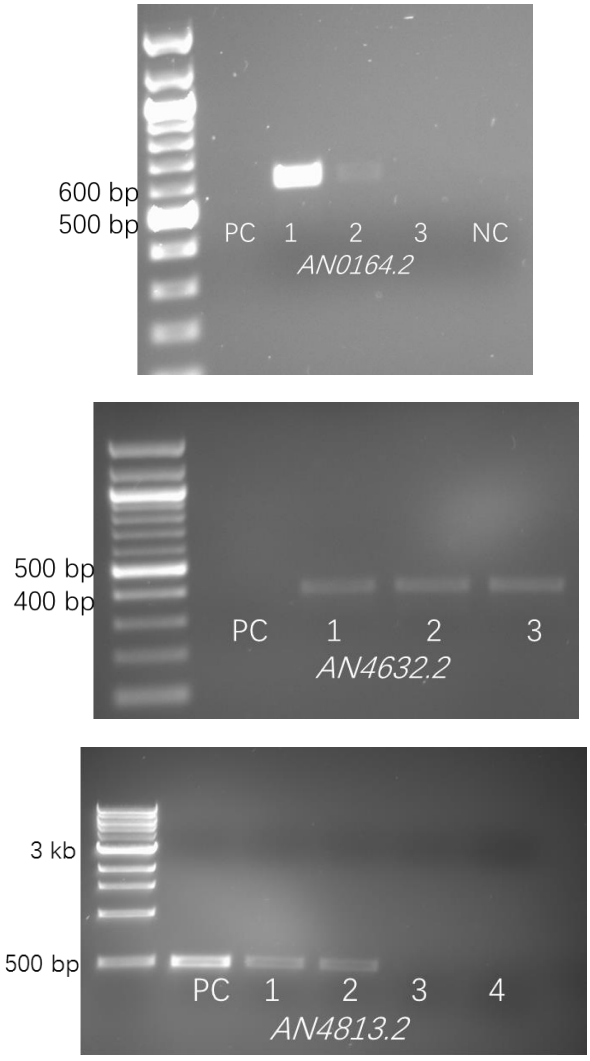

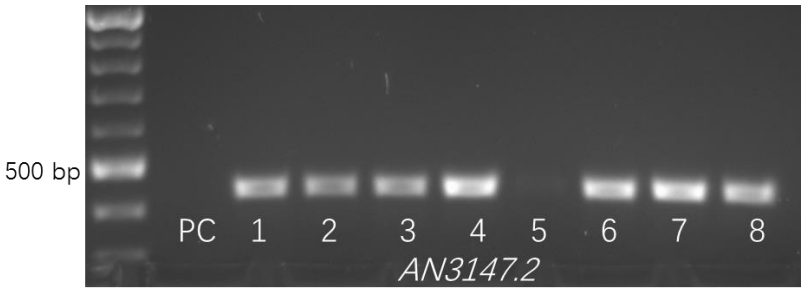

Appendix 36 Verification of the complementation of gene of interest. See annotation on individual gels for the gene being screened. PC indicates parental control with absence of a band. The presence of a band in the numbered complemented isolates indicates the reinsertion of the target genes (with an average size of approx. 500 bp).

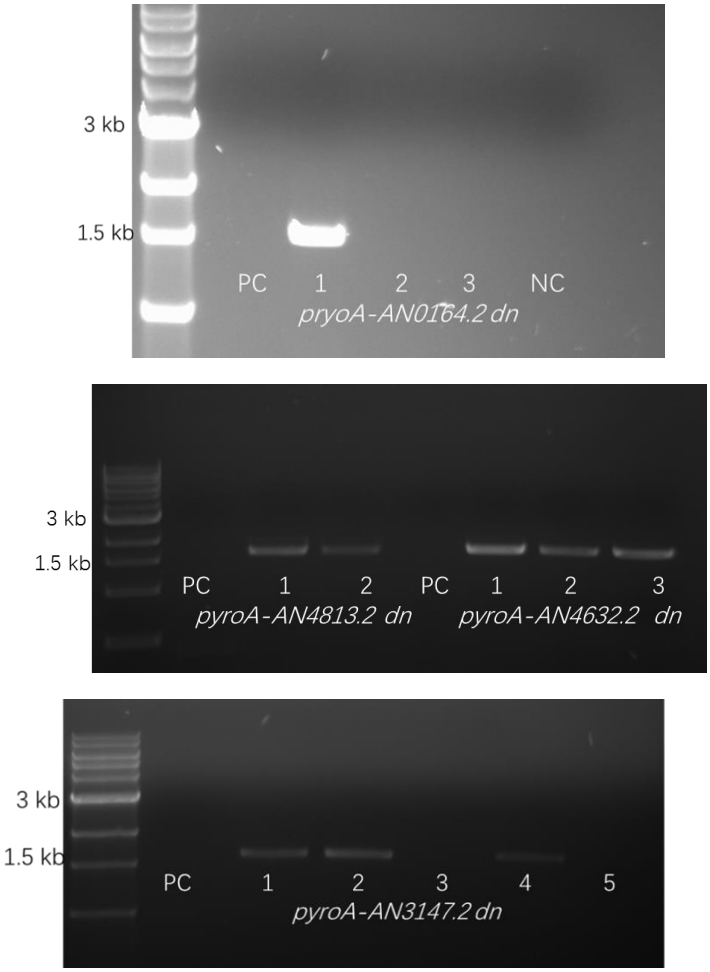

Appendix 37 Verification of the integration of the selectable *pyroA* marker at the correct target locus according to positional PCR diagnostics. See annotation on individual gels for the gene being screened. The letter dn indicates a fragment produced from the internal *pyroA* and the downstream flanking region of the target gene (with designed size to be approx. 1.5 kb). PC

indicates the parental control. Number indicates the screened complemented isolates. NC indicates negative control (genomic DNA minus).

Appendix 38 Primers used in the amplification of HMG gene deletion cassette in *A. fumigatus*

Primer	oligo-nucleotides (5' to 3')
AFUB042890 P1	AAGGCTCCAAAAGGAGGTTC
AFUB042890 P2	TAGTTCTGTTACCGAGCCGGACACCTTTTTGATGACCATGC
AFUB042890 P3	GCTCTGAACGATATGCTCCAACGTCAAAGGTTACCCGACAGC
AFUB042890 P4	TTCCCCTGTCTCATTCAAGC
AFUB042890 P5	CGTCGATAATTGGGAGTTGC
AFUB042890 P6	CAGGAGAACAGCCAAATTCC
AFUB069370_P1	ACTCTAGCCACTCAGTCCCA
AFUB069370_P2	TAGTTCTGTTACCGAGCCGGCTCGGAGGTGACGATGCTAC
AFUB069370 P3	GCTCTGAACGATATGCTCCAACCAGGCGCAGAGTCTAGTATGG
AFUB069730 P4	GAAGATTGGGGCTACTTTGC
AFUB069370_P5	TTAATGGCAACCCCCGGTTT
AFUB069730 P6	AGCTGACGATGTGTCCTGTG
AFUB067900_P1	GCTGTATGGCAGTCTTCGGT
AFUB067900_P2	TAGTTCTGTTACCGAGCCGGGATGGGCAGGAATAGGTCGG
AFUB067900_P3	GCTCTGAACGATATGCTCCAACTGGCTCAAACTGTCGTTTCT
AFUB067900_P4	GTTCGTTGCGCTTTCTCAGG
AFUB067900_P5	AGAACGAGGAGGGTGACTGA
AFUB067900_P6	TGTCCTGTCAGTGCATGGAC
AFUB042900_P1	GGGCAAAAGGACAAGCAGAG
AFUB042900_P2	TAGTTCTGTTACCGAGCCGGACGAGAGACAAGTGTAGACGT
AFUB042900_P3	GCTCTGAACGATATGCTCCAACCGGCGTCTCGAGTCTACTTC
AFUB042900_P4	CGAGCCATTGCGTCGATTTT
AFUB042900_P5	GCTGGTAGAGGGCAGTCTTG
AFUB042900_P6	GTCGTTGTGGATGGCTGGTA
AFUB009460 P1	TGCTTCCGTTCTCTCTCAGC
AFUB009460 P2	TAGTTCTGTTACCGAGCCGGGGACCTGGGTTGACACTACG
AFUB009460 P3	GCTCTGAACGATATGCTCCAACCAAACAAGCTGAAGAGGATCG
AFUB009460 P4	ACGAGTCGGGTGAATTTTGG
AFUB009460 P5	GGCTTCGAGGCCTAATCAC
AFUB009460 P6	AACCCATGATGAGACAGTCG
hph Fwd	CCGGCTCGGTAACAGAACTA
hph Rvs	GTTGGAGCATATCGTTCAGAGC
AFUB_037560 P5	CCATTTGCGAAACATTTCCT
AFUB_037560 P6	ACCAACTGGAAGGTCACAGC
AFUB_004890 P5	CACCAGTTGGTGATTGATCG
AFUB_004890 P6	TTGGGAATTAGGTGCATGGT

Appendix 39 Primers used in verification of HMG gene knock-out

Primer	oligo-nucleotides (5' to 3')
AFUB04890 vFw	GCTTTTGGAGAATGGATTGC
AFUB04890 vRV	AAGGCTTACCGGCCTTGTAG
AFUB09460 vFw	TGGAACCTCCCAAGAAACTG
AFUB09460 vRv	CGTAGCTGTCAGACCCTTCC
AFUB37560 vFw	GAAGAAGGGTACGTGGTTGC
AFUB37560 vRv	TCAGCACCGTTCATTTCAAG
AFUB42890 vFw	GTCGCAGGCTAAGTTTGTGG
AFUB42890 vRv	ATGAGATCGAACGCATTTGG
AFUB42900 vFw	AAGCACACCGGAAGTAATGG
AFUB42900 vRv	AAGGCTCCAAAAGGAGGTTC
AFUB67900 vFw	AGTACCCACCAAGGACATGC
AFUB67900 vRv	CATCACTCGACCACCACATC
AFUB69370 vFw	AGCAATGGTGAGTTGGAAGC
AFUB69370 vRv	GAACGAGTTCATGGGTCTGG
hph-vRv1_for_P1	CATCCACTGCACCTCAGAGC
hph-vFw2_for_P4	CTCCGGAGTTGAGACAAATGG
AFUB04890 PvU	GGTACAGAGCAGGGGGAATC
AFUB04890 PvD	GACGAGATGAGAGCCTGGAC
AFUB09460 PvU	GCTTTGGCAGACTGAGGAAC
AFUB09460 PvD	AACTGGGCACCAAAATTGAC
AFUB37560 PvU	GACGATACCTTGCCATCAGC
AFUB37560 PvD	CTCCGGAGTTGAGACAAATGG
AFUB42890 PvU	TGATGTCGCCACGAAAATTA
AFUB42890 PvD	CACGAAACTGAAACCCCAAC
AFUB42900 PvU	AGCCTTAAGAGGTGCGAATG
AFUB42900 PvD	TGCGGTTAGAGTGTGATTCG
AFUB67900 PvU	TTTCGCTGGATTTGGGTTAG
AFUB67900 PvD	TTCGTACCCAATTGCCTTTC
AFUB69370 PvU	CCAGGAATCAAAGCCATACG
AFUB69730 PvD	TGTATGCCCTCGAACAGGAC

Appendix 40 Primers used in construction of complementation plasmid and verification of complementation transformaion

Primer	oligo-nucleotides (5' to 3')
AFUB69370 up GoI fwd	CAGTGAATTCGAGCTCGGTACCCGCGGCCGCTGGCTTGATTTTCCCAGC
AFUB69370 up GoI rev	ACGCCGTCTGACTTTTGTGGTGAGCGCACCAGGAGACCAGAAG
AFUB69370 dn fwd	AATCTCGTACTCAACCCTCACTCGCTTCTTCTGGTCTCCTGGTG
AFUB69370 dn rev	CAGGTCGACTCTAGAGGATCCCCGCGGCCGCTTCTCCAGCTGACGATGTG

Appendix 41 Number of cleistothecia formed by wild type versus *Δku* strains of *A. fumigatus*.

	47-51X47-55	47-465X47-466
replicates	6	6
Minimum	3	162
maximum	835	1121
mean	363.5	441.0
SEM	127.6	150.4

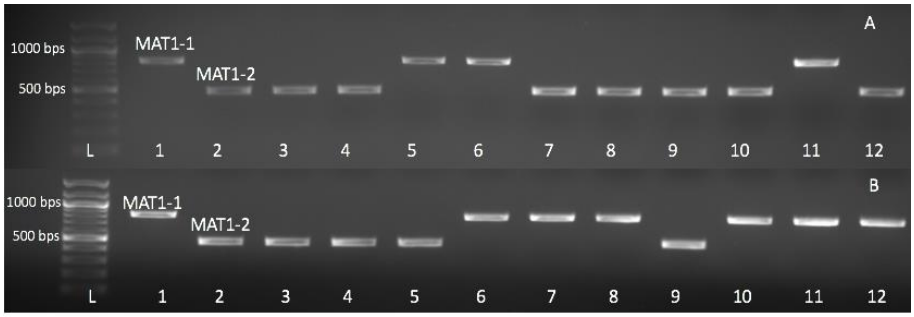

Appendix 42. **PCR assay to identify mating types of progeny of 47-51-Δ*nsdC* × wild-type strains crossing.** The lane1 and lane2 in **A** and **B** indicates *MAT1-1* strain 47-267 (834 bp) and *MAT1-2* strain 47-55 (438 bp), respectively. **A** presents the mating types of progenies from 47-51-Δ*nsdC*5 and 47-107 crossing. Strains determined in lane 4, 5, 6, 7 were selected and named as Δ*nsdC* x, Δ*nsdC* y, Δ*nsdC* z and Δ*nsdC* w. **B** presents the mating types of progenies from 47-51-Δ*nsdC*5 and 47-55 crossing. Strains determined in lane 5, 6, 9 and 10 were selected and named as Δ*nsdC* a, Δ*nsdC* b, Δ*nsdC* c and Δ*nsdC* d.

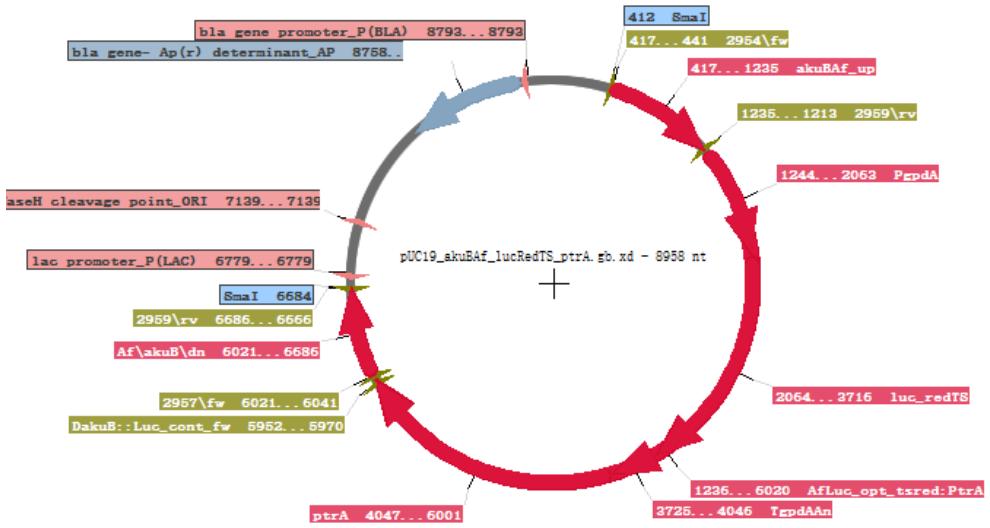

Appendix 43 The pUC19_akuBAf-lucRedTS_ptrA plasmid for deletion transformation in *A. fumigatus* strain 47-55. The rose line indicates the deletion cassette containing upstream flanking region of *kuB*, *LucRedTS, prtA* and downstream flanking region of *kuB*. The gray line indicates the fragment of the vector pUC19. The light blue line indicates selectable marker *Amp*.

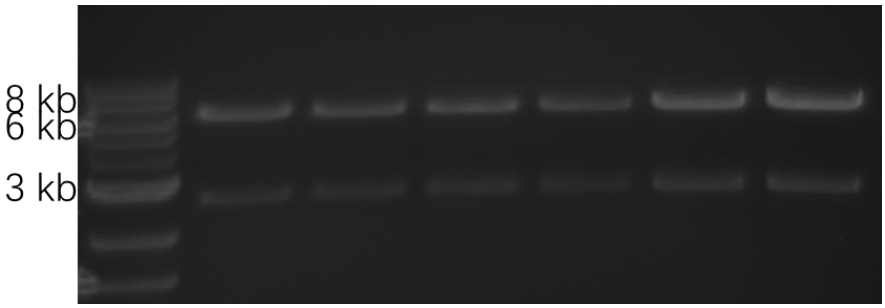

Appendix 44 The digestion of the transformation plasmid The pUC19_akuBAf-lucRedTS_ptrA plasmid. The plasmid was digested by *Sma*I, the *lucRedTS_ptrA* fragment gave size of approx. 6.2 kb.

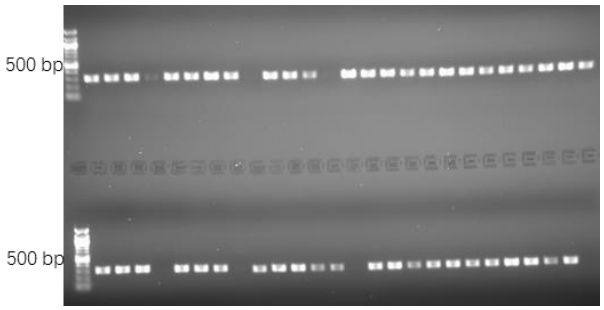

Appendix 45 Verification of *kuB* knock-out via colony PCR. The parental strain was 47-51 (MAT1-1). The presence of band (with approx. size 300 bp) indicates *kuB* fragment. The absence of band indicates the deletion of *kuB* in putative isolates.

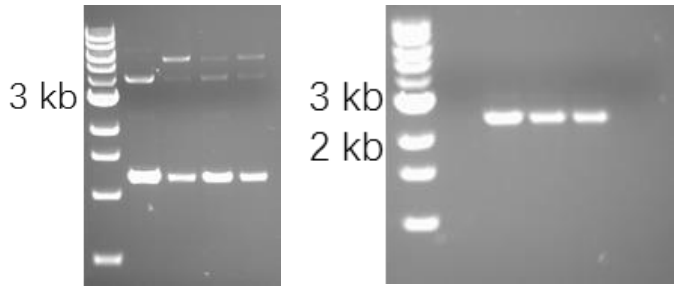

Appendix 46 Verification of intergaration of *prtA* at the correct target locus according to positional PCR diagnostics. The left image indicates the fragment produced with primers sets designed from the *kuB* upstream flanking region and the internal *ptrA* (with approx. size 5.5 kb). The right image indicates the fragment produced with primers sets designed from downstream flanking region *kuB* and the internal *ptrA* and the *kuB* downstream (with approx. size 1.6 kb).

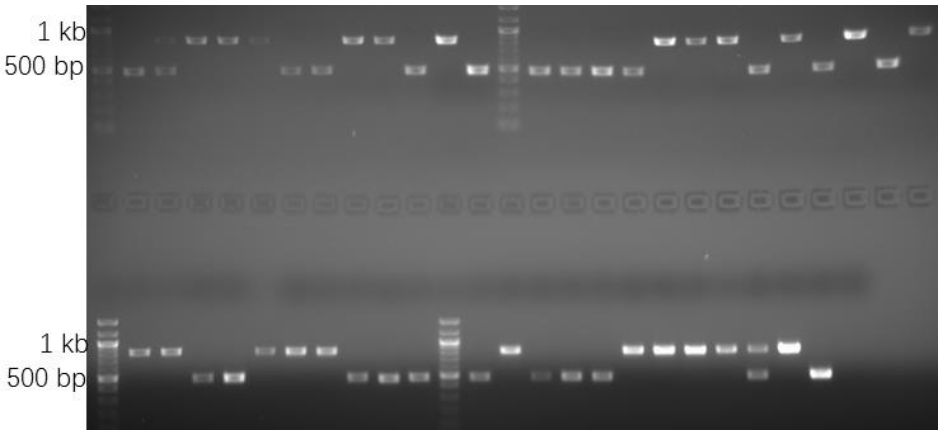

Appendix 47 The screen of the Δ*kuB* progenies from 47-51-Δ*kuB*8 and 47-55 crossing. The MAT1-1 progenies gave a size of approx. 834 bp, and the MAT1-2 progenies gave a size of approx. 438 bp.

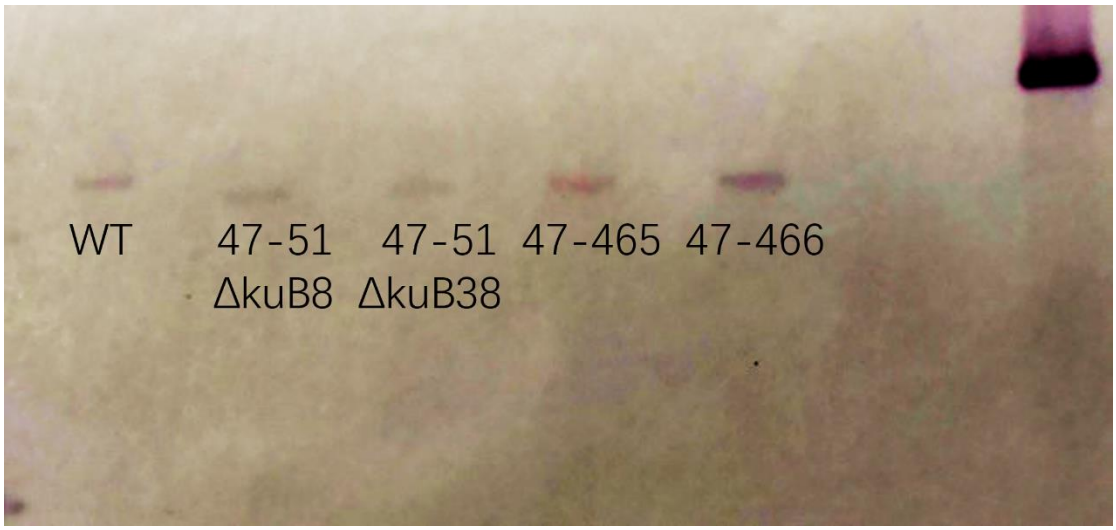

Appendix 48 Southern blotting of the Δ*kuB* strains. The genomic DNA of samples were digested with *Sac*II. The probe (approx. 1 kb in size) was

designed to bind the downstream flanking region of *kuB*. The *kuB* containing fragment of the wild-type (WT) strain was expected to produce a product size of approx. 7.1 kb in size after *Sac*II digestion, whereas the *kuB* deletant strain transformants with the *ptrA* insert of were expected to produce a product size of approx. 6.1 kb after *Sac*II digestion.

Appendix 49 The amino acid sequence alignment of AN3667 (XP661271.1), AFUA4G12410 (XP751590.2; AFUB069370), PaHMG5 (XP001905098.1) and Fmf-1 (XP9638833.3). Highly conserved residues are marked in red, while

lower conserved residues are marked in blue. The alignment was analyzed via Constraint-based Multiple Alignment Tool (COBAL; https://www.ncbi.nlm.nih.gov/tools/cobalt/cobalt.cgi?CMD=Web).

Appendix 50 The amino acid sequence alignment of AN1962 (XP659566.1), AFUA4G10820 (XP751745.1; AFUB067900) and *P. anserina* homolog PODANS_6_4110 (XP001909907.1). Highly conserved residues are marked in red, while lower conserved residues are marked in blue.

Appendix 51 The amino acid sequence alignment of AN2885 (XP754458.1), AFUA3G11610 (XP660489.1 AFUB037560) and *P. anserina* homolog PODANS_1_14230 (XP001905127.1). Highly conserved residues are marked in red, while lower conserved residues are marked in blue.

Apendix 52 The amino acid sequence alignment of AN10103 (XP750203.1) AFUA1G04550 (CBP89496.1; AFUB004890) and *P. anserina* homolog PODANS_1_11050 (XP001908768.1). Highly conserved residues are marked in red, while lower conserved residues are marked in blue.

```
EAA65860.1      1    -    MPLKLIRRGGSILRNFPGTGSLARPVRVFSPQHRVRCITFVARRSPISVTRGLPCSSSTVTT-LARSYATHDGPS  74
XP_752370.1     1   M[74]MPRNIIQGGGSILRYLHRSNALIRPSRVAIANGFIRRICVSMNSQLVSPTMKTFRPSVILSRPLINSFATTITPD 150
XP_001912962.1  1   M    ------------------------------------------------------TQLLSTVFGELGLAQYLDAFLEQGFDTWETIL  33

EAA65860.1     75   EEasSKSTKSTKTTKTKKTKKTKKAGKKPAVR---KTRKVLTEEQKEAR[4]KAEELKETKRKLKAAALQTPKLLPTLPWvN 152
XP_752370.1    151  DE--TETTKSTGSKTGKKNTKKRSSKAATKAkpKPRKKLTDKQKEAK   KAEKMKELVKQLKKTALEPPKKLIENPW-N 224
XP_001912962.1  34  DI--TESDLDTLGVKLGHRRKLQRRIANTRG-----------------  ------------------------------  62

EAA65860.1     153  AMKDKLSEVDKSDNPSPKEAFSRATELARRATPEERQRYVDQAAANKAANEAALKAWVDSHTPLQILEANNARRRLAQLQ 232
XP_752370.1    225  LTIATVAKGLQARGVNGTDFIMQCSQLAQSISAEERERIATEAEANKAANAAAYEAWIQQHTPRQIRDANAARRRLNKIK 304
XP_001912962.1  63  ----------------------IAPDASLVSPTQPSIEELRLQDAQRPDASRQDARDAGVLVVTKRKV--------RRHPK--  113

EAA65860.1     233  GKRrVSIIHDDRLVKPPTSAWIYFFMEKRDK---NALVVSDMAQDVAVQWKNLPASEKAPYLEKANADRARYEREYLEV      308
XP_752370.1    305  NTS-LRLLHDDRQVKRPRTAYLLYMLDRTAEGDFKYMTAKDISVRLTEEWKGLTATEKEKYFKQAEEDRERYRREYLEV      382
XP_001912962.1 114  --------PDENAPERPPSAYVLFSNKMREELKGRNLSFTEIAKLVGENWQSLNASEKEPYESQAQAIKEKYLSDLAEV[19] 203

EAA65860.1     309  YGQPVPKLKGNKKSSKDE       326
XP_752370.1    383  YGEE-PSTSRSTTASPSP       399
XP_001912962.1 204  HGSPPQGMLRSNRTSPPR[257]  478
```

Appendix 53 The amino acid alignment of AN1267 (EAA65860.1) AFUA1G10040 (XP752370.1; AFUB009460) and *P. anserina* homolog PODANS_1_7390 (XP001912962.1). Highly conserved residues are marked in red, while lower conserved residues are marked in blue.

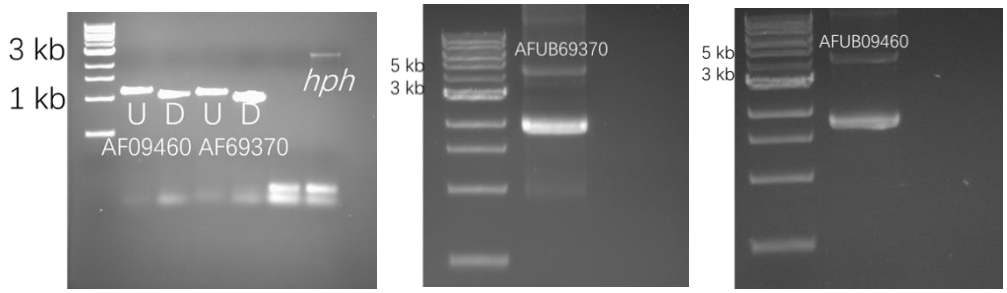

Appendix 54 Construciton of *hph* containing HMG gene deletion cassettes via fusion PCR. The upstream and downstream flanking fragments shows a band with aprrox. 1 kb in siza, and the *hph* fragment band with approx. 2.8 kb in size The AFUB69370 and AFUB09460 were synthesized with a size of approx. 4.8 kb.

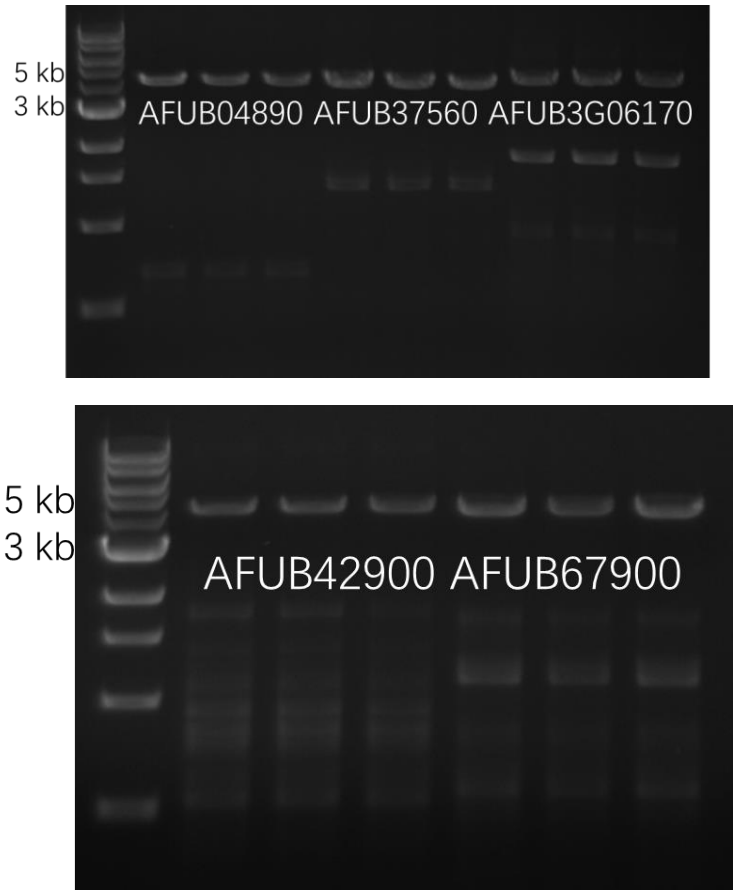

Appendix 55 Amplification of HMG genes cassettes. The approx. size of each deletion cassette was 4.8 kb.

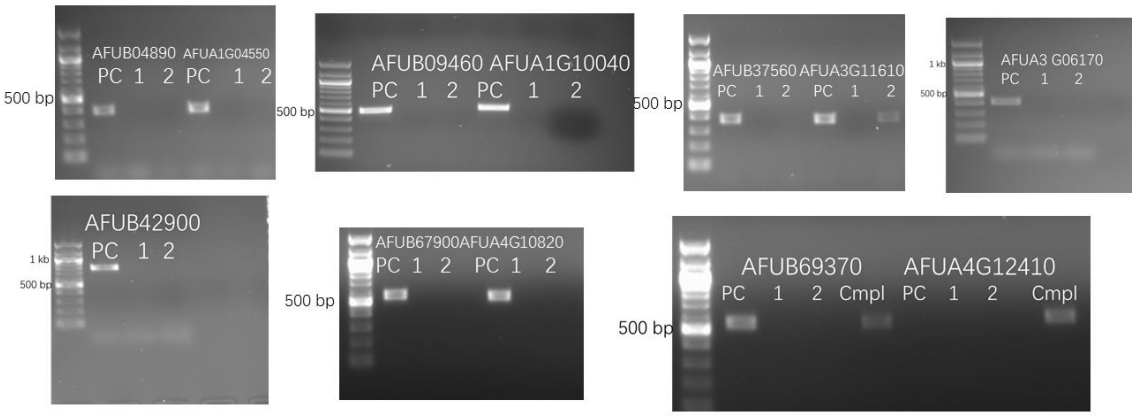

Appendix 56 Verification of the knock-out of the GoI in *A. fumigatus*. See annotation on individual gels for the gene being screened. Parental strains 47-465 and 47-466 were used as the positive control (PC) which gave the product with size approx. 500 bp. The designed primers band with in the ORF of GoI. Cmpl indicate the complementation strain. The absence of a band in the numbered transformants indicates replacement of the target genes whereas presence of a gene product suggests ectopic transformation.

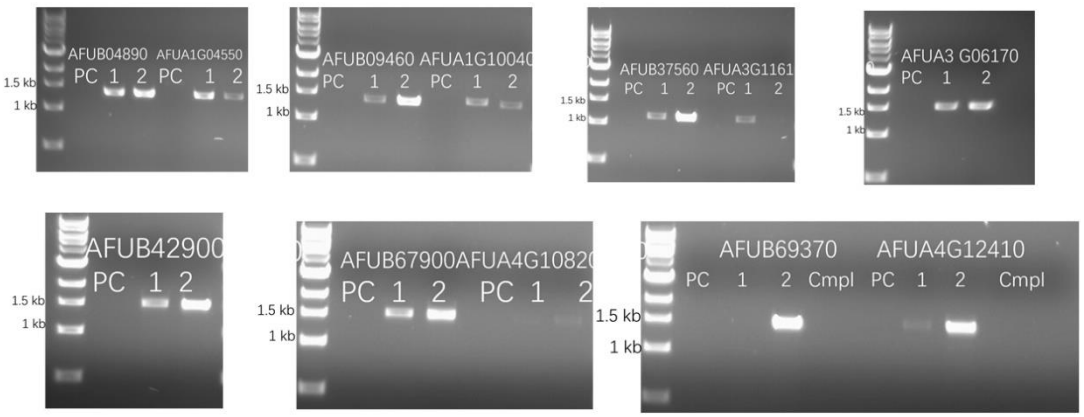

Appendix 57 Verification of the integration of *hph* in *A. fumigatus*. The parental strain 47-465 as 47-466 were used as the positive control (PC) which unable to produce a product. The fragment produced with primer sets designed from the internal *hph* ORF region and the downstream flanking region of the target gene. Diagnostic fragments were all designed to be approx. 1-1.5 kb in size. Cmpl indicate the complementation strain which did not gave a product.

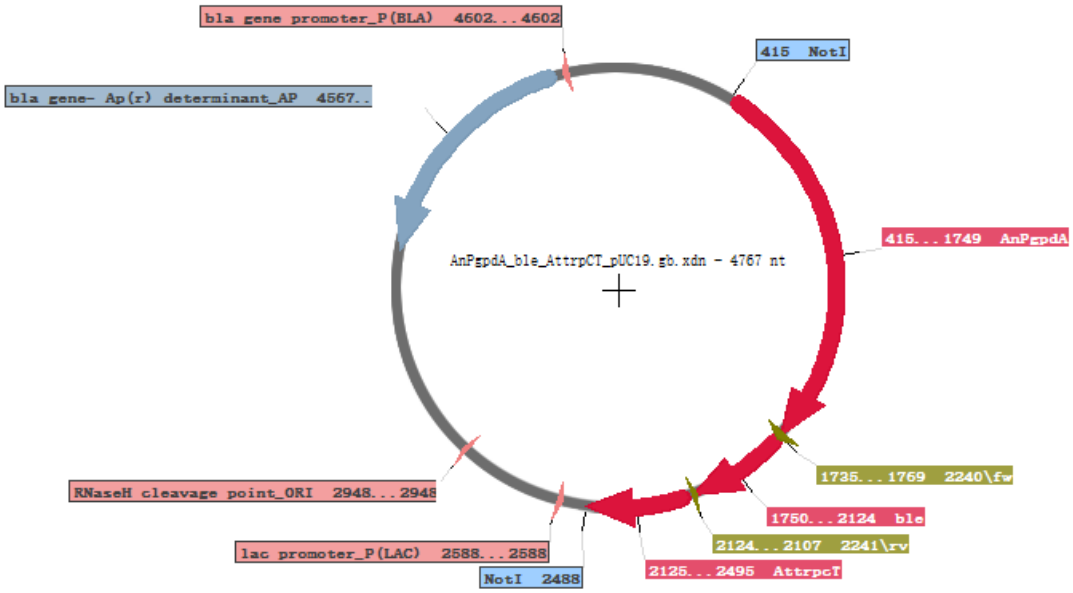

Appendix 58 The map of pUC19-ble containing plasmid. The rose line indicates the deletion cassette containing promotor AnPgpdA, *ble,* and terminor AttrpcT. The gray line indicates the fragment of the vector pUC19. The light blue line indicates selectable marker *Amp*.

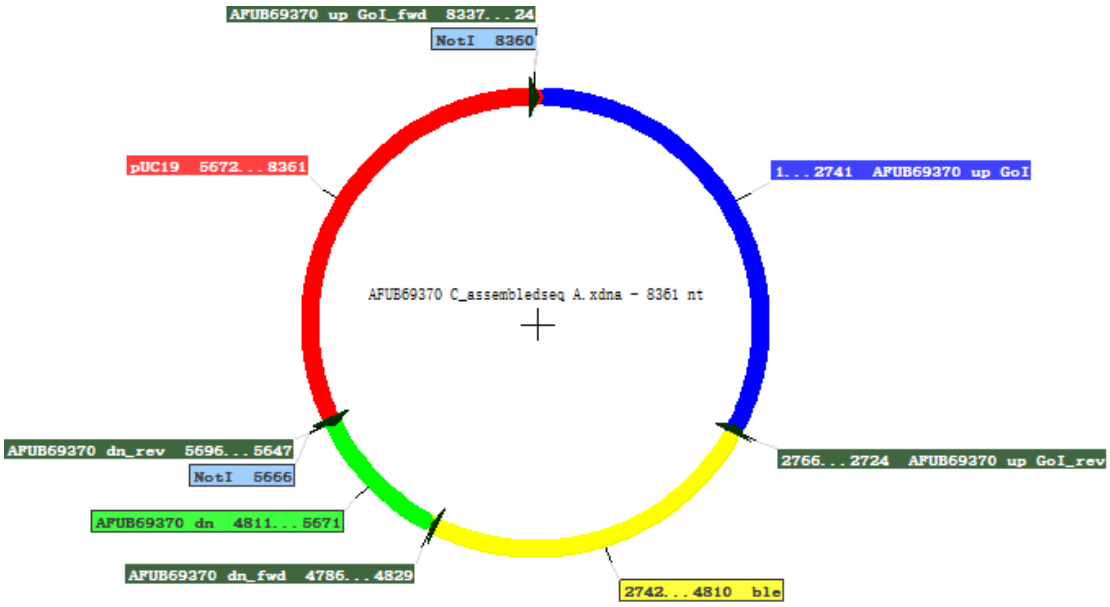

Appendix 59 The map of the pUC19-ble-AFUB69370 containing plasmid. The blue line indicates the upstream flanking region and gene of interest. The yellow line indicates the selectable marker *ble*. The green line indicates the downstream flanking region of the target gene. The red line indicates the fragment of the vector pUC19.

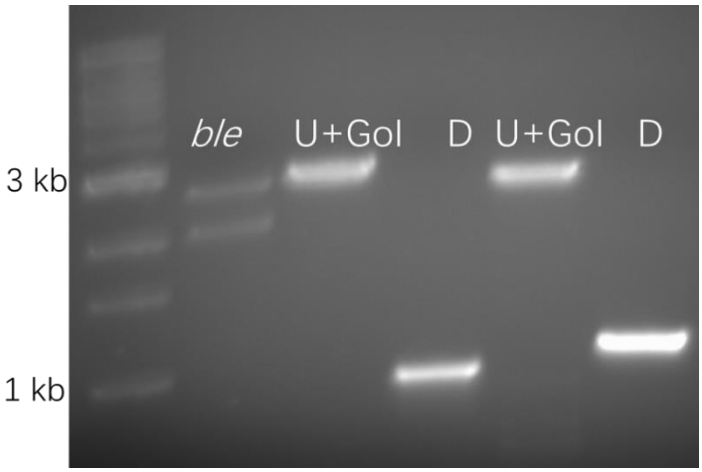

Appendix 60 Construction of pUC19-ble-AFUB69370 plasmid. See annotation on individual gels for the gene being screened. Lable *ble* indicates the fragment (with approx. size 2 kb) digested from pUC19-ble plasmid with *Not*I. U+GoI indicates a fragment from the upstream flanking and AFUB69370 ORF region which was approx.3 kb in size. D indicates the downstream flanking region of AFUB69370 which was apporx. 1 kb in size.

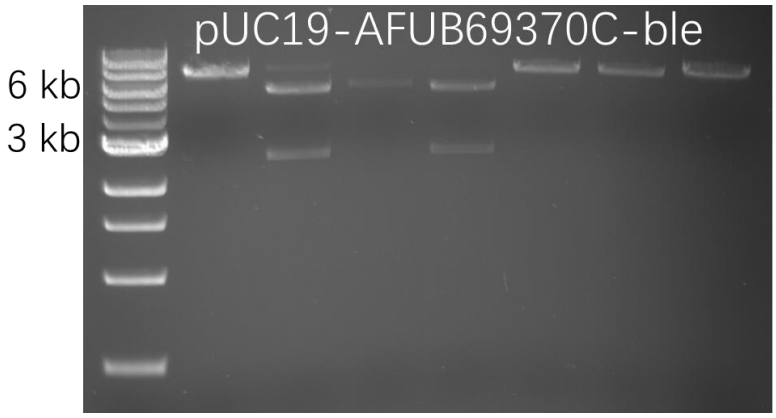

Appendix 61 Screening of pUC19-AFUB6930C-ble plasmid by digesting with *Xho*I. The target plasmids were digested into two fragment which were 5728 bp and 2633 bp.

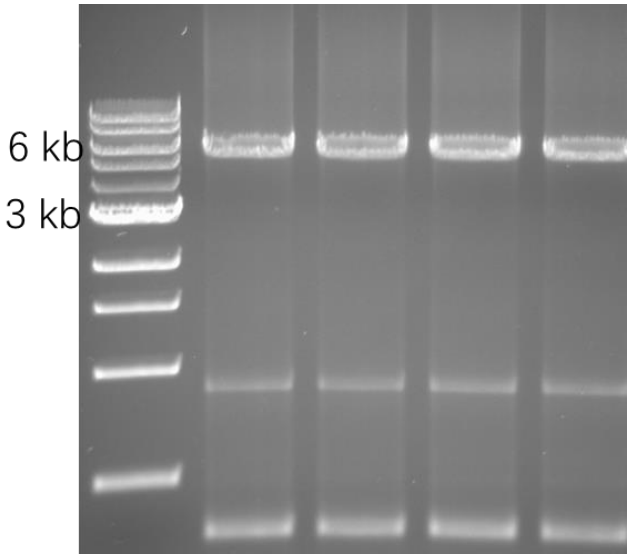

Appendix 62 Amplification of the complementation cassettes from the pUC19-AFUB6930C-ble plasmid. The size of the fragment was approx. 5.7 kb in size.

Appendix 63 Levels of fumagillin production in control and ΔHMG strains of *A. fumigatus* (MAT1-1 background)

Strain	Average±SEM (μg/mL)	Replicates
47-465	10.43±1.632	3
ΔAFUB04890M1a	13.13±0.8708	3
ΔAFUB04890M1b	16.00±1.069	3
ΔAFUB09460M1a	26.34±8.896	3
ΔAFUB09460M1b	58.30±6.565	3
ΔAFUB37560M1a	20.83±2.664	3
ΔAFUB37560M1b	132.4±34.06	3
ΔAFUB42900a	11.71±0.5324	3
ΔAFUB42900b	12.94±0.6295	3
ΔAFUB67900M1a	13.70±1.801	3
ΔAFUB67900M1b	12.17±3.237	3
ΔAFUB69370M1a	16.76±1.504	3
ΔAFUB69370M1b	14.69±0.5175	3
AFUB69370M1C	136.2±15.36	3

Appendix 64 Levels of fumagillin production in control and ΔHMG strains of *A. fumigatus* (MAT1-2 background)

Strain	Average±SEM (μg/mL)	Replicates
46-466	38.65±5.134	3
ΔAFUB04890M2a	66.50±16.69	3
ΔAFUB04890M2b	41.59±17.19	3
ΔAFUB09460M2a	155.2±6.916	3
ΔAFUB09460M2b	125.2±23.95	3
ΔAFUB37560M2a	14.04±1.502	3
ΔAFUB37560M2b	13.37±1.211	3
ΔAFUA3G06170a	57.66±4.869	3
ΔAFUA3G06170b	34.40±3.428	3
ΔAFUB67900M2a	21.34±3.171	3
ΔAFUB67900M2b	40.93±12.59	3
ΔAFUB69370M2a	22.31±7.010	3
ΔAFUB69370M2b	24.54±4.533	3
AFUB69370M2C	14.59±1.235	3

Appendix 65 Levels of pseurotin A production in control and ΔHMG strains of *A. fumigatus* (MAT1-1 background)

Strain	Average±SEM (μg/mL)	Replicates
47-465	192.6±46.04	3
ΔAFUB04890M1a	192.9±2.276	3
ΔAFUB04890M1b	220±45.32	3
ΔAFUB09460M1a	93.71±28.73	3
ΔAFUB09460M1b	128.9±17.61	3
ΔAFUB37560M1a	6.582±2.743	3
ΔAFUB37560M1b	207.9±37.12	3
ΔAFUB42900a	1.227±1.227	3
ΔAFUB42900b	90.42±17.12	3
ΔAFUB67900M1a	2.762±2.63	3
ΔAFUB67900M1b	108.8±52.27	3
ΔAFUB69370M1a	0	3
ΔAFUB69370M1b	0.7721±0.7721	3
AFUB69370M1C	30.34±4.541	3

Appendix 66 Levels of pseurotin A production in control and ΔHMG strains of *A. fumigatus* (MAT1-2 background)

Strain	Average±SEM (μg/mL)	Replicates
46-466	268±23.27	3
ΔAFUB04890M2a	258.5±4.792	3
ΔAFUB04890M2b	193.6±51.89	3
ΔAFUB09460M2a	178±8.021	3
ΔAFUB09460M2b	34.79±8.442	3
ΔAFUB37560M2a	23.75±13.78	3
ΔAFUB37560M2b	12.22±1.846	3
ΔAFUA3G06170a	169.8±23.93	3
ΔAFUA3G06170b	9.41±7.487	3
ΔAFUB67900M2a	0.3104±0.3104	3
ΔAFUB67900M2b	0	3
ΔAFUB69370M2a	1.177±0.6606	3
ΔAFUB69370M2b	1.347±0.7031	3
AFUB69370M2C	24.03±2.864	3

Appendix 67 Levels of gliotoxin production in control and ΔHMG strains of *A. fumigatus* (MAT1-1 background)

Strain	Average±SEM (μg/mL)	Replicates
47-465	84.08±35.66	3
ΔAFUB04890M1a	264.7±203.3	3
ΔAFUB04890M1b	98.31±23.33	3
ΔAFUB09460M1a	218.2±159.6	3
ΔAFUB09460M1b	45.23±3.605	3
ΔAFUB37560M1a	39.04±9.398	3
ΔAFUB37560M1b	29.19±3.359	3
ΔAFUB42900a	52.48±25.42	3
ΔAFUB42900b	55.26±24.39	3
ΔAFUB67900M1a	61.69±8.316	3
ΔAFUB67900M1b	66.08±14.74	3
ΔAFUB69370M1a	85.67±36.44	3
ΔAFUB69370M1b	23.4±2.384	3
AFUB69370M1C	34.73±3.28	3

Appendix 68 Levels of gliotoxin production in control and ΔHMG strains of *A. fumigatus* (MAT1-2 background)

Strain	Average±SEM (μg/mL)	Replicates
46-466	84.08±35.81	3
ΔAFUB04890M2a	76.33±20.97	3
ΔAFUB04890M2b	26.16±4.523	3
ΔAFUB09460M2a	34.66±4.912	3
ΔAFUB09460M2b	179.2±92.44	3
ΔAFUB37560M2a	67.34±13.18	3
ΔAFUB37560M2b	23.48±6.748	3
ΔAFUA3G06170a	90.67±8.834	3
ΔAFUA3G06170b	60.62±14.87	3
ΔAFUB67900M2a	85.2±49.13	3
ΔAFUB67900M2b	196.4±154.1	3
ΔAFUB69370M2a	113.7±86.79	3
ΔAFUB69370M2b	58.62±35.93	3
AFUB69370M2C	36.72±9.908	3